SCALE-UP OF CARBON/CARBON COMPOSITE BIPOLAR PLATES
DOE Contract DE-FC36-02AL67627

FINAL REPORT
November 2008

Executive Summary

This project was focused upon developing a unique material technology for use in PEM fuel cell bipolar plates. The carbon/carbon composite material developed in this program is uniquely suited for use in fuel cell systems, as it is lightweight, highly conductive and corrosion resistant. The project further focused upon developing the manufacturing methodology to cost-effectively produce this material for use in commercial fuel cell systems. United Technology Fuel Cells Corp., a leading fuel cell developer was a subcontractor to the project was interested in the performance and low-cost potential of the material.

The accomplishments of the program included the development and testing of a low-cost, fully molded, net-shape carbon-carbon bipolar plate. The process to cost-effectively manufacture these carbon-carbon bipolar plates was focused on extensively in this program. Key areas for cost-reduction that received attention in this program was net-shape molding of the detailed flow structures according to end-user design. Correlations between feature detail and process parameters were formed so that mold tooling could be accurately designed to meet a variety of flow field dimensions.

A cost model was developed that predicted the cost of manufacture for the product in near-term volumes and long-term volumes (10+ million units per year). Because the product uses low-cost raw materials in quantities that are less than competitive tech, it was found that the cost of the product in high volume can be less than with other plate technologies, and can meet the DOE goal of $4/kW for transportation applications.

The excellent performance of the all-carbon plate in net shape was verified in fuel cell testing. Performance equivalent to much higher cost, fully machined graphite plates was found.

Project Summary

The project was performed in three phases as follows:

Phase I. Design and fabrication of the pre-pilot development system, and technical investigation into the material concept.

Phase II. Detailed product development and performance verification

Phase III. Net shape molding development, process optimization, cost evaluation and performance verification.

In Phase I, a development system was designed and constructed that enabled the efficient manufacture of test materials. Raw materials sources then were reviewed and selected for investigation. Finally in this stage, prototype flat bipolar plates were generated through specific designed experiments to generate a relationship between raw material properties, material recipe and finished plate properties. UTC Fuel Cells helped to generate the finished bipolar plate target properties in conjunction with the DOE technical targets for bipolar plates.

Prototype flat plates were generated and tested by UTC Fuel Cells to demonstrate the potential of the Porvair plate.

Phase II focused upon generating a low-cost, net-shape moldable bipolar plate. The activities in this phase included the modification of the Phase I forming machine to enable more repeatable net-thickness sheets (bipolar plate precursor material). Several technical investigations were performed to generate highly uniform precursor materials that led directly to the formation of high quality molded bipolar plates in a prototype design. Investigations around forming, molding and carbonization variables were performed. Fuel cell testing was also performed to validate the performance of the material in use.

In Phase III the effort focused upon process optimization and extending the technology to a variety of fuel cell designs. Correlations between flow channel dimension and product shrinkage were developed to generate a tool for generating molding tooling to yield accurate flow field replication. Further, effort was placed on optimizing the process for product cost reduction. Statistical analysis of the process was implemented to drive continuous process improvements to eliminate part defects and improve product quality and yield. Finally, product performance was tested in the materials final version with an updated flow field pattern. Results again confirmed the excellent performance of the Porvair bipolar plate in testing performed by UTC Fuel Cells.

Phase I

Design and Construction of the Pre-Pilot Development System

The pilot-scale bipolar plate manufacturing process is a repeatable method for dispersing raw materials into a perform sheet. The overall process is as follows:

1) Raw materials dispersed in water are formed into a wet loaf material
2) The wet loaf is dried in a convection dryer
3) The dried loaf is then cut into four uniform thickness plates using conventional sawing and milling operations.
4) These "green" plates are then pressed and/or molded to net shape in a hot press
5) The molded plates are then carbonized under controlled conditions to produce a carbon composite plate
6) Depending on the application, the carbon composite plate may be sealed with chemical vapor deposited carbon to generate the final bipolar plate product.

The dry loaf material consists of a uniform mixture of carbon fibers, thermoplastic or thermosetting resin and potentially other additives that impart desirable characteristics to the final product.

After carbonization, the plate thermal and electrical conductivity is significantly enhanced, generating a product with properties unmatched by other carbon/graphite based technologies.

The process at this stage of the project is a developmental process. The forming operation is a batch operation, making at most four plates per batch; each batch requiring about 1 hour of forming time. The pre-pilot equipment is meant to provide Porvair with the capability to develop the material and process into a cost-effective bipolar plate product that can be made in high volume.

1.0 Design and Construction of the Vacuum Former

The pre-pilot-scale vacuum former was designed and built at PAM facilities. The system consisted of a stand and platform, a liquid ring vacuum pump, vacuum/pressure tanks, one polyurethane process tank and a specially designed forming box where the prototype materials are vacuum formed. Additional equipment needed for the operation and control of the system included hand, solenoid and pneumatic control valves, flow meters, mixers, level sensors, and control equipment. The utilities needed for the system includes a 220VAC electrical power, a water supply and water drain system (actually installed as a pump to a common plant water treatment system). Fig. 1.1 shows the assembled forming system.

The forming system functions as follows:

1) De-ionized water is batched into the supply tanks
2) Simultaneously the vacuum tanks are evacuated.
3) A screen filter is positioned in the forming pans and the pan "hats" re put in place.
4) During water fill, weighed raw materials are added to the tank and mixed in to the water
5) Mixing conditions are maintained that fully disperses the solids in the water. The mixer remains on during the remainder of the operation
6) When the vacuum tanks have been evacuated and the material is fully batched into the water, the forming operation can begin. To start the forming, a solenoid-operated valve

opens to feed slurry to the forming pan. When the pan is near full, the vacuum system is opened to begin forming the material loaf.

7) During forming a pneumatic valve controls the rate of forming from the forming pan. This is done through a feedback control loop with an in-line flow meter positioned between the forming pan and the vacuum tanks.
8) After forming has begun, a level sensor is positioned on the forming pan "hat" to control the addition of slurry to the forming station. The goal is to have a head of slurry of at least 5" above the forming loaf of material.
9) The system operates automatically from this point forward until all of the slurry has been discharged to the forming station and the remaining water in the system pulled out by the vacuum tanks.
10) The formed loaf of material is then removed from the system (on the stainless screen and support), and placed into a batch oven to dry fully.
11) After the forming sequence is complete, the vacuum system is isolated and vented, and the water collected in the vacuum tanks during the forming operation is discharged to the plant water treatment system.

Figure 1.1 Pilot bipolar plate material forming system

The system was designed in-house and built and installed by a local fabricator.

Before the system was used to form material loaves, its operation was debugged through initial trials using water only. The water flow meter was calibrated using water, and the flow control setpoints established to prevent overshoot and excessive cycling during operation. After this initial equipment shake-down, an initial batch was made to form a trial material loaf. No

difficulties were found in forming the initial loaf, so the control parameters were recorded and operation opened up for product development efforts.

2.0 Design and Construction of a Platen Press

After the loaves are dry they are cut into four individual green plates each. The plates are then pressed to densify the parts and to melt and flow the resin throughout the matrix. The hot press for the program was selected to have the following characteristics:

1) At least 100 tons of pressing pressure
2) Operating power, 480VAC, 3-phase power
3) Rapid closure and opening speeds to minimize press open times
4) Degas capability with control response times of 1 sec. or less
5) Platen size of about 24” x 18”
6) Daylight opening of at least 24”
7) Platen travel of at least 12”
8) Independent heating control for top and bottom platens
9) At least turn-lock, 220VAC, single phase receptacles for electric heaters per platen
10) Up-acting press to simplify mounting and installation

Obviously the most desirable press will be very expensive and require long lead times if purchased new. An alternative was to lease a press from a knowledgeable press manufacturer. We opted for the second alternative. In selecting the press, we performed several phone interviews with major press manufacturers and searched used press offerings from several used equipment dealers. Ultimately a used press was found having the desired capabilities in a reasonable machine footprint. The press was refurbished and upgraded to suit our needs, and a leasing arrangement was defined for the press. The press selected for this program is shown in Fig. 2.1, and met all of our requirements. The press was installed by Porvair maintenance personnel. Training to program and operate the press was provided on-site.

Press tooling for the manufacture of flat test plaques was then designed and purchased to conform to our needs. Figure 2.2 shows the flat plaque design loaded in the press. Tool steel was for the press tooling was purchased from DME, Inc., a major supplier of mold tooling equipment for the compression and injection molding industries.

The flat plate thickness is controlled in the press by narrow industrial shims. Shims were purchased that offered increments of 0.001” of pressed part thickness control from 0.020” up to 0.100”.

Heaters for the platens were selected as cartridge heaters operating at 220VAC, single phase power. The heaters were designed at 2 kW each, and were ½” diameter heaters to match the through holes of the flat press tooling. Heating control was performed with the press heating control system. One type J thermocouple per platen was used to provide temperature feedback to the control system.

After all equipment and tooling was in place and installed onto the press, initial trials were performed to debug the system and to establish the initial molding conditions. No operational issues were noted with the press, tooling or platen heating system.

3.0 Design and Construction of Roller Press

A roller press was envisioned to be capable of rapidly embossing the flow field pattern into the plate product prior to carbonization. A prototype roller press was constructed from a de-commissioned roller system to demonstrate the feasibility of pattern embossing using this method. The press consists of a flat base roller and a grooved top roller. The roll spacing is controlled by worm gears, and the roller rotation is controlled with a 90V DC motor. Figure 3.1 shows the roller press and the grooved roller. The roller press was built in-house using equipment on-hand from ceramic foam production equipment. The aluminum rollers were machined to our specifications by a local fabrication shop.

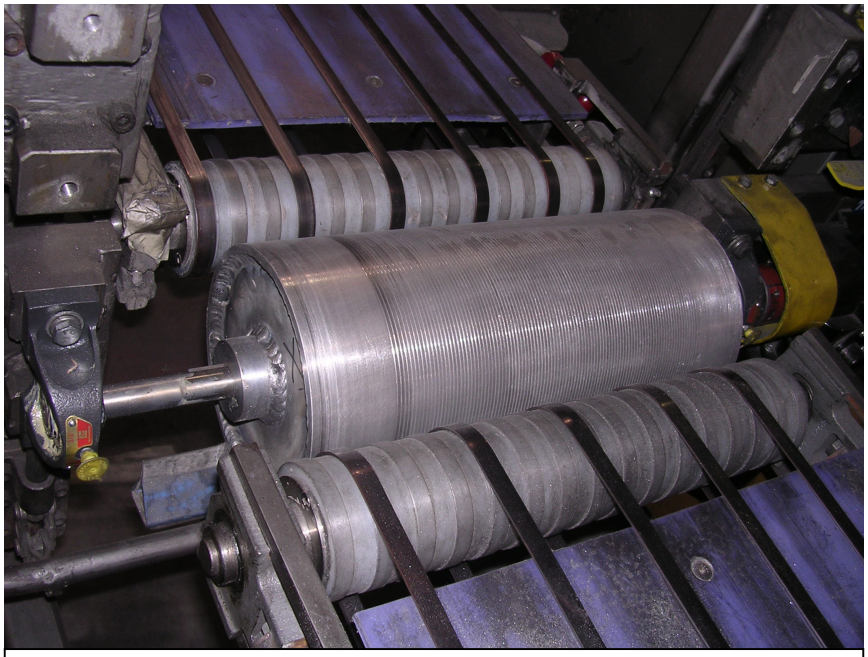

Figure 3.1. Photograph of roller press modified from a standard roller machine for this program.

4.0 Design and Construction of Vapor Infiltration Furnace

This furnace was the single largest equipment expense for the program. In the manufacture of sealed bipolar plates, the surface is sealed with a chemical vapor deposited carbon coating. Because the ideal coating conditions are not known, the furnace capability must be suitably flexible so that a variety of operational conditions can be established at temperatures as high as 1650°C.

In the process of seeking this furnace, a detailed furnace specification was developed. This is shown below:

CVI FURNACE SPECIFICATION

SPECIFIC REQUIREMENTS

Furnace Configuration: Top loading furnace or horizontal furnace

Hot Zone Dimensions: Minimum 16” width x16” height x32” depth useable region or equivalent for horizontal furnace. Cylindrical shape for top loading furnace, dimensions approximately 24” inside diameter x 32” height.. The hot zone is to be defined as the interior dimensions of a graphite or carbon-carbon composite retort box located inside of the heating elements.

Furnace Power Requirements:

The furnace power supply and controls shall be designed to operate from a 480 VAC, 3-phase source. Vendor to establish the ultimate power requirements. Provide suitable safety interlocks, loss of cooling water alarms, and undervoltage trips, etc. as needed.

Elements:

Graphite elements that are low cost for repair/replacement are preferred (stay away from specialized element design if possible). Also acceptable are carbon-carbon composite heating elements or other materials that may be suitable for the application.

Furnace Temperature Requirements:

Temperature uniformity shall be to +/-10°C at peak temperature (it is assumed that this uniformity level is standard for the industry). Please indicate what would be required to tighten the uniformity specification to +/- 5°C.

Thermocouples:

Thermocouples and sheath materials suitable to the environment are required for process and over-temperature control. The environment will encourage significant carbon deposition upon materials located into the hot zone region. Sheath materials should be compatible with this environment. (Gases are primarily methane and other light hydrocarbons. Some concentration of hydrogen and nitrogen will also be present).

A bank of 8-12 survey thermocouple connections is also desired. Interface of these survey thermocouples with the controlling PLC is desired. Please include this as an option in the proposal.

Include as an option the installation of an optical pyrometer capable of detecting load temperature.

Furnace Pumping Requirements:

The pumping system shall be designed to evacuate the chamber to less than 200 microns of mercury within reasonable time (typically less than 10-15 minutes), and shall enable the desired partial pressure control range at maximum total gas flow rate (see below).

Of particular importance is that the pumping system be suitable for the gases of use. High concentrations of methane will be present in the off-gas. Also present will be hydrogen gas. The pumps must be capable of safely pumping mixtures of methane, hydrogen and nitrogen. Off gas treatment (e.g., incineration) of the pump exhaust will be done by Porvair.

Specific pump specifications may be prescribed so that the pump equipment matches existing pumps in our facility (depending upon the ultimate sizing of the pumping equipment for this furnace).

Retort Box:

The retort design is left open, provided that the interior dimensions meet the specified requirements. An additional note is that operation will result in a significant amount of carbon/graphite deposition on the interior retort surfaces. A design with means of conveniently removing the retort box (or disposable box lining) for periodic cleaning (if necessary) or replacement is desirable.

Product Support:

Graphite rails positioned above the gas distribution system (or at the same level) are acceptable for product support. Product load support shall have a capacity of approximately 250 lb.

Furnace Operational Pressures:

The furnace shall have the capability of pumping down to a pressure of less than 200 microns of mercury. During operation, the furnace shall run at a programmable pressure setpoint between 1 and 100 torr. Partial pressure control shall occur through a combination of mass flow and exhaust valve control.

Furnace Pumping Configuration:

The pumping configuration should adequately control furnace setpoint pressure. It is further desired to isolate the interior methane gas from the exterior purge gas. A suitable method of venting the nitrogen purge gas to the pump line is desired to minimize internal and external gas mixing.

Pressure Measurement:

Pressure measurement shall be with good quality instrumentation.

Partial Pressure Control:

The furnace shall have partial pressure control using both mass flow control of gases and pump flow modulation through an actuated butterfly valve on the pump line. Suitable controls, linked to the furnace control system for programmable partial pressure set-point is desired.

Methane Gas Injection:

Methane gas shall be injected into the retort interior. Control of methane flow should be through suitable mass flow control means. Maximum desired methane flow rate is 15 scfm at maximum furnace operating pressure (see table below for approximate flows at differing furnace operating pressures). Methane gas injection may occur at the base of the retort box in a uniform injection pattern that spans the cross-section of the retort interior. The injection method used shall be reliable and resistant to plugging under the conditions of operation. During operation, methane gas flow may be from bottom to top or from top to bottom.

It should be noted that the given flow rates for methane and nitrogen as specified below will require significant power input to heat the gases to the furnace operating temperature. It is requested that a gas pre-heating system be included in the system design. The purpose of the gas pre-heating system will be to heat the flowing gases up to a desired temperature before injection into the retort chamber.

Nitrogen Gas Injection:

The furnace shall have the capability of nitrogen gas injection within the main chamber and within the retort box. Each stream shall be independently controllable. The gases injected into the retort chamber shall use the same gas lines as those used to carry methane (for methane dilution with nitrogen if needed). Mass flow control is desired on both nitrogen streams. Nitrogen gas injection shall be in the range of 4 scfm in the outer zone and 8 scfm in the retort zone at peak operational pressures. See table below for approximate flow rates at differing operational pressures.

Furnace Controls:

The furnace electronic controls shall be through a PLC with a computer screen interface for system programming and process indication. Plant compatibility requires that the PLC hardware be Allen Bradley SLC500/04 or better. Citect software is suggested (but not mandatory) for the computer interface, as it is used elsewhere in the plant.

Furnace Instrumentation, indication and alarms:

Provide industry-accepted standard instrumentation (prefer analog current and voltage indication) and alarms.

Cooling Water System:

Provide inlet and outlet for circulation loop. Provide suitable loss-of-flow indication tied to alarm system. Provide pressure relief where required.

This furnace specification was presented to several vacuum furnace manufacturers, including:

Advanced Vacuum Systems
Bethlehem Advanced Materials
Centorr
Thermal Technology
Seco Warwick
Materials Research Furnaces

A trip to each of these vendors was taken to interview the manufacturers and review the product specifications. After this initial interview, each manufacturer was asked to prepare a detailed final quote and product specification. After these quotations were received, the systems were compared to assist in selecting the most capable system for the best price.

After this review process, the Thermal Technology furnace was selected after they were motivated to reduce their pricing further due to competitive pressure and the slow equipment market at the end of 2001. A drawing of the furnace is shown in Fig. 4.1 prior to furnace fabrication.

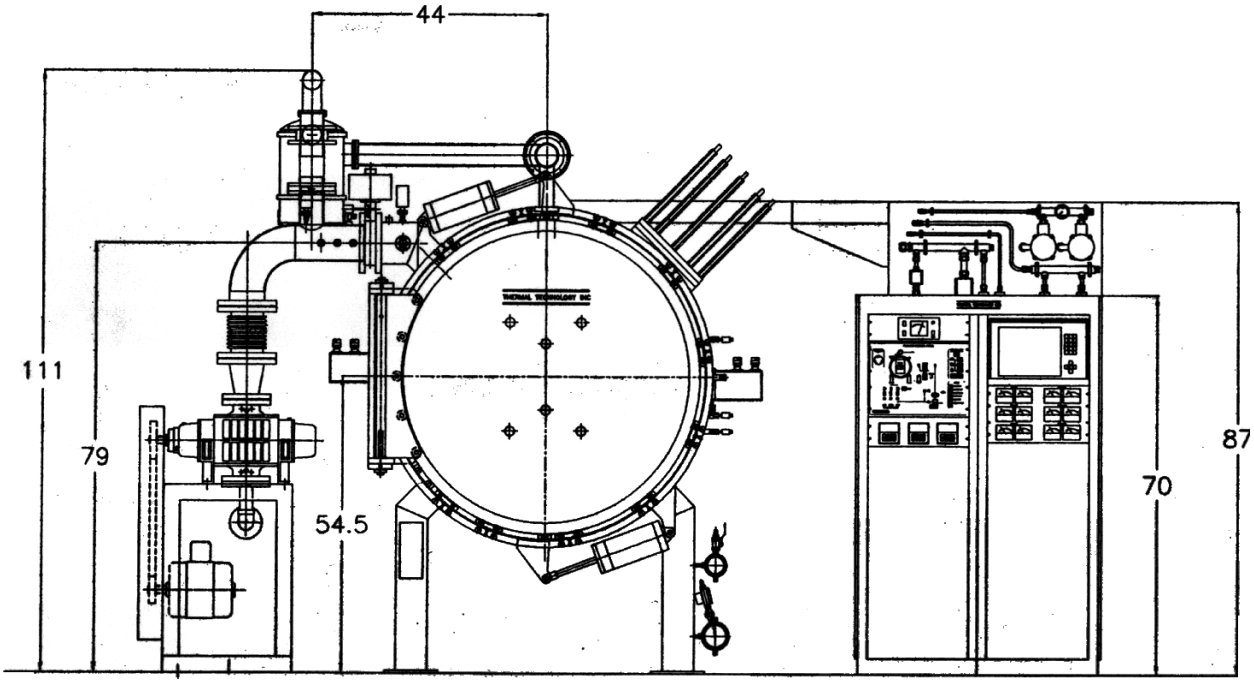

Figure 4.1. Drawing of conceptual furnace.

Prior to firm order placement, several iterations of the final furnace specification were prepared jointly by Porvair and Thermal Technology. After order placement, final drawings were prepared by Thermal Technology, and inspected and approved by Porvair. A trip was made to observe the initial furnace test-out at Thermal Technology before final shipment of the furnace to Porvair. The furnace was installed at Porvair in late May 2002 by Porvair maintenance personnel. The furnace as installed is shown in Fig. 4.2.

Figure 4.2. Installed vacuum furnace.

5.0 Design of Flow Field Pattern

For this demonstration program, we proposed to use UTC Power's standard flow field design. The design details are proprietary to UTC Power. At this stage of the program, we did not have product shrinkage data, so the flow field was designed to their final print.

6.0 Design and Construction of Dies for Flow Field Pattern

For the molding, a mold base was designed and constructed, and pattern inserts were constructed from standard tooling steel. The mold dies were made from graphite masters in a face EDM process. Hand polishing of the flow-field features followed to yield acceptable prototype dies.

7.0 Review of Available Carbon Fiber Sources

The carbon fiber product used in our process is milled carbon fiber. Sources of milled carbon at the time of this investigation included Fortafil and Zoltec. Other major carbon fiber suppliers include Cytec, SGL Carbon, Toho, Toray and Hexcel. Most applications for carbon fiber materials utilize continuous or chopped carbon fiber. Those companies manufacturing milled carbon fiber do so for relatively minor applications such as conductive filler in thermoplastic injection molding compounds.

The product specifications for this material are:

Characteristic	Limit
Flexural Strength	Minimum 240 ksi
Flexural Modulus	16.0 – 19.0 Msi
Shear Strength	Minimum 13.0 ksi
Bulk Density	300-400 g/L
Magnetic Material Content	No Visual Contamination – not reported on COA

In our studies, we reviewed Zoltec and Fortafil material, with essentially equivalent product specifications. Both Fortafil and Zoltec are reputable suppliers with more than satisfactory near-term product availability. Pricing in 2002 was also similar between both products. Because the Fortafil manufacturing facility (Rockwood, TN) is relatively close to Hendersonville, and because Fortafil has product support personnel frequenting the Charlotte area, we chose to use the Fortafil material in this program.

During product scale-up operations, we had an opportunity to audit Fortafil operations as part of our ISO9001 material qualification procedures. In the audit, we found no non-compliances and an excellent history of data collected for the 342 product that showed consistent manufacturing operations and conformance to product specifications.

8.0 Review of Available Binders

Binders in this program refers to the resin used to bind the fiber and other additives together in the as-pressed state. The same material also carbonizes with heat treatment and establishes a carbon bond. The material defined for use at the start of the program was a thermosetting phenolic resin. In early trials, however, it was found that the material acts like a thermoplastic, as it fails to set-up with applied heat and pressure in the molding operation. This results due to the loss of the water soluble initiator, hexamine in the product. As a result, a search for alternative binding materials was launched, yielding several candidate replacement materials.

Thermoset Materials

There are numerous types of thermoset materials available for the production of a variety of plastic components. These materials are generally low-cost and are available in large volumes. They are used either alone or are compounded with another material (clay, glass fibers, cotton flocks, carbon fibers, etc.) to produce higher strength composite materials. The lowest cost material is urea, which is used as a binding resin in OSB lumber manufacture. Phenol, melamine, polyester, polyvinyl, and a number of epoxy products are also common thermoset materials. These materials are generally used in either injection or compression molding, where the material (or a compound of thermoset and filler) is molded under heat and pressure to form a final-shape product. Currently there are several bipolar plates made through compression molding, but strength and electrical conductivity remain significant issues.

Urea and melamine products are similar thermoset materials. Melamines tend to have higher strength and moisture resistance, and are common in products such as countertops, school seats and desktops.

Phenol materials are the next most common thermoset material. These materials exhibit better strength and moisture resistance than the ureas and melamines. These products have been developed for a wide variety of plastic materials, and there is an almost endless supply of material alternatives in the phenol group. They are common precursors for use in “glassy” carbon-carbon components.

Other thermosets include vinyl-esters, polyesters and epoxies, among many others. All of the thermoset materials will behave differently to heat and will set up at different rates. Polyester materials, for example, are said to be less viscous before thermosetting, therefore encouraging flow and allowing for the use of a higher solids loading than some of the other thermoset materials. Vinyl esters, polyesters and epoxies are generally higher cost raw materials used widely in composite manufacture. Their carbon yield is low in carbonization processes.

One significant characteristic of the thermoset materials, as used in this program, is its response to thermal treatment. Carbon yield and structure formation resulting from polymer decomposition impacts strongly preform properties and characteristics, including carbon content, strength, permeability characteristics, and material warpage. Carbon forming materials are usually pitches or PAN materials, although phenol thermosets have been used in forming CC-composites. The liquid nature of the pitch-based materials may allow for some graphite crystal orientation before pyrolization renders it solid, whereas the phenol materials is set solid to begin with, and yields a non-crystalline carbon structure on carbonization.

The manufacturers of thermoset materials are numerous. Each manufacturer in turn has target market niches and a host of materials to support their customers. Major manufacturers of the basic resin products (urea, melamine and phenol) include Borden Chemical, DuPont, Georgia Pacific among other oil and chemical companies. Specialty companies have taken the basic industrial products and have expanded them technically to fit niche markets for plastic products. Thermoset materials manufacturers include Durez, Plenco, Glastic, Premix and others. The latter companies generally work toward manufacturing a product that can be thermoset molded into a finished plastic component through compression or injection molding processes. Each company has a product portfolio of materials that are used for a variety of applications. A vast array of material properties results from the many product offerings.

Thermoplastic Materials

Thermoplastic materials include nylon, polypropylene, polyethylene, polyvinyl chloride, etc. None of these materials are considered suitable for use in this program due to anticipated low carbon yields on carbonization. Further, the materials are of high melt viscosity and will be difficult to work with in the pressing operation, requiring significant time to first melt then re-solidify in the process.

Pitch Materials

Pitch materials are routinely used in the manufacture of graphite and carbon products. Pitch is manufactured from coal tar and petroleum residues, or from more controlled hydrocarbon products in a polymerization reaction. Mesophase pitch – considered the most important type of pitch to the carbon-carbon industry contains stable liquid crystal particles. The pitch may or may not be mixed with carbon cokes and powders prior to heating to produce a porous carbon or graphite product. Several sequential steps of pitch impregnation into the materials porosity followed by heat treatment serve to fill the material porosity and increase final density. In the manufacture of bipolar plates at PFCT, it is not necessary to completely fill the porosity of the

material, and so the pitch may be used in place of another material to provide component shape holding and carbon to the final product. A technical discussion will be scheduled to determine if trials using pitch should be performed.

Selection of Resins for Investigation

In initial testing, a standard product showed generally good processing characteristics, and yielded a final product with good strength and electrical conductivity (see detailed investigations in Phase I, task 12).

In the early portion of the program, we chose to use a Durez thermosetting resin, but quality issues during process scale-up encouraged our switch to an alternate supplier. Despite competitive pricing for the material, the alternate supplier offers smaller runs, longer shelf life and better customer service than does Durez. Later scale-up work would include a quality audit of the operation and a complete product qualification.

9.0 Review of Other Additives

Other additives to the material composition may include products to yield good green strength for product handling, as well as ingredients to improve the products properties.

For our customer, UTC Power, bubble pressure and flexure strength are the two key properties to optimize.

Because bubble pressure is known to depend upon the pore size of the material microstructure, a means of reducing the nominal pore size of the material was needed. One method of doing this is to add a particulate material (graphite powder) to provide reduced material porosity and therefore increased bubble pressure. As we would later discover (see Task 12), the addition of graphite powder significantly improves the plate properties and dramatically reduces product material costs.

For this reason, we investigated sources and grades of graphite powder. We worked closely with three potential sources of graphite material, Superior Graphite, Asbury Carbons, and Timcal. Several other graphite suppliers exist, and were contacted for our program, but the breadth of products from Superior, Asbury and Timcal span every known grade of material, and all suppliers are leaders in the industry. Further, all three suppliers specialize in materials from different sources.

Timcal is a manufacturer of highly pure synthetic graphite powders. Their products are very clean and come in a variety of size grades.

Asbury is a manufacturer of all types of carbon, coke and graphite powders. Their graphite powders are primarily sourced from scrap materials (known as secondary graphite sources) resulting form the waste from steel electrode machining. However, Asbury also sources natural and primary synthetic graphite powders.

Superior offers graphite powders from both synthetic and natural sources. Their synthetic graphite is sourced from coke residuals. All products are processed to 2500℃, driving off impurities in the process.

Sourcing of the graphite material in this program was a large undertaking, and several investigations, quality reviews and audits were performed in the process. Summaries of this activity are provided later in this report.

10.0 Modification of Water Wetting Angle

A key product property for bipolar plates is material wettability. In the operation of non-porous bipolar plates, the product needs to be either highly hydrophobic so that water generated on the anode plate rolls easily along the flow channels by air pressure, or highly hydrophilic so that the water flows along the flow channels to the air exit. In the UTC Power porous plate the product must be highly hydrophilic so that water easily penetrates the porosity of the bipolar plate material.

Several investigations were performed in this program to identify a means of treating the plates to impart wettable characteristics at low materials and process costs.

The standard method for imparting water wettability to the porous plates is to perform a chemical

Experiment 1

Eight coupons were selected – two from each of four materials. Half of the materials were carbonized, while the other half were simply pressed. These materials were treated in a tin-oxide solution (2:1 by volume water to colloidal tin oxide @ 15% solids – Nyacol) by vacuum filling in a sequence of 20-10-10 minutes of vacuum hold and vacuum release. Half of these materials were then carbonized in a 4.5-day duration carbonization cycle (04/19/02 – 04/24/02). Table 1 shows material types and properties. Wettability is quantifited by the time required to absorb a 6 l droplet into the porosity of the material.

Substr.	Type	Mass (g)	Density (g/cc)	Mass after SnO2 (g)	Wettability After SnO2	Mass after Pyrol. (g)	Wettability After Pyrol.
W1	50% powder Carbonized	4.38	0.96			4.43	~ 40 sec
W2	50% powder Carbonized	4.36	1.00	4.452	> 1 min		
W3	50% powder Pressed	4.54	1.04			4.06	> 2 min
W4	50% powder Pressed	4.56	1.04	4.662	> 30 sec		
W5	15% powder Carbonized	4.63	0.97			4.74	~ 30 sec
W6	15% powder Carbonized	4.62	0..97	4.450	> 5 min		

W7	15% powder Pressed	4.92	1.09			4.34	> 5 min
W8	15% powder Pressed	4.87	1.08	4.976	> 1 min		

The purpose of the short study was to determine if carbonized materials first treated with SnO_2 would retain their wetting characteristics better than just with colloidal SnO_2 treating alone. None of the materials, however, showed good wetting characteristics (through the time required to soak a droplet of water into its surface). Carbonization appears to have improved the wetting characteristics somewhat. Retention of the properties was not examined due to the poor wettability of the materials.

Experiment 2

In this study, the addition of titanium and zirconium oxides were added to the raw materials prior to forming. The parts were then processed as normal. These oxides were chosen as candidates for improving wettabilty based on their predicted stability during both the pyrolysis reaction and later in the aggressive aqueous, electrochemical environment seen in fuel cell.

In this study, a more repeatable measurement method was adopted, and is known as "wick-fill." In this method, a sample plate is placed in a container, which is filled with water slowly over a five-minute interval. The sample is then allowed to soak in the water for 30 minutes. The sample is then removed, patted dry, and weighed. The sample is then submerged and vacuum filled with water according to the standard procedure required in other testing, patted dry and reweighed. The wick fill is simply the ratio of water uptake by wicking to that by vacuum filling and is reported as a percentage. See section 3.1 for a fully detailed description of wettability testing.

Experimental Design

A factorial design to study wettability changes in bipolar plates affected by additions of oxides during the batching process:

Sample	TiO2/ZrO2	Coarse/Fine	10% / 5%	Heat Treat/Not
TIZR1	-	-	-	-
TIZR2	+	-	-	+
TIZR3	-	+	-	+
TIZR4	+	+	-	-
TIZR5	-	-	+	+
TIZR6	+	-	+	-
TIZR7	-	+	+	-
TIZR8	+	+	+	+
TIZR9	Control			

Powder Characteristics

TiO2(c) -325mesh titanium oxide (rutile)**(actual measured aps=1.2 micron)
TiO2(f) 1 micron titanium oxide(anatase)

ZrO2(c) -325mesh zirconium oxide
ZrO2(f) 1 micron zirconium oxide

Results

Following are the results from the averages in wick fill percent for each experimental group.

Experimental Group	**Average (Wick Fill %)**
Titanium Oxide	56.6%
Zirconium Oxide	54.1%
Fine	58.3%
Coarse	52.38%
5% Powder added	54.3%
10% Powder added	56.4%

Heat Treatment

All coupons were oxidized at 650 F for 12 hours in an air furnace for the purpose of determining if light oxidation of the plates encourages improved plate wetability.

Experimental Group	Average (Wick Fill %)
Pre Heat Treatment	53.1%
Post Heat Treatment	**69.5%**

Conclusions

- The most powder size seems to be more important than amount or type, fine powders being better than coarse.
- The best alternative at this point looks like 10% Titanium oxide in a fine powder.
- The heat treatment had the most drastic improvement (+16.4%).
- The average wick fill on the heat treated samples are better than those processed using tin chloride.(Tin Chloride treatment averages 68%)

11.0 Production of Preliminary Samples

Porvair created and delivered prototype samples to UTC Power on a regular basis during the development of the porous bipolar plate product. The activity was regular from the out-set of the program, even prior to having all of the processing equipment in-place, as there was a high degree of pull from our customer. In the early stages, before we had pressing capability, we sent to UTC Power personnel “green” product that could be pressed using their in-house equipment. The parts would then be sent back to Porvair for carbonization using in-house furnaces as availability allowed.

Once the full capability was in-place, the rate of product development increased significantly, and we quickly defined a product recipe and process parameters that yielded a product meeting UTC Power’s material requirements. Once this milestone was achieved, we manufactured a set of 30 blank plates for property verification at UTC Power.

Initial plates at UTC Power were measured for compliance to their internal materials specification. Bench-scale testing included standard measurements (flexure strength, electrical conductivity, bubble pressure, permeability, and leaching/contamination). After a series of parts showed passing results, UTC Power proceeded to build fuel cell stacks to further evaluate the performance of the product. Figure 11.1 shows polarization curves for the first few parts tested in single cell testing at UTC Power. As seen in the figure, the first net shape part (LD designating low-density) was lacking in performance in comparison to bill-of-material (BOM) plates. After improving our net-shape product offerings, the performance quickly improved to yield performance very close to the BOM product.

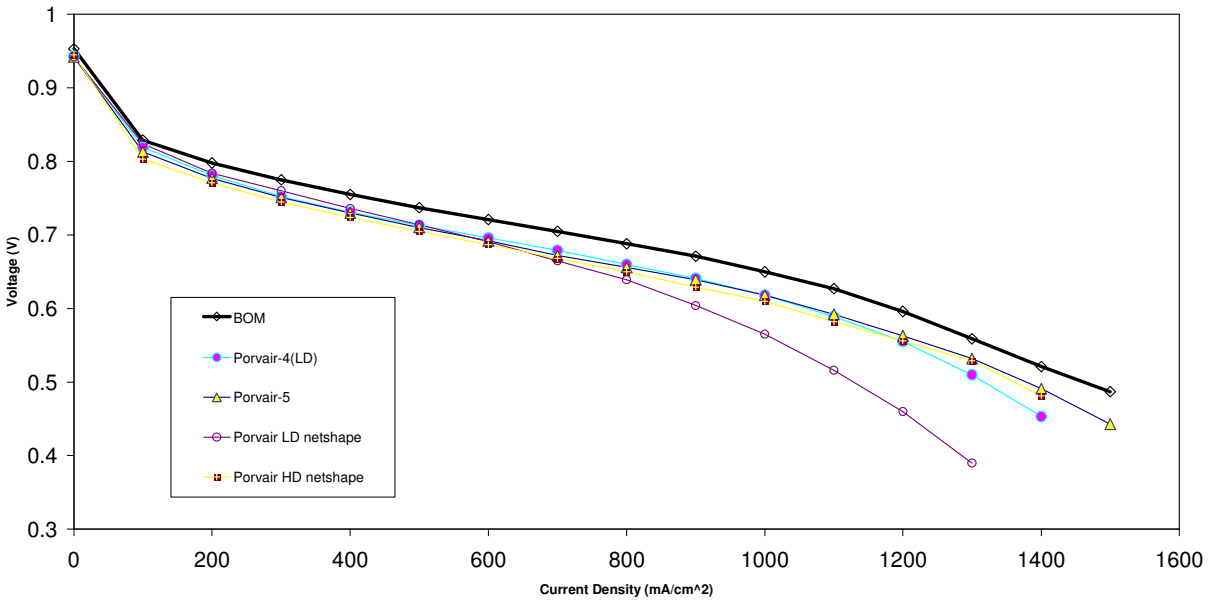

Figure 11.1. Early fuel cell test results from a group of Porvair test parts.

12.0 Experimental Design on Compositional Variables

Because composition influences final product properties so strongly (much more so than process parameters), a great deal of effort was put into the design of the material system. As mentioned earlier, the initial material consisted of 70 wt% milled carbon fiber, and 30 wt% phenolic resin. After carbonization, approximately 50 wt% of the phenolic resin is converted to carbon, and therefore the final product consisted of approximately 85% milled fiber carbon bonded with 15% carbonized resin. The subsequent product is very porous and must be densified in the chemical vapor infiltration process (development described later) to either seal the plates or to make them of smaller porosity (to meet bubble pressure requirements for the porous UTC Power bipolar plates).

Because CVI treatment is an expensive process, it was desired to improve the product properties through compositional changes. Several investigations were performed to improve the materials.

Experiment 1

An experimental design focused around vacuum forming of materials was performed in a two-level fractional factorial design. The experimental variables investigated are shown below. Table 12.1 shows the individual composition experiments. The loaf materials were formed, cut to the sizes desired, pressed to consistent thickness, carbonized and CVI treated. The materials were cut to 2x2 coupons following carbonization. Bubble point was measured following carbonization, and bubble point and permeability were measured following each of the two 12-hour CVI cycles.

Also measured were material geometric dimensions and weight following each step of the process.

Independent Variables Investigated:

Table 12.2 shows the experimental plan for this investigation. Specifics of raw materials are not disclosed.

Table 12.1

Experiment	Binder Type	Binder Amount	Preform Thickness	Additive Amount	Binder (lbs)	Graphite (lbs)	Fiber (lbs)
1	A	15	0.120	0	0.6	0	3.4
2	B	15	0.120	15	0.6	0.6	2.8
3	A	30	0.120	15	1.2	0.6	2.2
4	B	30	0.120	0	1.2	0	2.8
5	A	15	0.150	15	0.6	0.6	2.8
6	B	15	0.150	0	0.6	0	3.4
7	A	30	0.150	0	1.2	0	2.8
8	B	30	0.150	15	1.2	0.6	2.2

Forming

Loafs were formed in total four pound batches, mixed with 100 gallons of water. The standard procedure was followed. Two loafs of each material were formed. Some materials did not form well. 50% yield was realized on experiments 2 and 8. Experiment #6 did not form well, and yielded no test results (0% yield). All of the poor-forming materials were made with the Durez 29217 phenolic material.

Pressing

The materials were pressed at PFCT, using 0.070 thick shim material. In general, materials formed with resin A and cut to 0.150 thickness yielded thickness near 0.080 thickness. Thinner-cut materials, and those formed with resin B yielded thickness near 0.070. The incompletely compressed materials probably yielded data that is influenced by the initial compression.

Carbonization

The materials were carbonized at PFCT in the lab vacuum furnace. A one-day cycle with maximum temperature of 1010°C was used. The materials were bound in a graphite fixture, held tight with graphite bolts. A layer of 1/8" graphite felt was used between the fixture and the adjacent experimental plate. It was found that the plates were stuck together lightly following carbonization. On mechanical release from one-another, the plates were shown to have warped somewhat. In addition, it was found that materials formed with resin A expanded in thickness significantly following carbonization. Those materials formed with resin B shrunk slightly. Table 2 shows this data. The material from experimental composition #8 was cut to approximately 5x5 before carbonization.

Table 2. Carbonization Data

Expt.	Resin	Wt. B4 (g)	Wt. After (g)	Wt. Loss (%)	Thk. B4 (in)	Thk. After (in)	Thk. Chg. (%)
1	A	95.0	87.1	8.3	0.071	0.084	+18.3
2	B	92.1	81.0	12.1	0.065	0.061	-6.2
3	A	109.1	91.0	16.7	0.071	0.078	+9.9
4	B	82.0	72.0	12.3	0.070	0.066	-5.7
5	A	111.9	103.2	7.8	0.077	0.086	+11.7
6	B	--	--	--	--	--	--
7	A	102.3	85.4	16.6	0.079	0.090	+13.9
8	B	32.1	28.2	12.3	0.068	0.064	-5.9

Expt.	After Pyrol Observatrions
1	Bow, ~3/8"
2	Twist, ~1/4"
3	Twist and Bow, ~1/4"
4	Light Twist, ~1/8"
5	Light Bow, ~1/16"
6	--
7	Bow, ~3/8"
8	Warp, ~1/4"

CVI Process

Following carbonization the materials were cut into 2x2 coupons for testing and CVI treatment. The materials were then measured for size and mass, and tested for bubble point. Two identical bubble point coupons were selected from each experimental sheet for CVI testing. In the CVI tests, one of each of the test materials was loaded near the base and near the top of the reaction zone in the CVI reactor. A standard CVI process was then run (peak temperature 1200°C, soak for 12 hours, methane flow 2100 cc/min, Argon flow 500 cc/min, pressure 5 torr), and the parts were tested for bubble point, perm, weight gain and dimensional change. The same materials were then run in the reactor for a second identical trial. Table 3 shows the run results.

It is interesting to note that the bottom-located samples (on average) gained less weight overall, but exhibited a higher measured bubblepoint. The differences may be attributed to slightly differing CVI conditions at the coupon locations (top and base of reaction zones). The samples at the top probably experience conditions that are slightly depleted in overall carbon, and may contain gases that are probably higher in average molecular weight.

Table 3 CVI Results

Expt.	BP aft PYRO	Location	Wgt Gain From CVI 1	Perm From CVI 1	BP From CVI 1	Wgt Gain from CVI 2	Total Wgt Gain	Perm From CVI 2	BP From CVI 2
1	12.5	top	72.47%	~1000+	19	31.26%	126.39%	150.58	26
1	12.5	bot	62.96%	~1000+	20	28.28%	109.05%	181.70	28
2	19.5	top	35.59%	236.14	32	15.33%	56.37%	10.48	55
2	19.5	bot	31.45%	192.57	34	13.94%	49.78%	8.90	59.5
3	17.5	top	44.17%	482.73	28	18.63%	71.02%	19.54	41.5
3	17.0	bot	44.86%	640.37	24.5	19.86%	73.63%	46.85	37
4	17.0	top	44.56%	775.42	23	21.83%	76.12%	108.58	32.5
4	17.0	bot	39.82%	614.65	26	19.25%	66.74%	70.32	39
5	20.0	top	52.85%	325.22	28.5	17.94%	80.27%	71.82	44
5	20.0	bot	49.27%	296.60	33	17.66%	75.63%	9.73	51.5
7	15.0	top	54.63%	1264.78	21	26.01%	94.85%	193.54	29
7	15.0	bot	48.20%	1051.64	22	23.32%	82.76%	140.65	32.5
8	26.5	top	24.27%	50.10	41.5	8.18%	34.44%	0.06	91
8	26.5	bot	22.34%	55.86	48	9.15%	33.53%	1.66	86

Statistical Results

Data analysis was performed on bubble point and permeability measurements to determine the influence of the independent variables in the study (resin type, resin amount, graphite amount, and before-pressing thickness). Averages and t-ratios were calculated, including variable-variable interactions. Results are shown in Table 4 below. For this set of data (average of 3 vs. an average of 4 – one data point missing due to poorly formed loaf #6), there are 5 degrees of freedom, leading to a critical t-ratio of 2.02 at 90% confidence, and 2.57 at 95% confidence. Only graphite powder addition was shown to influence the data with this level of confidence. However, through observation, resin type clearly had a strong influence on results, and material thickness is expected to influence results through material compaction. A surprising result was

the lack of significant influence by the resin content. Higher resin contents did show higher bubble point results, but not significantly so. High standard deviations probably attributed to the lower than expected t-ratios for some of the variables.

Variable-variable interactions were found to be non-significant.

From the study, it was clear that the resin B is preferred over resin A. The reasons for this include the fact that resin B acts like a thermoset material, and does not require mold cooling during pressing to remove (bringing the cycle time from 1.5 hours to less than 15 minutes per pressing), and because resin B induces shrinkage instead of expansion to the material thickness. Shrinkage is preferred as it may allow for better thickness control of the material throughout the process.

A simple linear model was developed based upon the data of this experimental design so that trends outside of the experimental regime could be approximated. A model was developed from carbonized bubble point data and from CVI 1 data using both graphite powder and material thickness variables. The resulting equations are shown below, using data from resin B resin (as this material is preferred for future use):

Carbonized:

$BP = 21 + 0.40(X_1-7.5) + 275(X_2-0.135)$

Where X_1 = the weight percent of graphite powder addition
X_2 = the pre-pressing material thickness

CVI 1 Base

$BP = 36 + 1.0(X_1-7.5) + 600(X_2-0.135)$
$PERM = 287.69 – 32.7(X_1-7.5)$

CVI 1 Top

$BP = 32.17 + 0.917(X_1-7.5) + 467(X_2-0.135)$
$PERM = 353.89 – 42.15(X_1-7.5)$

These models were used to project results out to thickness and graphite powder loadings beyond the trials investigated in this analysis. Non-linearity in the trends will limit the usefulness of these models, but they do provide for starting places for subsequent investigations. The carbonized results are particularly intriguing in that it may be possible to hit target properties with very little or no CVI treatment required. Permeability testing was performed for only one carbonized sample (#8, BP = 26.5, Perm = 294). Figure 1 shows a chart of material thickness vs. graphite powder content projected to achieve differing levels of material bubble point. Some of these target combinations could be experimented with to produce a material that is near target properties following the carbonization stage.

With the CVI'd materials, permeability was found to be a strong function of graphite powder loading only. The models were therefore made with only that parameter. Figure 2 shows a plot of material thickness and permeability vs. graphite powder content. Two curves are shown for each target bubble point – one for materials processed at the top of the CVI furnace, and one at

the base. The range between should produce materials within 10 points of the target throughout the furnace zone. The permeability curves (a function of only graphite powder loading) is overlaid to show how quickly this property falls off with increased graphite powder content. It would appear that non-permeable plates would be produced for graphite loadings much greater than 15% and 12 hours CVI processing time. However, this parameter is expected to be somewhat non-linear and tests would be needed to bear-out the predictions.

Another interesting feature is the bubble point and permeability relationship with the overall density of the material. Density was found to be a strong function of graphite powder addition. Less significant influences to the material density were binder type and initial material thickness. Figure 3 shows bubble point and permeability as a function of material density. Carbonized materials produce bubble points that appear to be very closely related to material density. Following CVI 1 and CVI 2, the relationship scatters somewhat due to the complex nature of the CVI process, but still appears to follow the general trends well. Permeability falls off very quickly with increasing density. Open porosity appears to close off quickly as the density of the material surpasses 1.5 g/cc.

Conclusion:

The study found that graphite powder loading has the most significant influence on material properties (bubble point and permeability). Of the two resins investigated, resin B was greatly preferred for its capability to be pressed and removed from the press at temperature, and because it induced material shrinkage instead of expansion (thought to be more controllable in the thermal processes used). An undesirable feature of the resin B resin in comparison to resin A is the fact that this resin does not provide high green handling and initial machining strength. A consequence of that was noted in trying to produce material #6 at 15% resin addition.

Models were developed that point to future compositions for experimentation, using graphite powder loading and material thickness as key variables. Maps of composition were generated to point to desired properties after both carbonization and one CVI treatment cycle.

The density of the material appears to correlate well the bubble point and permeability. For carbonized materials, the bubble point may be controlled with good accuracy by controlling the density of the part. The CVI process tends to scatter the correlation somewhat, but still demonstrates basic trends with the material density. Permeability is less correlated with density, and shows extremely rapid fall off as the density increases.

Table 4. Statistical Averages and T-ratios

	Pyro BP	CVI 1 Base BP	CVI 1 Top BP	CVI 1 Base Perm	CVI 1 Top Perm	CVI 2 Base BP	CVI 2 Top BP	CVI 2 Base Perm	CVI 2 Top Perm
Resin A	16.3	24.9	24.1	747	775	37.3	35.1	94.7	109
Resin B	21.0	36.0	32.2	288	354	61.5	59.5	27.0	39.7
T-ratio	1.56	1.75	1.52	1.83	1.33	1.88	1.60	1.34	1.27
15% resin	17.3	29.0	26.5	496	529	46.3	41.7	66.8	77.6
30% resin	19.0	30.1	28.4	591	643	48.6	48.5	64.9	80.4
T-ratio	0.47	0.14	0.30	0.29	0.31	0.14	0.37	0.03	0.04
No powder	14.8	22.7	21	889	1013	33.2	29.2	131	151
15% powder	20.9	34.9	32.5	296	280	58.5	57.9	16.8	25.5
T-ratio	2.39	2.05	3.01	3.16	4.60	2.03	2.11	3.83	4.50

0.120 thick 0.150 thick T-ratio	16.6 20.5 1.19	26.4 34.3 1.10	25.5 30.3 0.80	611.9 468 0.45	624 556 0.19	40.9 56.7 1.03	38.8 54.7 0.92	76.9 50.7 0.45	72.3 88.5 0.26
Resin/Amount & Powder/thk T-ratio	0.47	0.64	0.16	0.43	0.32	0.49	0.35	0.01	0.13
Resin/powder & Amt/thk T-ratio	0.06	0.47	0.42	0.21	0.32	0.65	0.73	0.86	0.41
Resin/thk $ Amt/powder T-ratio	0.25	0.22	0.47	0.08	0.40	0.24	0.61	0.31	0.65

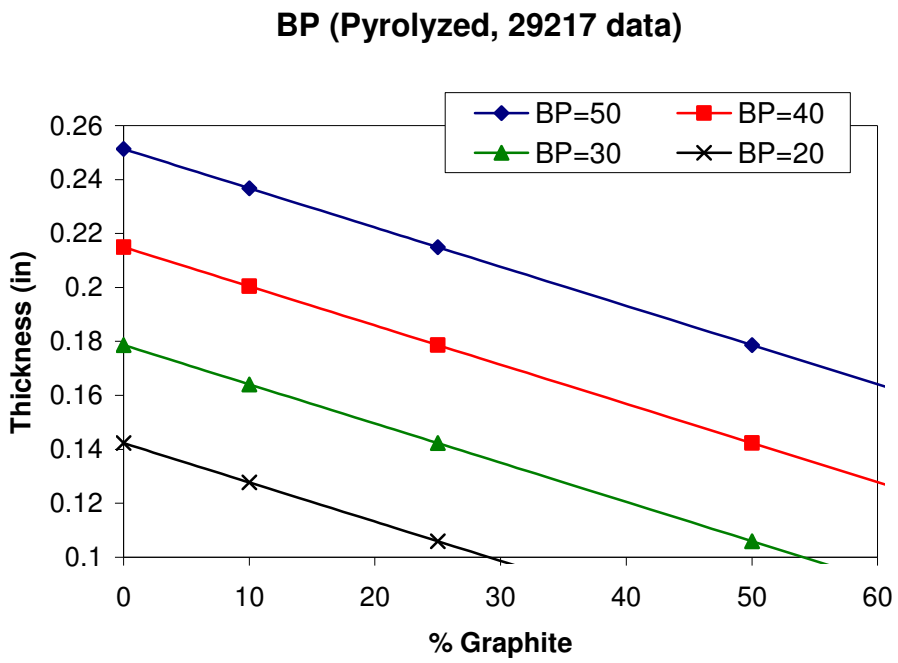

Figure 2. Model predictions for carbonized materials.

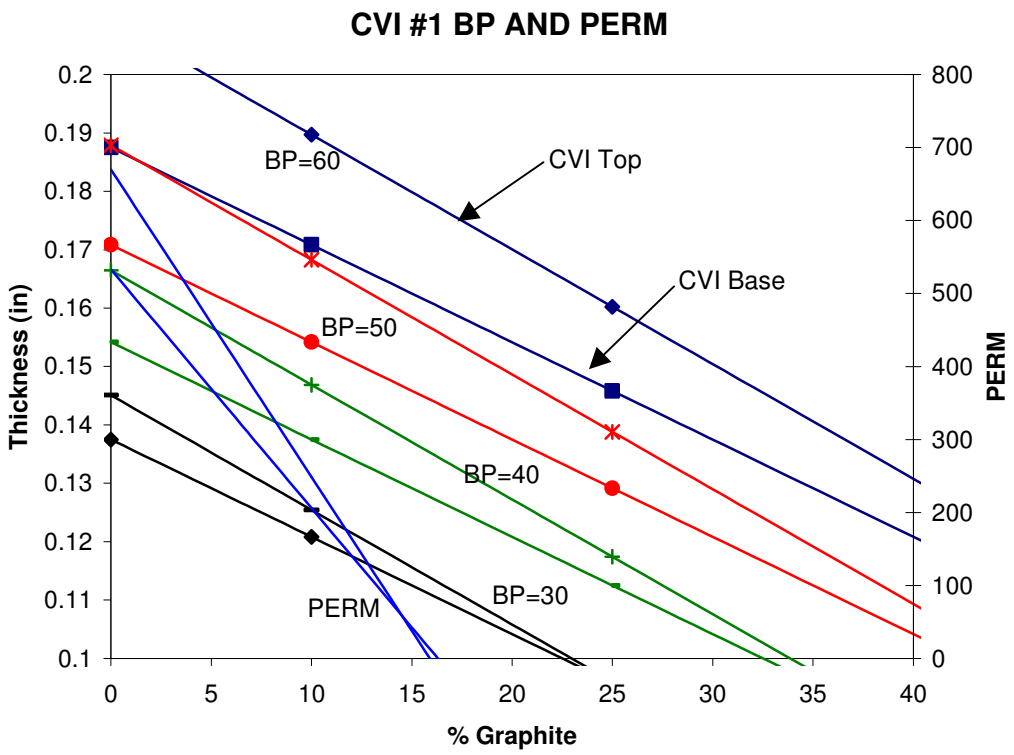

Figure 3. Model predictions for materials CVI treated for 12 hours. Permeability is shown as a function of graphite loading only.

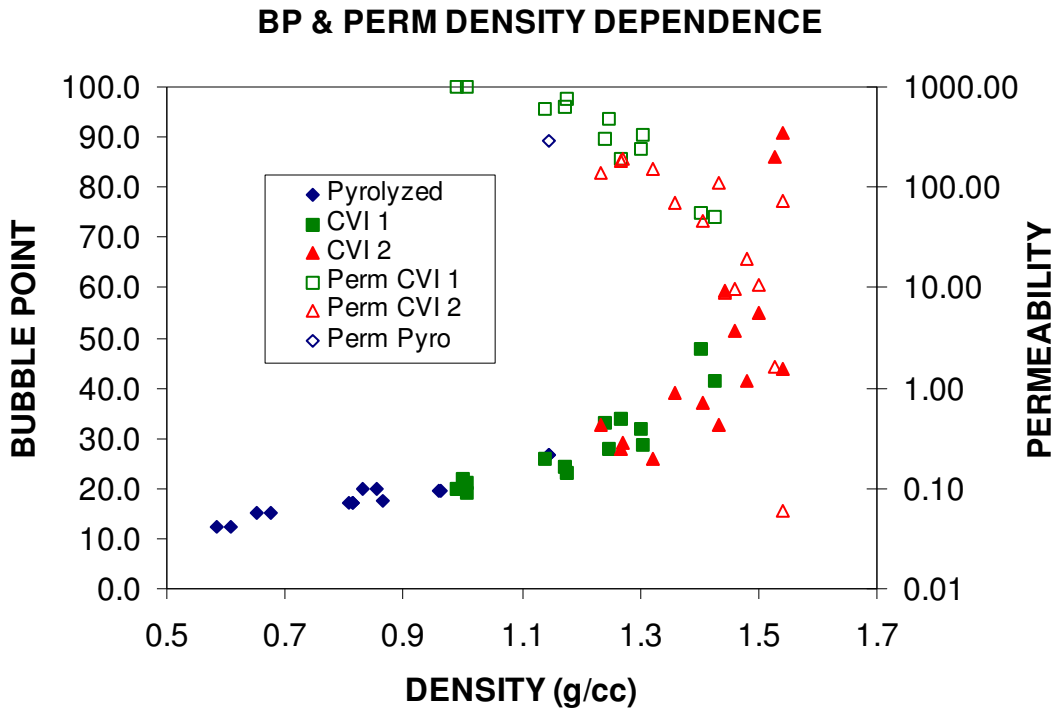

Figure 4. Bubble point and permeability dependence on density. Carbonized materials follow density closely. CVI processes tend to scatter the relationship somewhat. Permeability falls off very quickly over densities of about 1.5 g/cc.

Experiment 2

An experimental design focused around vacuum forming of materials was performed in a two-level fractional factorial design. The experimental variables investigated are shown below. Table 1 shows the individual composition experiments. The loaf materials were formed, cut to the sizes desired, pressed to consistent thickness, pressed with the anode flow pattern, pyrolyzed and CVI treated. The materials were cut to 2x2 and 2 x 6 coupons following carbonization. Bubble point, permeability, strength and conductivity was measured following carbonization and CVI treatment. The CVI process was run under conditions of 1200°C, 5 torr for 4 hours duration.

Also measured were material geometric dimensions and weight following each step of the process.

Independent Variables Investigated:

Graphite Powder Amount:	
Graphite Powder Size:	Fine and coarse
Carbon Fiber Type:	Fiber A and Fiber B
Forming Rate:	1 gpm, 5 gpm

Table 5

Experiment	Powder Amount	Powder Size	Fiber Type	Forming Rate
1	1	20	A	1
2	2	20	A	5
3	1	-300	A	5
4	2	-300	A	1
5	1	20	B	5
6	2	20	B	1
7	1	-300	B	1
8	2	-300	B	5

Forming

Loafs were formed in total four pound batches, mixed with 100 gallons of water. The standard procedure was followed. Some materials formed better than others. Materials using fine powder size required careful agitation in order to fully wet the powder materials. At higher content, there tended to be a cake residue of the powders on top of the loaf (typically about 1/8 of the total powder in this residue form). Materials using high powder loadings also tended to be much softer and weaker. Significant abrasion could be achieved with handling. The as-machined plates had to be handled with care.

Each loaf was cut to an equal number of materials sliced to 0.150 and 0.120 thickness. The 0.150 materials were used for flat pressing, while the 0.120 materials were used for flow field embossing.

Pressing

The materials were pressed at PFCT, using 0.070 thick shim material. All of the flat-pressed materials compressed easily to the shim thickness under maximum press tonnage (about 115 tons). Some of the embossed materials did not press completely to the shim thickness. These were generally materials made with coarse powders, as will be shown in the final data analysis below.

Carbonization

The materials were pyrolyzed at PFCT in the lab vacuum furnace. A four-day cycle with maximum temperature of 1300°C was used. The materials were stacked and weighted with graphite plates and blocks. Stack heights were 3-4 plates, separated by graphite plates. Flat pressed materials generally stayed flat, while embossed materials retained slight warpage (typ. ~ ¼" warpage). Uniform material shrinkage in thickness following carbonization was not found in this study, as it was for the same resin in Composition #1. A mixture of slight shrinkage to material expansion was found.

Table 6. Carbonization Data

Expt.	Wt. B4 (g)	Wt. After (g)	Wt. Loss (%)	Thk. B4 (in)	Thk. After (in)	Thk. Chg. (%)	Warpage Observations
1	93.3	81.7	12.4	0.066	0.068	2.5	Light, ~1/8"
2	104.8	92.5	11.7	0.066	0.064	-1.9	Light, ~1/8"

3	90.9	79.6	12.4	0.071	0.069	-1.8	Light, ~1/8”
4	110	97.6	11.3	0.075	0.069	-8.0	Twist, ~1/4”
5	87.5	76.5	12.6	0.069	0.068	-2.2	Twist, ~1/4”
6	105.6	92.5	12.4	0.068	0.065	-3.9	Light, ~1/8”
7	98.2	85.5	12.9	0.074	0.073	-1.2	Warp, ~1/4”
8	102.4	92.3	9.9	0.073	0.072	-1.5	Bow, ~1/4”

Carbonization Properties

Following carbonization the materials were cut into 2x2 and 2x6 coupons for testing and CVI treatment. The materials were then measured for size and mass, and tested for bubble point, permeability, strength and electrical conductivity in the pyrolyzed state. Results showed that bubble points were either near or beyond the UTCFC target for both the flat and the embossed materials. As a result, it was decided that CVI operation would be performed for a very short duration to examine the influence of the process to enhance material strength properties. A standard CVI process was then run (peak temperature 1200°C, soak for 4 hours, methane flow 2100 cc/min, Argon flow 500 cc/min, pressure 5 torr), and the parts were tested for bubble point, perm, weight gain and dimensional change.

Table 3 shows results from the pyrolyzed material testing.

Table 7 Carbonization Results

Expt.	Flat or Pattern	Simple Geometry Density (g/cc)	Bubble Point	Per m	Flexure Strength (psi)	Flexibility (%)	Simple Geometry Conductivity (S/cm)
1	Flat	1.08	32	182	5164	3.4	269
1	Pattern	0.80	38	76	1221	3.2	154
2	Flat	1.33	70	11.2	7077	4.3	527
2	Pattern	0.96	>100	0	997	3.1	311
3	Flat	1.12	44	130	3631	2.9	220
3	Pattern	0.77	50	69	1032	3.3	176
4	Flat	1.23	84	2.2	5225	4.0	373
4	Pattern	0.90	94	3.4	1269	3.1	204
5	Flat	0.97	32	327	2910	3.0	165
5	Pattern	0.75	38	153	862	3.4	126
6	Flat	1.23	76	19.5	5226	3.9	371
6	Pattern	0.94	>100	0.6	1684	4.8	259
7	Flat	1.05	38	269	5776	3.6	221
7	Pattern	0.75	38	216	436	1.3	168
8	Flat	1.21	92	11.2	5771	5.1	348
8	Pattern	0.86	82	9.7	522	2.4	177

Statistical Results

Data analysis was performed on the measurements to determine the influence of the independent variables in the study (graphite powder amount, graphite powder size, fiber type,

and forming rate). Averages and t-ratios were calculated, including variable-variable interactions. Results are shown in Table 4 below for flat plates. For this set of data (average of 4 vs. an average of 4), there are 6 degrees of freedom, leading to a critical t-ratio of 1.94 at 90% confidence, and 2.45 at 95% confidence. Only graphite powder addition was shown to influence the data with this high level of confidence. None of the other variables in the experimental design influenced the material properties to any significant extent, and no variable-variable interactions were found to be significant. As in composition study #1, higher levels of graphite powder addition enhance material properties significantly. Some of the benefits include higher densities achieved on initial compaction leading to higher strength, higher electrical conductivity, and the capability of meeting target bubble point prior to CVI treatment. Results for the embossed materials were similar to the flats, except that the bubble points were generally higher (indicating greater material compression in the patterned regions). Embossed material strengths, calculated based upon the simple geometry of the plates seem to be low, however, a complete analysis of the actual moment of inertia of the complex actual geometry of the plate was not done. The material strength is expected to be the same as that measured for the flat materials.

Density Dependence

As with the previous composition investigation, most material properties can be well correlated with net material density. Figures 1, 2, and 3 show the density dependence of bubble point/permeability, electrical conductivity and strength respectively. Both pyrolyzed and CVI'd properties are shown in the figures. An important note is that CVI'd material strengths are generally higher for the same material density than as pyrolyzed.

Pressing Tonnage and Characteristics

From earlier testing and observations, it is apparent that the pressure required to compress graphite loaded materials to a given thickness reduces with increased graphite loading. Further, highly graphite loaded materials require less overall compression to achieve targeted BP/perm characteristics (i.e., can start with a thinner substrate and still achieve properties with highly loaded graphite compositions). These characteristics add up to successful material molding at overall lower pressures with highly graphite-loaded materials.

A screening study was done to examine the pressure required to compress the experimental materials (not all of the compositions were tested, however). Coupons approximately 4"x4" were cut from the materials and pressed to different pressure setpoints without shims. The resulting compression of the material and the tonnage applied were assembled and charted to derive the materials compression characteristics. Figure 4 shows these results in comparison to some materials from Comp. 1 DOE. As the graphite loading in the material increases, higher final material densities are achieved at lower pressing pressures. This implies that the compression applied by the press goes into compacting the materials tightly, and that there is little resistance to this compaction when graphite powder loadings are increased. The data shows that successful molding of the materials to the final desired material densities and porosity properties can be easily achieved with highly loaded graphite materials at loadings of less than 100 tons. It is also possible that less warpage issues will be present when less material compression is applied.

Wetability

A very simple and fast test was done to determine the materials as-pyrolyzed wetting characteristics. Both flat and embossed materials were tested. A droplet was placed on the material and timed for the droplets full soak into the material. Results show that high graphite loadings are worse for wetability. At low loadings, droplets soak into the material in less than 30 seconds (typ.). High graphite loaded materials hold the droplets on the surface for 10 minutes or longer.

The differences could have to do with the average pore size of the material or the nature of the material. Materials with lower net density and lower bubble points (avg. 1.06, low graphite powder addition) tended to pull the droplets in quickly, while materials with high density (avg. 1.25, high graphite powder addition) tended to retain the droplet on the surface. It is unknown if the material type or its net structure influences drop absorption more.

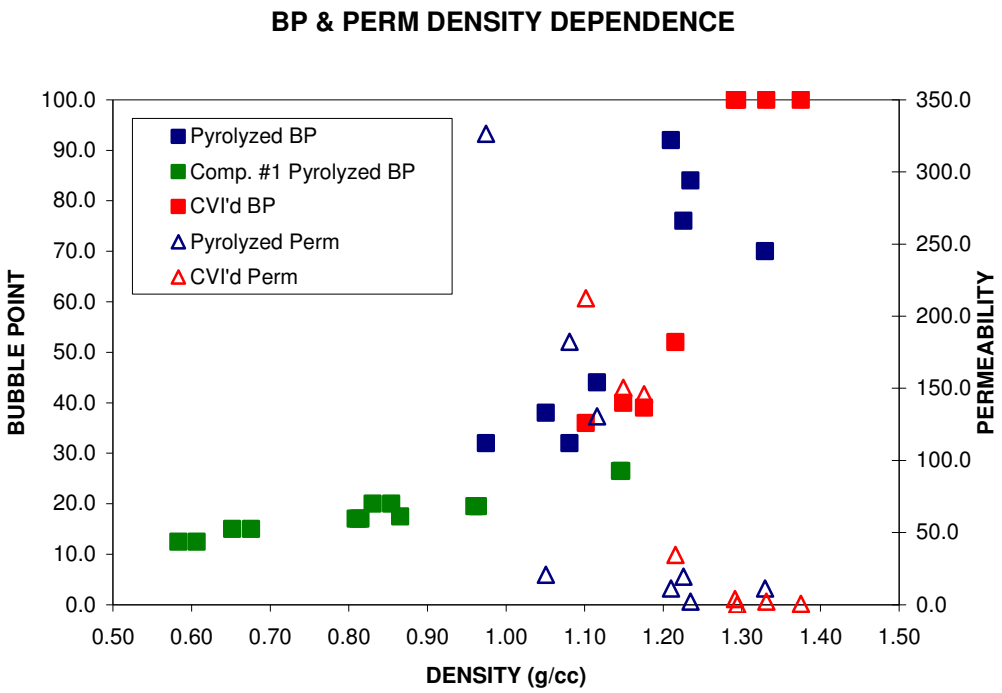

Figure 1. Bubble point and permeability material density dependence.

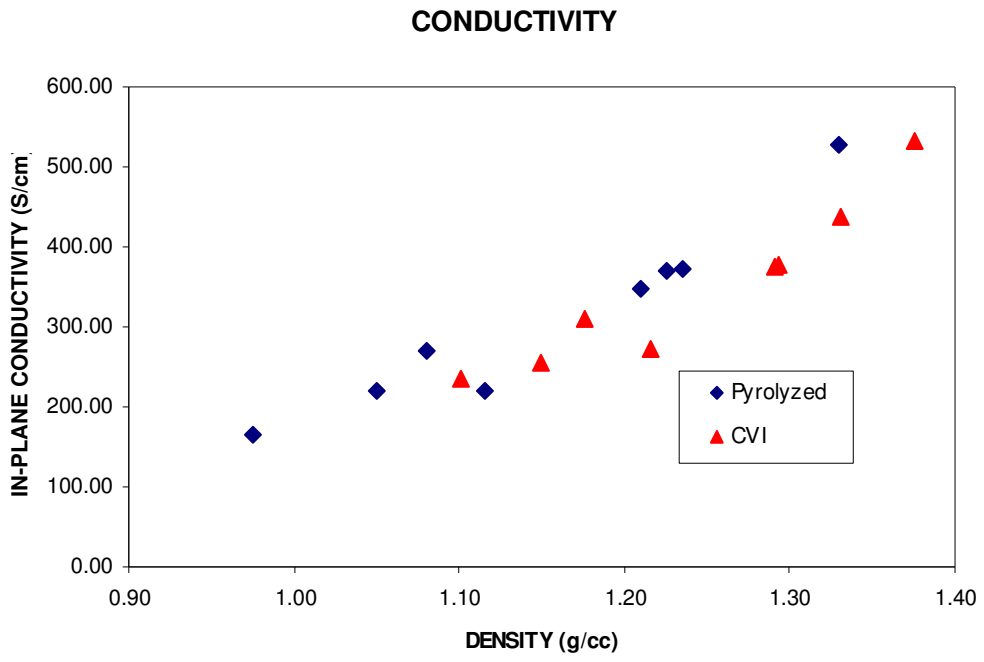

Figure 2. In-plane material conductivity density dependence.

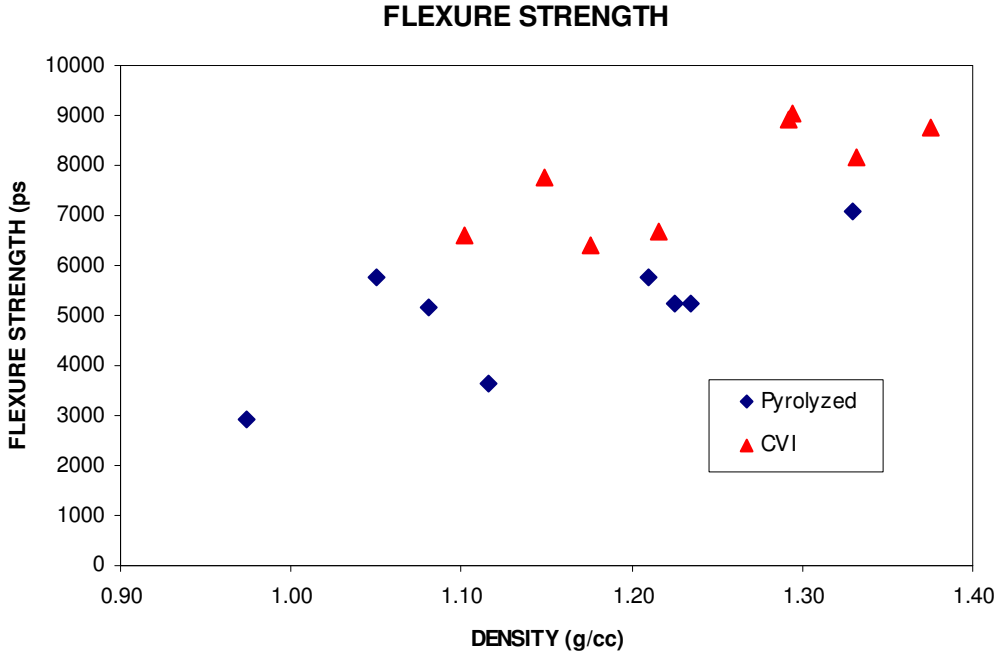

Figure 3. Fluexure strength density dependence. CVI process enhances material strength at equivalent material density.

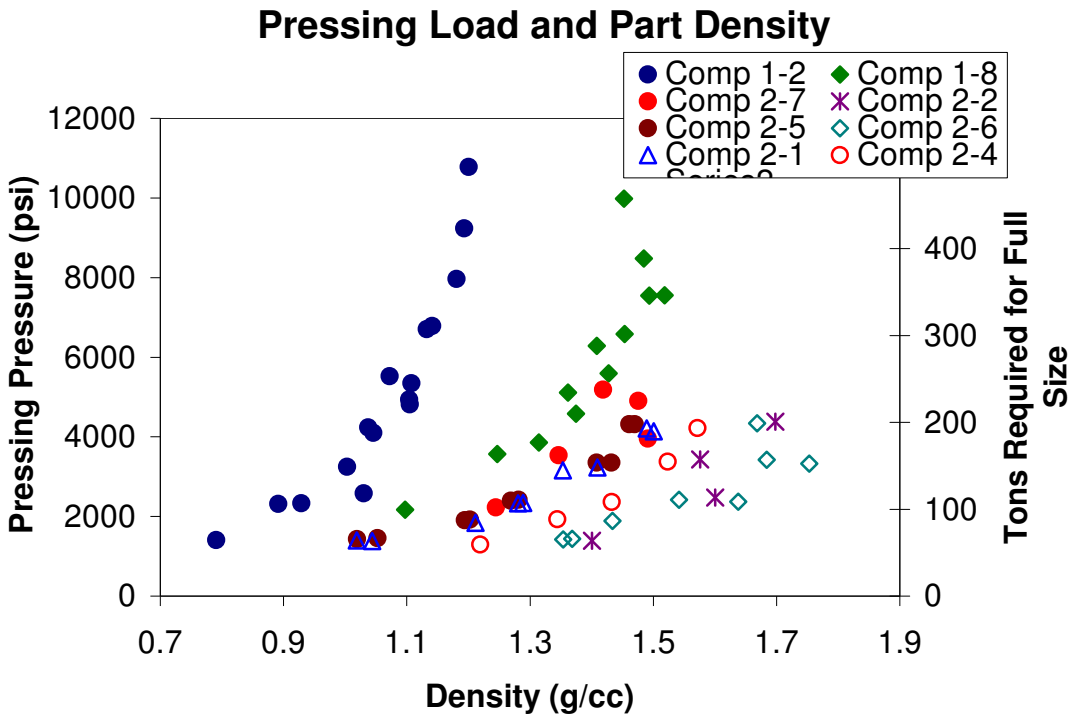

Figure 4. Material pressing response and tonnage required for compressing full size materials. Higher graphite loaded materials achieve higher final densities at lower compression pressures.

Conclusion:

The study found that graphite powder loading has the most significant influence on material properties (bubble point, permeability, conductivity and strength). None of the other variables influenced the results to statistically significant degrees. No variable interactions were found to be significant. Results point to the use of higher graphite powder additions to improve all material properties, and to enable hitting target properties with no CVI treatment and with less overall compression during the pressing stage of material manufacture.

Embossed material manufacture was successful. In general, the embossed materials exhibited somewhat higher bubble points and somewhat lower permeabilities than their flat counterparts. Warpage of the embossed plates was minimal, but remains a significant issue toward the manufacture of embossed water transfer plates.

Models were developed that point to future compositions for experimentation, using graphite powder loading and material thickness as key variables. Trends point to the continued use of higher graphite powder loadings, although this begins to introduce practical difficulties in material forming. Forming with high powder loadings and with (in particular) the smaller particle size powder yielded a loose cake of powders on top of the loaf material. Green loafs were also weak and easily abraded at higher powder loadings.

The density of the material appears to correlate well the bubble point, permeability, conductivity and strength. As discovered in the first composition study, bubble point and permeability may be controlled by controlling the density of the part through compression and carbonization.

The final CVI treatment in this program was unnecessary to achieve target regions of bubble point for most of the composition materials. As a result, the process duration was minimized (4 hours) in this study. One significant advantage to the final material properties that the CVI process offers is a boost to the strength of the material (as can be seen in Fig. 6). Average strengths of CVI'd materials were higher than pyrolyzed materials at equivalent density.

A pressing characteristics study was also done as part of this experimental investigation. It was found that lower compression pressures are required to compact highly graphite-loaded materials to a given density. Their compaction is easier than with highly fiber-loaded materials. This characteristic allows for the prediction of the press tonnage required to compress a full size plate to final thickness, and may allow for less plate stress retention which could reflect back to more desirable plate flatness characteristics.

A wetability test was performed to examine the capability of the materials to absorb water with no further surface treatment. Pyrolyzed only materials were tested. Results showed that the materials formed with high graphite loadings retained droplets on the surface more readily than those formed with low graphite powder loadings. Low graphite addition at the compression ratios examined in this program improves wetting characteristics. The influence of net compression is not known, but it is expected that the materials formed with higher graphite powder additions will improve in wetability somewhat when not overcompressed.

Compositional Variables Experiments Conclusion

The two compositional experimental studies showed that the addition of graphite powder significantly improved the properties of the bipolar plates for both porous and for sealed bipolar plates. For porous bipolar plates, the studies proved that the bubble pressure and permeability properties could be simultaneously achieved in the process without the need for Chemical Vapor Infiltration. For the UTC Power product, this finding significantly improves the cost effectiveness of the materials and process as follows:

- Use of significantly lower cost raw materials
- Elimination of an expensive process step
- Improves process throughput as CVI bottleneck step is eliminated

Further product development and compositional optimization occurred later in this project, and are detailed in later sections.

13.0 Experimental Design on Pressing Variables

A key process step is pressing of the product where the green sheet material is molded into a net-shape product. The molding of the product occurs through both an initial embossing of the green plate, followed by resin melting and product flow. After a short time under heat and pressure, the resin begins to crosslink and form the final pressed structure of the part. In the pressing process, the low density (~0.6 g/cc) green part is consolidated to a carbon/polymer composite material with a density around 1.25 g/cc, depending on the design of the part.

The initial pressing conditions were defined by the resin supplier for platen temperature and material hold duration. The first experimental investigations of the pressing parameters were performed in conjunction with a material study, designed to improve the achievement of bubble pressure in the product.

DEGAS INSTALLATION AND TRIALS

Introduction

This document will describe the process of press de-gas installation and the results of initial trials.

Installation

Press de-gas operation required significant electrical modifications to enable the safe, reliable operation of the de-gas cycle. The press was taken down on Tuesday, July 22 to begin the modifications. Modifications were documented carefully so that press operation could be re-established to normal conditions. The press was maintained in working order between modification shifts (we used first shift for modifications) so that second shift can continue with pressing production activities. On Friday, July 25, the press was down until operational in the de-gas mode. A PLC was installed to facilitate modifications without introducing unsafe conditions. Saturday afternoon press modifications were complete.

Initial Trials

Sunday morning (July 27) de-gas trials were initiated. Attempts were made to operate under the following conditions:

Press Temperature:	185°C
Shim Size	0.080”
Initial Clamp Duration	5 sec
Open Time	60 sec
Re-clamp Time	2 min

When this set of conditions was set, operation resulted in exploded parts upon release of clamp pressure to begin the degas portion of the cycle. Conditions were evaluated to map out the range of operating conditions that could yield satisfactory results. At the same time, moisture levels within the parts were evaluated.

It was found that for initial clamp times greater than 15 seconds, un-damaged parts could be obtained with a press temperature setpoint of 185°C. The following process conditions were evaluated with the noted observations.

Temperature (°C)	Shim Size (in)	Clamp Time (sec)	Plate Condition	Observations
185	0.080	5	Normal	Violent Explosion
185	0.080	4	Normal	Violent Explosion

185	0.080	3	Normal	Violent Explosion
185	0.080	10	Normal	Moderate Explosion
185	0.080	15	Normal	Plate Damage (1 of 2)
185	0.080	20	Normal	No Damage
175	0.080	5	Normal	Violent Explosion
175	0.080	5	Dried in Vac Oven	Violent Explosion
175	0.080	3	Normal	Violent Explosion
175	0.080	20	Normal	Plate Damage (Bulging)
175	0.080	15	Normal	Violent Explosion
165	0.080	5	Normal	Violent Explosion
165	0.080	3	Normal	Violent Explosion
155	0.080	3	Normal	Mild Explosion
145	0.080	3	Normal	Part Damage (Bulging)
185	0.082	10	Normal	No Damage
185	0.082	5	Normal	No Damage
185	0.081	10	Normal	No Damage
185	0.081	5	Normal	No Damage
185	0.081	5	Normal (Repeat)	No Damage (Very Mild Bulging)
185	0.080	10	Normal (Repeat)	Plate Damage (Mild Bulging)
185	0.080	5	Normal (Repeat)	Explosion
185	0.080	10	Normal (Repeat)	Plate Damage (Mild Bulging)
185	0.080	10	Normal (Repeat)	Plate Damage (Bulging)
185	0.080	10	Normal (Repeat)	Explosion (Plate Ripping)

From the conditions investigated, it was apparent that the target shim size (0.080, current production shim producing average density ~1.22 g/cc) could not be used effectively with a degas cycle, unless initial clamp times of 20 seconds could be used. Unfortunately, this duration of time defeats the purpose of a degas cycle. Experts in the pressing industry and at UTCFC have indicated that early degas sequences are more beneficial to successful degassing of parts. At 20 seconds, the part resin has completely melted and has partially cured.

Degas Open Time

Experiments were run to evaluate the impact of degas open time of final part thickness. Production target thickness is 1.98 mm following the pressing operation. This thickness is achieved (with normal variation in the process) using shims of 0.080” thickness. Moving to thicker shims moves the average thickness target up to 2.01 mm (the part tends to shrink slightly from the set shim size). Measurements were taken using degas times of 30 and 60 seconds, with the following results:

Temperature (°C)	Shim Size (in)	Clamp Time (sec)	Open Time (sec)	Avg. Thickness (mm)	Observations
185	0.081	10	60	2.052	No Damage
185	0.081	5	60	2.053	No Damage
185	0.081	5	30	2.035	No Damage
185	0.080	10	60	2.012	Plate Damage (Mild Bulging)

185	0.080	10	30	1.990	Plate Damage (Bulging)

Based upon the results, it is apparent that clamp open time impacts pressed plate thickness. Further, because it is not possible to use shims of 0.080" thickness due to significant plate damage concerns, it was clear that a shorter clamp open time must be utilized to keep part thickness down. At the present time, production target thickness is 1.98 mm, which is achieved using no degas and a shim size of 0.080", yielding an average part density of 1.22 g/cc, and centering the Bubble Pressure rejects between the high and low limits. Going with a shim size of 0.081" will move the average density to near 1.20 g/cc, pushing more bubble pressure rejects to the low side, and most likely increasing the quantity of bubble pressure rejects altogether. Some historical data:

Week Ending	Shim Size Used	Low BP Rejects	High BP Rejects	Total BP Rejects
7/12	0.082	18.3%	2.5%	21%
7/19	0.080	9.8%	5.5%	15%
7/26	0.080	10.8%	1.9%	13%

Moving to thicker shims will drive up the percentage of bubble point rejects, unless the impact of the degas operation is significant enough to tighten the bubble point distribution.

Pressing Rejects

One hundred plates were pressed with the degas cycle defined above. Observations showed that about 10% of the plates pressed in this manner exhibited some type of reject-able damage (significant part bulging, moderate part explosions, etc.). The current press reject rate is low (< 1%) using no degas cycles. These parts are in carbonization, and data will be collected on Wednesday, July 30. These parts will yield information regarding part bubble pressure and density variation. A number of parts will also be cut for coupon testing in original and skim-cut thickness (0.025").

Part Moisture

Moisture measurements were made of parts waiting for pressing. Because of the press down-time experienced waiting for press degas modifications, some parts were waiting in their bags for several days. Parts 5-6 days old were collected and dried in a vacuum oven for up to 4 hours at 50°C (operating pressure about 200 microns mercury). Part moisture ranged from 0.35 to 0.47% by weight. Weight loss was measured at about 1 hour intervals, and was stable after two hours under heat and vacuum. Parts pressed dry showed similar explosion characteristics as parts pressed without drying under similar degas conditions. Additional investigation is required to determine if degas conditions can be optimized by better controlling the moisture in the parts, but the moisture levels in the parts is very low. Additional measurements are being taken to evaluate the propensity of parts to absorb ambient moisture when exposed to the plant environment for extended periods of time.

Recommendations

It is recommended that the test parts be run through testing to evaluate their properties and variation in properties. Skim cut samples will be taken to evaluate thin section bubble pressure

and density compared to non skim-cut parts. Parts taken from standard pressing conditions will be tested in the same way as a basis for comparison. PFCT would like to wait for these results before proceeding with the above degas procedure so that we can evaluate the impact of this process on net product yield and quality improvement.

14.0 Experimental Design on Vapor Infiltration Variables

At the start of this project, it was envisioned that the Chemical Vapor Infiltration process would be a fully integral part of our bipolar plate manufacturing process. However, after initial materials development results showed that UTC Power porous plate properties could be obtained without the expensive CVI treatment, CVI processing was investigated for the purposes of sealing the surface against hydrogen permeability for sealed bipolar plate applications. Investigations were run to identify the key process variables that control the rate and location of carbon deposition, and the quality of the hydrogen seal.

Experiment 1

A Design of Experiments was drafted to optimize and to help broaden our understanding of the CVD process. It was executed according to plan during the months of February and March. This report contains the plan, execution, observations, and conclusions of that DoE.

Current State

Under the 'current state' conditions at which CVD is normally performed, the control of the furnace vacuum level is entirely dependant upon the capacity of the vacuum pumps due to the volume of gas being introduced into the chamber, coupled with the pressure set-point. Under those conditions, the butterfly (controlling) valve opens 100% and the pumps are only able to maintain a chamber pressure. One of the objectives of this DoE was to identify parameters under which the flow is not overbearing on the pumps and the butterfly valve can 'control' the chamber pressure.

At present, the above parameters are run for six hours. Every hour, the CH4 is turned off for 15 minutes to 'clean out' the system. (This pulsing was carried over from the small reactor where the system was much dirtier after each run without it) A 6-hour trial run without the pulses, showed a minimal increase in soot and a questionable coating. (one plate very little coating, the other plate, same as usual). It is unknown whether the pulses help significantly with sooting on the large reactor.

Additionally, micrographs of parts processed under current conditions reveal a thin black layer in between the pulse coatings. (Each pulse is recognizable under a microscope. E.g. a 6 pulse run will have 6 layers) The plate from the trial run without pulses showed no black layer. It is thought that some sooting is occurring during or near the 15 minute breaks.

Input

Constant:

Total Gas Flow	.5 scfm
Process Time	3 hours
Part density	GAPC = 1.13 – 1.20 g/cm3 (approx.)

S500 = 1.23-1.24 g/cm3

Variable:	+	-
Temp	1350	1450
Pulse	yes	no
Pressure	5 torr	10 torr
Ratio (Ar:CH4)	3:1	1:3

Accounting for gas flow of .5 scfm, the gas flows (scfm) were .375:.125 (3:1) and .125:.375 (1:3)

Design

A two-level design was selected. Four variables in eight experiments should yield results in which main effects are free of interactions and interactions are confounded with each other in pairs: 12=34 13=24 14=23

See Figure 1.

1	-	-	-	-
2	+	-	-	+
3	-	+	-	+
4	+	+	-	-
5	-	-	+	+
6	+	-	+	-
7	-	+	+	-
8	+	+	+	+

Fig. 1 Two-level, four variable, eight experiments – design matrix

Experiments

Fig. 2. Four variables, eight experiments (Exp 1 and 8 switched from actual matrix design)

	1	**2**	**3**	**4**	**5**	**6**	**7**	**8**
Temp	1350	1350	1450	1350	1450	1350	1450	1450
Pulse	Pulses	No Pulses	Pulses	Pulses	No Pulses	No Pulses	Pulses	No Pulses
Pressure	5 torr	10 torr	10 torr	10 torr	5 torr	5 torr	5 torr	10 torr
Ratio	3:1	3:1	3:1	1:3	3:1	1:3	1:3	1:3

The experiments were randomized to eliminate possible extraneous variables associated with time. The random order selected is: 1, 5, 2, 7, 3, 8, 6, 4.

Material & Loading Configuration

Each experiment contained 5 GAPC parts (windows not cut out) and 20 S500 parts. They were configured in the furnace as shown in Figure 3.

Of the 20 S500 parts, three were cut into the pattern shown in Figure 4 prior to the run, for hydrogen permeability testing afterwards. These three parts (numbered 1, 10, & 20) were located in positions 2, 12, and 24.

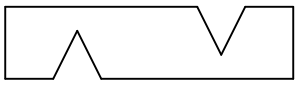

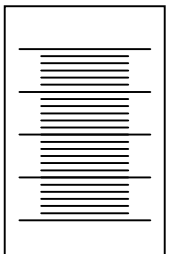

Fig. 3 Material configuration in furnace. Long lines indicate GAPC parts, shorter, S500

Fig. 4 Cut part for Hydrogen Perm testing.

Tracking

The location and orientation of each plate was critical to the data collection and analysis, so each plate was numbered sequentially for each experiment in an E-# pattern, where E = the experiment number and # = the plate number 1 through 20. For example, a S500 part from experiment 4 might be "4-16". This number was etched into the part in the top right corner. Special care was taken to ensure that the plates were loaded with the scribed number at the top right, facing the front of the furnace. The GAPC parts used in this DoE were numbered the same with the exception of the addition of the letter "G" before the plate number. A GAPC plate, then, would be numbered "4-G3", for example. These numbers were also etched into the plates and the plates were loaded such that the numbering was in the top right corner of the part and faced the front of the furnace. Plates were loaded identically for all eight experiments without exception.

After each experiment, samples were taken from the GAPC parts in a domino five pattern (four corners and center) to be polished. (25 samples per run) The samples were named according to the plate they were removed from and their location in the plate (TL=Top Left, TR=Top Right, BL=Bottom Left, BR=Bottom Right, & C=Center). E.g. The top left sample from the 3rd plate in experiment 6 would be "6-G3-TL".

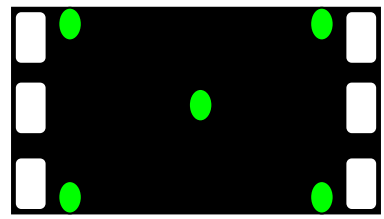

Fig. 5 Configuration of sampling from GAPC plates

Output

The following is a brief breakdown of the measureables:

- Weight gain (requires before and after weight)
- Thickness increase (measured before and after on Alanjack)
- Coating thickness (microscope)
- Presence of soot layer (microscope)
- Hydrogen permeability (three pre-cut samples)
- XRD
- Furnace conditions during and after the run were documented (pressure trace, soot collected on exhaust filter cartridges, etc).

Procedure

Before run:

1. Record weights on all plates and 6 thickness measurements on all S500 plates (Alanjack).
2. Load plates into furnace according to configuration seen in Fig.3 and with numbering beginning at G1 and 1 at the front of the furnace and ending with 20 and G5 at the back.
3. Begin run

During run:

1. Monitor pressure trace, butterfly valve position, and ensure temperature and flow set-points are maintained.

After run:

1. Once the furnace has cooled to at least 200ºC, crack open the door and allow to cool to at least 100ºC.
2. While cooling, review pressure trace and document differential pressure readings on Run Summary.

3. Fully open door and visually inspect inner and outer chamber walls for excessive soot.
4. Unload plates, verifying that each plate was loaded in proper orientation.
5. Inspect plates and make notes on Run Summary regarding appearance and carbon build-up if any (rate carbon build-up on 1-5 scale).
6. Disassemble the exhaust manifold consisting of the large U-pipe and the filter chamber.
7. Remove filter cartridges and visually inspect, rating soot build-up on a 1-5 scale.
8. Clean filters (vacuum then soak and wash in acetone bath) and reassemble exhaust manifold.
9. Using a mirror and flashlight, visually inspect chamber exhaust tubes for excessive carbon build-up. Remove and clean if necessary.
10. Using the mirror and flashlight visually inspect ceramic diffusion plates for carbon build-up or plugging. Replace if necessary.
11. Record weights on all plates and 6 thickness measurements on all S500 plates (Alanjack).
12. Place all plates in large Ziploc bag along with the Run Summary.
13. Acquire plate set for next experiment and repeat all of the above.
14. Samples for micrographs and XRD cut one experiment at a time, mounted and polished as time permits throughout course of DoE.

Samples for Micrographs

Samples for micrographs were cut according to the detail above and mounted five samples to a mount. Since each plate had five samples, the one mount contained all the samples for one plate. Each experiment then had five mounts. The samples were mounted in the following order: TL, TR, BL, BR, C. The direction of this order was easily discernable by a white arrow on the backside of the mount pointing toward the “TL” sample.

Coating Thickness Measurements

In order to characterize coating thickness, several steps had to be taken to achieve the measurements. First, a slide with a dot having a nominal diameter of .1 mm (Bausch & Lomb Omnicon Test Plate 3) was placed on the microscope (ZEISS ICM 405) and magnified 1000X. A digital photograph was then taken of the dot through the camera attachment. Each sample was then examined at the same resolution and a photograph of the coating was taken as well. Sample photographs were saved as JPEG’s named their respective sample names. (Samples were thoroughly examined before the photograph was taken to ensure that the area photographed was representative of the entire coating on the sample.) Once all the samples had been photographed, each picture was inserted onto a slide in Microsoft Power Point and printed out. All photographs when inserted were considerably small and were enlarged to ‘snap’ to the size of the slide. This ‘snap’ function ensured that each photograph was enlarged exactly the same percentage.

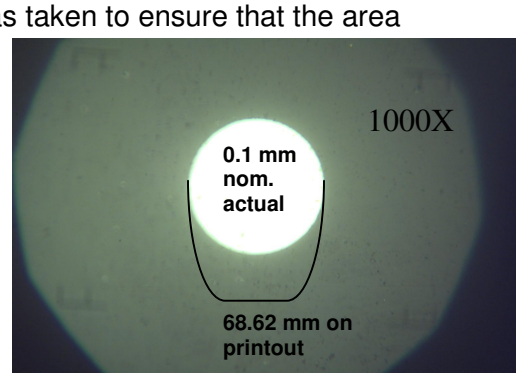

Fig. 6 Photograph of .1mm nominal diameter dot

A calibrated set of calipers was then used to manually measure the .1mm dot on the printout. That measurement, 68.62mm, was then used in the conversion equation, C=((X*0.1)/68.62)*1000, where ‘X’ equals the manually measured coating

thickness in millimeters and 'C' equals the coating thickness in microns. (0.001mm=1 micron or µm) The coating thickness of each sample was manually measured, converted, and recorded. Being that the purpose of this measurement is to compare coating thickness to one another rather than obtain an accurate coating thickness measurement, the fact that the 0.1 mm diameter dot is a nominal 0.1 mm, is irrelevant.

Hydrogen Permeability

Hydrogen permeability tests were performed according to standard procedure (ASTM D1434).

Observations

Pressure control

For these experiments, the total gas volume was reduced from 1 scfm to .5 scfm. In every instance where the butterfly valve was checked, it was observed operating between 13-25% and the pressure set-point was being maintained.

Sooting

As mentioned above, micrographs of parts processed under 'current state' conditions reveal a thin black layer between the pulse coatings, therefore the 'pulsing' was included as an input variable to investigate its affect on the layering of the coating. Figure 7 shows layers in the coating from Experiment 8, which had no pulsing. Similar layering was observed on many samples irrespective of the pulsing.

It was also believed from prior experience in the small reactor that the pulsing (or lack of) contributed to the build-up of 'soot' throughout the furnace exhaust system. After each run of this DoE the filter cartridges were inspected and given a rating of 1, 2, 3, 4, or 5. A rating of "1" was assigned if the filters were clean and a "5" if the filters had collected so much soot that they were plugged. Figure 8 shows the ratings of each experiment.

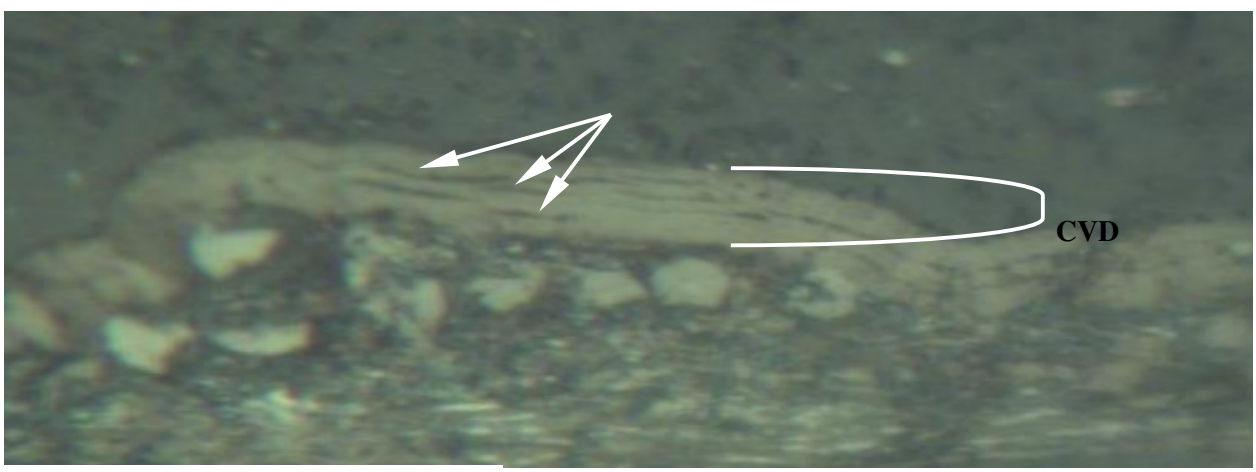

Fig. 7 Layers in Coating (1000X)

Exp.	Pulses?	Rating
1	Yes	1
2	No	3
3	Yes	1
4	Yes	3
5	No	1
6	No	4
7	Yes	3
8	No	5

Fig. 8 Filter Ratings

Averages and t-ratios were calculated using these ratings and the pulses were determined to play no significant role in the soot build-up. (Stdev 1.51, T=1.17, T-crit (6df,0.05)=2.447) However, upon comparing all the variables in each experiment with the cleanliness ratings, a pattern did emerge. The runs that received anything but a "1", all had high pressure and/or high ratio. While the runs that received 1's had a mixture of high and low pressure, they all had low ratio. Three of the four runs with low ratio received 1's. The one that did not, had high pressure, high temperature and no pulses. It would appear while the pressure (t=0.70) may contribute somewhat, the ratio is most likely the driving force behind the soot build-up in the exhaust, which would bring light to it having the highest t-ratio of any of the variables (t=2.11) Future trials with less variables and more repeat data would be needed to better determine the role and benefit, if any, of the pulses.

XRD

Six samples were taken from each experiment to be used for XRD (X-ray Diffraction) evaluation. It is of interest to know whether the coating deposited during the CVD process is the same form of carbon as the bipolar plate substrate and XRD is the most common way to make that determination.

The first sample (6-G1-TL) was evaluated after being glued to a piece of glass then having all of its material removed by sanding until presumably only the carbon coating on the bottom side was left, a visual judgment when the layer was so thin that glass was showing through it. The second sample (6-G5-TL) was also glued to a piece of glass. After the top layer of coating was sanded off, the glass was placed on a hot plate to soften the glue. The sample was removed, flipped over, and re-glued to the glass. After the coating on that side was sanded off, that sample was evaluated – presumably the substrate material only. The results of both evaluations were compared and found to be identical, (both coating and substrate same form of carbon) with the exception that the one of the coating only had a higher number of intensity counts. It was subsequently determined that there would be no real benefit to evaluate all 48 samples.

Uniformity

It was observed that the samples from the bottom of the plates frequently had a thicker coating than those from the top. (See Figures 9 & 10) In order to quantify this difference for analysis, the coating thickness of each bottom sample was subtracted from the coating thickness of its corresponding top sample to produce a number (usually negative) that represented the uniformity of the coating. For example, the samples pictured below would produce a –3.03 (4.55-7.58=-3.03) while a uniform coating would produce a zero (top-bot=0 ⟶top=bot).

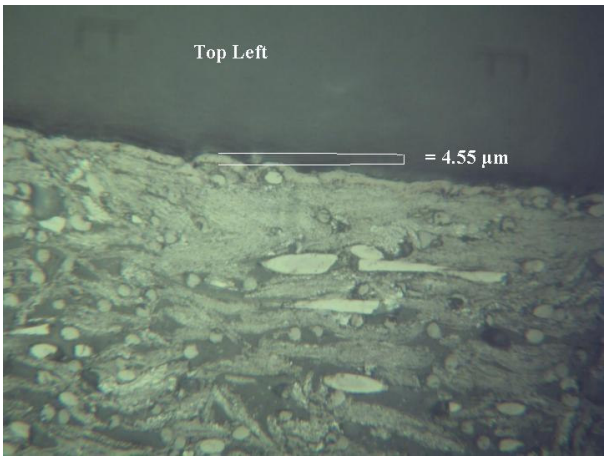

Fig. 9 Coating Thickness Top Left

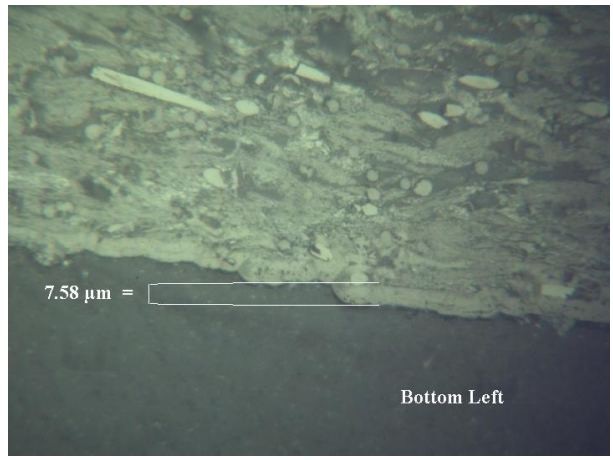

Fig. 10 Coating Thickness Bottom Left

Carbon Build-up

During many of the experiments, carbon built up on the parts where they contacted the furniture. In a few experiments, the build-up also occurred on the surface of the plate in areas where there were no contact points. Currently, this build-up is considered damaging to the part as it deforms the surface. Each experiment was given a number based on the amount of carbon build-up. A rating of "1" was assigned if there was no build-up, and a "5" if the build-up covered the part. Figure 11 shows the ratings. Standard deviations and T-ratios were calculated and while no variable qualified as a 'significant' factor (t-crit=2.447, 6df,0.05)(temp & pulse: t=0.00), pressure and ratio stood out as possible contributors (t=1.87). Cross-referencing the ratings with only the experiment parameters of pressure and ratio, it is interesting to note that the only two experiments with no build-up were at low pressure and low ratio. The four experiments that received 3's either had high pressure and low ratio, or low pressure and high ratio. The two experiments that received 5's both had high pressure *and* high ratio. Based on these findings, it is probably safe to assume that regardless of the un-qualifying t-ratios (which are terribly conservative in their calculation) the most powerful players in the carbon build-up are pressure and ratio.

Exp.	Rating
1	1
2	3
3	3
4	5
5	1
6	3
7	3
8	5

Fig. 11 Carbon Build-up

Infiltration vs. Deposition

Due to the porosity of the bipolar plates, sealing the surface through CVD creates a light-weight, yet strong and hydrogen impermeable product. The difference between CVI (chemical vapor infiltration) and CVD (chemical vapor deposition) is basically the location of the carbon deposit. In a CVI process, the carbon deposits into, or 'infiltrates' the substrate. In a CVD process, the carbon is primarily deposited onto the surface of the substrate. It is an underlying objective of this DoE to begin to understand the parameters that control that deposition. In this picture, the coating can easily be observed having sealed over the surface. On closer inspection, however,

the coating can be seen on the surface of all exposed areas inside the part, gradually becoming thinner further into the substrate. That coating, when viewed through the microscope, can be seen much clearer than in this photograph. It is quite distinguishable from the substrate in its appearance and coats over or 'outlines' all of the exposed area, crossing over from fiber to powder without seam or break exactly as it does over the outside surface of the part. In the

data, this is represented by a higher weight gain and a thinner coating thickness and indicates that the carbon deposited slow, leaving the inside of the substrate exposed for some time before the surface was sealed off.

Sealing

Three parts from each run were tested for hydrogen permeability to qualify sealing. No parts from any experiment qualified.

Data Analysis

For this study, of particular interest are weight gain (WGN), overall coating thickness (CTG) and the top-bottom thickness as a measure of uniformity (UNF) as discussed in the previous section. Figure 13 contains the averages of those outputs from each experiment.

Exp	WGN	CTG µm	Fig. 12 CVI vs CVD
			UNF µm
1	1.87%	2.03	-0.19
2	2.16%	1.46	-0.47
3	1.54%	1.68	-1.43
4	4.22%	1.78	-2.45
5	1.64%	1.70	-1.36
6	3.66%	5.18	-0.34
7	3.26%	8.48	-3.71
8	3.55%	7.56	-3.76

Once all the data had been collected, the first step was to do a statistical analysis, in order to get a picture of the primary or main effects of each variable on the critical outputs. The averages from the data (Fig. 13) were used to calculate t-ratios. For this calculation, only 6 degrees of freedom are available and at 95% confidence a t-ratio greater than 2.447 would be necessary to consider a variable significant. As is evident in Figure 14, only one variable qualifies as significant using this method of calculation. With only 6 degrees of freedom, these numbers are considered conservative, and while they do not clearly signify strong relationships, they do begin to point in a particular direction. With a t-ratio of 2.52, the ratio of Argon to Methane appears to be a significant variable, especially with regard to weight gain.

Fig. 13 Output Averages

		Temp	Pulsing	Pressure	Ratio
Weight Gain	Stdev	0.01	0.01	0.01	0.01
	T-Ratio	0.65	0.04	0.35	2.52
Coating Thickness	Stdev	2.82	2.82	2.82	2.82
	T-Ratio	0.75	0.13	0.24	2.40
T-B Coating	Stdev	1.45	1.45	1.45	1.45
	T-Ratio	1.66	0.45	0.61	1.66

Following closely behind is temperature (t=0.65) and behind it, pressure (t=0.35). Based on the t-ratios and general observations, it was determined that the pulsing had no real impact on the critical outputs and was therefore removed from the continuing analysis.

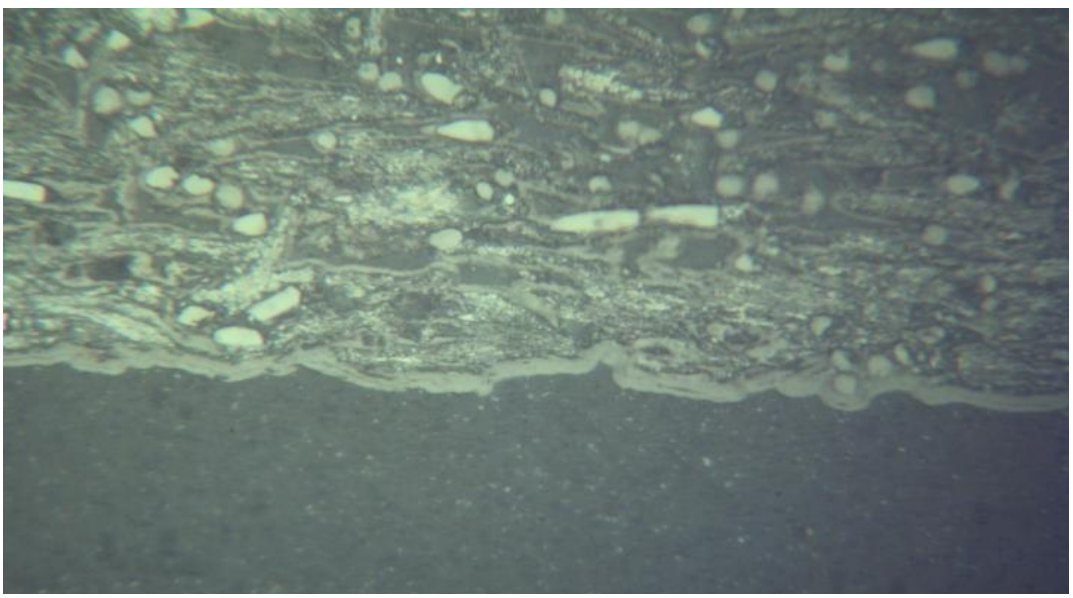

Fig. 14 Standard Deviations and T-Ratios

The second step in the data analysis was attempt to understand the relationships of the variables to each other and the effect of that interaction on the critical outputs. T-ratios were calculated for the interactions and none qualified as significant. However, none were disqualified for the continuing analysis as, once again, these calculations were conservative and it is strongly believed that the interaction of certain variables are, in fact, significant. The analysis was therefore moved to the next step, which was to build a math model. Since building a math model requires that significant or possibly significant variables and interactions be established, other means of detecting these effects were implored.

It is a strongly held belief, based on past experience, that temperature, pressure, and ratio *all* are in some way significant variables, regardless of their low t-ratios. For that purpose, all three were automatically included individually in the math model.

In order to identify variable *interactions* worthy of inclusion, comparative slope charts were created. Comparative slope charts compare variable interactions by plotting the effect of one variable at high and low levels of another variable. If the two resulting lines are significantly out of parallel, it is because the level of one variable influences the effect of the other, and their interaction can be considered significant. For example, figure 15 is the comparative slope chart for the effect of the temperature/ratio interaction on coating thickness. Due to the difference in slope, this interaction was considered significant and was included in the model for coating thickness. The three-way interaction in figure 16 between temperature, pressure and ratio on uniformity (T-B coating thickness) was the strongest interaction of the DoE, according to the slope charts and was also included in the model.

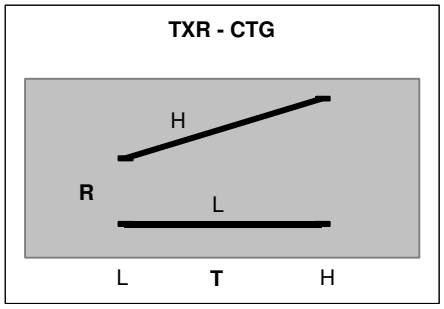

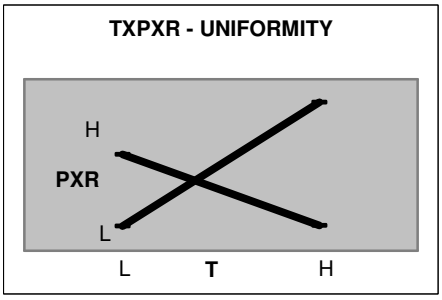

Figs. 15 & 16
Comparative Slopes Charts

Based on the charts, significant and possibly significant interactions were identified and included in the linear math model. Figure 17 shows those identified.

	T	P	R	T/P	T/R	P/R	T/P/R
Weight Gain	X	X	X			X	X
Coating Thickness	X	X	X		X		
T-B Coating	X	X	X	X	X	X	X

Fig. 17 Variables Included in the Linear Models

<u>Models</u>
Empirical linear models for each critical output were created based on the above findings for use in generating predictive graphs of the variable effects. The models are as follows:

Weight Gain = 2.750E-02 – 5.000E-05(T-1400) + 5.000E-04(P-7.5) – 7.125E-03(R-1.667) – 1.125E-04(P-7.5)*(R-1.667) – 3.750E-07(T-1400)*(P-7.5)*(R-1.667)

Coating Thickness = 4.134 + 0.0154(T-1400) - 0.1055(P-7.5) - 1.812(R-1.667) - 0.00599(T-1400)*(R-1.667)

T-B Coating = -1.71375 – 0.017025(T-1400) – 0.1255(P-7.5) + 0.6384375(R-1.667) + 0.001135(T-1400)*(P-7.5) + 0.002391(T-1400)*(R-1.667) + 0.0339375(P-7.5)*(R-1.667) – 0.000347(T-1400)*(P-7.5)*(R-1.667)

Using the above models, the following predictive graphs were created. (Figures 18 & 19). The purpose of such a graph is to plot the effect of different levels of one or several variables on a particular output, based on the empirical models. Use of these types of graphs help to understand basic trends of variables and effects that may otherwise be unnoticeable in the raw data. For example, the 'Differential Thickness' graph below shows a wide space between the varying pressure lines at '1350 C' while the lines are closer together in the '1450 C' group, revealing that varying the pressure at low temperature has a greater impact on uniformity than does varying the pressure at high temperature. This also indicates that at higher temperatures uniformity is more
dependent on a variable other than pressure, while at lower temperatures pressure plays a significant role. The graph also shows the lines are closer together at low concentrations (3) than they are at high concentrations (0.333), indicating that the effect of changing the pressure at high concentrations has a greater impact on uniformity than does changing the pressure at low concentrations. This leads to a reasonable conclusion that a higher concentration of process gas greatly increases the effect of temperature and pressure on uniformity, or as will be noted later, greatly increases the distance the 'sweet spot' moves relative to the parameter change.

Due to the nature of the sealed bipolar plate product, uniformity of the coating is the number one critical characteristic. It is very important that the plates receive a uniform layer of carbon across the entire surface, as this layer is the medium that seals the plate; if it has great variation, the plate may or may not be sealed in all areas. This graph was used to understand the controlling factors of that variation.

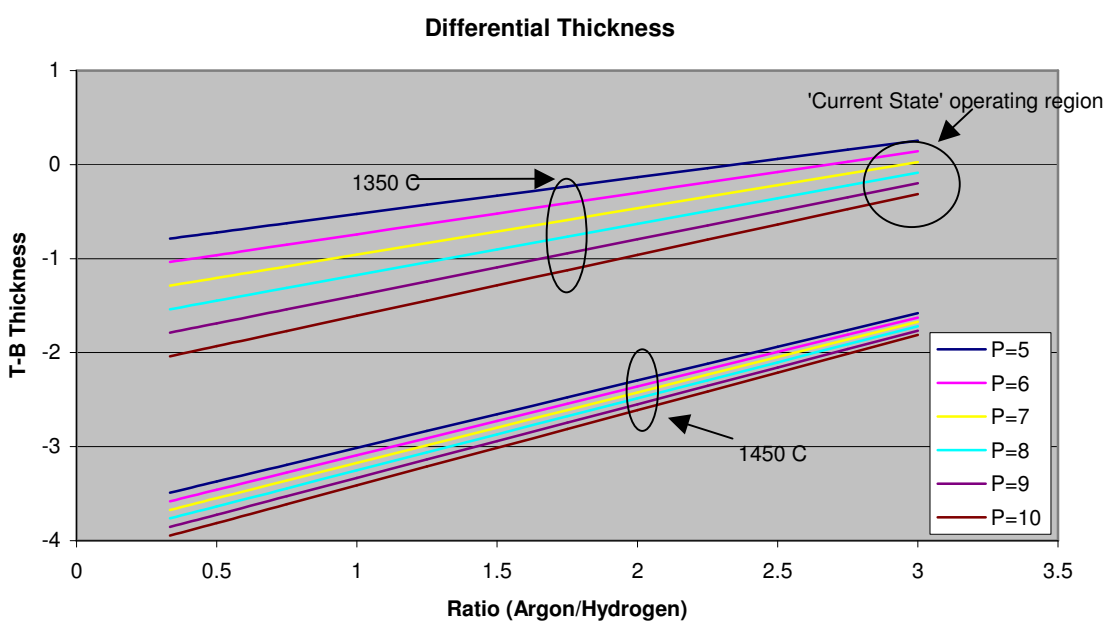

Fig. 18 Differential Thickness Model

Additionally, while assumed but heretofore unqualified, Figure 18 confirms that the parts previously processed at 'current state' conditions (found on page 1) should have received a uniform coating. This is evidenced by the location of the operating region in reference to the "zero" T-B Thickness grid line.

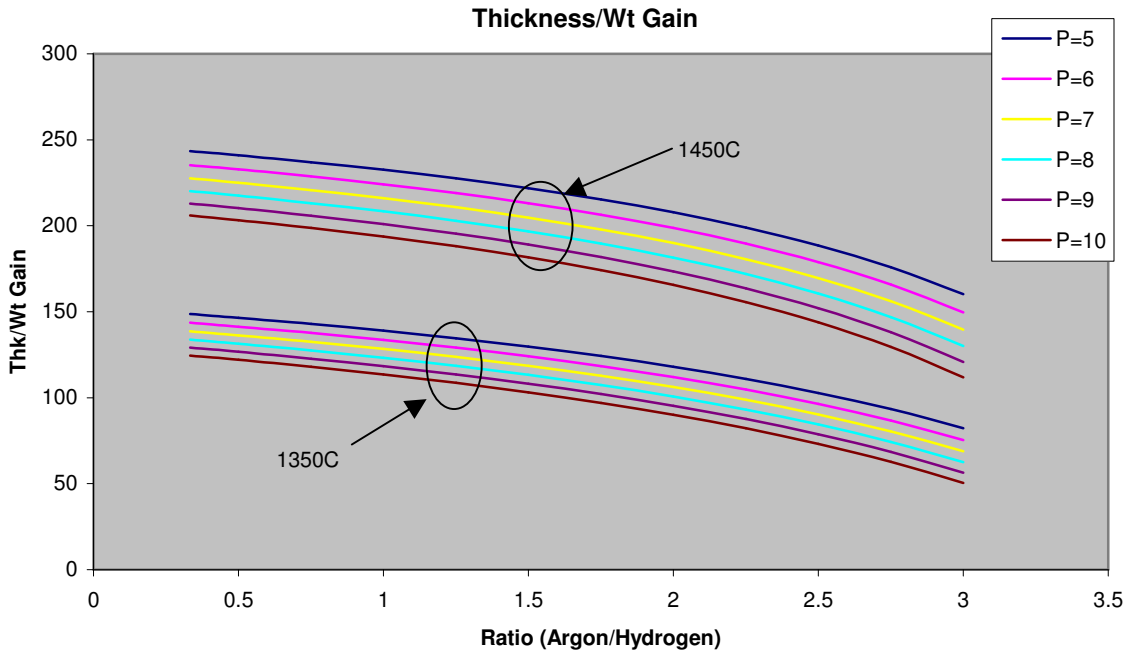

Fig. 19 Thickness/Wt Gain Model

Another, albeit not critical but preferred, characteristic of this product is that it be lightweight due to the large numbers that must be assembled as a unit for use. Being that a thicker coating presumably provides a better seal, it is preferred to maximize coating thickness while minimizing weight gain. In the Thickness/Wt Gain model above this is represented by higher numbers on the vertical axis. This chart was used to identify the trend of the variables toward that goal and indicates that higher concentration at higher temperatures and low pressure give the best result. It has already been concluded however that those conditions create poor operation conditions in the reactor with regard to sooting as well as non-uniform coating. It appears certain trade-offs will be necessary in the process to achieve desirable results in all areas.

Conclusions

Main Effects

The simple chart at right, outlines in general the effect of temperature, pressure and ratio (shown as concentration) on weight gain (WGN) and coating thickness (CTG). The "+" indicates an increase and the "-" indicates a decrease. These responses are significantly greater at higher concentrations.

	WGN		CTG
Temperature	+	-	+
	-	+	-
Pressure	+	+	-
	-	-	+
Concentration	+	+	+
	-	-	-

Fig. 20 Basic Main Effects on Weight Gain and

Interactions

The 'possibly significant' interactions for the critical outputs can be found in Figure 17 on page 14.

Uniformity

Based on past experience in the small reactor, it is known that within the reactor there is a zone in which the carbon deposits uniformly. This has been referred to as the "sweet spot" (hereafter referred to as the 'zone'). If the zone is low in the chamber, then the bottom of the plates will receive more coating than does the top. Conversely, if the zone is high in the chamber, then the top of the plates will receive more coating than the bottom. Ideally, the zone would sit in the middle of the chamber relative to the plates, such that the plates fall completely within its boundaries and thus the entire plate receives the same amount of deposition. It is also known that with changes of temperature and pressure, this zone moves primarily up or down and that those two parameters interact with one another to facilitate the zone movement. To date, our knowledge of this interaction is minimal. However, using the uniformity (t-b) data, it is possible to 'see' the zone in the chamber and chart it's movement in response to parameter changes.

Since the uniformity data was the result of top coating thickness minus the bottom coating thickness, negative uniformity numbers indicate that the coating on the bottom of the plate is thicker than the top. Positive uniformity numbers indicate that the coating is thicker on the top of the plate than it is on the bottom. Therefore, it is reasonable to assume that the movement of uniformity numbers from negative to positive is an indication of the zone moving from low in the chamber to higher in the chamber.

Using the model as a guide, a 'working' model was developed that allows the user to scroll through temperatures and pressures and watch the graph of the critical outputs change accordingly. Using this model, the zone, was seen to move down with an increase in temperature (Figs. 21 & 22) and down with an increase in pressure (Figs. 23 & 24). It can be concluded then, if the temperature is increased, the zone drops, so the pressure must be decreased to bring the zone back up. While the exact coefficient of this relationship is still unknown, the basic knowledge of their directional impacts is valuable.

In the charts on the following page, the zone is represented by the green line, labeled "variation" and is charted based on the math models found above. The "Variation" and "Thickness" lines are plotted against the primary y-axis, while the "Weight Gain" (yellow line) is plotted against the secondary y-axis.

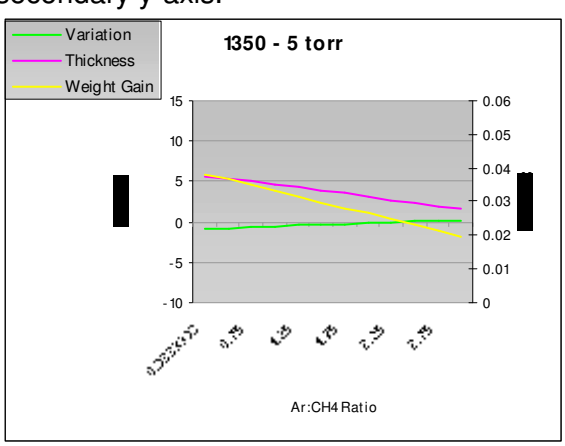

Fig. 21

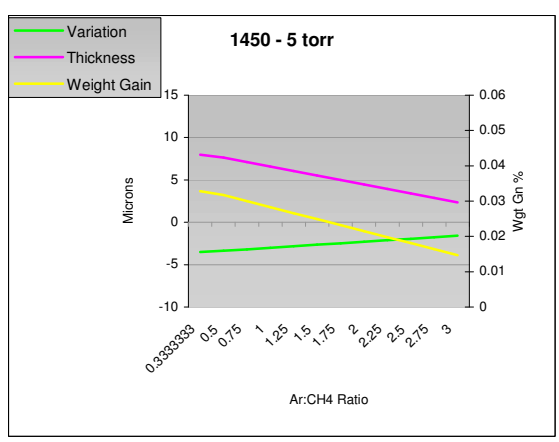

Fig. 22

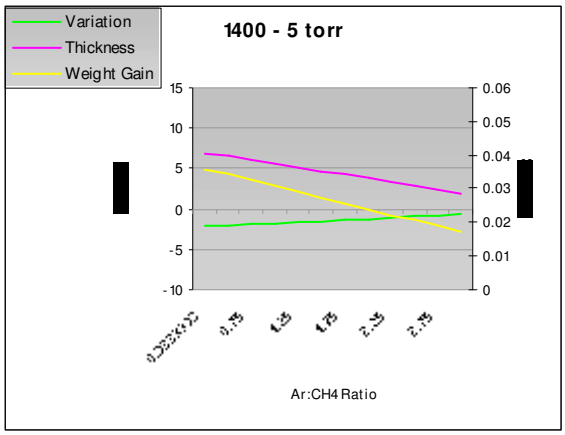

Fig. 23

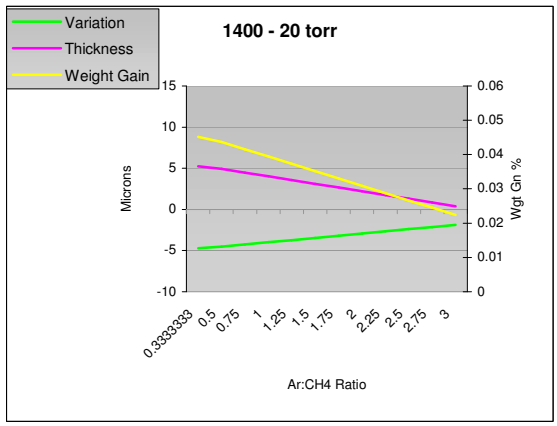

Fig. 24

Optimized process

The data set from this DoE seems to show that the most desirable conditions for maximizing thickness and minimizing weight gain are the most undesirable for uniformity. It appears that a low temperature and low pressure allows the carbon to deposit more slowly and uniformly. Unfortunately, those conditions allow the carbon to infiltrate the substrate and cause more weight gain. Future trials should explore exposing the parts to high temperature for a short time in an effort to seal the surface quickly, then lowering the temperature to allow the carbon to build slowly and uniformly on the initial layer.

Based on the data, the following combination may be a possible parameter set for good all-around results:

Temp	1450	Temp	1320
Pressure (SP)	5 torr	Pressure	5 torr
Gas Ratio	1:3 Ar:CH4	Gas Ratio	1:1 Ar:CH4
Flow	0.5 scfm	Flow	0.5 scfm
Time	1 hour	Time	5 hours

It will take an actual trial to confirm if these parameters are reasonable.

<u>Summary</u>

The findings from this Design of Experiments have shed light on several key issues regarding the CVD process.

- Decreasing the total gas volume being introduced into the chamber by 50% allows the controlling valve to control at approx. 20% and removes the burden of maintaining pressure from the pumps.
- The use of pulsing does not appear to aid in the cleanliness of the exhaust manifold, nor does it appear to contribute to the layering of the carbon.
- Parts previously processed most likely received a uniform coating.
- The temperature & pressure are large contributors to the ‘zone’ and can be adjusted in conjunction with one another to move the zone up and down.
- The ability to seal the surface of the parts quickly and then slowly build the carbon layer seems to be the key to depositing a uniform coating while minimizing weight gain.
- Higher temperatures promote fast deposition while lower temperatures slow the deposition down.

- Weight gain works opposite of coating thickness, with regard to temperature. (i.e. as coating thickness increases at high temps, weight gain decreases)
- Three hours at any of the conditions in this DoE, does not produce a carbon coating sufficient to seal the parts.
- All critical outputs are influenced more significantly at higher concentrations of process gas than at lower concentrations. (i.e. the coating thickness difference from high temp to low temp at high concentration is significantly greater than the same difference at low concentration)
- Pressure and Ratio control the carbon-build up on the plates. High pressure and/or high ratio for three hours result in carbon build-up.
- Ratio seems to be the key to the filter cleanliness – important if runs longer than three hors are needed.

15.0 Construction of Testing Facility for H_2 Permeability

Because the product must resist the passage of hydrogen fuel from one side of the plate to the other, most types of plates must be physically sealed against hydrogen gas transport. The test method used to evaluate hydrogen gas permeability through the bipolar plates is ASTM D1434-82(1998) Standard Test Method for Determining Gas Permeability Characteristics of Plastic Film and Sheeting. In this test method, the sample of known face area is mounted in a sealed region. Both faces of the sample are flushed with hydrogen prior to pressurizing one side only of the sample. The un-pressurized side is vented to a calibrated capillary tube containing colored capillary fluid. During the test, the rate of movement of the capillary tube fluid is proportional to the permeability of the test sample.

The bench-scale test rig was designed and built in this program. Figure 15.1 shows the test device after construction. After initial trials, it was found that thermal drift was an issue with this test method (as temperature fluctuations caused expansion or contraction of the gas in the lines, moving the capillary fluid independent of product permeability). For this reason, a room temperature water bath was used to provide a consistent thermal atmosphere to the test equipment.

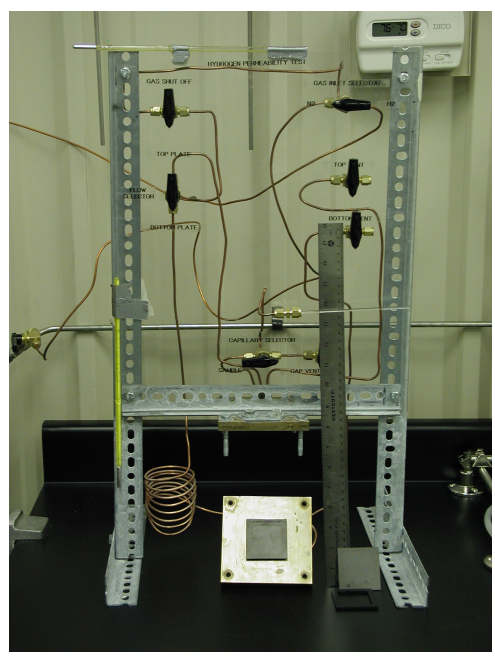

Figure 15.1. Photograph of test apparatus for measuring hydrogen

16.0 Construction of Testing Facility for Water Permeability and Gas Bubble Pressure Test

For the development of porous bipolar plates, two specific property requirements for UTC Power products include the plate bubble pressure and water permeability. For this program, a bench-top bubble pressure and permeability test fixture were designed and fabricated. The key considerations for the design of the rig is the satisfactory sealing against the test fixture in a manner that seals well, but does not introduce excessive stresses to the plate. For the net-shape molded parts, the design of the flow-field must be accounted for, and therefore requires the manufacture of special gaskets to ensure a good seal against the plate and fixture.

The test fixtures were made from polycarbonate material to ensure that a good view of the plate could be obtained during the test. The fixture was clamped initially with nuts and bolts to ensure uniform clamping pressure. These were later replaced with quick connect hand clamps.

For bubble pressure measurement, a supply of clean nitrogen at a controlled pressure was provided to the fixture base. On introduction of the nitrogen to the system, excess water is pushed through the plate and out the vent port. The point at which gas first forces its way through the porosity of the saturated bipolar plate is defined as the bubble pressure of the plate.

To test for plate water permeability, the nitrogen line is replaced with a water source, and the vent is directed to a small flow meter to indicate water flow through the face of the plate at a defined supply pressure.

17.0 Construction of Testing Facility for Electrical Conductivity

A key performance property is the electrical conductivity within and through the plane of the material. The standard in-plane measurement method is ASTM C-611 Standard Test Method for Electrical Resistivity of Manufactured Carbon and Graphite Articles at Room Temperature. In this test method, two contacts drive electrical current through a known-dimension test strip, while two additional contacts detect the voltage drop across the test section. The conductivity results from a simple calculation of product conductivity (in S/cm):

$$k = \left(\frac{I}{V}\right)\frac{l}{A}$$

Where V is the voltage drop, I is the current through the test specimen, l is the length between the voltage contacts, and A is the sample cross-sectional area. For the Porvair carbon/carbon plates, the conductivity is much higher than other graphite bipolar plates available. Our measurements generally indicate more than 300 S/cm conductivity. Most resin-bonded graphite bipolar plates have conductivity on the order of 50-100 S/cm.

Probably a better indicator of electrical performance, however, is the through-plane electrical conductivity. This parameter provides information on the transfer of electricity through the plate material in the direction of energy transport. Unfortunately there is no simple and unambiguous way of measuring this parameter, due to the thinness of the plates. The commonly accepted method is as follows:

Using freshly polished copper contact plates compress the test sample between compliant layers of carbon fiber non-woven fabric. The total contact resistance is then calculated by evaluating the current passing through the face of the test sample and the voltage drop. Subsequent compressing of the sample to about 1000 psi provides an indication of the approximate conductivity of the sample, after first subtracting a similar calibration trace for the compression of the non-woven carbon fiber fabric itself. Figure NN shows a continual increase in test sample conductivity, and a steadily decreasing resistivity with increasing loading pressure. Presuming that the test sample is not compressing during the test, the through plane conductivity of the bipolar plate material should remain the same regardless of the test pressure. The contact resistances however (from platen to conformable non-woven, and from non-woven to the test material) will significantly decrease within increasing pressure. Because the trend is continuing to increase at 1000 psi loading pressure, it can be said that the through-plane conductivity of the bipolar plate material is considerably higher than 70 S/cm.

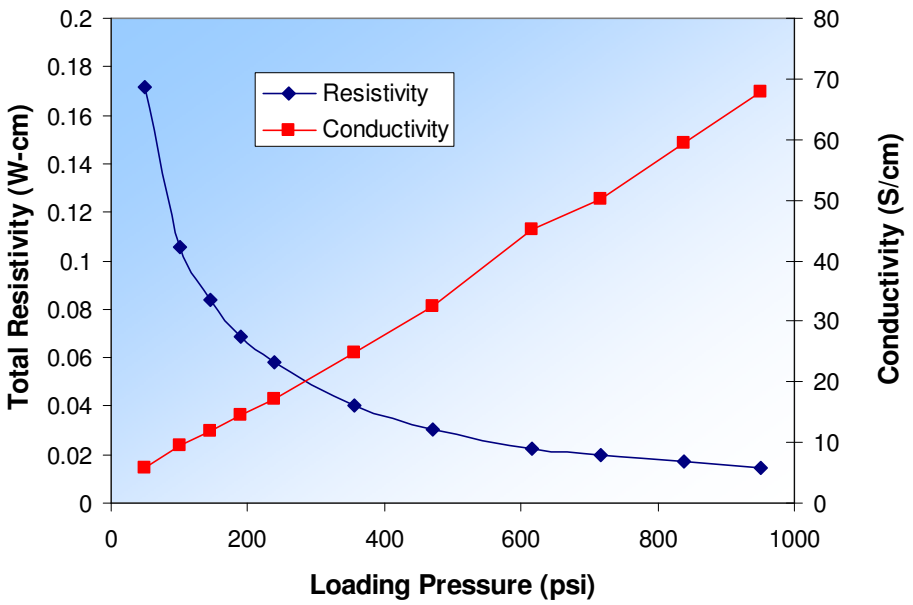

18.0 Construction of Corrosion Cell for Corrosion Measurements

Corrosion testing is highly important to fuel cell materials durability. In the fuel cell environment, the electrochemical cells in operation generate highly corrosive conditions, especially on the cathode side of the system. On the cathode side, oxygen is catalyzed to enable reaction with hydrogen ions crossing the PEM membrane, and liquid water is generated in the process. The combined electrochemical conditions generate severe corrosion conditions that are simulated in the laboratory with sulfuric acid, sometimes with additional corrosive additives. We have found the test methods to vary by fuel cell manufacturer. However, the conditions for most fuel cell tests include 0.1M sulfuric acid. Some companies specify the addition of 10 ppm hydrofluoric acid as well, as it is thought that fluoride ions from the membrane will be present in the fuel cell. Operation at 80℃ is generally standard.

Our corrosion test cell included a chemical hood, glass test ware with covers and a temperature-controlled hot plate. Acids of the recommended concentrations were added and

test samples were submerged in the solutions for specified durations. Duration of the test varied from 100-500 hours. Solution level is adjusted daily to ensure consistent concentration.

Weight loss and strength loss in 3-point bending were measured to gauge the severity of corrosion to the test materials. We performed this test very infrequently over the course of the program, as our materials, being 100% carbon in make-up, are highly resistant to corrosion

19.0 Second Level Experimental Design Testing Interactions of Best Composition, Pressing and Infiltration Variables

The initial compositional experimental design showed that product properties could be significantly improved through the addition of graphite powder to the mixture. The graphite powder has the benefit of dramatically improving strength, electrical conductivity and bubble pressure properties. To further optimize the material composition, additional experimental investigations were performed.

EMBOSSED MATERIAL FACE-AREA SHRINKAGE

Introduction

Shrinkage numbers are required for accurate die fabrication. Measurements have been taken of the outer pattern dimensions to determine the shrinkage rate of the material compared to die pattern design. Channel depths have not been measured to this point.

Measurements

Pattern dimensions were measured on a group of 19 embossed materials on-hand. These materials were generally subject to differing pressing and pyrolyzation conditions as most were experimental. Many materials were not measured as they were either broken, cut up for property testing, or sent to UTCFC for evaluation/testing. Measurements were taken using calipers. Channel dimensions from the outer walls of the outer-most flow channels were recorded on both sides of the plate for both the plate length and width. Table 1 shows the recorded dimensions

Table 8

			Water-Side				Air-Side			
Part No	ht avg	density	Lg avg	Wd avg	Srk Lg %	Srk Wd %	Wd 1	Lg avg	Srk Lg %	Srk Wd %
V129C-L1	0.0671	0.9190	11.9420	5.6098	1.3058	1.5819	5.4470	11.9230	1.4628	1.6787
V134A-R1	0.0665	0.8377	11.9105	5.6002	1.5661	1.7515	5.4390	11.9070	1.5950	1.8231
			11.9240	5.6097	1.4545	1.5848	5.4630	11.9138	1.5393	1.3899
V121A-R2	0.0633	0.8736	11.9225	5.6220	1.4669	1.3684	5.4655	11.9150	1.5289	1.3448
V121B-R2	0.0643	0.8781	11.9295	5.6128	1.4091	1.5292	5.4600	11.9250	1.4463	1.4440
V113A-R1	0.0613	0.8231	11.9108	5.6040	1.5640	1.6842	5.4485	11.9088	1.5806	1.6516
V119B-L1	0.0626	0.8623	11.9023	5.6113	1.6343	1.5556	5.4640	11.9033	1.6260	1.3718
V119C-L2	0.0540	0.8786	11.9083	5.5905	1.5847	1.9211	5.4335	11.9078	1.5888	1.9224
V119C-R1	0.0470	0.7559	11.9250	5.5978	1.4463	1.7924	5.4490	11.9233	1.4607	1.6426
V119C-L1	0.0540	0.8786	11.9200	5.6137	1.4876	1.5146	5.4530	11.9208	1.4814	1.5704

V112C-L1	0.0678	0.8400	11.9213	5.6102	1.4773	1.5760	5.4630	11.9085	1.5826	1.3899
V112B-R1	0.0692	0.7813	11.9370	5.6142	1.3471	1.5058	5.4665	11.9308	1.3988	1.3267
V119C-R2	0.0488	0.6915	11.9200	5.5863	1.4876	1.9942	5.4305	11.9315	1.3926	1.9765
V121B-R1	0.0674	0.8403	11.9145	5.6092	1.5331	1.5936	5.4535	11.9198	1.4897	1.5614
V121B-L2	0.0688	0.8459	11.9280	5.6053	1.4215	1.6608	5.4595	11.9263	1.4360	1.4531
V136B-R1	0.0675	0.8920	11.9135	5.6112	1.5413	1.5585	5.4600	11.9085	1.5826	1.4440
V134B-L1	0.0680	0.9112	11.8933	5.6038	1.7087	1.6871	5.4550	11.8870	1.7603	1.5343
V134C-R2	0.0670	0.9124	11.9183	5.6230	1.5021	1.3509	5.4625	11.9113	1.5599	1.3989
V134C-R1	0.0678	0.9168	11.9125	5.6248	1.5496	1.3187	5.4625	11.9028	1.6302	1.3989

Averages and standard deviations are shown in Table 2

Table 9

	Water-Side		Air-Side	
	Srk Lg	Srk Wd	Srk Lg	Srk Wd
Average	1.499	1.607	1.534	1.543
Std Dev	0.096	0.176	0.093	0.195

Because better than 99% of the material formed will reside within three standard deviations of the mean, these values will be used to estimate the achievable tolerances with the uncertainty in shrinkage. Table 3 shows the estimates.

Table 10

	Water-Side				Air-Side			
	Max Lg	Min Lg	Max Wd	Min Wd	Max Lg	Min Lg	Max Wd	Min Wd
3 Shrinkage Bounds	1.787	1.211	2.135	1.079	1.813	1.255	2.128	0.958
Deviation from target Using 1.5% shrinkage	-0.035	+0.035	-0.037	+0.024	-0.039	+0.030	-0.036	+0.031

Using this information (assuming that the shrinkage remains consistent), better than 99% of the materials formed will be less than 0.035” from target size. It is unknown what final tolerances UTCFC requires with their materials.

Consistent processing will tend to improve the results (reduce the standard deviation of the material face area shrinkage).

One interesting note is the differing shrinkage between the length and the width on the water-side. About 0.1% shrinkage difference is noted. The width measurements also yielded greater deviation in shrinkage than the length. It is not known at this point if the die would need to be produced with the differing shrinkage specifications to account for the shrinkage difference between the length and the width of the materials.

<u>Embossed Channel Depth Measurements</u>

Measurements were taken of numerous sections of embossed materials (all material from V107A composition). Channel depth was measured on a depth gauge using a narrow pin tool. The tool was zeroed on the top of a rib before moving into a channel to record the channel depth. More than 450 measurements were recorded yielding the following results:

	Air Side	Water Side
Average Depth (in)	0.0194	0.0189
Std Dev (in)	0.0006	0.0006
Average Shrinkage (%)	3.1	5.4
Std Dev (%)	3.0	3.3

Internal Porosity

One of the key issues discovered with the manufacture of plates was the tendency for the formation of internal porosity. The effect would be high levels of compression on the outside of the plates and low levels within, resulting in weak materials after machining. This was found to be caused by press temperatures that are too high and by not allowing the gases generated during pressing to escape from the part Figure NN is a micrograph of a plate cross-section shown a significant quantity of internal porosity (plate run under normal pressing conditions with no press degas cycles. Figure NN shows a cross-section with a pressing degas cycle applied. Because the trial samples were machined product at this stage of the program, pressing degas was considered an important parameter to add to our standard pressing operation.

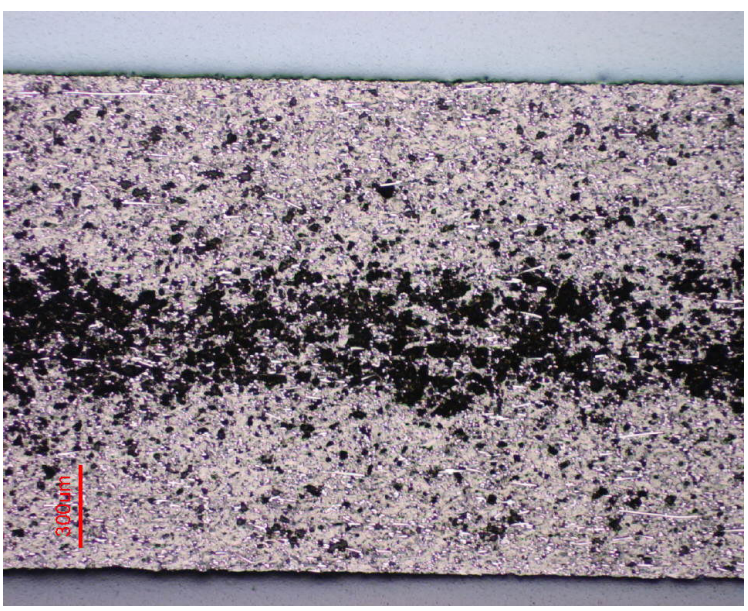

DENSITY UNIFORMITY MEASUREMENTS

Introduction

Density measurements were taken of parts as formed and cut to weight, as carbonized without pressing, as pressed and as carbonized to evaluate the in-plate density variation at each point in the process (six plates from each). Each plate was cut into approximately 45 sections and measured for length, width, thickness and weight. Geometric density was calculated and the results plotted to examine density variation across the plate. The figures below show some surface maps (higher quality contour maps are being generated to aid in evaluation of the data). The tabulated data is included in a separate document.

Results

Table 1 shows the final data summarized from all of the measurements.

	Average Density (g/cc)	Average Deviation (g/cc)	Average Minimum (g/cc)	Average Maximum (g/cc)	Normalized Deviation (%)
Formed	0.842	0.009	0.825	0.865	1.1
Formed then Carbonized	0.803	0.016	0.757	0.827	2.0
Pressed	1.244	0.031	1.145	1.292	2.5
Carbonized	1.162	0.045	1.045	1.238	3.9

As seen, the product density variation increases with each processing step. The finished product experiences density deviations that swing across a large range. Low density areas, although infrequent, could be subject to low bubble pressure.

As seen in the surface plots, the plates (in all conditions) tend to have lower density areas near the outer edges of the plate, and higher density areas near the plate center.

It is important with this product to keep the density variation minimal so that the entire plate maintains properties within property specifications. The cause of the variation at each step needs to be identified and steps taken to eliminate these causes. Potential causes of variation include:

Forming: Inconsistent or non-uniform forming conditions (pressure and flow)
Pressing: Platen temperature uniformity, platen flatness, composition uniformity
Carbonization: Composition uniformity, processing uniformity, stacking arrangement, etc.

As a means of checking the composition uniformity, the coupons from the forming measurements will be carbonized and re-measured to evaluate if the density variation increases, which would indicate regions of resin variation in the product.

NORMALIZED DENSITY VARIATION
CARBONIZED WF119E2 (1 = 1.152G/CC)

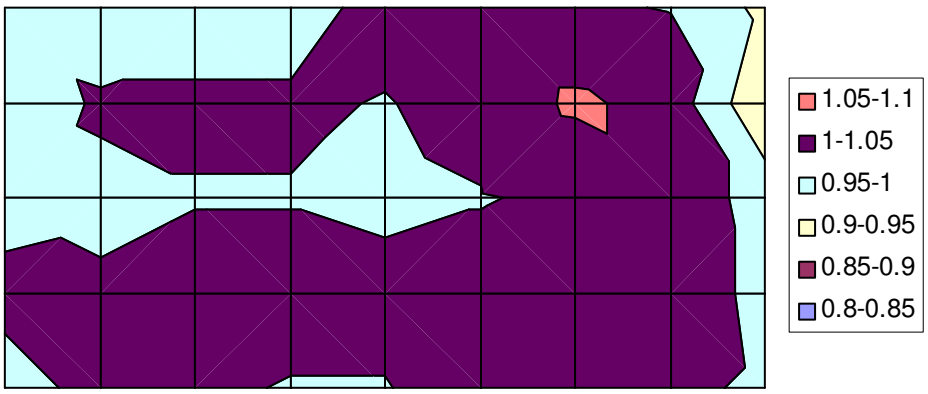

NORMALIZED DENSITY VARIATION
CARBONIZED WHI28E3 (1 = 1.178G/CC)

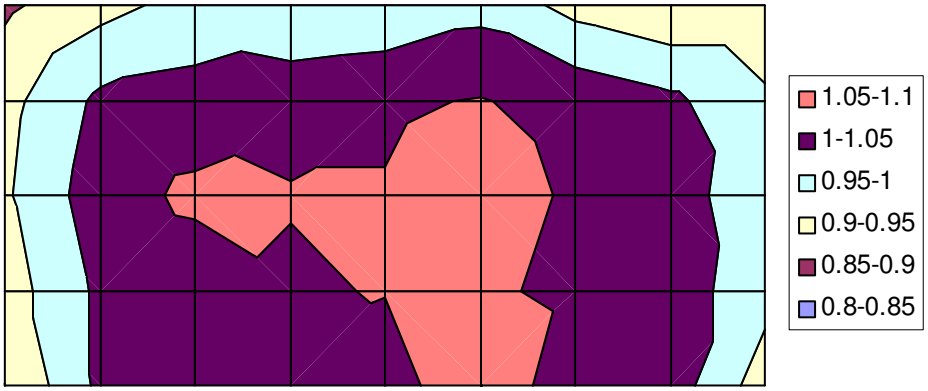

NORMALIZED DENSITY VARIATION
CARBONIZED WE119B4 (1 = 1.148G/CC)

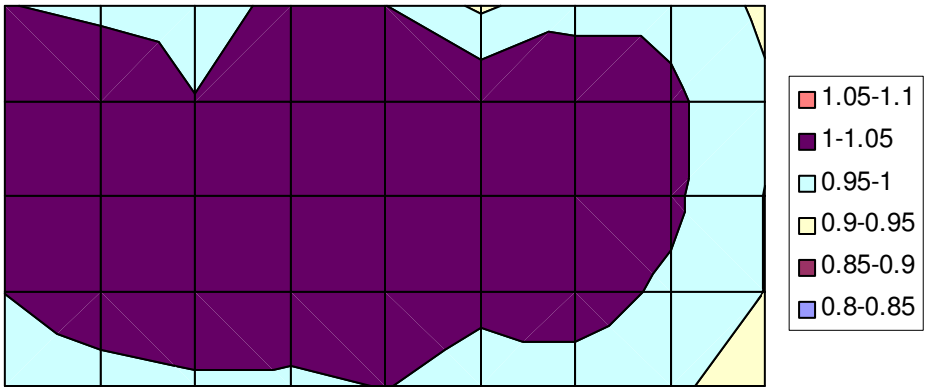

NORMALIZED DENSITY VARIATION
CARBONIZED WE133E3 (1 = 1.160G/CC)

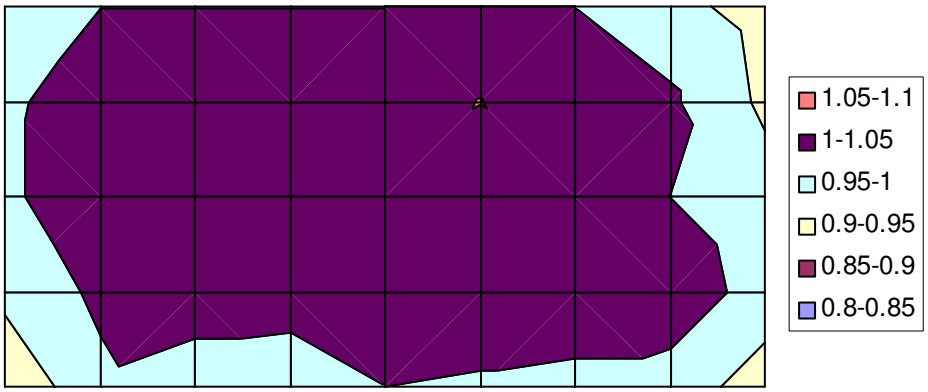

NORMALIZED DENSITY VARIATION
CARBONIZED WI12804 (1 = 1.166G/CC)

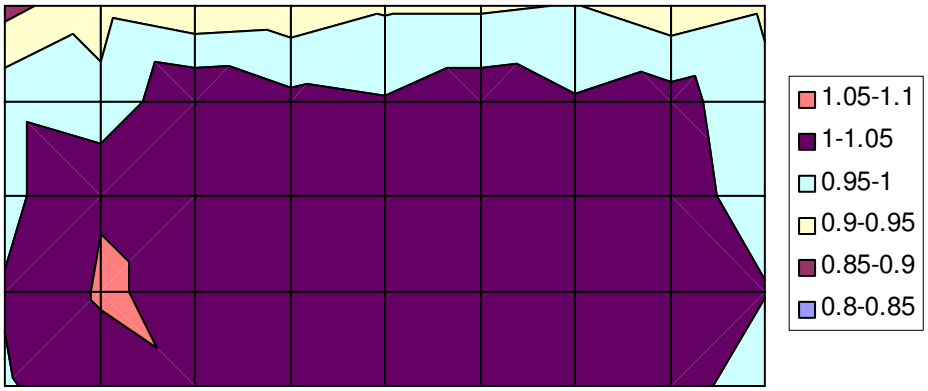

NORMALIZED DENSITY VARIATION
CARBONIZED WK128K2 (1 = 1.168G/CC)

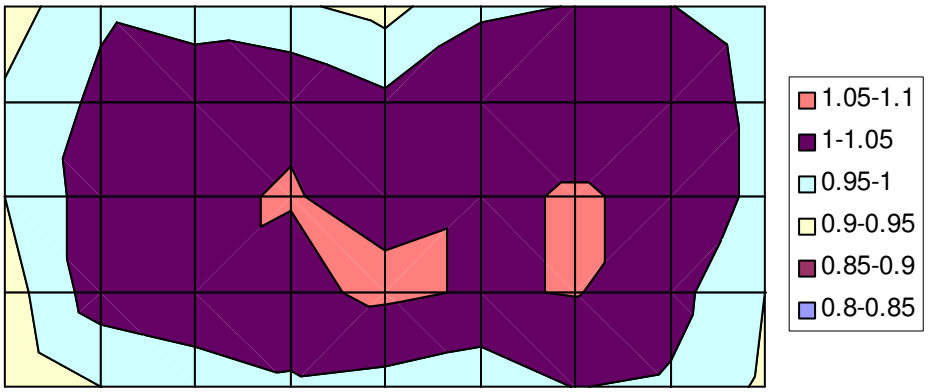

NORMALIZED DENSITY VARIATION
PRESSED WG136E2 (1 = 1.255G/CC)

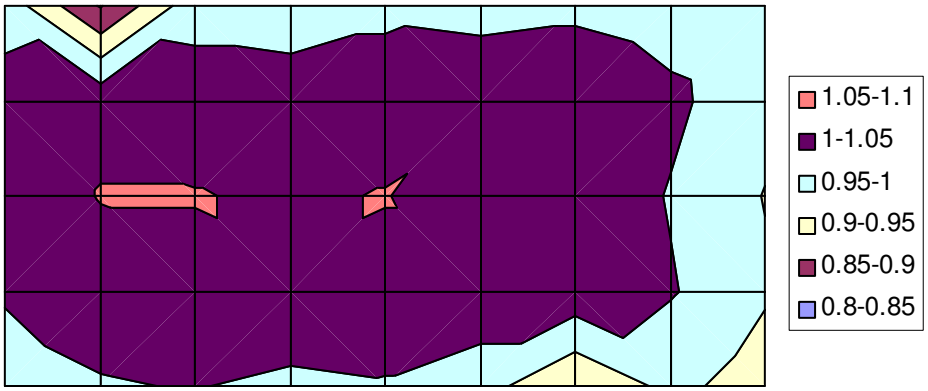

NORMALIZED DENSITY VARIATION
PRESSED WG136E1 (1 = 1.202G/CC)

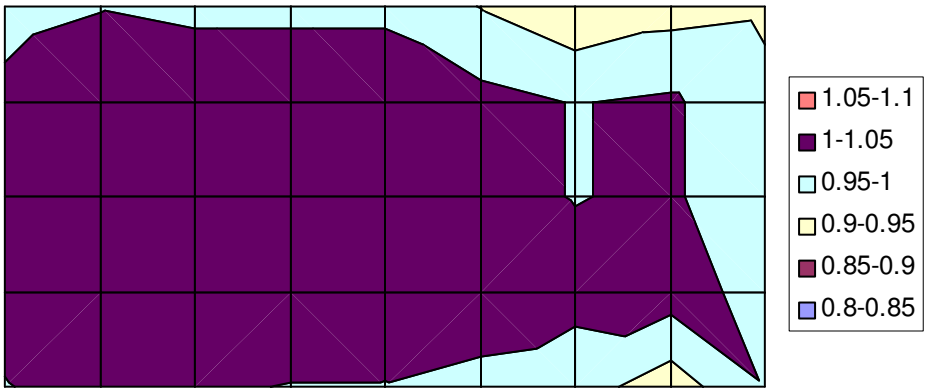

NORMALIZED DENSITY VARIATION
PRESSED WL135I3 (1 = 1.245G/CC)

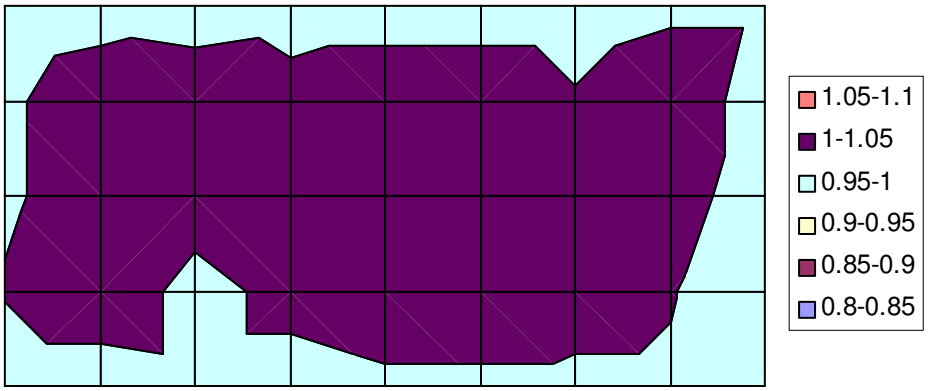

NORMALIZED DENSITY VARIATION
PRESSED WL135I2 (1 = 1.270G/CC)

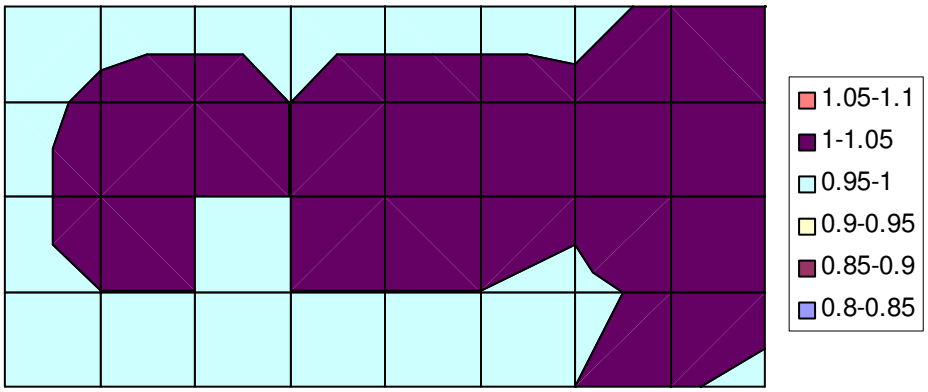

NORMALIZED DENSITY VARIATION
PRESSED WL135I1 (1 = 1.224G/CC)

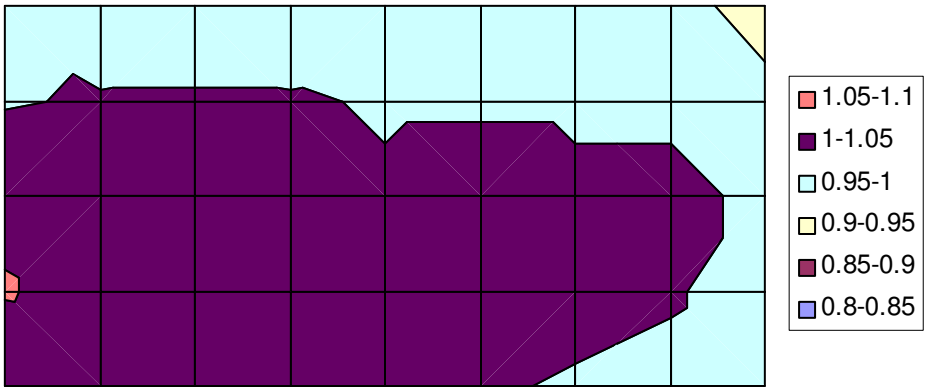

NORMALIZED DENSITY VARIATION
PRESSED WD135F3 (1 = 1.264G/CC)

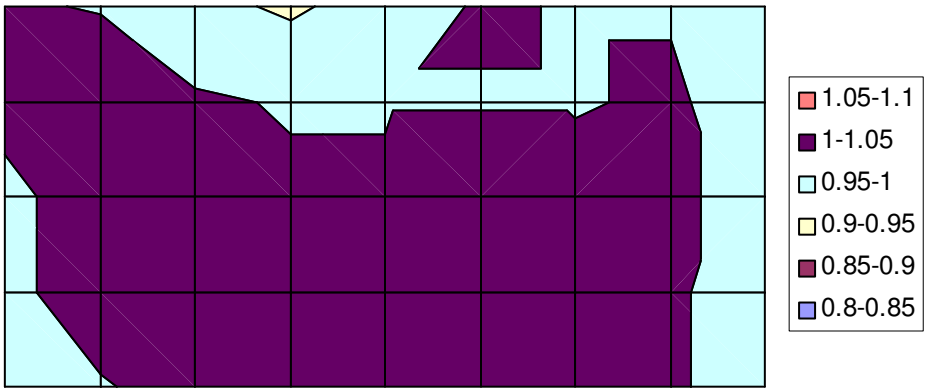

NORMALIZED DENSITY VARIATION
FORMED WJ135F1 (1 = 0.844G/CC)

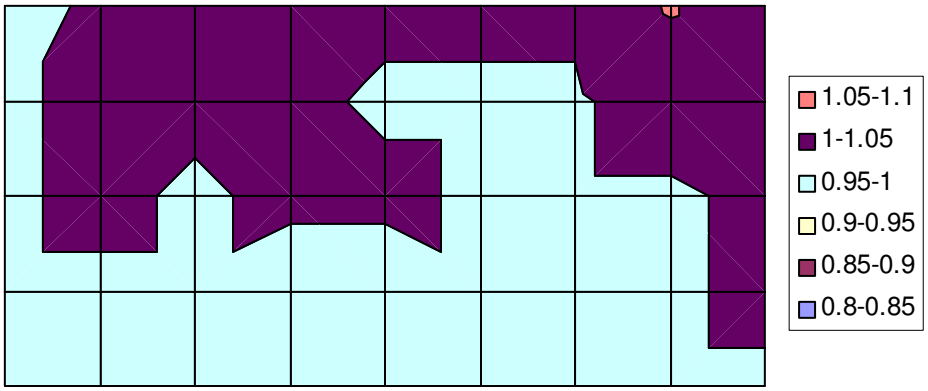

NORMALIZED DENSITY VARIATION
FORMED WJ135F2 (1 = 0.842G/CC)

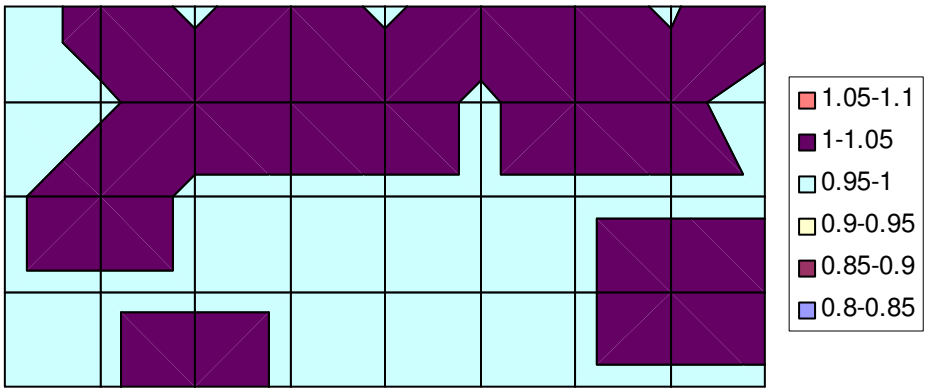

NORMALIZED DENSITY VARIATION
FORMED WJ135F3 (1 = 0.838G/CC)

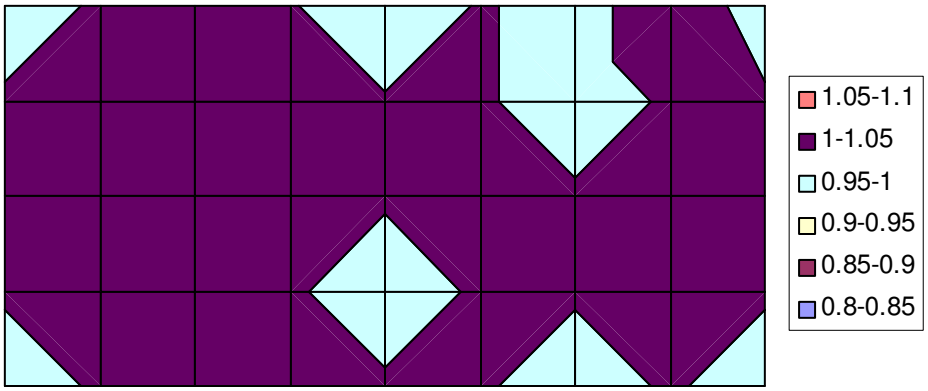

NORMALIZED DENSITY VARIATION
FORMED WJ135G1 (1 = 0.831G/CC)

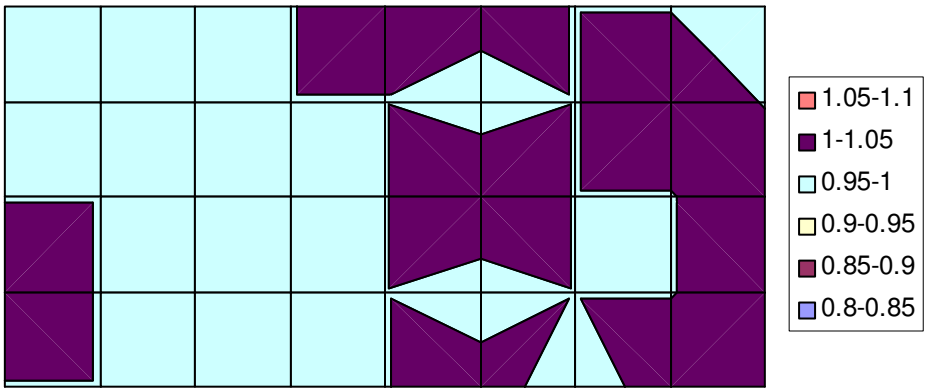

NORMALIZED DENSITY VARIATION
FORMED WD135K3 (1 = 0.845G/CC)

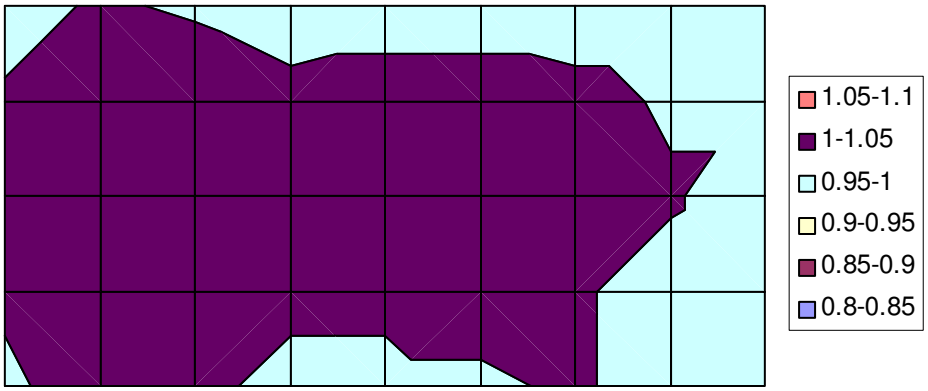

NORMALIZED DENSITY VARIATION
FORMED WD135K2 (1 = 0.854G/CC)

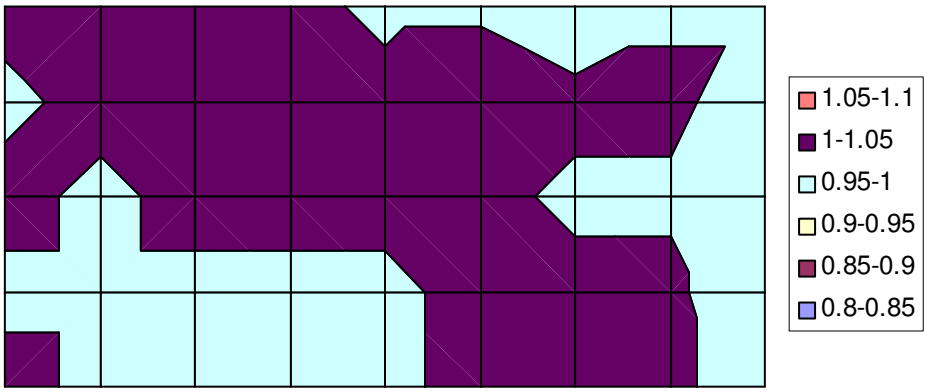

FORMING SYSTEM SOLIDS MEASURMENTS

Introduction

Because dispersion of raw material ingredients is a key factor in determining product consistency, measurements were taken of the baseline system to establish the degree to which mixture uniformity is achieved. Measurements were taken of the percent solids concentration of the suspension mixture over the course of a run before mixing modifications. The date of the sampling was May 20. Samples were taken from the liquid top at the start of a run and during the run. Samples were also taken from the exit of the system, just before entering the forming pans.

Samples of the liquid furnish were taken using a sampling cup. The mass of solution was taken for each sample, and the sample drained through filter paper to yield the captured solids of the suspension. The solids were then dried fully, and weighed to yield the percent solids of the sample.

Results

Table 1 shows the measured percent solids for the samples taken.

Sample Location	Tank Level	Sample Weight (g)	Dried Solids Weight (g)	% Solids
Holding Tank Surface	Full	113	0.674	0.60
Holding Tank Surface	½ Full	114	0.749	0.66
Holding Tank Surface	¼ Full	118	0.732	0.62
Pan A	Full	116	0.824	0.71
Pan A	¼ Full	116	0.867	0.75
Pan B	Full	112	0.875	0.78
Pan B	¼ Full	118	0.945	0.80
Pan C	Full	113	0.865	0.77
Pan C	¼ Full	115	0.965	0.84
Pan D	Full	114	0.857	0.75
Pan D	¼ Full	126	0.904	0.72
Mixing Tank Surface	Full	115	2.21	1.92
Mixing Tank Surface	¼ Full	135	2.31	1.71
Mixing Tank Surface (repeat)	Full	120	2.53	2.11
Mixing Tank Surface (repeat)	¼ Full	129	2.56	1.98

Results show that the samples appear to have consistent solids content during the course of the run for samples taken in the same location. However, samples taken in different locations show different solids contents. Samples taken from the holding tank surface are routinely lower than those taken near the forming trays. This indicates a preference for the solids in the mixture to reside near the bottom of the tank. There was also a variation from pan-to-pan (pans A and D showed slightly lower solids % than pans B and C).

The measurement uncertainty has not been evaluated, so the error in measurement is unknown. Measurements were taken before any mixing modifications. This study will be repeated with the new mixers, blades and baffles in the holding tanks to determine if improvements have been made in dispersion. The influence of the difference in solids content between holding tank top and bottom, and from pan-to-pan is unknown.

FORMING SYSTEM SOLIDS MEASURMENTS – AFTER MIXING MODIFICAITONS

Introduction

Mixing tank modifications were made to enhance material dispersion in response to recommendations. Baseline measurements of system solids content were run before any mixing changes, and a report prepared detailing the results. Baseline results showed that, while the percent solids were consistent with tank level, significant differences were found when samples were taken from the top of the tank and at the pan. The table below shows these results.

Mixing enhancements were made to increase slurry dispersion. These changes included larger mixers, larger impellers and a second impeller on the mixing shaft for each tank. In addition, baffles were installed in the tanks to prevent flow swirl and to encourage additional top-to-bottom mixing action. The changes appear visually to induce a greater degree of dispersion to the mix.

Following these mixing equipment modifications, the solids measurements were repeated to measure the dispersion effectiveness. Table 1 shows the results of the solids measurements.

Results

Table 1 shows the measured percent solids for the samples taken.

Sample Location	Tank Level	Before Modifications % Solids	After Modifications % Solids
Holding Tank Surface	Full	0.60	0.79
Holding Tank Surface	½ Full	0.66	0.81
Holding Tank Surface	¼ Full	0.62	0.76
Pan A	Full	0.71	0.80
Pan A	¼ Full	0.75	0.77
Pan B	Full	0.78	0.81
Pan B	¼ Full	0.80	0.79
Pan C	Full	0.77	0.79
Pan C	¼ Full	0.84	0.81
Pan D	Full	0.75	0.75
Pan D	¼ Full	0.72	0.72
Mixing Tank Surface	Full	1.92	2.56
Mixing Tank Surface	¼ Full	1.71	2.51
Mixing Tank Surface (repeat)	Full	2.11	2.31
Mixing Tank Surface (repeat)	¼ Full	1.98	2.27

Results show that significant uniformity improvement in solids measurement has been achieved through the improved mixing conditions installed into the system. Better solids uniformity from tank top to bottom and over the course of the run was measured than before the mixing enhancements were implemented.

20.0 Post CVI Process Steps

Post CVI process steps include part inspection, property measurement, part bonding and part trimming. Very little work related to this program was done in this area, as the key activities are either customer-specific (as with product inspection criteria) or was addressed in other areas of the program (i.e., bonding in Phase II).

21.0 Cost Estimation

END OF PHASE I PRODUCTION COST ESTIMATE

Process and Estimates

The process of making bipolar plate materials currently entails the following steps:

1) Batching:
2) Mixing:
3) Forming:
4) Drying:
5) Loaf Measurements:
6) Machining:
7) Preform Measurements:
8) Pressing/embossing:
9) Pressed Measurements:
10) Carbonization:
11) Carbonized Measurements:
12) Testing:
13) Inspection:
14) Packing and shipping:

Yields and Materials

1 loaf creates ~ 4 plates.
4 plates creates ~ 3 acceptable plates for customer at present

Materials:

Total per loaf: 1825 gm, yields 4 plates at 150 gm per plate.

The total direct costs at this stage of the product development is as follows (assuming 80% product yield):

Materials	$5.90
Labor	$22.24
Consumables	$6.05
Utilities	$3.44
Total Cost/Plate	$37.62

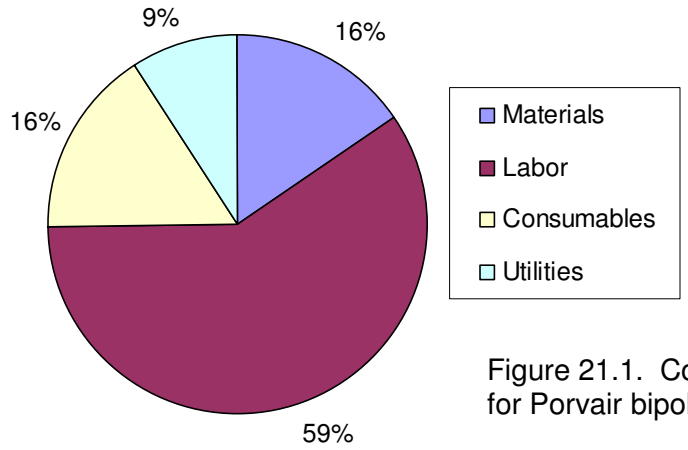

Figure 21.1. Cost break-down for Porvair bipolar plates.

Figure 21.1 shows the breakdown of costs graphically. Obviously the key to driving costs lower in the program is automating many of the manual operations in the process, and so reduce labor costs. This activity was done in later portions of the program.

22.0 Fuel Cell Performance Testing

Fuel cell testing at our primary sponsor (UTC Power) site occurred numerous times in the first phase of the program. Most testing was associated with materials qualification testing and fuel cell performance of blank plates machined to net shape at UTC Power. The testing effort began about September 2002, and continued with a rapid effort through December 2003, at which point UTC Power qualified the product for introduction into their product. The following describes some reporting text related to the fuel cell testing from the Phase I period.

Fuel cell testing at UTC Fuel Cells continued in September 2002. Testing of two 20 cell and two single cell tests were completed in September. Single cell tests investigated materials made without wettability enhancement, and with a paper-made preform material. Results in both cases were good. The paper-made product performed exceptionally well and generated a great deal of excitement at UTCFC. The test run without wettability enhancement demonstrated that the material could perform well without the extra step and cost of wettability enhancements. Additional work in this area is needed to demonstrate that the performance is maintained over long periods of time. The 20 cell tests performed adequately, but not up to expectations. Some early indications of potential problems included test station difficulty, “bad” cells (meaning cells not wetted, cracked or plugged), and high gas cross-over. Post-test tear-down will assist in determining the causes for the reduced performance. Despite the reduced performance relative to expectations, the tests did pass performance qualification limits set by UTCFC, and performed good enough to maintain momentum with the product. Additional cell testing is scheduled for late October and November.

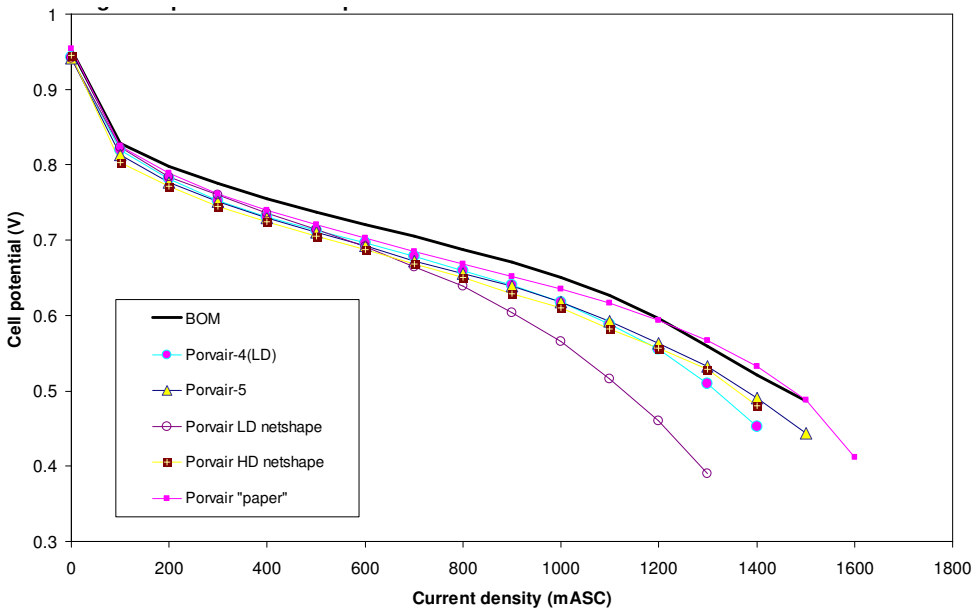

Figure 22-1. Fuel cell performance testing in early part of program. Chart shows continuous improvement in fuel cell performance as product development efforts improved the product.

In the timeframe September 2002 to December 2002, the single cell performance data of Fig. 22.1 was generated. Performance of the product improved steadily through the testing effort, resulting in the qualification of the Porvair product for the demonstration fuel cells. Most of the testing effort was performed by UTC Power independent of this program, as part of their own product qualification effort**.**

Additional fuel cell performance testing occurred at UTC Power in later phases of this project .

23.0 Fuel Cell Durability Testing

Following the initial fuel cell performance characterization and subsequent performance improvement as material development efforts resulted in continual improvements, some longer-term testing was performed to evaluate the product stability over time.

Early program durability testing showed the evidence of performance degradation over time, as shown in Fig. 2. In this early testing, UTC Power found that the Porvair plates, while generally performing very well the rate of performance decreased more rapidly than their standard bipolar plate materials. This performance degradation was thought to be related to the state of product uniformity. Figure 3 shows a density uniformity map taken of parts made in this early stage of the program. As seen in the figure, a high density area exists in one portion of the plate. It is theorized that this high density area impacted fuel cell performance. Product uniformity is critical to achieving a stable level of fuel cell performance in this program.

The uniformity issue prompted rapid product improvement efforts, which improved the product, and led to a round of fuel cell testing outside the scope of this program (funded internally by UTC Power) aimed at qualifying the product for use.

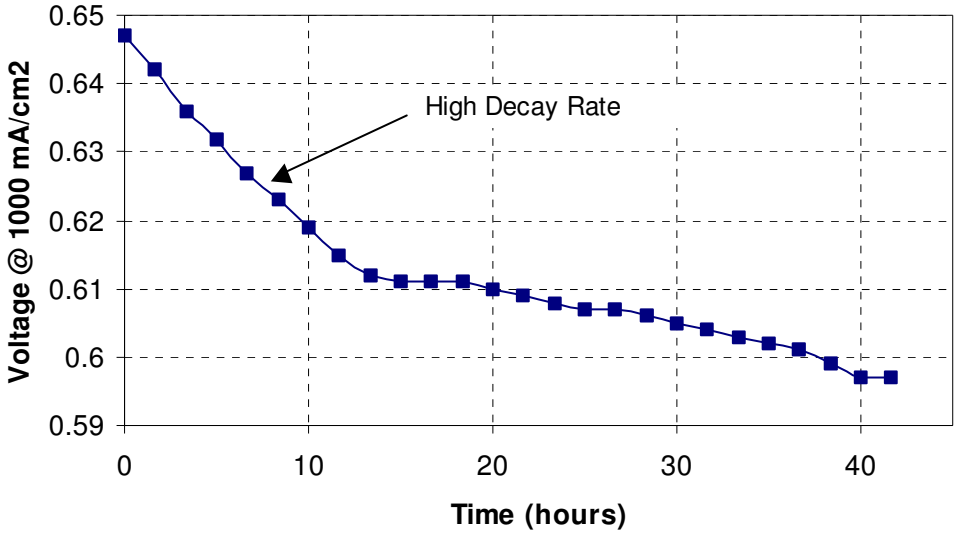

Figure 23.1. Fuel cell durability testing, showing a high rate of voltage decay for the Porvair plates tested in this early stage of the program.

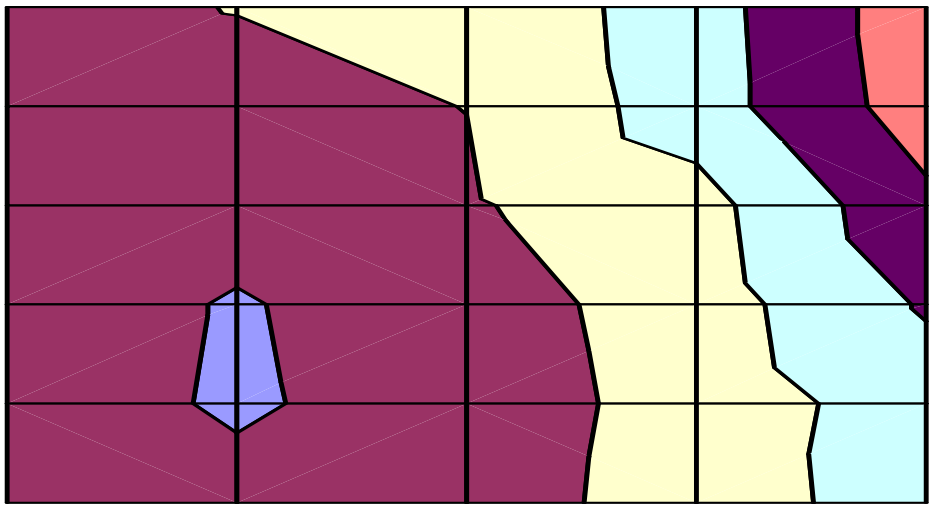

Figure 23.2. Density mapping of Porvair plate material. The density is found to increase from 1.00 g/cc in the upper right corner (orange region) to more than 1.20 g/cc near the lower left (blue region).

24.0 Review Meeting

A review meeting was held on Jan 24, 2003 .

25.0 Interim Report

Interim reports were submitted as annual reports and quarterly reports.

26.0 Go/no-go Decision on Process

During the review meeting with DOE personnel on January 24, 2003, the progress to that point was reviewed, along with our program scale-up plans and market opportunities. A letter from our program manager was received shortly thereafter providing the interest from the Department of Energy to proceed to the next phase of the program.

Phase II

II.- 1. Develop Hybrid (Near-Net Shape) Molded/Machined Technology

Following the decision to re-focus the effort on the development of the next-generation forming technology for fully molded bipolar plates, a new forming system was designed and built. The forming system is improved from the original in that it allows for net thickness sheet formation (instead of loaves that must be sub sequentially machined into net thickness). Further, the improved system offers the flexibility of manufacturing sheets in groups of plates that extend through the entire run of parts. Sheet weight may also be controlled on demand to offer the flexibility of forming different weight sheets, or using the functionality to provide process control.

An outline of the improved system is shown in Fig. 1.1.

A Photograph of the layout of the system is shown in Fig. 1.2. The mixing and distribution system are PLC controlled to automate these operations and minimize variation. Operators use a control panel to direct the introduction of water to the system and to direct the mixture flow through a magnetic separator for iron particle removal (iron particles being present in some of the raw material ingredients). After mixing and magnetic separation, the mixture is distributed to an actively mixed holding chamber where it is batched sheet-wise to a forming head that creates a single sheet.

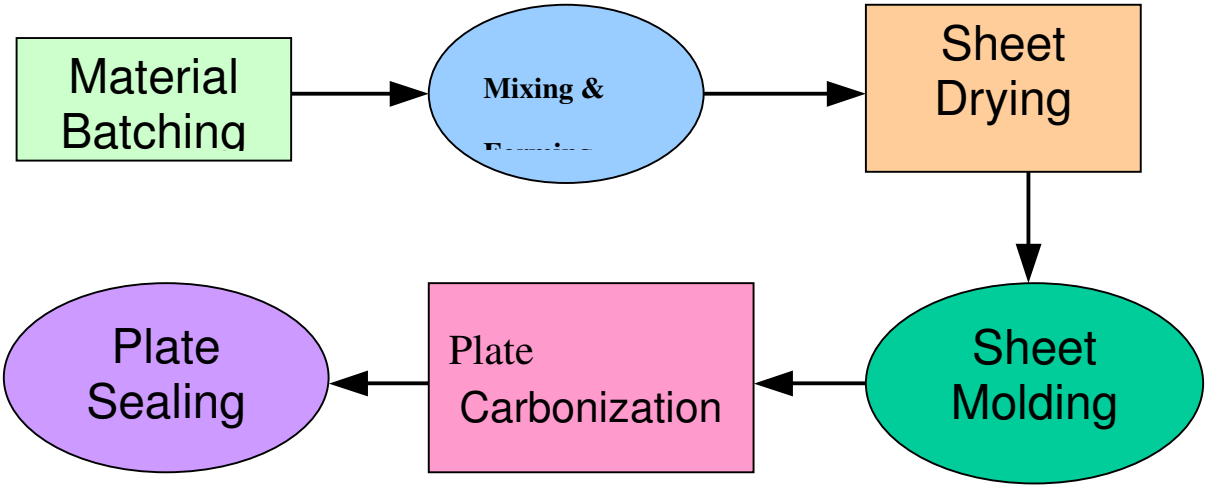

Figure 4.1 Outline of improved process flow.

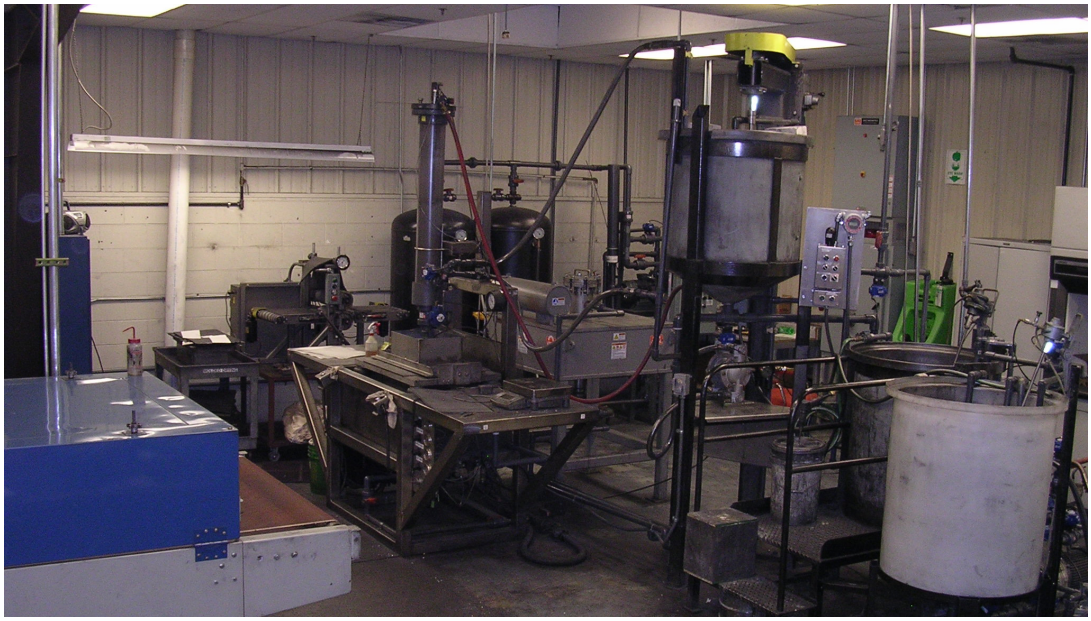

Figure 1.2 Equipment installed for the manufacture of net-shape molded plates.

1.1 Optimize Phase II Forming System

Several investigations were performed to characterize and optimize this system. Individual reports from the efforts will be reported here to describe the studies.

MIXING EXPERIMENT REPORT

Introduction

A short mixing investigation was performed to evaluate the effect of three variables on sheet-to-sheet weight consistency (within sheet uniformity was also measured). The standard sealed molded composition (GAP – series) was used. The standard premixing procedure was used. This experiment evaluated the influence of the holding tank mixing conditions (mixer speed and rotation direction) and the influence of sensor rinsing between sheets.

The experimental layout is provided in the plan document.

Results

Sheet-to-sheet Uniformity

Figure 1 shows the sheet-to-sheet weight for the four experiments run. Data was found to follow the same trend seen with the use of this system – sheet weights degrade slowly throughout the run. However, this trend appears to be more significant for experiments 1 and 4 than for experiments 2 and 3. Experiment 3 in particular appears to have produced mostly stable sheet weights when noisy sheets are removed.

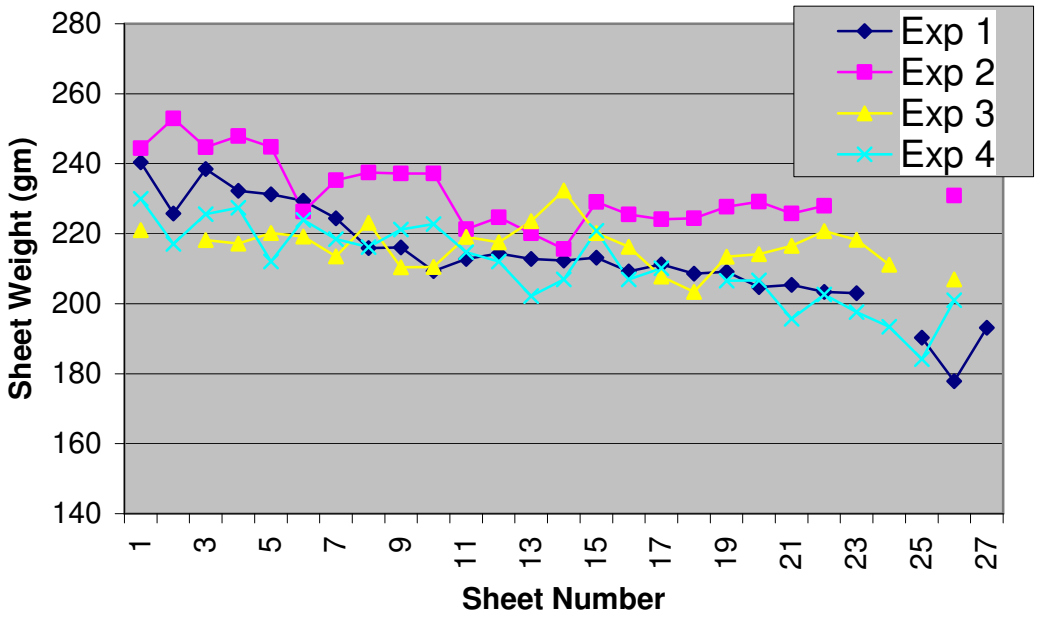

Figure 1. Sheet weight trend for experimental runs.

The data were fitted with linear curves, producing the following data (Table 1). As seen in the table, experiments 2 and 3 showed considerably less slope than experiments 1 and 4. Experiment 3 showed a liner fit slope much lower than all experiments. The curve fit slope was averaged with respect to the experimental conditions to examine the effect of each variable on sheet-to-sheet consistency. Table 2 shows the results.

Table 11. Experimental arrangement and sheet weight linear curve fit results.

Experiment	Mix Rotation	Mix Speed (rpm)	Probe Rinse	Linear Slope (gm/sheet)	Linear Intercept (gm)
1	CW	400 +/- 10	Yes	-1.7114	236.6
2	CW	300 +/- 10	No	-0.9425	243.4
3	CCW	400 +/- 10	No	-0.2877	220.3
4	CCW	300 +/- 10	Yes	-1.3029	228.4

As can be seen in Table 2, differences were resolved for the experimental conditions of the experiment, although statistically significant differences were not found with the limited data set (only four experiments). The most surprising result was the significant effect that the rinsing operation appeared to have on the sheet uniformity. With sensor rinsing, the sheets tended to lose significantly more weight from sheet to sheet. Observations during the run noted that the rinsing operation (consisting of a spray nozzle connected to a garden hose) tended to drip a great deal. Operators were instructed to discharge this water prior to starting a sheet. The rate of drip was not measured.

Table 12. Slope of linear fit averaged per experimental condition. Significant effect indicated by t-ratio greater than 4.3 for this experiment.

	Average Slope (gm/sheet)	T-ratio
CW Rotation	1.33	0.84
CCW Rotation	0.80	
300 rpm	1.12	0.17
400 rpm	1.00	
Rinse	1.51	2.32
No Rinse	0.62	

It appears that the rotation of the mixer can have a strong impact on sheet uniformity. Observations during the run noted that the mixing seemed significantly more active with the rotation counterclockwise than when it was clockwise. When counterclockwise, the blade rotation pushes the fluid up toward the top of the tank and away from the tank bottom, where the solution is pulled for transfer to the batching tube. It is thought that this type of mixing (CCW) would be beneficial in encouraging heavier particles to be more uniformly distributed in the mix and keep the mixing momentum away from the pump entrance (tank bottom). More investigation is needed to confirm this as a contributing variable. Mixing speed may have an influence as well. Higher speeds tended to produce better results.

<u>Within Sheet Uniformity</u>

Four sheets were punched in 11 places (per standard practice), and measured for weight uniformity. The within sheet weight standard deviation was measured for each sheet with the results shown in Table 3, along with notes taken after the premixing step.

Table 13. Within sheet uniformity results, and notes taken after premixing step.

Experiment	Average Standard Deviation (%)	Notes (general and in 500 ml cylinder)
1	4.65	Flocks sinking slowly, ½ of flocks floating after 1 hour, flocks appear clustered, medium size flocks
2	6.34	Meduim size flocks, clustering together, Flocks sinking moderate rate
3	4.73	Small flocks sinking quickly, ½ of flocks floating after 1 hour
4	6.47	Small flocks sinking quickly, ¼ of flocks floating

The within sheet standard deviation was evaluated statistically with the following results (Table 4). Surprisingly the data indicate that the mixer speed significantly influences the within sheet uniformity. While this result would provide valuable insight into the problem of within sheet uniformity, this result should be reviewed and investigated in more detail, as many other factors might contribute to uniform sheet production. One other factor has to do with the mixture chemistry and solution chrematistics. Table 3 shows operator notes for the experiment. Experiments 1 and 3, producing the better within sheet measurements, had similar solution characteristics with the solution tending toward floating. Further investigation is needed to clearly pinpoint the significant variables.

Table 14. Within sheet variable evaluation. Significant effect indicated by t-ratio greater than 4.3 for this experiment.

	Average Within Sheet Standard Deviation (%)	T-ratio
CW Rotation	5.5	0.09
CCW Rotation	5.6	
300 rpm	6.4	22.5
400 rpm	4.7	
Rinse	5.6	0.02
No Rinse	5.5	

<u>Summary</u>

This experiment evaluated mixing conditions in the holding tank that may contribute to sheet-to-sheet consistency. The variables investigated included holding tank mixer rotation direction, mixer speed, and batching tube sensor cleaning. A linear curve fit to the sheet-to-sheet weights was used to evaluate the consistency results. Results showed that none of these variables produced showed statistically significant effect. The practice of rinsing the sensor (shown to have the greatest impact – negative to sheet consistency) is thought to have imparted significant variation to the operation of the system, influencing results. Mixer rotation direction

counterclockwise, pushing the material to the top of the tank) showed benefit to sheet consistency, as did higher mixer speeds.

Within sheet variation was measured and evaluated statistically. Surprisingly, the results showed extremely high correlation of sheet uniformity with mixer speed. It is thought that some other variables are also contributing to within sheet uniformity, despite the high correlation with mixer speed. Future analysis will pay close attention to the relationship between mixer speed and sheet uniformity.

Additional testing is needed to further investigate holding tank mixing variables, as the results of this test showed enough evidence that the property can be strongly influenced by conditions in the holding tank.

Bipolar Plate Mixing DOE Report

Summary

The objective of this experiment was to investigate the impact of mixing variables on within-sheet uniformity and sheet-to-sheet uniformity within a standard bipolar plate batch. This experiment targeted a number of variables within the mixing process, primarily downstream at the holding tank. These included the holding tank mixer rotation and mixer speed, the size of the blade used in the holding tank, the number of blades for mixing and the amount of mixing in the Saturn-6 chamber. The mixer in the Saturn-6 traditionally remained idle until the entire sheet of material was pumped over to the chamber, thus not agitating the sheet mixture until the chamber was full. The opposite extreme was introduced for this DOE by mixing the sheet material as it was pumped into the Saturn-6 chamber.

The assumption was made that the material batching process in the mixing tank did not affect the sheet uniformity or sheet-to-sheet uniformity, which was based on the results of the order of addition experiment BP-04-001.

By way of analysis on the effects of each variable independent of one another, the optimal levels for each variable gave the following “best case” prediction.

Mixer Direction:	CCW
Mixer Speed:	400 RPM
Blade Size:	12 inch diameter
Number of Blades:	2
Saturn-6 mixing:	As soon as material enters the chamber

One test batch was run at the above conditions and the results did not meet expectations. The sheet-to-sheet uniformity rose to 4.217% standard deviation with a negative slope of –1.3997. The goal for sheet-to-sheet uniformity is 2%. Experiment 6 produced sheet-to-sheet uniformity of 1.47%, with one 12” blade and lower speed being the only differing parameters from above. Looking at All Combinations Analysis, blade size alone accounted for 86% of the variation. Blade size combined with the number of blades accounted for 98%. Creating a model based on the slope analysis points to two 10” blades or one 11” blade for optimal sheet-to-sheet uniformity, achieving near-zero slope. Further experiments are recommended to test this analysis as true. Based on this same model, one 12” blade is best for our current production process. Thus, the following mixing settings are recommended at this time with further experiments to follow.

Mixer Direction:	CCW
Mixer Speed:	400 RPM

Blade Size:	12 inch diameter
Number of Blades:	1
Saturn-6 mixing:	As soon as material enters the chamber

A second mixing experiment was performed to evaluate further the influence of mixing variables on consistent sheet-to-sheet weights. The report of this effort follows:

Bipolar Plate Mixing DOE

Introduction

The objective of this experiment was to investigate the impact of mixing variables on within-sheet uniformity and sheet-to-sheet uniformity within a standard bipolar plate batch. This experiment targeted a number of variables within the mixing process, primarily downstream at the holding tank. These included the holding tank mixer rotation and mixer speed, the size of the blade used in the holding tank, the number of blades for mixing and the amount of mixing in the Saturn-6 chamber. See Figure 1 for physical layout of system operation.

Figure 1 **Holding Tank and Saturn Six Chamber**

Material is pumped into the Holding tank from the lower Mixing tank where all the ingredients are added and mixed together. The shaft in the Holding tank is angled down into the tank. One blade is attached to the bottom of the shaft and one can be attached about 12" from the bottom. One sheet of material at a time is pumped into the Saturn Six chamber. This sheet of material then dispenses into the pan below to form a sheet.

The assumption was made that the material batching process in the mixing tank did not affect the sheet uniformity or sheet-to-sheet uniformity, which was based on the results of the order of addition experiment BP-04-001.

The measurables recorded at each batch included the sheet wet weight and dry weight, coupon dry weight and fired weight. Beginning with the 4th sheet formed and every 6th sheet thereafter, 11 coupons were punched from each sheet to measure within sheet uniformity. The coupons

were punched out of dry formed sheets. The locations for each punched coupon are estimates and not punched to exact specifications. See Figure 2.

Figure 2 **Location of 11 coupons in a sheet for within sheet uniformity**

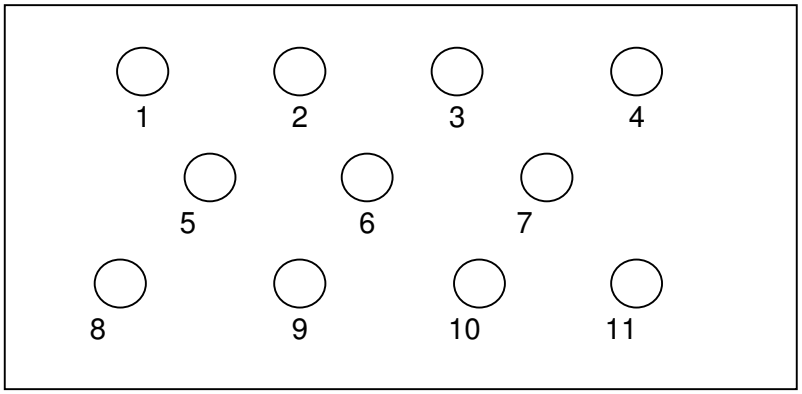

Once the coupons were weighed dry they were fired in the continuous furnace. Their fired weights were taken and compared with the dry weights to evaluate consistent and expected weight loss.

Design of the Experiment

There are five variables in this two-level design of eight experiments. The mixer direction and mixer speed were included in a previous mixing DOE. Those results did produce extremely high correlation of sheet uniformity with mixer speed, but further investigation in this relationship was advised. Higher speeds did tend to produce better sheet-to-sheet uniformity.

With regard to mixer direction, it appeared that the rotation of the mixer had a strong impact on sheet uniformity based upon the results of the previous mixing DOE. It was thought that mixing counter-clockwise, pushing the material up, would be beneficial in encouraging heavier particles to be more uniformly distributed in the mix and keep the mixing momentum away from the pump entrance at the tank bottom. More investigation in this idea was recommended to confirm mixer direction as a contributing variable.

No investigative study has been conducted this far on the blade size or number of blades for optimal mixing conditions. These two variables were taken as experimental variables to see what, if any, difference they made in sheet uniformity and batch production.

The mixer in the Saturn Six normally remained idle until the chamber was completely filled with batch material. This allowed for possible settling of the particles, as well as increased foam production. Continuing to mix the material as it enters the chamber might reduce the amount of foam or at least maintain the material distribution within the mix.

The eight experiments were run in random order to guarantee that the effects by cofactors would be divided fairly and any possible extraneous factors associated with time would be eliminated. Table 1 lists the design matrix for the eight experiments.

Table 1 Design Matrix for Mixing DOE, two-level, five variable, eight experiments

Run Order		Mixer Direction	Mixer Speed	Blade Size	Number of Blades	Saturn-Six Mixing Time

6	Experiment 1	CW	300 RPM	8”	1	Full
3	Experiment 2	CCW	300 RPM	8”	2	Empty
4	Experiment 3	CW	400 RPM	8”	2	Empty
7	Experiment 4	CCW	400 RPM	8”	1	Full
5	Experiment 5	CW	300 RPM	12”	2	Full
2	Experiment 6	CCW	300 RPM	12”	1	Empty
8	Experiment 7	CW	400 RPM	12”	1	Empty
1	Experiment 8	CCW	400 RPM	12”	2	Full

Cofactors

A number of cofactors were taken into consideration throughout this design of experiments as having possible emphasis on the results of forming.

- The question arose as to whether all the material in the mixing tank circulates through the deflaker. After a certain amount of time it is estimated that all the material should pass through the deflaker. Without doing too much work on this, it is estimated that after 20 minutes all of the material will have gone through the deflaker at least once. This does not propose to be a problem at this time.

- The location of the blade on the mixing shaft remained constant due to the design of the shaft.

- The mixing blades in the Saturn-6 remained the same and were not altered for variation in mixing pattern or circulation direction.

- No dispersant was added to the batch material. It’s use and performance is still under investigation.

- The parameters for drying sheets remained constant to standard production. This is an area for further independent investigation.

- Premixing of the material was done in bags, as opposed to buckets.

Procedure Alterations

It should be noted that for experiments 1 and 5, 2-3 grams of Nitric Acid were added to the Resin during predispersion in the Silverson mixer to lower the pH of the Resin. It was revealed that the addition of Nitric Acid to the Resin would reduce the foam creation in mixing and possibly eliminate the need for pH balancing later on in the mixing process. This step was removed and recommended for investigation in a separate DOE.

The shaft in the mixing tank consistently fell off the mixer during the mixing operation in the holding tank. This occurred an average of once per experiment and was due mostly to removing the shaft for regular changes of the blade sizes and amounts.

Results and Discussions

Sheet-to-Sheet Uniformity

The sheet weights vary greatly at the end of the batch due to lack of material in the bottom of the tank and the probability of entraining air. Because of this, only the first 22 sheets were taken into account for sheet-to-sheet uniformity. Experiment 1 produced sheet weights that grew heavier through the batch process, thus resulting in a very high positive slope. This behavior did not fit our model. The results of this experiment heavily skewed the data and because of this, experiment 1 was rerun to check results. The results of exp. 1 rerun were consistent with the sheet weight trend of the original exp. 1. Although the slope came closer to zero, it remained too high to include in the analysis. Table 1 shows the output results for all of the experiments, including exp 1 rerun and exp 9—best case.

Table 1 Mixing DOE Output Variables Results

Experiment (1st 22 sheets)	Slope	%StDev for Avg. Sheet Weight	Variance for Avg. Sheet Weight	% StDev for Avg. Coup Weight	Variance for Avg. Coup. Weight
TARGET→	**<0.1**	**2%**		**1%**	
1	6.8114	15.71	2325.73	17.0	0.1169
2	0.751	2.6	54.76	3.92	0.0044
3	0.532	2.73	73.94	6.90	0.0181
4	1.4105	6.12	370.32	8.33	0.0252
5	-0.8773	2.56	57.40	4.50	0.0068
6	-0.3285	1.68	19.05	4.51	0.0037
7	-0.4616	5.42	255.73	10.75	0.0419
8	-0.7193	3.27	67.51	16.90	0.0122
1 rerun	4.6249	10.22	1019.64	13.07	0.0628
9 “best case”	-1.3997	4.21	134.88	6.22	0.0111

During the run of Experiment 1 there was a lot of foam sitting atop the surface of the batch while in the holding tank. It is thought that because of the smaller blade size, the lower speed and the clockwise direction of the mixer, the mixing power was not strong enough to break the foam on the surface until the entire batch level dropped closer to the blade. Therefore, the weights earlier in the batch were lighter than those later on when the material in the foam was mixed into the rest of the batch, accounting for the high positive slope in the sheet weight as a function of sheet number in the batch.

To determine whether a significant impact occurred in each independent variable between levels, the F-Ratio test was conducted for each variable. Table 2 lists the results of the F-Ratio test for sheet-to-sheet uniformity.

Table 2 F-test results at 95% Confidence Level

	Mixer Direction	Mixer Speed RPM	Blade Size diameter	Number of Blades	Saturn Six Mix Time

	CW	CCW	300	400	8”	12”	1	2	Full	Empty
Variances	644.42	123.50	572.91	183.6	662.72	92.73	708.93	61.22	661.8	93.67
F value	5.218		3.120		7.147		11.58		7.066	
F Critical one tail	1.429		1.430		1.430		1.429		1.430	

If the F value is greater than the F Critical value then there is significant difference in variance at a 95% Confidence Level. As can be seen there was significant difference in each of the five variables. The greatest significance for sheet-to-sheet uniformity was in the number of blades. Two is better than one. Next in significance was the blade size. The larger blade is better. Following these results, we ran a test under these prescribed conditions, experiment 9. Unfortunately the results were no better and in some cases worse than other experiments.

A model was created based upon the experiment results through the use of Minitab Statistical Analysis package. Table 3 shows the model predictions based on the blade size, the number of blades and the Saturn six mix time set at varying parameters.

Table 3 Model results for reaching Zero Slope

Blade Size	Number of Blades	Saturn Six Mix Time	Slope
8	1	Empty	1.3747
8	2	Empty	0.6413
10	2	Empty	-0.2437
11	1	Empty	0.0472
12	1	Empty	-0.3953
12	2	Empty	-1.1287

Charlie Hendrix, a friend and mentor to Selee and PFCT who is well versed in statistical analysis, shared some advice and direction toward how to properly and accurately analyze data of this sort. When analyzing the data, he removed the results of Experiment 1 because they are so “off the wall” that they heavily skewed the data. He ran a stepwise regression analysis, which is based on comparing the averages and finding the main effects in the data. A linear model was fit to the data to acquire a slope of zero. This model produced results that agreed with the Minitab model. In Charlie’s model, he found the single most important variable was Blade Size. The second important variable was number of blades. The equation for the slope of the line is shown below.

Slope = 4.986 – 0.397*(Blade Size) – 0.550*(Number of Blades)

Using this equation, Table 4 lists the predictions made for reaching a slope of zero. Note that BS is blade size and NB is number of blades. The slope for one 8" blade predicts the worst slope. This is in agreement with Experiment 1, which used one 8" blade and had a high slope of 6.81. Notice the slope for two 10" blades is –0.0783 and for one 11" blade is 0.0747. These two cases predict to reach closest to zero. These results do correlate to those of the Minitab Analysis model, which predicts one 11" blade to reach a slope of 0.0472, even closer to zero.

Table 4 Results of slope equation to reach zero slope

BS	NB	Slope
8	1	1.26
8	2	0.71
9	1	0.863
9	2	0.313
10	1	0.466
10	2	-0.084
11	1	0.069
11	2	-0.481
12	1	-0.328
12	2	-0.878

Another type of analysis is the All Combinations analysis in which every kind of combination of the 5 variables is evaluated to see which accounts for the greatest variation. Blade size alone accounts for 86% of the variation. The combination of blade size and number of blades accounts for 98% of the variation. No two other combinations come close to accounting for more variation than 98%. For three variable combination, mixer direction, blade size and number of blades account for 99%. This is not a significant difference from 98%. Thus, the analysis once again points toward blade size and number of blades for the most significant influence.

Within-Sheet Uniformity

An analysis of variation among coupons within sheets was also carried out with the help of Charlie Hendrix. His results on the analysis of variation, nested-design, on the dry weights of the coupons, with 95% confidence limits, are listed in Table 5. The coupon weights are combined for the 4 sheets in each experiment.

Table 5 Analysis of Variation on Coupon Weight within a batch

	Exp	1	2	3	4	5	6	7	8
Coupons	StDev	0.1592	0.0555	0.1223	0.0883	0.0816	0.0608	0.1876	0.1068
	Var.	0.0254	0.0031	0.0150	0.0078	0.0067	0.0037	0.0352	0.0114

Further analysis of coupon variation within sheets resulted in no one variable having statistical significance. However, mixer direction has a marginal effect with a t-ratio of 2.31. The T-critical value at 95% confidence level is 2.46. The model equation for this analysis is shown below.

StDevWithinSheets = 0.198 – 0.0598*(Mixer Direction)

A comparison was made between the dry weight and the fired weight of the coupons to test uniformity in weight loss after firing. The amount of weight loss is expected to be between 18-19%. After pressing, parts lose only about 1.5% of pre-press weight. After firing in the continuous furnace, parts lose about 12.5% of pre-fired weight. These measurements are based on a batch made process. The current parts used in this DOE are composed of a little different chemistry. That difference accounts for an added 4.5% weight loss in the parts after firing. Thus a total of 18.5% weight loss is expected. Note, these coupons were not pressed before being fired. Table 6 lists the results of percent weight loss for each sheet. The full list of weight loss by each coupon can be found in the appendix. The results vary between 18% and 24% weight loss from firing.

Table 6 Average Percent Weight Loss for each sheet of Coupons fired

Sheets	**Exp1**	**Exp2**	**Exp3**	**Exp4**	**Exp5**	**Exp6**	**Exp7**	**Exp8**

4	21.11	22.55	19.58	18.88	19.78	17.46	18.80	19.73
10	20.78	20.31	19.19	18.93	20.24	17.71	18.89	19.38
16	24.54	19.52	19.15	19.06	19.60	17.99	19.63	20.57
22	22.86	19.66	18.52	19.51	19.74	19.71	17.97	19.56

This difference of 6% in variation of weight loss can be due to any number of reasons. One might be due to material loss in forming, through the screen. Another possible reason is moisture in the parts. Maybe the parts were not fully dry before they were fired. The parts could also be losing material in handling of the coupons. The range from 18% to 24% is not necessarily unacceptable. At this point in development, no standard acceptable weight loss has been set.

Recommendations

Significant effort and time was spent analyzing this data. At the present time there is not a standard method for analyzing the data produced from experimental testing that is practiced by all in-house. It would be highly beneficial to develop a method of analyzing data that would produce accurate statistical results and conclusions for all to use. The Stepwise Regression analysis is a thorough test to run for statistical analysis on data of this type. Another additional test to run is an All Combinations analysis, which discovers the main effects in any combination of the variables used.

Key findings in Mixing DOE results

- Mixer Direction of CCW is better than CW
- Blade Size of 12” is better than 8”
- For Number of Blades, 2 is better than 1.
- The combination of blade size and number of blades remains to be seen which is best—further testing to be carried out in this area.
- Mixer speed appears to be insignificant according to the model, but due to the results of different experiments, the influence of mixer speed requires further investigation.
- Within-Sheet uniformity is not highly affected by the variables in this Mixing DOE
- Experiment 1 was repeated and produced the same results in sheet weight as a function of sheet number formed in the batch. It is speculated that there is some interaction going on but has yet to be found.
- The variable parameters for Experiment 1 and 4 did not fit our model and are most undesirable.

Further mixing experiments are recommended to test the validity of the outcomes predicted by the models. The specifications for experiment 6 mirror those of the best-case prediction except for the speed. The results of Experiment 6 held the best sheet-to-sheet uniformity. Therefore, a short follow-up mixing DOE will target the impact of mixer speed on the sheet-to-sheet uniformity and different blade sizes and numbers based on the results of the slope-analysis model that pointed toward two 10” blades or one 11” blade to reach zero slope.

Until the next mixing DOE is carried out and the results evaluated, it is recommended to run under the following parameters.

Mixer Direction:	CCW
Mixer Speed:	400 RPM
Blade Size:	12 inch diameter
Number of Blades:	1

Saturn-6 mixing: As soon as material enters the chamber

Through applying the learning from this experiment, we were able to identify mixing conditions that minimized sheet-to-sheet weight variation.

The within sheet variability is even more important to improve in this program. Our long-term target for within sheet uniformity is <1% standard deviation on 11 punched coupons (punch pattern shown in the figure above). When the new forming process was begun, our within sheet uniformity averaged between 6-10% standard deviation. The following report shows an a study designed to understand the important variables controlling within sheet uniformity.

ORDER OF ADDITION EXPERIMENT REPORT

Introduction

An experiment was performed to evaluate the effect that the order that ingredients are introduced to the system has on sheet uniformity. The experiment was performed as indicated in the experimental plan.

Results

Within sheet uniformity

Every third sheet was punched to obtain discs used for basis weight measurement. The pattern was as in the drawing below (Fig. 1). The exact positions were not punched, but were only approximate. Sheet trimming, also was approximate in placement relative to the untrimmed sheet.

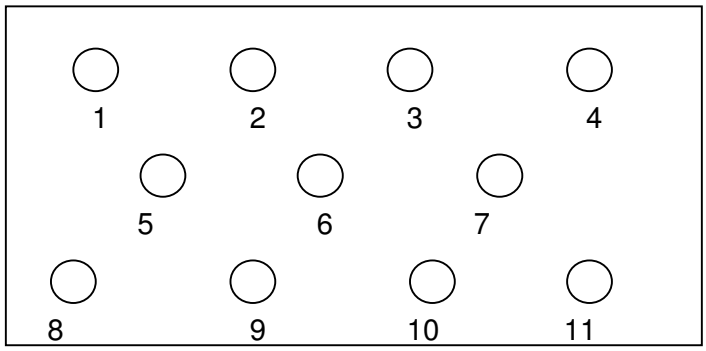

Figure 1. Pattern used for within sheet uniformity evaluation.

Figure 2 shows the experiment-wide average normalized punch weight. As can be seen, there was a tendency for the punches to be somewhat lighter (~4%) near the edges of the sheet compared to the central portion of the sheet.

Figure 3 shows sheet punch standard deviation for each experiment. Experiment 6 stands out as having the highest level of punch deviation (poorest uniformity). This experiment was repeated with similar results. Figure 4 shows the experiment-wide average sheet deviation against sheet number in the batch. As stated above, every third sheet of the run was punched and measured. Figure 4 shows that within sheet uniformity improves after the first 6 sheets have been run, and in general throughout the run. Removing the first two measured sheets (the 3rd and 6th sheets of the run) from the data set yields Fig. 5. Clearly outlier sheets are eliminated, suggesting that experiment 6 may not be in error, but influenced strongly by the first two measured sheets of the run.

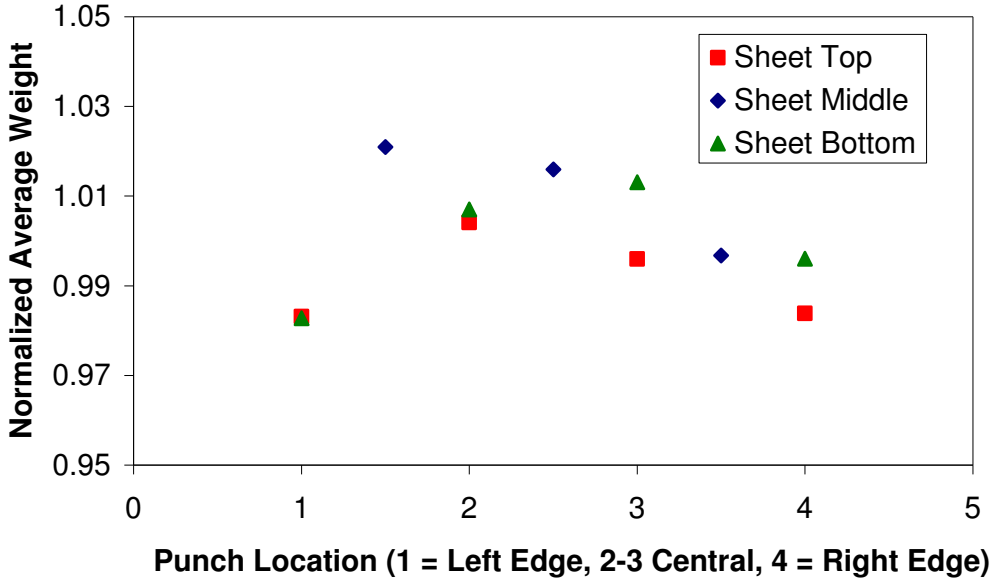

Figure 2. Normalized average punched disc weight (experiment wide average) relative to sheet position. Data shows sheets are slightly lighter on edges and heavier in the middle.

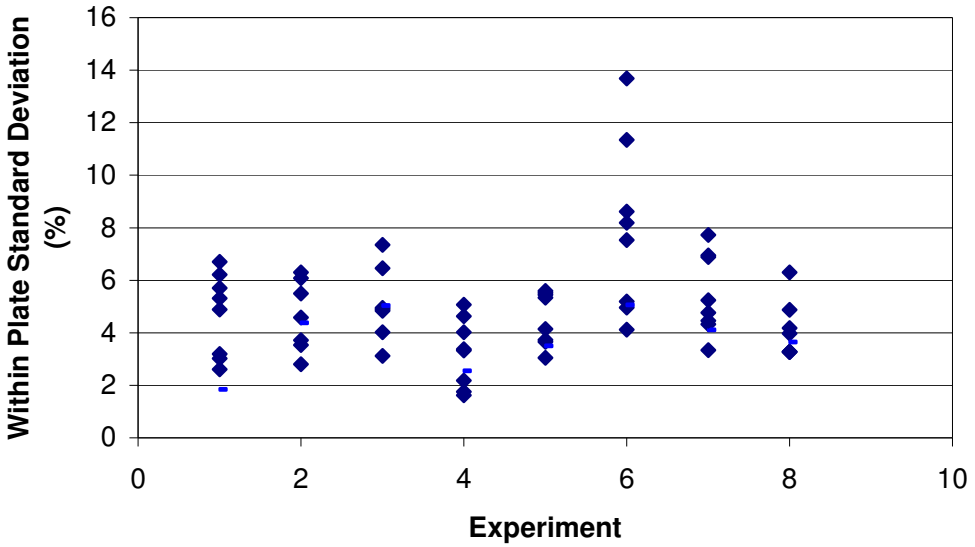

Figure 3. Within sheet standard deviation vs. experiment.

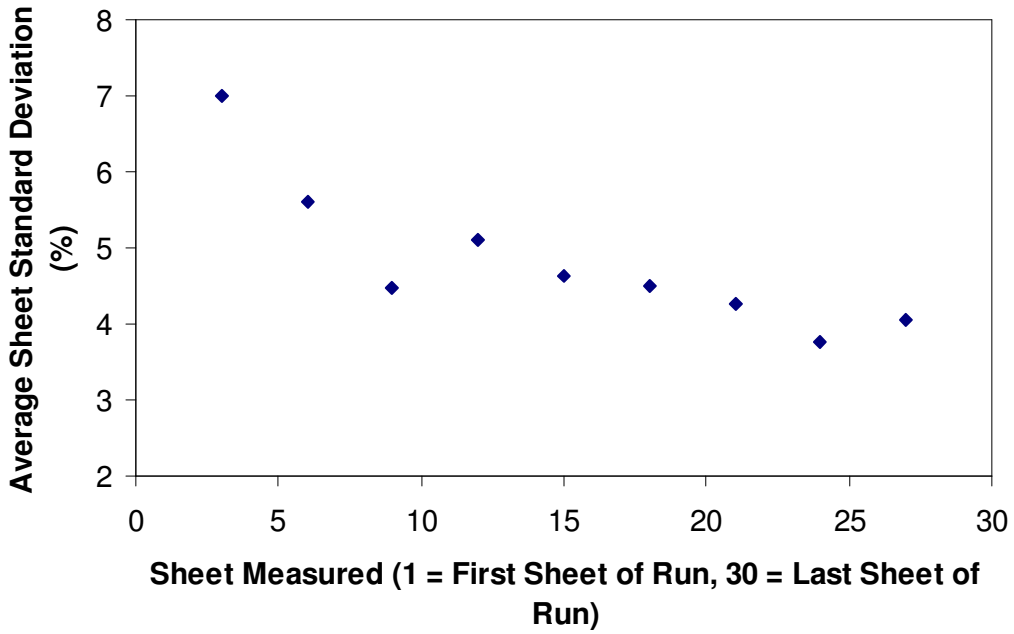

Figure 4. Within sheet standard deviation vs. sheet sequence. Start of run shows more non-uniformity than bulk of run.

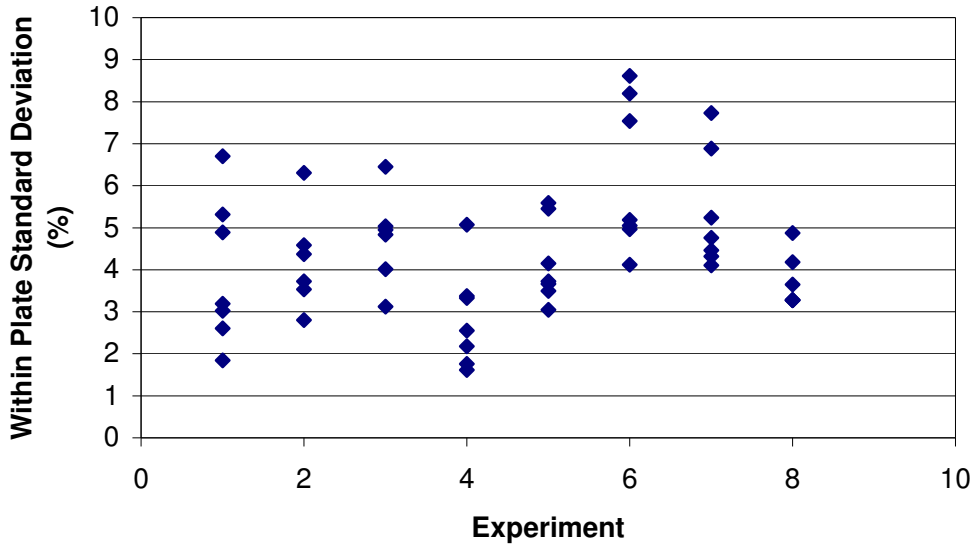

Figure 5. Within sheet uniformity standard deviation with first two sheet measurements removed.

Table 1 shows a statistical summary of the experimental investigation for all data and for data with the first two measured sheets removed. As seen, the only variable that showed a significant effect upon the results was resin ball milling vs. no ball milling. A significant effect is defined by a statistical t-ratio greater than 2.4 for this experiment. Ball milling the resin showed a positive impact on within sheet uniformity. However, for this study (7 variables in 8 experiments), main effects may be confounded with two level interactions. For this experiment, the resin mixing is confounded with the following variable interactions

Resin Mixing = Premix/Bag & Natural Location (variables 4 & 2)
= Natural Deflake Time & Total Deflake Time (variables 1 & 7)
= B1000 Order & Matrix Sinlge/All Addition (variables 3 & 5)

It is possible for a variable interaction to be significant without the main variables having a significant effect. However, this is usually not the case. A mirror image of this experiment would need to be run to fully determine if the resin mixing most significantly effects within sheet uniformity, or if it is one of the above two-level interactions.

Table 15. Summary of statistical results for within sheet uniformtiy. Significant effect is indicated by t-ratio greater than 2.4 for this experiment.

		All Sheets		1st Two Measured Sheets Eliminated	
Variable #	Variable	Average Stdev(%)	T-ratio	Average Stdev(%)	T-ratio
1	Natural Deflake 20 min 60 min	 4.3 5.4	1.18	 3.9 4.9	1.36
2	Natural Loc.		0.92		0.61

	In Tank Holding Tk	4.4 5.3		4.2 4.6	
3	B1000 Order 1st 2nd	 4.6 5.1	0.49	 4.3 4.5	0.22
4	Premix Premix Bag Mix	 4.9 4.8	0.07	 4.3 4.5	0.36
5	Matrix Single All	 5.3 4.4	1.00	 4.7 4.1	0.68
6	**Resin Mixing** **Ball Mill** **Disperse**	 **4.0** **5.7**	**2.22**	 **3.7** **5.1**	**2.80**
7	Deflake Time 5 Min Duration	 5.1 4.6	0.59	 4.6 4.2	0.49

The best combinations of the above variables were run in three batches to manufacture sheet with low within sheet variation. These variables were as follows:

20 minute natural deflake time
Natural in holding tank
B1000 added before matrix
Premix matrix (very small effect)
Add matrix all at once
Ball mix resin
Deflake for duration

Results did not show improved sheet uniformity compared to other experiments in this study. The net within sheet standard deviation was measured to be 7.5% for the sheets measured (two batches have not been measured and recorded as of the time of this report). This is worse than any of the experimental batches. Other sources of variation (operator, equipment, water temperature, water quality, pH resolution and measurement, etc.) could have contributed to the poor within sheet uniformity results indicated in this experiment.

Sheet-to-sheet Uniformity

Data collected to date has shows a significant decrease in sheet weight as the batch material is consumed. A sheet weight loss at a rate of approximately 2 gm/sheet (trimmed sheet) has been noted for most runs. Figure 6 shows the sheet-by-sheet weight for the experiments.

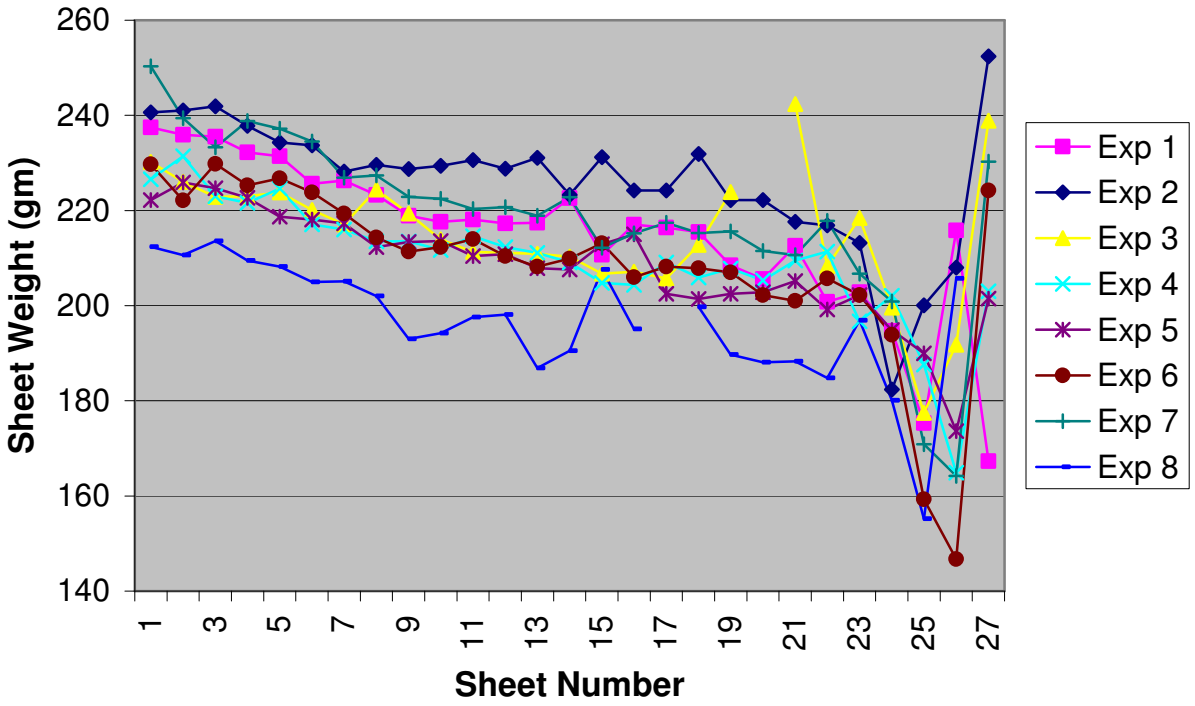

Figure 6. Sheet to sheet weight variation through experimental batch runs.

Examining the data in Fig. 6, it is apparent that most compositions showed significant weight loss throughout the run. However, two runs showed relatively constant sheet weight through a large portion of the runs. These are experiments 1 and 2. Neither of these runs showed better than average within sheet uniformity. As will be reviewed below, experiment 2 showed chemistry behavior of excellent suspension and very little flock settling over time. Experiment 1 notes on chemistry behavior are incomplete.

Solution Chemistry Observations

During experiment operation, samples were taken after mixing and pH adjustment, placed into a 500 ml flask and allowed to settle. The final filtrate volume was recorded after two hours. Experiment 1 filtrate volume was not recorded or photographed. The character of the filtrate varied considerably for the experiments. Experiment 2 held flocks in suspension (even overnight). Most of the other solutions showed rapid material settling. Most solutions showed significant flock clustering (flocks sticking together). Some experiments did not require pH adjustment. Those that did required a small amount of nitric acid addition to achieve near 7 pH. No clear trend was established between filtrate volume and within sheet uniformity, as seen in Fig. 7. Sheet-to-sheet uniformity may be impacted by the solution behavior, as discussed above. Experiment 2, showing little or no suspension settling, produced the most uniform weight sheets throughout the run. Solution chemistry that provides excellent flock dispersion without flock clustering is thought to be key to the success of both within-sheet and sheet-to-sheet uniformity.

While experiment 2 showed good sheet-to-sheet uniformity, it did not produce better than average within sheet uniformity.

Figure 7. Photographs of solution chemistries.

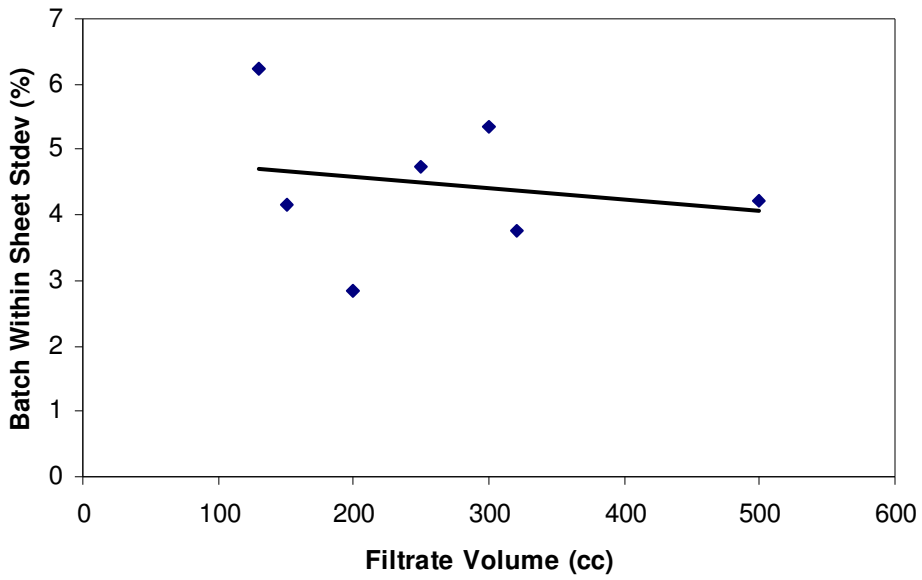

Figure 6. Trend of filtrate volume and within sheet uniformity. No clear trend is evident.

Conclusion

This experiment was run to evaluate material order of addition and some mixing variables on resulting sheet uniformity (both within sheet and sheet-to-sheet). Statistical review of the data indicates that within sheet uniformity was influenced by only a single variable (resin ball milling vs pre-dispersion – with ball milling preferred for within sheet uniformity). However, because seven variables were investigated in eight experiments, the effect of this variable may be confounded with two-level variable interactions. To fully clarify this, an additional eight experiments mirroring those run here would need to be run. This work is not planned.

It was found that within sheet uniformity improves as the batch run progresses. The first few sheets show poorer within sheet uniformity than those formed later in the batch.

It was found that sheet-to-sheet weight decreased from the start of the run to the end of the run. Sheets decrease through the bulk of the run at a rate of approximately 2 gm/sheet (for trimmed sheets).

Best condition sheets were run with a combination of variables that had the indication of best case within sheet uniformity. Although only one of three batches was measured in time for this report, the best-case conditions did not show any improvement in within sheet uniformity. Uniformity was actually worse for this run.

Solution chemistry varied considerably from experiment to experiment. It is not known if this variation resulted from the conditions of the experiment, or from run-to-run variation. Some indication of improved sheet-to-sheet uniformity was apparent for a solution with good solution dispersion (slow settling rate).

Additional study is needed with solution chemistry, material composition, and additional mixing parameters to improve both within-sheet and sheet-to-sheet uniformity.

A study on forming variables with the system was performed to improve product uniformity. Here variables were learned that improved the uniformity over what had been seen before.

Bipolar Plate Forming DOE Report

Summary

The purpose of this experiment was to optimize forming techniques to improve sheet uniformity and sheet-to-sheet uniformity within a batch. This experiment will target six variables within the forming process—3 control variables and 3 "noise" variables. The 3 control variables are Vacuum Control, Saturn Six Fill Method, and Pan Rinse. The 3 outside variables, or "noise" variables, are pan agitation, vacuum exposure time, and mix time within the Saturn Six before the material is dispersed into the pan. The main effects of this experiment on within-sheet uniformity were Saturn Six fill method, rinsing the pan and the mix time inside the Saturn Six. It appears that vacuum control, pan agitation and vacuum exposure time had very little effect.

The greatest effect to within-sheet uniformity was held by the Saturn Six fill method. The analysis showed that filling from the top was better than bottom fill. Filling from the top of the Saturn Six is most undesirable due to the influence it has on sheet-to-sheet uniformity. Bottom filling reduces the foam amount in the Saturn Six and therefore reduces the amount of foam fed into the pan. This allows the mixture to be well mixed as it flows into the pan and result in higher sheet-to-sheet uniformity within the batch.

Knowing that bottom fill is the way we wish to proceed, it is best recommended to form incorporating the following changes:

- Saturn Six bottom fill method
- No Rinsing of the Pan in between sheets formed
- Mixing in the Saturn Six for 30 seconds produced better uniformity than mixing for 10 seconds

Introduction

The purpose of this experiment was to optimize forming techniques to improve sheet uniformity and sheet-to-sheet uniformity within a batch. This experiment will target six variables within the forming process—3 control variables and 3 "noise" variables. The 3 control variables are Vacuum Control, Saturn Six Fill Method, and Pan Rinse. The 3 outside variables, or "noise" variables, are pan agitation, vacuum exposure time, and mix time within the Saturn Six before the material is dispersed into the pan.

CONTROL VARIABLES

Vacuum Control—Normally, the vacuum remains wide open, i.e. not throttled, pulling 100%. This is a variable of interest to determine the necessary amount of vacuum. For this DOE, a ball valve has been implemented so that the amount of vacuum can be changed by throttling the valve, i.e. opening the valve varying degrees of rotation.

- Throttled—45°
- Not Throttled—wide open

Saturn Six Fill Method—The Saturn Six chamber is just downstream from the holding tank. One sheet of material is pumped into the Saturn Six at a time from the holding tank.

Traditionally the method of filling the Saturn Six has been from the top of the chamber. This method appeared to create more foam in the chamber, which is not desired. This DOE aims to determine the best fill method into the Saturn Six from the holding tank.

- Top Fill
- Bottom Fill

Wash Pan—One sheet of material is dispersed from the Saturn Six chamber at a time into the pan located below the Saturn Six. The material empties in to the pan and sits about 4 inches full. The vacuum pulls the water out, lowering the level in the pan, and a thin sheet of material is left on the screen, while material residue is left on the sides of the pan. Normally this does not get rinsed off until the end of the batch, 25-30 sheets later. For this DOE, we will investigate the influence on within sheet uniformity by rinsing the pan between every sheet formed for an entire batch or not rinsing at all and letting material possibly build up after each sheet.

- Rinse
- No Rinse

"NOISE" VARIABLES

Agitate Pan—Compressed air is fed to chambers under the pan under pressure causing the pan to vibrate, thus settle the material in the pan uniformly.

- On
- Off

Vacuum Exposure Time—The time allotted for vacuum pull on the pan of material into the sheet.

- 25 seconds
- 60 seconds

Mix Time within the Saturn-6—The time allotted for one sheet of material to be mixed in the Saturn Six chamber before it is dispersed into the pan.

- 15 seconds
- 30 seconds

DESIGN LAYOUT

Table 1 is the layout of the DOE plan. This is a four experiment, two level design with a three-variable outer array and another three-variable inner array. Three variables are "control" variables while the other 3 variables are "noise" variables. Table 1 lists the design matrix for the four experiments. The first 2 sheets of each batch will be eliminated as will the last several. The sheets needed for this DOE are numbers 3 through 18. This will enable greater uniformity among the sheets within the batch.

Table 1 Design Matrix for Forming DOE

Exp No.	VacCtrl	FillMthd	WshPan	AgtPan	VacTime	MixTime	Sheet No
1	1	1	1	1	1	1	3-6
				1	2	2	7-10
				2	1	2	11-14
				2	2	1	15-18

2	1	2	2	2	2	2	3-6
				2	1	1	7-10
				1	1	2	11-14
				1	2	1	15-18
3	2	1	2	2	2	2	3-6
				2	1	1	7-10
				1	2	1	11-14
				1	1	2	15-18
4	2	2	1	1	1	1	3-6
				1	2	2	7-10
				2	2	1	11-14
				2	1	2	15-18

Results and Discussions

Within-Sheet Uniformity

The interests in the results of this DOE are primarily with within-sheet uniformity. With the use of Minitab Statistical Analysis, the main effects found for coupon variance are Saturn Six fill method, washing the pan and the amount of time the material mixes in the Saturn Six before dispersing into the pan. Saturn Six fill method held the strongest effect, a t-ratio of 2.64, with top fill being better than bottom fill. Bottom fill is more desirable to maintain better sheet-to-sheet uniformity. Washing the pan and the mix time have about the same effect with t-ratios of 0.98 and –1.02, respectively. Not washing the pan in between sheets is better, while mixing in the Saturn Six for 30 seconds instead of 10 seconds appears to be better. The effects of vacuum control, pan agitation and vacuum exposure time appear to be minimal. Table 2 lists the coupon data.

Table 2 Coupon Data and Results

Experiment	Sheet	CoupAvgWt	CoupStDev	Coup Var	Coup%StDev
1	4	**1.854**	0.0567	**0.0032**	3.061
1	8	**1.894**	0.0626	**0.0039**	3.304
1	12	**1.885**	0.0444	**0.002**	2.358
1	16	**1.644**	0.1233	**0.0152**	7.500
2	4	**1.866**	0.0907	**0.0082**	4.863
2	8	**1.738**	0.1328	**0.0176**	7.643
2	12	**1.805**	0.1478	**0.0218**	8.188
2	16	**1.904**	0.1345	**0.0181**	7.063
3	4	**1.855**	0.0764	**0.0058**	4.117
3	8	**1.789**	0.0787	**0.0062**	4.399
3	12	**1.834**	0.1196	**0.0143**	6.523
3	16	**1.828**	0.0877	**0.0077**	4.799
4	4	**2.035**	0.1063	**0.0113**	5.224
4	8	**1.966**	0.0916	**0.0084**	4.657
4	12	**1.927**	0.1192	**0.0142**	6.184
4	16	**1.9560**	0.1377	**0.0190**	7.040

Sheet-to-Sheet Uniformity

Sheet-to-sheet uniformity was explored in terms of slope. The slope of the sheet weights as a function of sheet number paints a picture of the uniformity within a batch. Breaking down the data to look only at the slope per 4 sheets in each experiment allows us to see the effects of the "noise" variables. Chart 1 in the appendix displays the slopes for all 4 experiments. Table 3 depicts the sheet data and results.

Table 3 Output Variables for Sheet Data

Exp	PanAgt	VacTime	MixTime	Sheets	slope	sheets avg wt	sheets stdev	sheets var	sheets %stdev
					Target→ 0				**Target → 1%**
1	Off	25	10	3--6	-0.87	310.725	2.661	7.083	0.856
1	Off	60	30	7--10	-2.68	305.2	4.193	17.580	1.374
1	On	25	30	11--14	-2.15	300.625	5.396	29.116	1.795
1	On	60	10	15--18	-7.39	275.025	10.105	102.103	3.674
2	On	60	30	3--6	-2.17	305.125	2.985	8.909	0.978
2	On	25	10	7--10	-3.04	294.1	4.557	20.767	1.549
2	Off	25	30	11--14	2.42	314.2	3.136	9.833	0.998
2	Off	60	10	15--18	-5.64	304.85	7.665	58.750	2.514
3	On	60	30	3--6	-3.42	305.65	6.507	42.337	2.129
3	On	25	10	7--10	-8.39	289.775	11.094	123.069	3.828
3	Off	60	10	11--14	1.38	297.5	4.974	24.740	1.672
3	Off	25	30	15--18	-2.03	290.125	4.717	22.249	1.626
4	Off	25	10	3--6	-0.33	330.625	0.971	0.943	0.294
4	Off	60	30	7--10	-0.81	321.375	3.953	15.622	1.230
4	On	60	10	11--14	1.66	321.55	2.417	5.843	0.752
4	On	25	30	15--18	-1.97	314.525	4.213	17.749	1.339

Based on the results of the slopes, it appears that experiment 4 produced slopes closest to zero, with Experiment 1, sheets 3-6 and Experiment 3, sheets 11-14 also reaching close to zero. The settings for Experiment 4 include Saturn Six fill method from the bottom, Vacuum pull wide open and no rinsing between sheets.

Conclusions and Recommendations

The main effects on the coupon variances are Saturn Six fill method, pan washing and mix time in the Saturn Six. Vacuum control, pan agitation, and vacuum exposure time have minimal effect on the coupon variances.

Key findings in Forming DOE results:

- Saturn Six top fill produces better within-sheet uniformity but the bottom fill produces better sheet-to-sheet uniformity.
- Longer mix time for the sheet material in the Saturn Six produces better within-sheet uniformity.
- Not rinsing the pan in between each sheet produces better within-sheet uniformity.

- Best sheet-to-sheet uniformity was produced by Experiment 4 conditions—Vacuum Control wide open, Saturn Six bottom fill method and no rinsing of the pan between sheets formed.

It is not clear which fill method for the Saturn Six should be recommended. Further examination of this may be required to reach more conclusive evidence in determining the strongest effect of the fill method. However, it is recommended to mix longer in the Saturn Six before dispersing material into the pan. Pan agitation did not have an effect on the sheet uniformity, nor did vacuum exposure time or vacuum control. It is advised to continue running at current set conditions for these 3 variables. Therefore, the recommended state to run forming production follows:

Vacuum control:	Wide open, not throttled
S6 Fill Method:	Bottom Fill
Wash Pan:	No washing/rinsing in between sheets per batch
Pan Agitation:	On
Vacuum Time:	25 seconds
Mix Time in S6:	30 seconds

A capability study was performed after characterizing the system and making changes designed to improve product uniformity. A report of the performance of the system after the indicated changes is provided:

Bipolar Plate Process System Performance Study

Phase-I saw significant improvement in both the "With-in Sheet" Uniformity and "Sheet to Sheet" Uniformity. The controlled changes made as a result of the Design of Experiments have proven to be successful and continues to drive the improvements.

With-in Sheet uniformity improved from a standard deviation consistently above .9 grams to consistently less than .05 grams. A marked improvement in with-in sheet uniformity was also noticed by the tighter control obtained over plate dimensional characteristics (shrinkage variation reduced). The second measure for with-in sheet, R-Bar, has also improved from > .35 grams to < .07 grams consistently showing that both the With-in Sheet and the Sheet-to-Sheet uniformity are progressing in the right direction. Graph No.1 shows the standard deviation improvement and R-Bar from before and after Phase-I.

Sheet-to-Sheet Uniformity has also seen marked improvement from batch slopes around the –2.0 mark down to consistently having slopes at +/-.5 and better. The R-squared values for the sheet-to-sheet data have begun to show much more predictability in the run of plates through a batch. Initial standard deviation values were typically in the 9 to 16 grams window. Batches running at the end of Phase-I are typically in the 2 to 5 grams window. Graphs No. 2 & 3 are included below, which show the before and after Phase-I Slopes and R-squared data.

Description of Measures:

- With-in Sheet Uniformity:
  - Standard Deviation is used but is not all-inclusive to defining the uniformity of a sheet. The effects of the "Sheet-to-Sheet" uniformity can influence this and can be misleading.
  - The R-Bar value is representative of all of the sample plugs taken from 4 sheets with in a batch. The desired value is "0" which would mean that not only with in a

sheet are all plugs equal, but between all 4 sheets the plug weights are equal as well. This is the ultimate measurement for Uniformity.

- Sheet-to-Sheet Uniformity:
  - Standard Deviation and the Range are used but are not all-inclusive to the batch dispersion characteristics and can also be misleading at this point (Not until the capability of dispersion with in a batch is achieved will standard deviation be effective in monitoring this portion of the process).
  - The slope of line constructed from the weights of the plates in one batch shows the trend of the batch. The desired value is a slope that is "0". The slope by itself is also not all-inclusive as to the batch being successful or not.
  - R-squared is used to monitor how tightly about the slope the sheet weights fall for a given batch. The desired value is "1".

Summary of Improvements:

- Batching:
  - Improved the weighing of materials and placed tighter controls and tolerances on the weights for improved repeatability.
- Mixing:
  - Optimized mixer configurations, blade speeds, and types of blades. The ideal blade setup at the end of Phase-I is two 10" blades, rotating CCW, located off center of the tank, and rotating around 400 RPM.
  - Significant relationship has been established between a low level in the hold tank and erratic weight control in the formed sheets during the end of the batch-forming run. This is contributed to significant air entrapment and foam creation. The foam causes problems with the repeatability of the individual sheet weights, which is primarily due to the adhesion of material to various components in the system.
- Chemistry:
  - At the end of Phase-I, significant information on the chemistry of the compositions was gained regarding optimal bubble points, permeability, and mixing characteristics. This composition will continue into to Phase-II as the "Frozen Process" until controlled, justified changes based on experimentation are proven. Changes will be controlled, documented, and verified.

Baseline vs. End of Phase-I Uniformity Graphs:

Graph No. 1 (With-in Sheet):

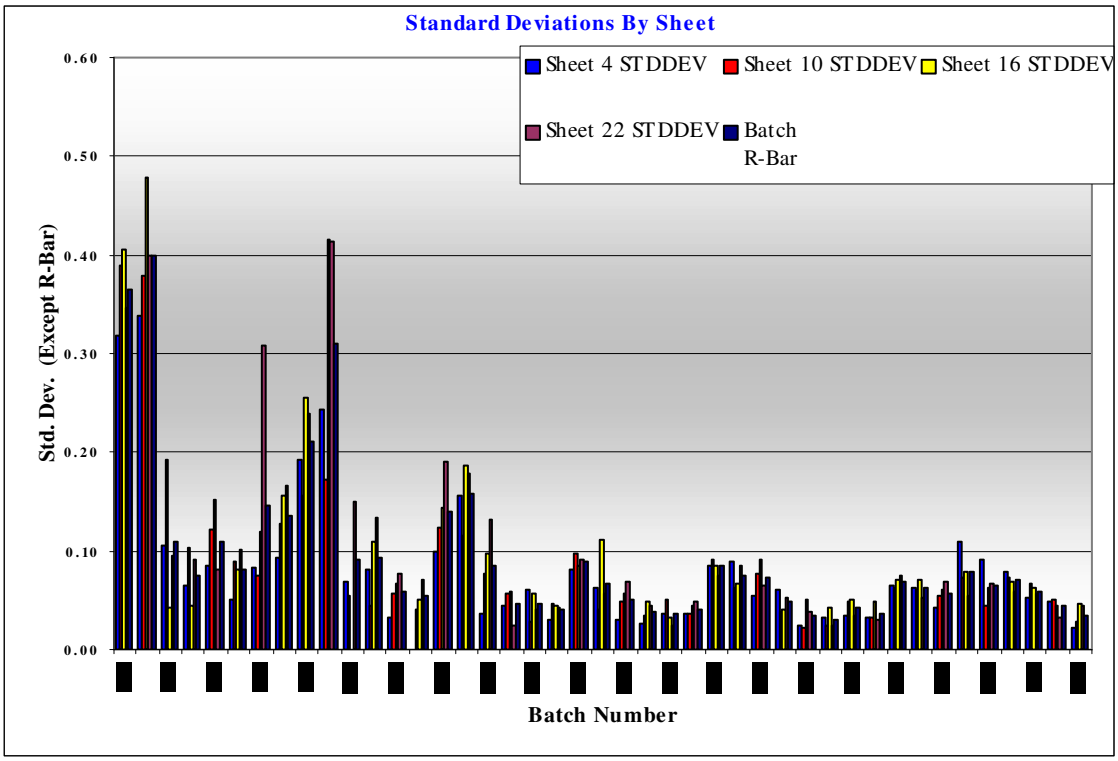

Graph No. 2 (Sheet to Sheet Slope and R-squared):

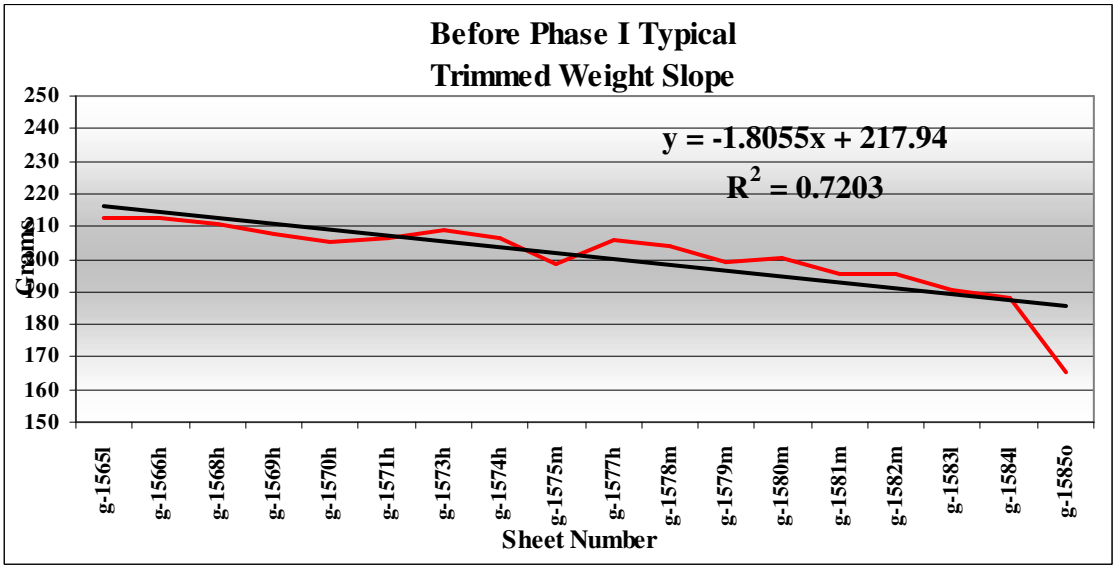

Graph No. 3 (Sheet to Sheet Slope and R-squared):

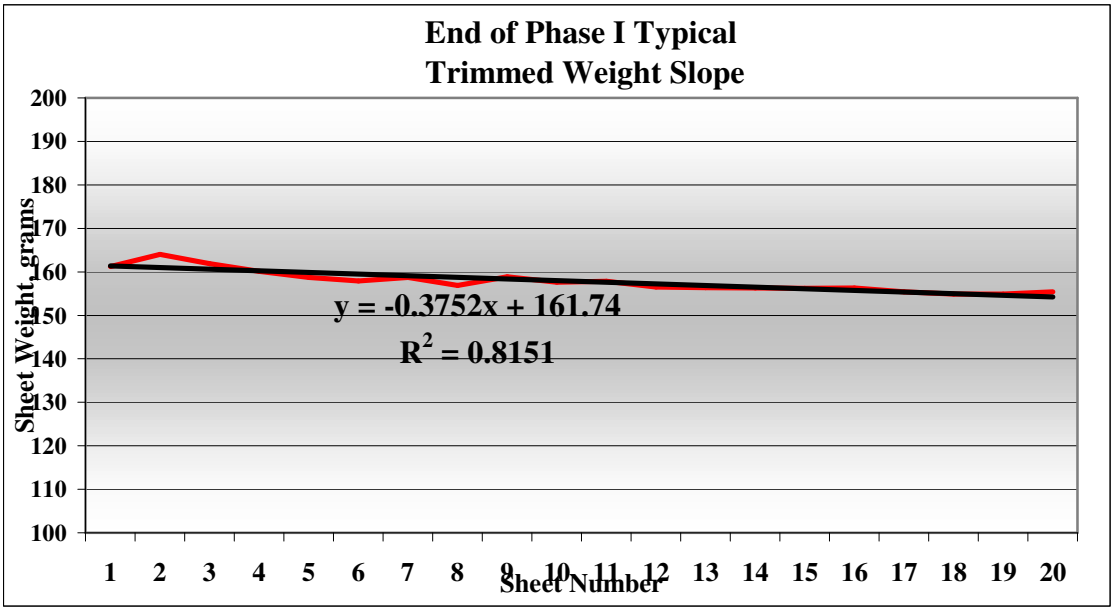

1.2 Optimize Sheet Composition

The scope of this task was changed during the performance of the program. The original intent of this subsection was to develop a material composition that could be effectively molded on one side and remain flat on the other. In this way, a single-sided plate could be supplied in net shape, and a double-sided plate could be provided needing only machining on one side. However, as we began exploring this concept, it became clear very quickly that we would have more success focusing on fully molded plates. Therefore, the materials development activities in this subtask were re-focused to the net-shape molding portion of the program (Task 5.1). Several composition reports describing the activity are reported in that section.

1.3 Molding Trials

Some work was done with flat plate molding for the purpose of characterizing material machining capability. Reports are included below for specific studies.

FLAT SHEET MANUFACTURING EVALUATION

Introduction

UTC Fuel Cells expressed interest in Porvair flat plate materials as an interim step to supplying fully molded bipolar plates. The use of the Porvair material in flat sheet configuration would serve as a basis for material durability testing prior to fully molded plate evaluation. Porvair has set about manufacturing a flat plate material that would meet key UTC requirements:

- Size per customer drawing
- Perm meeting customer requirements

- Bubble pressure meeting customer requirements
- Part strength reasonable per discussions with UTC personnel
- Material composition similar to that of molded plate materials

The first step in the evaluation was to manufacture parts with a wide density range (through modification of sheet weight in forming) so that a target density could be achieved and so that the relationship between permeability and plate bulk density could be established. After this trend was measured and established, additional batches would be run in the target range to set final run parameters and provide UTC with test materials.

Permeability of Plates

It was noted immediately that permeability measurements were difficult with these thick flat plate materials. Permeability measurements indicated low permeability and measurements that did not correlate well with product density. The first initial screening batch was processed as follows:

- Parts initially made in full sheet size (~16”x12”) through carbonization
    - Parts were then measured for weight and dimensions
- These parts were cut in half to plates of size approximately 8”x12”
- These plates were measured for weight, dimension, permeability and bubble pressure (some samples also taken for strength measurement)

Permeability is measured in two locations on a plate using a small testing circle. Water is pressurized to 30 kPa and collected for 30 seconds per measurement after the plate has been vacuum filled with water. The locations are approximately as shown in Fig. 1.

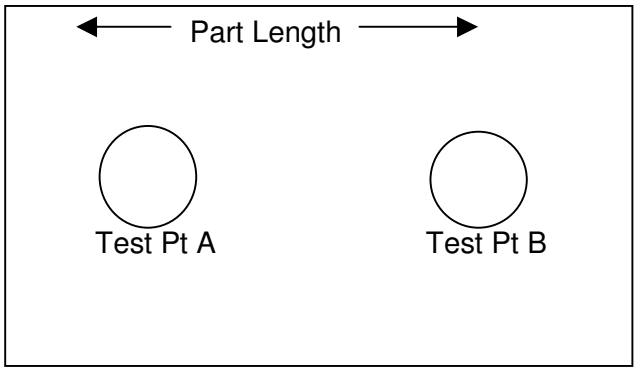

Figure 1. Schematic approximate locations for spot-permeability measurement.

For the first batch made, because the parts were cut in half prior to testing, the test locations were actually as shown in Figure 2.

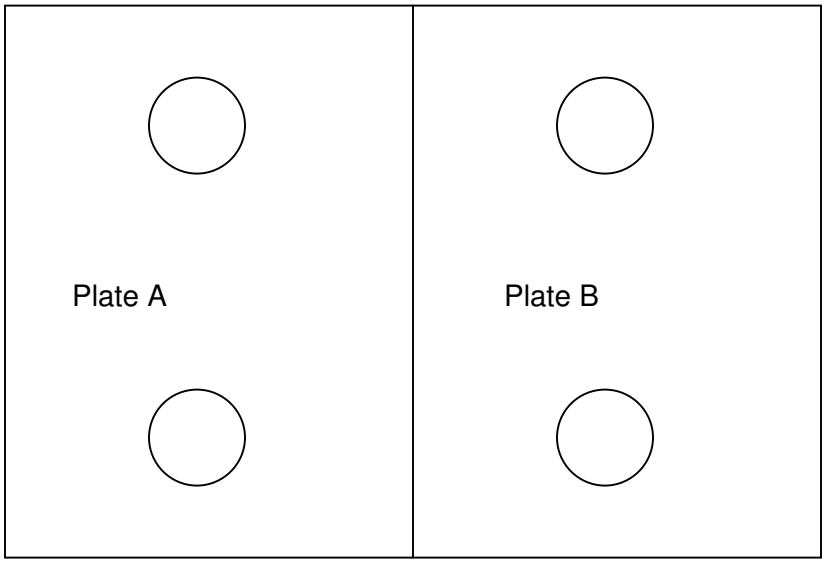

Figure 2. Initial batch layout and permeability measurement locations.

Some difficulty was encountered in measuring the permeability of this material, so two vacuum cycles were used to encourage water flow. The results of testing were promising and showed good correlation of permeability with overall plate density, as shown in Figure 3 (flexural strength is also shown in this figure).

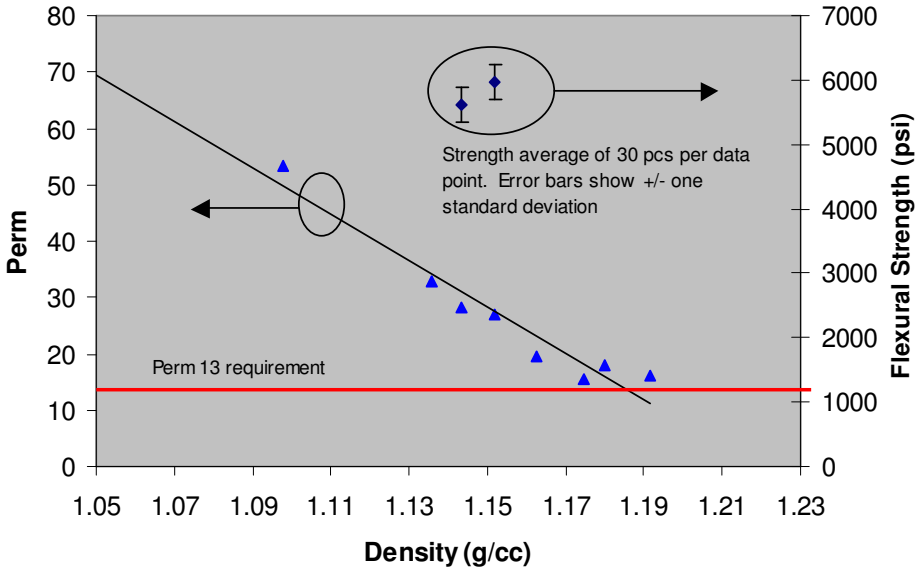

Figure 3. Perm and strength measurements from initial flat plate trial.

Density variation was noted with these plates both as carbonized and after cutting in half, as shown in Table 1 (note that basis weight of the preform sheet was modified to enable the achievement of a wide range of plate density).

Table 16. Plate density in g/cc.

Sheet #	Full Sheet Density	Density Plate A	Density Plate B	Average A, B Density
2	1.023	1.046	1.055	1.051
3	1.022	1.045	1.055	1.050
4	1.022	1.050	1.052	1.051
5	1.023	1.047	1.054	1.051
6	1.114	1.147	1.143	1.145
7	1.113	1.138	1.159	1.149
8	1.116	1.143	1.151	1.147
9	1.069	1.094	1.098	1.096
10	1.112	1.136	1.152	1.144
11	1.140	1.168	1.175	1.171
12	1.068	1.100	1.101	1.100
13	1.060	1.089	1.100	1.095
14	1.063	1.097	1.101	1.099
16	1.074	1.093	1.117	1.105
17	1.067	1.091	1.105	1.098
18	1.065	1.093	1.099	1.096
19	1.053	1.080	1.089	1.084
20	1.048	1.064	1.082	1.073
21	1.132	1.156	1.163	1.159
23	1.147	1.180	1.192	1.186
24	1.145	1.170	1.179	1.174
25	1.015	1.033	1.045	1.039
Average	**1.068**	1.094	1.103	**1.098**

It was apparent that after cutting the sheets, the density calculated for the cut sheets was greater than that calculated for the whole sheet prior to cutting. Density is calculated by dividing the plate weight by the length, width and thickness of the whole plate. Length is measured in two locations and width in three using calipers. Thickness is measured in 10 locations around the perimeter of the plate using a dial micrometer. It was noted that the cut edge of these plates measured somewhat thinner than the non-cut edges.

After this initial run, preforms were cut before being pressed into plates. These plates were then measured for permeability in locations similar to Fig. 1. At this point, however, the permeability measurements indicated issues with permeability capability that we believe are related to where the measurement is taken relative to the first and subsequent batches. This led to a study of the density uniformity of the material.

Uniformity Evaluation

Product uniformity was evaluated through destructive test and measurement. Process plates were first characterized for their variation in density. Figure 4 is a schematic layout of coupon measurement locations. Coupons were cut on a bandsaw and measured for length, width, thickness, weight and permeability. Figure 5 shows the average coupon density across a plate. As can be seen, the middle section of the plate is denser than the exterior. Figure 6 shows the corresponding thickness variation through the plate.

1	6	11	16
5	10	15	20

Figure 4. Layout of sample coupons

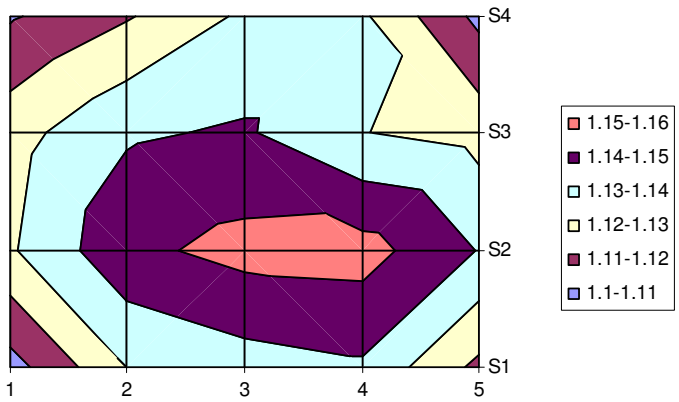

Figure 5. Density layout of carbonized plate.

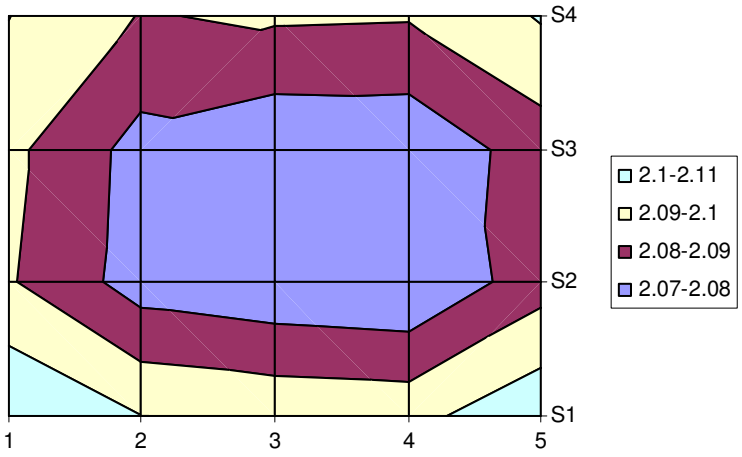

Figure 6. Thickness layout of carbonized plate.

The thickness variation alone is not significant enough to induce the density variation seen throughout the plates. The additional variation seen in the plate density may also be attributed to variation in preform sheet weight.

Pressed plate thickness variation was measured for thickness and density variation. Figure 7 shows plate density variation, while Figure 8 shows thickness variation. As can be seen in the figures, the plate is found to be both more dense and slightly thinner in the central region of the plate. The thickness difference is small (typically less than 0.002 in.), and probably results from either or both slight deflection in the molding tool during pressing and the additional shrinkage encountered in more dense regions of the plate over the density ranges targeted.

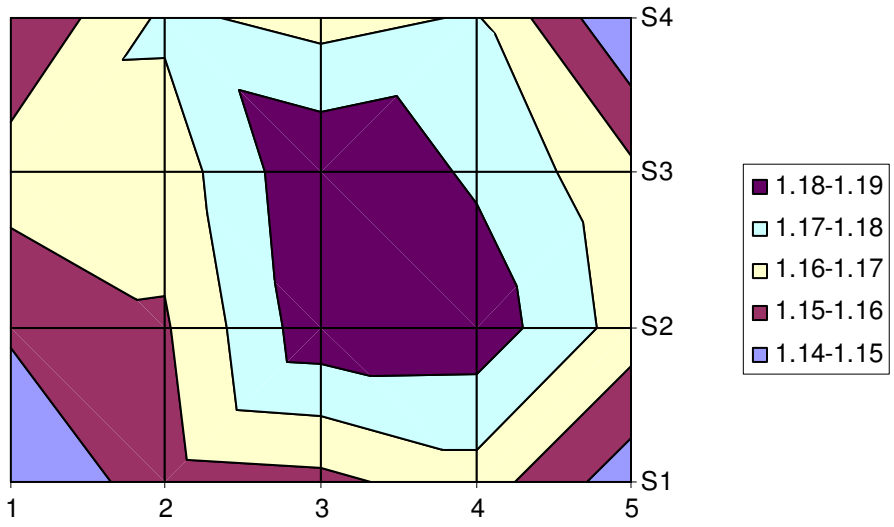

Figure 7. Pressed plate density variation (g/cc).

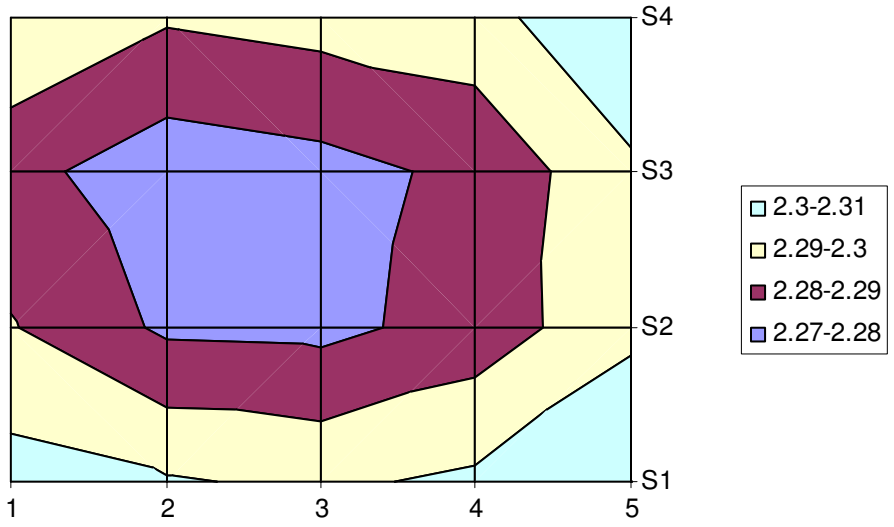

Figure 8. Pressed plate thickness variation (mm).

From the pressed plate sampling, the uniformity in basis weight was measured, and is shown in Figure 9. As may be seen, the pressed coupon weight per unit area variation is similar to that of the pressed plate density variation.

Figure 10 is a chart of the average of our normal punched coupon basis weight measurements (here measured in the standard 11 punches per sheet pattern). As can be seen, the same general trends are found as with the pressed part basis weight variation. A basis weight standard deviation from 0.5% to 3% of the mean coupon basis weight has been measured in flat sheet samples. The average standard deviation for these coupons is 1.38%, which is similar to that found in thin sheets. Based upon this level of variation, there would exist approximately 0.06 g/cc variation in final part density (+/- 2 standard deviations) within the plate. This is in general the level of density variation that has been detected through carbonized plate uniformity measurements. From permeability measurements on these flat sheets, this level of variation will introduce approximately 25 permeability units difference from the low to high density regions over the plate, with about 60% of the plate having perm uniformity of better than +/- 7 perm units, and 90% of the plate being within +/- 13 perm units. To be in a safe region, the average plate permeability would have to be greater than about 30 perm units.

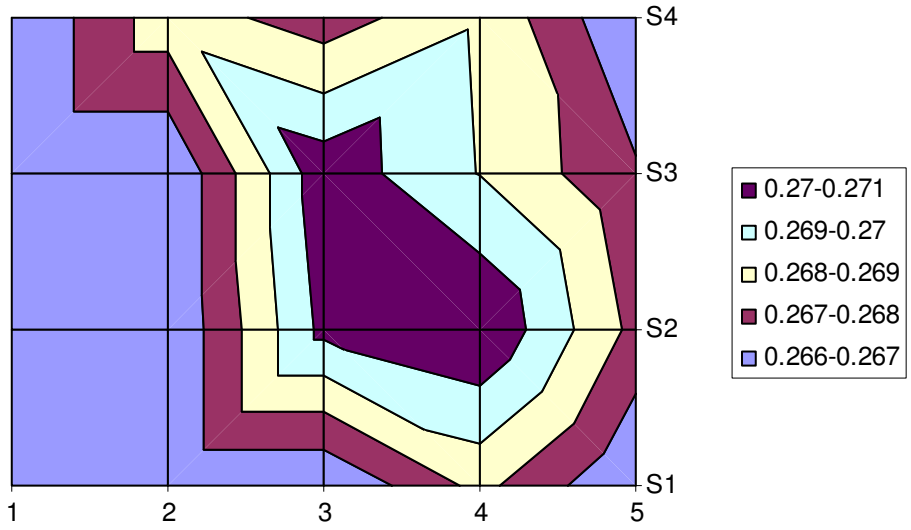

Figure 9. Pressed coupon weight uniformity (gm/cm2).

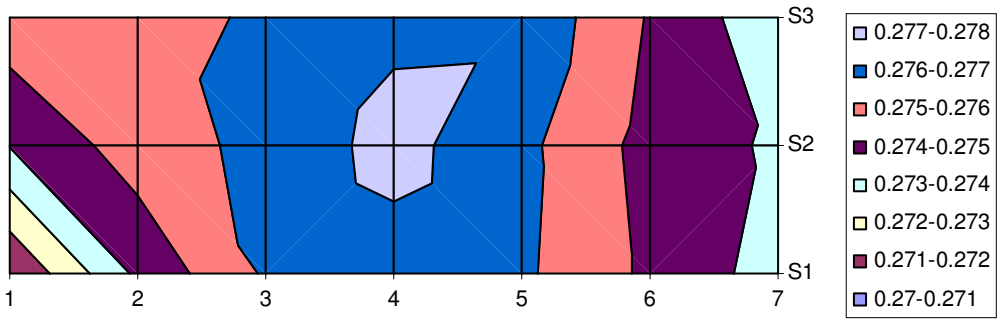

Figure 60. Formed sheet coupon weight uniformity (gm/cm2).

Permeability Evaluation

Permeability achievement in the flat plate configuration has been challenging. It has been found that a single vacuum fill cycle has yielded permeability data that vary greatly, and that are significantly lower than the target values. Parts vacuum filled in two complete cycles (two cycles of the 20-10-10 procedure) have permeability increases of as much as 70%, and tend to trend better with coupon density. However, it has been found that the permeability uniformity throughout a plate (when sampled in coupons) is still worse than desired. Figure 11 shows an example of permeability uniformity mapping. In this mapping, permeability is lower on the edges of the plates than in the center in general. It is thought that better plate wettability and vacuum filling would improve permeability vs. density trending, and would introduce a perm uniformity pattern similar to the coupon density mapping. This particular plate recorded an un-cut average plate density of 1.09 g/cc. The average coupon density was measured to be 1.12 g/cc, with a range from 1.08 – 1.15 g/cc. Permeability varied from 1.3 (most likely an outlier point) to 36.5 with an average coupon perm of 16. Obviously a lower target density is required to prevent the plate from having any low permeability areas. Such plates have been made and are in the process of mapping evaluation.

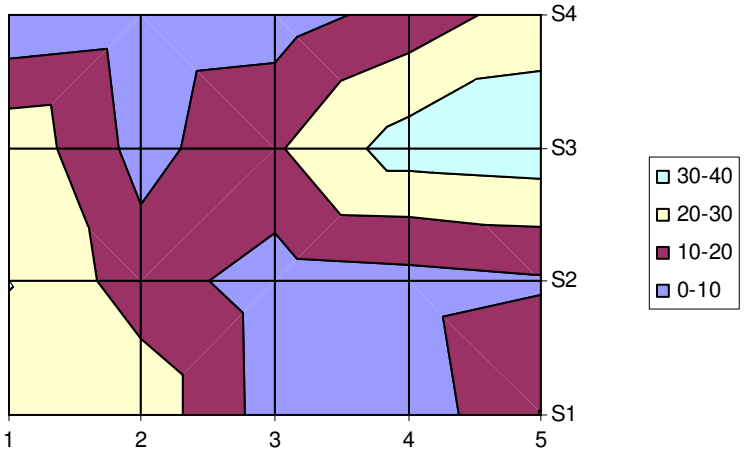

Figure 61. Permeability mapping example.

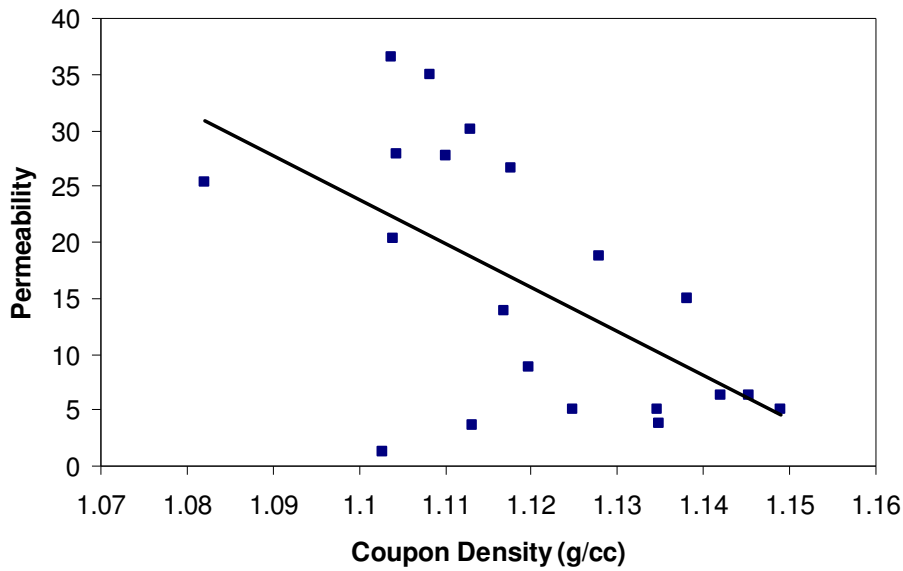

Figure 62. Coupon permeability variation with density.

Conclusion

The flat plates made to this point using the molded plate composition appear to be highly sensitive to basis weight variation – more so than with the molded plates. This is probably due partially to the design of the molded plate and partially due to the improved wetability and thinness of the molded plate. The studies presented in this report, however, indicate that the variation in sheet weight is not worse than that achieved with thin sheets. However, the variation that does exist tends to put heavier basis weight toward the center part of the sheet – making the sheets denser in the middle part of the plate. The plan to improve the performance and uniformity of the flat plates includes the following:

- Manufacture plates at lower density (targeting 1.05 g/cc) to move the average permeability to near 30
- Run trials with laminated sheets to improve overall plate basis weight distribution
- Run forming trials to attempt to improve sheet basis weight uniformity to better than 1% standard deviation

FLAT SHEET MANUFACTURING EVALUATION II

Introduction

This report follows upon improvements in flat sheet manufacture over the last two weeks to address density and permeability variation found in thick flat sheet material. It was found in the

previous study that the thick sheets were found to have more than desired final density variation, leading to part permeability variation that was greater than desired. This was combined with manufacturing parts with target density slightly too high so that areas of the flat sheet were below target permeability. Potential causes for the variation included the following

- Two plates cut from single plate – exaggerating positional variation of plate non-uniformity
- Formed sheet basis weight variation
- Selecting proper target density to ensure no low permeability areas
- Permeability variation introduced by thickness of part and vacuum fill procedure

Several investigations and improvements were implemented to improve sheet uniformity. Uniformity of preform sheet, pressed plate and carbonized part were evaluated. Permeability mapping was executed to determine the variation in plate permeability following process improvement.

Uniformity Requirements

The goal for the flat plate product is to have no area with permeability less than the spec. Further, according to the UTC specification, the plate should be as uniform as possible, with measurements within 20% of the plate mean. To achieve this level of uniformity in properties, improvements are needed in both the plate uniformity and in the permeability measurement system. Uniformity of this level would yield the following variation within a plate (Table 1):

Table 17. Acceptable permeability variation (**average perm assumed to be 25**) based upon varying levels of uniformity.

Variation	Min Perm	Max Perm
+/- 20%	20	30
+/- 30%	17.5	32.5
+/- 40%	15	35
+/- 50%	12.5	37.5

At present, even with the recent improvements, the flat plates reside in the +/-40% range for permeability uniformity (based upon 15 measurements per plate, and the present measurement method). Part of this variation is attributed to variation in the measurement system itself. Additional variation is attributed to the fact that the parts are not in a wettable condition, and may not fill with water adequately during the vacuum fill process. A gage R&R study on permeability with flat plates has not achieved a level better than 40% variation using non-wettable plates with the standard vacuum fill method. An R&R study on wettable molded plates has not been performed, but is expected to be better. We will be working on this and on the full plate permeability test in following months.

Forming System Evaluation

As reported previously, the standard deviation for parts made with the standard sheet forming method averaged 1.38%. This level of variation imparts approximately 0.06 g/cc density variation, and 25 permeability units variation in the plate, which is approximately the level of variation detected in uniformity evaluation in carbonized plates. Several investigations were

performed to improve the uniformity of the formed sheet. Some of the variables investigated include:

- Use of pan vibration during forming
- Modifications to suspension introduction to pan
- Use of pressure drop increasing materials in center of pan
- Laminating thinner sheets
- Forming sheet to net dimension (no trimming)

The last item modified the pan so that the sheet size was reduced from 16”x12.5” (sufficient for S600, of interest when the pans were designed and built) to 14”x7”. The following observations were made resulting from this investigation.

- Use of vibration has a small, negative effect upon sheet uniformity
- Modified suspension introduction design had a small, positive effect upon sheet uniformity
- Pressure drop increasing materials moved the dense regions from the center of the sheet to other areas on the sheet, but did not improve uniformity (actually made uniformity somewhat worse)
- Lamination of two thinner sheets improved material uniformity somewhat, but could not get away from having at least two light plate corners (with sheet layout scenario’s tried). This is due to the typical pattern of sheet uniformity, where more material is deposited in the sheet center, and less around the sheet perimeter. Laminating did not help this situation.
- Significant improvement was realized when forming sheets to near-net size.

Plates of each type described above were pressed, carbonized and tested. In general, permeability uniformity improvement tracked basis weight uniformity improvement. Figure 1 shows some uniformity trends from the above experiments. The figures show coupon uniformity across the sheet for the conditions identified. In the figure, oval refers to the insertion of a porous sheet in the center of the forming tray to impart additional forming pressure drop and so improve sheet uniformity. Wood box refers to the use of a wood box to obtain forming in the center of the pan only to realize near-net dimension parts. As can be seen, significant uniformity improvement resulted from the use of the near-net dimension forming. Lamination also improved uniformity, but not as significantly as did the near-net forming. For this reason, near-net dimension forming was used for further investigations.

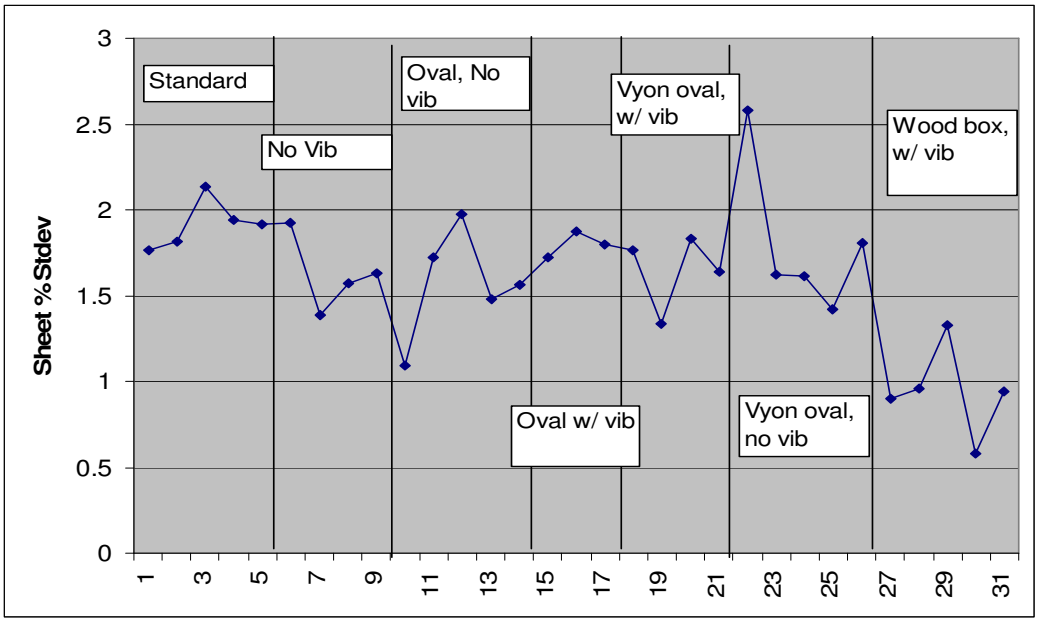

Figure 6. Coupon uniformity measurements from a variety of forming conditions.

Pressing Uniformity

Additional pressed plate measurements were made in this timeframe. Previous measurements using standard run and trimmed sheets showed pressed plate thickness to be within 2 mil across the plate. However, data showed that the part tended to be somewhat thinner in the central portion of the plate.

Plate measurements on near-net formed plates found plates to be high uniform after pressing. Table 2 shows some of these measurements compared to pressed plate measurements for laminated plates. The numbering outline is as shown in Figure 2.

11	12	13	14	15
6	7	8	9	10
1	2	3	4	5

Figure 6. Layout for uniformity measurements.

Table 18. Comparison of pressed plate thickness and density uniformity for laminated and near-net dimension plates.

	Laminated Pressed Plates				Near-Net Dimension Pressed Plates			
Coupon	Pressed Thickness (mm)	Pressed Density (g/cc)	Pressed Thickness (mm)	Pressed Density (g/cc)	Pressed Thickness (mm)	Pressed Density (g/cc)	Pressed Thicknes s (mm)	Pressed Density (g/cc)
1	2.044	1.158	2.044	1.143	2.153	1.185	2.151	1.210
2	2.05	1.191	2.046	1.185	2.161	1.180	2.159	1.195
3	2.048	1.172	2.06	1.184	2.165	1.168	2.174	1.177
4	2.047	1.147	2.048	1.168	2.16	1.182	2.152	1.169
5	2.054	1.181	2.041	1.161	2.157	1.187	2.143	1.202
6	2.034	1.173	2.044	1.167	2.171	1.175	2.144	1.187
7	2.03	1.199	2.03	1.209	2.149	1.190	2.145	1.206
8	2.035	1.209	2.034	1.203	2.155	1.199	2.153	1.190
9	2.036	1.198	2.044	1.199	2.149	1.202	2.148	1.185
10	2.032	1.169	2.034	1.188	2.152	1.182	2.145	1.179
11	2.04	1.171	2.039	1.164	2.148	1.195	2.147	1.199
12	2.042	1.195	2.046	1.197	2.154	1.188	2.152	1.185
13	2.05	1.192	2.046	1.187	2.156	1.184	2.162	1.182
14	2.047	1.197	2.048	1.189	2.159	1.167	2.160	1.166
15	2.044	1.166	2.05	1.167	2.151	1.189	2.154	1.180
Average	2.042	1.181	2.044	1.181	2.156	1.185	2.153	1.187
Stdev	0.0074	0.0176	0.0074	0.0184	0.006	0.010	0.008	0.013
%Stdev	0.36	**1.499**	0.36	**1.556**	0.297	**0.842**	0.389	**1.091**
max-min	0.024	0.061	0.030	0.066	0.023	0.035	0.031	0.045
max-min (in)	**0.00095**		**0.00118**		**0.00091**		**0.00122**	

As can be seen in the table, pressed plate thickness is relatively stable regardless of part pressed, and the maximum thickness difference over a part is approximately 0.001". Parts laminated show pressed plate density variation of approximately 1.5%, where parts near-net dimension formed show pressed plate density variation of approximately 1%. Please note that the parts were run to different basis weight and shim size, but with similar target densities.

Figure 3 shows the average thickness variation measured by plate area. Ends are defined as the narrow ends of the plates – top and bottom. Edges are the wide edges of the plate – right and left. Middle is defined as the center-most section of the plate. As can be seen in the figure, the plates on average are slightly thinner in the center portion of the plate. The difference however is minor, about 0.2 – 0.5 mil. It is not believed that pressing is the leading cause of density variation in the parts.

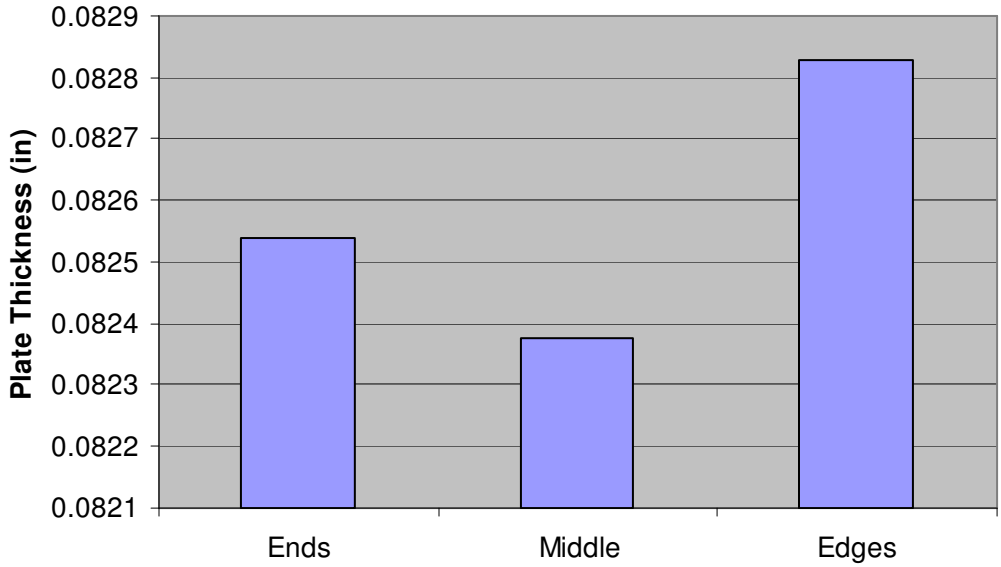

Figure 3. Average pressed thickness variation by part area.

Permeability Uniformity

Carbonized parts were measured for permeability uniformity non-destructively by locating the perm measurement area on a region of the plate. The pattern used was a grid of 3x5 measurements, matching the destructive press coupon measurements. Table 3 shows some measurements for permeability and perm uniformity for parts run

Table 19. Permeability mapping for various plates.

Coupon #	Standard	Standard	Laminated	Near-net	Near-net	Near-net	Near-net
1	17.7	19.6	16.9	32.3	27.5	29.9	16.2
2	14.0	17.4	10.3	38.3	35.9	20.9	24.5
3	18.4	12.8	12.5	26.9	26.9	29.3	22.7
4	14.7	9.1	15.5	38.9	34.1	30.5	25.7
5	9.6	6.8	16.2	38.9	31.1	35.9	26.3
6	26.5	18.1	11.8	28.1	23.9	21.5	15.6
7	21.3	18.9	19.1	20.3	19.2	23.9	15.0
8	17.7	15.8	11.0	21.5	18.0	23.3	14.4
9	17.7	14.3	13.2	23.9	28.1	25.1	18.0
10	9.6	8.3	9.6	31.7	38.3	44.9	29.3
11	17.7	10.6		24.5	18.6	19.8	15.0
12	22.1	12.1		23.3	22.7	24.5	22.1
13	19.9	6.8		30.5	21.5	23.9	19.2
14	19.1	9.8		31.7	26.3	28.7	31.7
15	7.4	5.3		28.7	27.5	29.3	28.1

Average	16.9	12.4	13.6	29.3	26.7	27.5	21.6
Min	7.4	5.3	9.6	20.3	18.0	19.8	14.4
Max	26.5	19.6	19.1	38.9	38.3	44.9	31.7
Stdev	5.1	4.8	3.2	6.1	6.3	6.5	5.9
%Stdev	30.4	38.6	23.2	20.8	23.5	23.7	27.1
%Variation	60.8	77.1	46.5	41.7	46.9	47.4	54.3

The data shows that the permeability uniformity improved significantly in moving from the standard forming method to the near-net dimension forming method. There is also an indication of uniformity improvement with laminated sheets, although not enough measurements were taken under that condition. The %variation shown in the table should be an estimate of the batch being within the average plate permeability. Note that no conditions come close to the proposed goal of +/- 20%. The variation measured is thought to be partially real and related to density variation through the part, and part attributed to the gage error of the perm test using the thick, non-wettable plate materials.

Figure 4 shows the average perm by plate region for the near-net dimension plates. The middle portion of the plates shows on average slightly lower permeability than the edges or ends of the plates, indicating that additional uniformity improvement is possible.

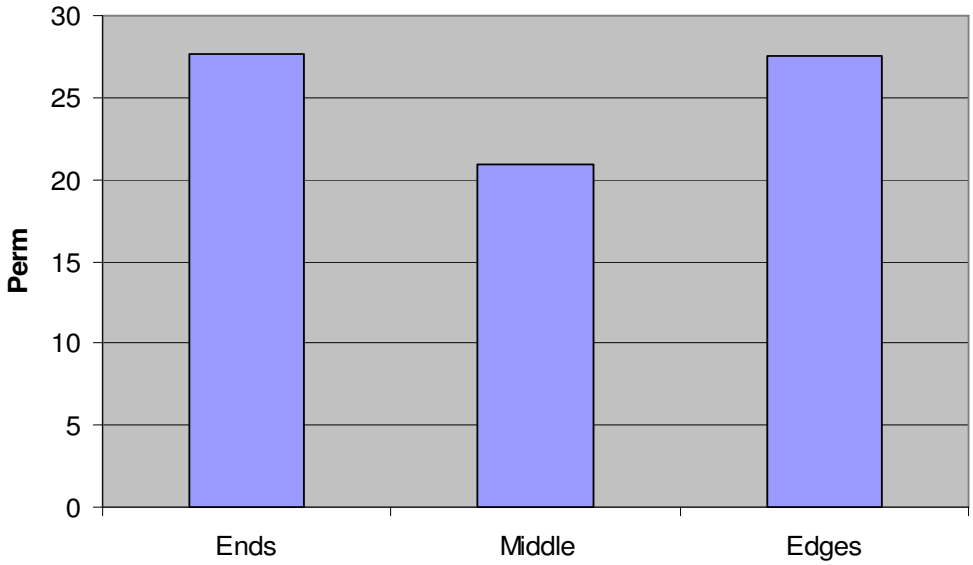

Figure 4. Perm average by plate region.

Conclusion

Investigations into plate uniformity root cause have led to significant improvements in plate uniformity. Several potential improvements were investigated, including

- Improvements in the suspension distribution to the forming pan

- Laminating sheets to improve uniformity
- Forming near-dimension sheets from center of forming pan
- Investigating press uniformity

Characterization of sheet basis weight uniformity found that forming plates to near-net dimension greatly improved sheet uniformity, yielding sheets on the order of 1% or better standard deviation, using the standard basis weight uniformity measurement. Laminating sheets was also found to be beneficial to sheet uniformity, but not as beneficial as forming to near-net dimension. Several plates were made and characterized (typical data was reported above) using the near-net fabrication method. Subsequent permeability tests showed permeability capability and uniformity significantly improved, but still worse than the uniformity spec of +/- 20% of the mean. Part of the permeability variation measured is thought to be attributed to the permeability test method itself, especially considering the poor gage R&R results of previous tests when using thick, non-wettable plates. Improvement in the perm measurement accuracy and repeatability will result when testing thinner plates that are wettability-enhanced. However, variation in density and permeability still exists in the plates. Work is continuing to further improve plate uniformity.

1.4 Manufacture Test Plates

As mentioned in 1.2, we found that the execution of the program would be of greater use by focusing on net-shape molded plates instead of near-net-shape molded plates. As a consequence, plate manufacture for hybrid molded/machined bipolar plate testing did not occur in this program. Instead, this effort was directed toward net-shape molded part manufacture in task 6 and Phase III of the program.

1.5 Fuel Cell Testing

As mentioned in 1.2, we found that the execution of the program would be of greater use by focusing on net-shape molded plates instead of near-net-shape molded plates. As a consequence, fuel cell testing for hybrid molded/machined bipolar plates did not occur in this program. Instead, this effort was directed toward net-shape molded part fuel cell testing, and is reported in task 6 and Phase III of the program.

1.6 Process Development Finalization

As mentioned in 1.2, we found that the execution of the program would be of greater use by focusing on net-shape molded plates instead of near-net-shape molded plates. As a consequence, process development finalization for hybrid molded/machined bipolar plates did not occur in this program. Instead, this effort was directed toward net-shape process optimization for net-shape molded parts, and is reported in task 5.5 and Phase III of the program.

2. Inherent Wettability Development

2.1 Develop Wettability Test Method

In Phase 1, Task 10.0 defined the importance of the plate to be either highly hydrophobic or highly hydrophilic for success in performance of fuel cell assemblies, as is the case for most bipolar plate designs depending upon the functionality of the plate. Further investigation in this

area of manufacturability was done to identify a means of treating the plates to create a wettable surface on the bipolar plates. UTC Power has a proprietary technology that is an expensive secondary treatment step that makes the porous plate surfaces wetting to water. This can only be applied to UTC Power products.

As part of ongoing study in this area and in an effort to find a secondary method of making the surface of the bipolar plates highly hydrophilic that is just as effective and less expensive, an experiment was carried out to examine methods of treatment. The addition of titanium and zirconium oxides were made to the original composition mixture prior to forming. These oxide additives are highly stable in fuel cell environments, non-poisoning to the membrane and catalyst, and are used in small concentrations (typically less than 2%). The parts were then processed as normal. These oxides were chosen as candidates for improving wettabilty based on their predicted stability during both the pyrolysis reaction and later in the aggressive aqueous, electrochemical environment seen in fuel cell.

Experimental Design

A factorial design to study wettability changes in bipolar plates affected by additions of oxides during the batching process:

Sample	TiO2/ZrO2	Coarse/Fine	10% / 5%	Heat Treat/Not
TIZR1	-	-	-	-
TIZR2	+	-	-	+
TIZR3	-	+	-	+
TIZR4	+	+	-	-
TIZR5	-	-	+	+
TIZR6	+	-	+	-
TIZR7	-	+	+	-
TIZR8	+	+	+	+
TIZR9	Control			

Powder Characteristics

TiO2(c) -325mesh titanium oxide (rutile)**(actual measured aps=1.2 micron)
TiO2(f) 1 micron titanium oxide(anatase)
ZrO2(c) -325mesh zirconium oxide
ZrO2(f) 1 micron zirconium oxide

Results

Following are the results from the averages in wick fill percent for each experimental group.

Experimental Group	**Average (Wick Fill %)**
Titanium Oxide	56.6%
Zirconium Oxide	54.1%
Fine	58.3%
Coarse	52.38%
5% Powder added	54.3%

10% Powder added	56.4%

Heat Treatment

All coupons were oxidized at 650 F for 12 hours in an air furnace for the purpose of determining if light oxidation of the plates encourages improved plate wetability.

Experimental Group	Average (Wick Fill %)
Pre Heat Treatment	53.1%
Post Heat Treatment	**69.5%**

Conclusions

- The most powder size seems to be more important than amount or type, fine powders being better than coarse.
- The best alternative at this point looks like 10% Titanium oxide in a fine powder.
- The heat treatment had the most drastic improvement (+16.4%).
- The average wick fill on the heat treated samples are better than those processed using tin chloride.(Tin Chloride treatment averages 68%)

Test Apparatus

Due to the time-consuming nature of wick-fill testing, Porvair built an apparatus to test plates ten at a time. The device is simply a stand holding plates at specific heights. The stands were built for testing the series 500 plates which are 7 ¼" wide. In the case of these full size plates, use a fish tank with a Plexiglas partition and one stand in each side holding a total of ten plates.

The stands consist of a series of 5 slots, each .725 inches higher than the last. This is a tenth of the height of a part standing up on its long side. Five plates are placed in each rack on either side of the fish tank. Then have the tank in a sink and begin filling one side at a rate so that the first plate is entirely submerged in 5 minutes. After 7 minutes, all five plates are submerged and the water spills over the partition to begin filling the second 5 plates. 35 minutes after the water starts flowing, testing of the wick fill weights begins. Following is a chart outlining the procedure for obtaining the wick fill weight.

- **Wick Fill Procedure Using the Tank and Stands**

Time	Event
Setup	Place parts in positions 1-10, put the racks in the tank, and the tank in the sink. Fill a ¼ " of water on both sides of the partition to bring the level up to the bottom of plates 1 and 6
0:00	Start the appropriate water flow; Plate one begins submersion. No activity is required for 35 minutes
0:30	Plate 2 begins submersion
1:00	3 Begins submersion
1:30	4 begins submersion
2:00	5 begins submersion
5:00	1 is submerged
5:30	2 is submerged
6:00	3 is submerged

6:30	4 is submerged
7:00	5 is submerged, water starts spilling over into the other side of the tank and 6 begins submersion
7:30	7 begins submersion
8:00	8 Begins submersion
8:30	9 begins submersion
9:00	10 begins submersion
35:00	Remove plate 1, pat dry and record wick weight.
35:30	Remove plate 2, pat dry and record wick weight.
36:00	Remove plate 3, pat dry and record wick weight.
36:30	Remove plate 4, pat dry and record wick weight.
37:00	Remove plate 5, pat dry and record wick weight.
42:00	Remove plate 6, pat dry and record wick weight.
42:30	Remove plate 7, pat dry and record wick weight.
43:00	Remove plate 8, pat dry and record wick weight.
43:30	Remove plate 9, pat dry and record wick weight.
44:00	Remove plate 10, pat dry and record wick weight.

Current Best Solution

An addition of titanium oxide into the batching process followed by a heat treatment is the most promising alternative to the tin chloride treatment. Wick fill percents of up to 80% have been achieved with a simple addition of titanium oxide. A heat treatment could further enhance wettabiltiy.

2.1 Investigate Material Additives

In addition to developing the best fit for a method to test the wettability of the plates, the materials to be added to the plates to induce wettability were also examined.

Study of Material Additives

Following the study outlined above, a second experimental design was carried out to further investigate the addition of Titanium Oxide and Zirconium Oxide to bipolar plates.

A factorial design to study wettability changes in bipolar plates affected by additions of oxides during the batching process was followed. See the following table below.

Sample	TiO2 / ZrO2	2% / 8%	Mic / Submic	Floc / not
OXAD1	-	-	-	+
OXAD2	+	-	-	-
OXAD3	-	+	-	-
OXAD4	+	+	-	+
OXAD5	-	-	+	-
OXAD6	+	-	+	+
OXAD7	-	+	+	+
OXAD8	+	+	+	-

The fourth variable is a heterogeneous flocculation experiment. Flocculated samples were mixed differently. The additive powder was put in 3 gallons of water and placed in the high shear mixer. Using ammonium hydroxide, the pH was adjusted to 9. The graphite was added. Finally, nitric acid was added to the mixture while still being stirred until the pH was 4. The mixture was then added to the batching process as normal.

Formulations

	Component Weight in g							
Sample	PVA	Fiber	Resin	Graphite	TiO2(C)	TiO2(F)	ZrO2(C)	ZrO2(F)
OXAD1	113.4	340	680	1122.7	-	-	-	56.7
OXAD2	113.4	340	680	1122.7	-	11.3	-	-
OXAD3	113.4	340	680	1049	-	-	-	425.3
OXAD4	113.4	340	680	1049	-	85.1	-	-
OXAD5	113.4	340	680	1122.7	-	-	11.3	-
OXAD6	113.4	340	680	1122.7	11.3	-	-	-
OXAD7	113.4	340	680	1049	-	-	85.1	-
OXAD8	113.4	340	680	1049	85.1	-	-	-

Powder Characteristics
TiO2(c) -325mesh titanium oxide (rutile)**(actual measured aps=1.2 micron)
TiO2(f) 32 nm aps micron titanium oxide(anatase)
ZrO2(c) 1 micron zirconium oxide
ZrO2(f) colloidal zirconium oxide

Pressing and Pyrolisis
Pressing was done according to normal procedure, pressing at 180F for 300 seconds at standard pressure 3000psi. Parts were then fired on a normal cycle.

Results
Following are the results from the averages in wick fill percent for each experimental group.

Averages	
ZrO2	56.97%
TiO2	**58.50%**
1%	**59.07%**
7.50%	54.78%
Sub Mic	54.66%
Micron	**58.14%**
Floc	52.37%
Not Floc	**60.17%**

Conclusions

- pH Flocculation did not seem to help wettability
- The sub micron additives seem to block the vacuum forming system.
- Best results were not as good as tin chloride treatment.

Tin and Tin Oxide Addition

Formulations

Tin oxide was selected for its high surface energy. Direct additions of tin oxide as well as an addition of tin with a post-pyrolysis heat treatment were investigated. All batches were run as 480g single sheet runs in the large rig(#1). An additional screen was used because the single sheet runs tend to stick to the batching screen and break apart.

	Component Weight in g							
Sample	PVA	Fiber	Resin	Graphite	Tin Oxide	Tin		
TINOX1	24	72	144	192	-	48		
TINOX2	24	72	144	192	-	48		
TINOX3	24	72	144	192	48	-		
TINOX4	24	72	144	192	48	-		

TINOX1 was lost in batching.
15 gallons water was used in each batch.

Pressing and Pyrolisis

The single sheets were pocked and thickness varied. 2.5 and 4 inch square coupons were cut from usable portions of each loaf. These were cut directly from the vacuum formed single thickness sheets and pressed. Pressing was done nov 1 2002 according to normal procedure, pressing at 180F for 300 seconds at 3000 psi.

Pyrolysis was performed in the labvac furnace. It was assumed that under pyrolisis conditions, tin oxide would at least partially reduce and slightly evaporate. To avoid possible contamination, we used the smaller furnace.

Results

Following are the results from the averages in wettability for each experimental group.

Experimental Group	Average (Wick Fill %)
Tin Oxide	**41.5%**
Tin	18.8%

All coupons were then oxidized using the same temperature cycle as the tin chloride process, 650 F for 12 hours. The coupons were all destroyed in the heat treatment.

Conclusions

- These additions do not merit further study.

The tin additions seemed to have a negative effect on wettability (compared to 50% average on a standard plate). An attempt to oxidize the tin destroyed the plates.
Therefore, Porvair will continue to produce wettable bipolar plates that have undergone the Tin Chloride Treatment supplied by UTC Power.

Zirconia and Titania Addition

The purpose of the study is to add ceramics oxides to the current porous graphite plate composition to make the plate more wettable to water and to eliminate the tin treatment if possible.

The preliminary choices of ceramic oxides are TiO2 and ZrO2. T-R TiO2 is from Kerr-McGee with a predominant particle size of 0.3 micron. The purity is 99.5%. The surface area is 5.5 m2/g. MS2 ZrO2 (Magnesium) has an average particle size less than 1 micron with a purity level of 99%.

There are five batches. The detailed compositions are given below.

	Standard	**Batch 29**	**Batch 21**	**Batch 22**	**Batch 23**
Graphite	**49.6%**	**47.24%**	**45.09%**	**46.32%**	**43.33%**
Fiber	**18%**	**17.14%**	**16.36%**	**16.8%**	**15.72%**
PE	**3%**	**2.86%**	**2.74%**	**2.8%**	**2.62%**
Resin	**28%**	**27.52%**	**26.27%**	**26.99%**	**25.25%**
TR TiO2		**4.76%**	**9.09%**		
MS2 ZrO2				**6.62%**	**12.64%**
Forming Fiber	**0.5%**	**0.48%**	**0.45%**	**0.47%**	**0.44%**

The amount of the oxides is adjusted according to the density difference between TiO2 (4.4g/cc) and ZrO2 (5.7 g/cc). Batch 29 and Batch 22 will have the same volume amount of oxides, so are Batch 21 and Batch 23. The relative rations among the rest of the components are maintained the same among all five batches.

The wettability will be evaluated with wick fill test on the amount of water absorbed.

PERM and bubble point will also be measured.

Experimental results:

Standard production procedures for plates were used to prepare all the five batches. Green sheets were formed, pressed and fired.

Table 1 is the weight gain after wick fill test, conductivity of the samples and their average density and % density

Table 1

Batch #	**Weight gain**	**Conductivity. S/CM**	**Density, g/cc**	**%Density**
21	**29.9%**	**544**	**1.14**	**51.4%**
29	**27.1%**	**512**	**1.16**	**53.3%**
22	**22.4%**	**490**	**1.27**	**58.2%**
23	**26.5%**	**415**	**1.32**	**58.1%**

Table 2 is the PERM

Batch #	**PERM/Wickfill**	**PERM/Vacfill**
21		**40.3**

29		**27.9**
22		**27.9**
23		**27.8**
22	**16.8**	**20**
23	**24.4**	**31.8**
Standard	**23.8**	**26.6**

Discussions:

Addition of oxides greatly improves water absorption ability of graphite plates from 7.04% to more than 22%. However, water drop test indicates that it takes 15 to 30 seconds for water droplets on Tin treated plates wicking inside. For plates with oxides, it takes about 4 to 5 minutes.

Addition of oxides decreases the electrical conductivity as anticipated. Plates with TiO2 generally have better electrical conductivity. It is believed that vacuum firing would make TiO2 more electrical conductive due to the formation of oxygen vacancy.

All plates with oxides show good PERM property. It is interesting to know that there is difference in PERM property when different water fill methods are used. PERM is a little bit lower with wick fill method.

2.2 Manufacture Test Plates

Through the experiments described in 2.2, it was found that the best wettability enhancement method available was the tin treat process originally prescribed by UTC Power. Superior water wicking into the porosity of the plates was achieved with the tin treatment process. The process is proprietary to UTC Power, and is not described in this report.

2.4 Fuel Cell Testing

Two-cell testing occurred at UTC Power. A description of the testing and test results follow:

Summary:

This Porvair net-shape molded two-cell build was built to evaluate Porvair's latest

material. The air, coolant, and fuel flow fields were molded for these two cells at Porvair.

The cell shows better IR based on the H_2 pump than typical cells, however the IR is the highest of all Porvair material received thus far. This is caused by two factors; the better mold quality yields decreased surface roughness on the ribs, and the reduced fiber content in the material increases through plane resistance. However, despite this IR difference performance is excellent on H2/Air. Mass transport losses are indicated by the l21 hr load calibration to start at 1600 mA/cm². The decay rate of the cell at 1000 mA/cm^2 hold was much lower in comparison to past cells, thought in part to be due to the increased uniformity in permeability and the higher pressure drop on the air flow fields.

Below are the graphs of interest for this two-cell, along with any comments about the testing performed and what was learned.

Performance vs. Time:

The net shape Porvair Hydrogen/Air performance is approximately 5 to 10 mV higher at the cell's peak performance when compared to batch material from Porvair. Figure 2 below shows how quickly the break-in of the cell took. The cell peaked at approximately 60 hours and then various testing was performed. Due to test stand availability only 121 hours of testing were performed.

Figure 1. Performance comparison on H2/Air vs. Time

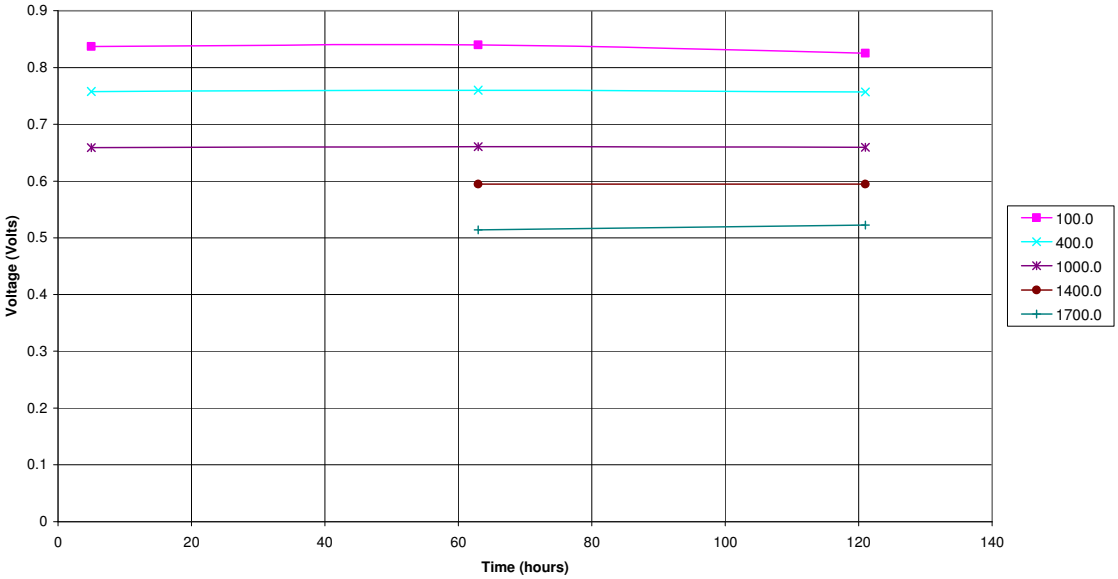

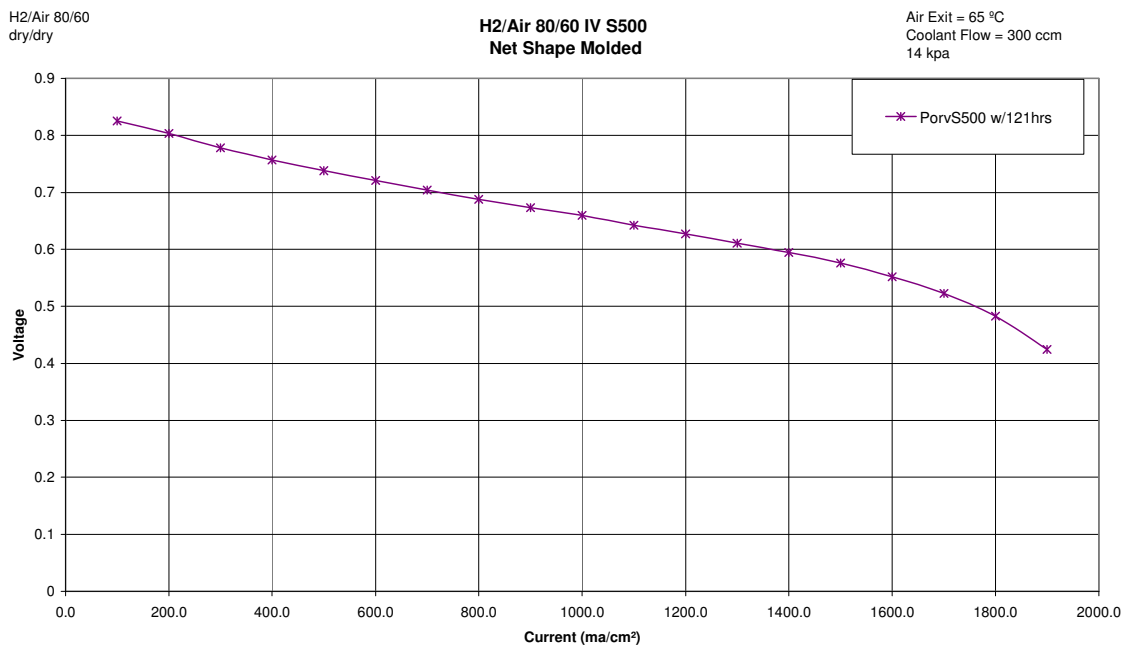

Figure 2. Polarization curve for net-shape molded plates evaluated at UTC Fuel Cells.

The net shape S500 Porvair Hydrogen/Air performance shows the onset of mass transport

limitation at 1600 mA/cm^2, with a limiting current of 1900 mA/cm^2 after 220 hours. The interesting thing to note is that the limiting current density is much further than previous cells. Again this is attributed to the flow field design primarily, and to the improved uniformity of the molded plates.

Conclusions:

This cell met all criteria except the run-time decay rate. Even though the decay was much lower than in previous testing it was still slightly above our target. This decay rate may be artificially low due to the design of the flow fields, however the improved plate uniformity should not be discarded as another contributing factor.

2.5 Process Qualification

Basic Procedure

Porvair Fuel Cell Technology's bipolar plate team adopted the tin oxide deposition process developed and used by UTCFC. The testing plan followed for qualification of the equivalency of the same PFCT process is UTC proprietary and therefore cannot be included in this report. The testing reported includes a modified wick fill test of wettability, bubble point data on wick filled and vacuum filled parts, and wick fill permeability. .

UTCFC Baseline

Ten plates treated by UTCFC stand as a basis for comparison to our process. The plates are flat and were made in the vacuum forming process by Porvair and then treated by UTCFC at their facility. The wick fill percentage is reported below.

UTCFC Treated	
Mean	71.3%
Median	70.8%
Max	77.6%
Min	66.7%
St Dev	3.9%

Process Qualification

Three test runs of 60 flat plates each (standard planned batch size) were treated in the PFCT rig. The same battery of tests were run on ten parts chosen from each batch of 60.

Qualification Run 1

	ID	MWF%	MWFBP(kPa)	VFBP(kPa)	Pre BP(kPa)	(DW)(g)	WW(g)	VFW(g)
1	**V303-1**	76.8%	73	75 / 76	62/70	145.29	175.73	184.93
2	**V280K-L**	62.8%	XXXXXXXX	XXXXXXXX	62/64	142.13	167.11	181.93
3	**W009B1-3**	78.1%	73	75 / 76	68/72	148.53	179.35	188.01
4	**W008A3-2**	79.6%	70	72 / 77	65/68	148.62	183.04	191.86
5	**W00-E1-2**	75.4%	73	76 / 78	66/67	145.82	175.36	185
6	**W2008A2-2**	78.5%	69	64	65/68	148.59	182.46	191.75
7	**W2008A4-3**	77.7%	83	68	65/67	146.88	177.52	186.33
8	**W008A1-4**	80.4%	82	64	60/68	146.75	178.72	186.51
9	**W2009B4-1**	76.6%	73	73 / 74	63/65	147.90	179.09	188.64
10	**W009B1-1**	77.5%	82 / 84	79 / 82	70/72	148.75	180.3	189.44

Mean	76.3%
Median	77.6%
Max	80.4%
Min	62.8%
St Dev	5.0%

MFWF% Modified(2hr soak) Wick Fill %
MWFBP Modified wick fill bubble point
VFBP Vacuum fill bubble point
Pre BP Bubble point before treatment
DW Dry Weight
WW Wick Weight
VFW Vacuum Fill Weight
WFPRM Wick Fill Perm

Qualification run 2

	ID	MWF%	MWFBP	VFBP	Pre BP	(DW)	WW	VFW	**WFPERM**
1	**V2359D2-1**	80.4%	72/74	72/74	69/88	**146.31**	181.17	189.68	9.05
2	**V353F3-4**	79.4%	70/71	74	62/66	**147.88**	178.6	186.55	3.55
3	**V362B1-1**	79.0%	62/64	58/64	1.165	**144.59**	178.89	188	7.94
4	**WB014D2-2**	78.3%	61/61	54/60	62/68	**146.8**	181.94	191.68	17.68

5	**V363A3-1**	79.7%	71/71	68/68	60/66	**145.78**	178.88	187.3	3.62
6	**V2363A2-2**	80.6%	50/64	56/62	54/56	**142.8**	177.29	185.6	17.68
7	**V2363A2-4**	81.0%	64/66	64/66	54/56	**145.34**	180.68	188.96	11.40
8	**V2356A4-1**	79.6%	54/66	52/64	52/60	**144.78**	178.69	187.37	26.74
9	**W010B4-4**	83.5%	66/68	66/68	60/64	**145.39**	182.67	190.01	19.19
10	**V264B4-1**	82.9%	68/68	64/68	48/56	**144.24**	181.1	188.69	12.23

Mean	80.5%						
Median	80.0%						
Max	83.5%						
Min	78.3%						
St Dev	1.7%						

Qualification run 3

	ID	MWF%	MWFBP	VFBP	Pre BP	(DW)	WW	VFW	**MWFPERM**
1	**W2002D2-2**	**78.5%**	70/72	80/80	55/58	148.5	184.89	194.88	7.03
2	**V2356B2-2**	**75.8%**	78	84/84	52/56	149.16	180.83	190.93	4.93
3	**W2002C4-2**	**76.4%**	76/80	78/82	64/73	148.99	181.42	191.45	7.07
4	**V2364F4-3**	**76.2%**	68/78	82/82	54/76	148.63	178.37	187.66	0.86
5	**W002E3-2**	**74.7%**	72/72	75/76	60/61	150.48	181.12	191.49	2.92
6	**W2002D3-1**	**75.0%**	77/77	76/78	60/63	147.07	176.11	185.79	2.70
7	**W2002H4-1**	**77.3%**	78/88	80/84	66/70	147.39	179.76	189.25	2.37
8	**WB013B4-1**	**74.8%**	66/72	60/70	58/68	147.46	179.02	189.66	8.39
9	**V303**	**74.1%**	68/73	70/74	68/72	144.76	176.67	187.83	5.76
10	**WB013N2-3**	**74.2%**	62/66	62/64	55/60	148.92	182.06	193.6	10.64

Mean	75.7%						
Median	75.4%						
Max	78.5%						
Min	74.1%						
St Dev	1.4%						

Data indicate good performance of the net-shape molded Porvair plates (as indicated by wick fill percentage 70% or greater in the qualification. Only one part showed poorer performance. This part V280K-L was found to be defective and outside the normal range for density. The three qualification runs were sufficient to successfully qualify the tin treatment method.

3.0 Low-cost Machining

This activity, meant to be a tie-in to reduce part costs in the interim period between composition development and net-shape molded part development. Faster than anticipated success with net-shape molding made the execution of this activity unnecessary. Funds devoted to the task were applied to net-shape molding development instead.

4.0 Low Cost Bonding

It is of a clear benefit to the customer to purchase bipolar plate products that are already bonded anode-to-cathode. In this way, a complete bipolar cell can be purchased and in-house

bonding steps be eliminated at the customer's site. In this program, we evaluated a simple means of bonding plates together, and investigated materials for bonding to our carbon-carbon bipolar plates.

4.1 Investigate Automated Bonding Systems

Automated systems designed for dispensing and distributing uniform lines of bonding adhesive in a uniform manner are common in the adhesives industry. No new technology is required if one were to be able to use dispensed adhesives. In this task, we contacted Loctite to explore options for dispensing adhesive uniformly. While several automated systems were available, it made the most economic sense to purchase a simple pneumatic extruder system and adapt it to an existing 3-axis CNC machining center. The Figure 4.1.1 shows the setup – a Loctite pneumatic disperser mounted to the head of a CNC. The arrangement allowed for us to evaluate bonding quickly and easily, using a number of candidate materials.

We found no issues with this system. The amount of material could be easily controlled through the pneumatic settings or the rate of traversal of the CNC machine. Corners and edges were easily formed and placement accuracy was excellent. Introducing a positive stop on the adhesive flow could make improvements to the system, as the flow continues even after air pressure to the pneumatic cylinder has shut off. This introduced the need to move the fixture off of the plate edge after completion of the adhesive application.

Following adhesive application, the part is assembled – anode to cathode, and pressed in an existing hydraulic press under a pressure of about 100 psi. Heat may or may not be applied to encourage rapid curing of the adhesive (depending upon the product).

We bonded a few hundred plates for trials and customer evaluation in this program.

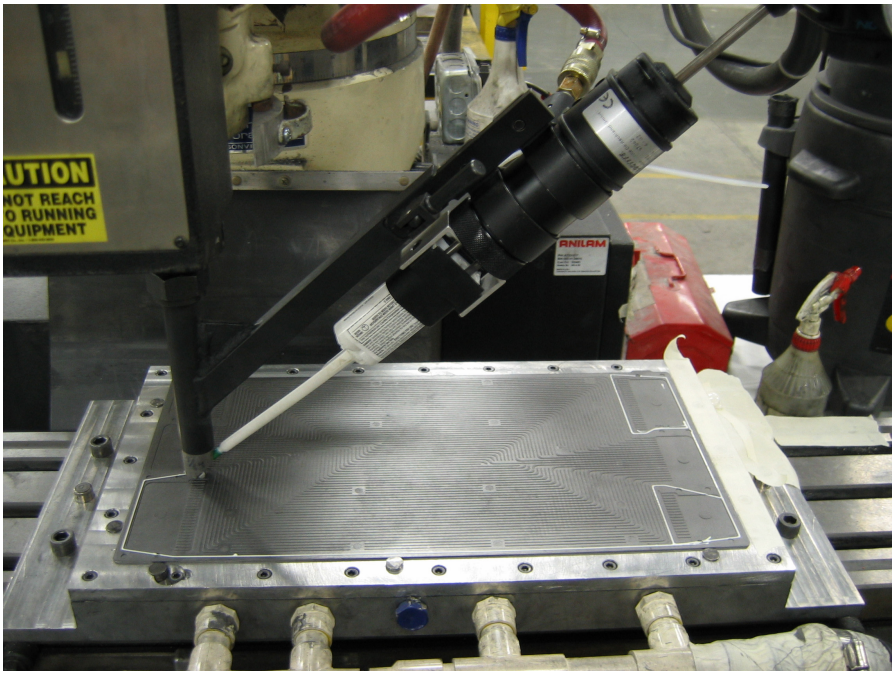

Figure 4.1.1. Automated bond application apparatus.

4.2 Investigate Bonding Systems

In this program we evaluated several adhesive products from a variety of suppliers. The breadth of adhesive choices was very large. Advice was sought from the various manufacturers in selecting products suitable for use in fuel cells. Most companies were found to have previous experience in bonding bipolar plate materials (generally graphite or polymer/graphite composite plates), and were aware of most of the issues, including corrosion resistance, water exposure resistance, wettability, adhesion to graphite products, and leaching of contaminants.

Additional product characteristics that were found to be of high importance to our products included the ability to be effectively extruded and the capability of generating a good seal once cured. Several products were found to be effective bonding materials internally. One product (Loctite E100CN) was selected for use in prototype bonding trials. No adhesive bonding customer qualification of this product was performed, however.

One issue that we encountered early on was the sensitivity of the system to overfill seal surface areas and run-over into adjacent flow channels. Figure 4.2.1 shows a bonded plate with one surface removed. In the region shown, where the seal area becomes compressed, we found that the adhesive tended to flow on compressing into the two closest flow channels. To correct this, it was necessary to increase the CNC speed when applying adhesive to this region, and effectively reducing the amount of adhesive applied in that region. Several destructive trials revealed the proper machine settings to enable effective bonding without overflow into adjacent channels. A better plate design, that includes an overfill channel was suggested to the customer as a way of ensuring that overfill issues will not be encountered. The chief issue was the zero-bondline design that squeezes the adhesive into an extremely thin later that is therefore extremely sensitive to the quantity of adhesive applied to the area. Non-uniform bonding pressure can inadvertently push adhesive into adjacent flow channels and create bonding quality issues. Very small bonding overflow channels would ensure proper bonding despite variations in adhesive application.

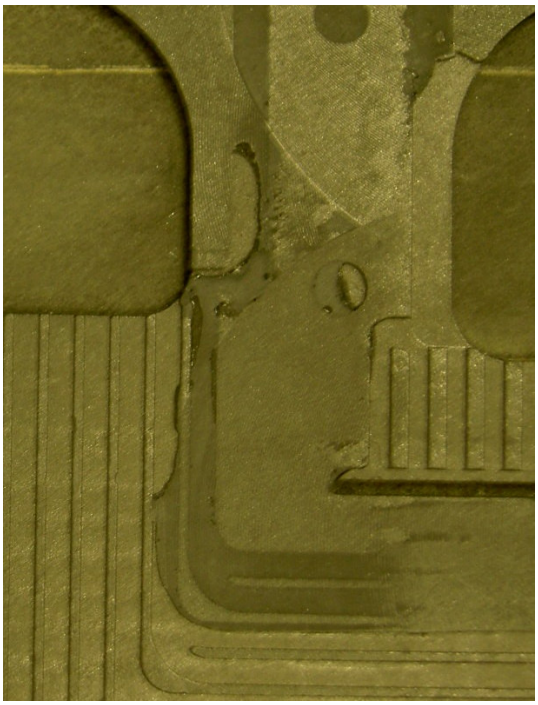

Figure 4.2.1. Photo of adhesive bleedover.

4.3 Demonstrate Low Cost Bonding Process

The modified CNC bonding system was used with the E100CN product to generate 40 bonded carbon/carbon bipolar plates for customer evaluation (Customer proprietary). The adhesive was applied to the plates in less than 1 minute. The anode and cathode plates were then joined in a fixture that ensures proper alignment and clamped into a hot bonding press to ensure good adhesive cure. The cure cycle for the adhesive selected was 5 minutes at a press temperature of 120°C.

Subsequent testing of the bondline confirmed that the method worked well, although improvements could still be implemented to improve overall product yield. About 80% of the parts made and tested passed the bonding leak tests. Of those that did not pass, it was found that nearly all failed due to difficulties associated with sealing the plate against the test fixture gaskets. This has been a chronic problem in our experience. In seal testing, it has been much more common to experience a failure of the gasket that seals the plate to the test fixture than an actual failure in the adhesive bondline. Issues are associated with wearing out the elastomer gasket materials from repeated use, slight mis-alignment of the bipolar plate to the test fixture, and ensuring uniform compression of the elastomer gasket against the bipolar plate. Any slight warp or curveature in the plate can lead to leaks in the gasket locally due to non-uniform compression in that area. This latter issue was addressed in this program, and is described in section III of this report.

From this investigation, we determined that the sealing method developed is robust, generating high yields for effective bonding. However, more work needed to be applied to the design and use of the bond test assembly, and to improving the local warp shown for the specific bipolar plate design evaluated in this program.

After assembly, the parts were boiled in water 24 hours and re-tested. No bondline failures were found to be introduced after the boiling test.

4.4 Definition of Next Steps

Because we had limited call to bond bipolar plates, we determined that no additional work would go into the development of the bonding system. A cost-effective and functional system was demonstrated for low-volume applications. Extending this to higher volumes would be a straight-forward engineering exercise.

5.0 Net-shape Molding

This activity was cancelled and re-worked for the work scope change effected in December 2004 (called Phase III).

5.1 Investigate Material Composition

In this task, we investigated the make-up of the composition to yield acceptable bubble pressure, permeability and net-shape molding performance. Several investigations were run leading to a final product composition. The summary reports follow:

Compositional DOE #1 UTFC

Objective

The objective of the compositional DOE is to optimize the mechanical strength and electrical conductivity of new plates and at the same time to meet the perm and bubble point specification. This preliminary DOE# 1 serves as a screening test to select the best composition for the future DOEs.

Variables and levels

The compositional DOE #1 consists of five variables and four levels. They are:

- Graphite: V11=Graphite A V12=GRAPHITE B
  V13=Graphite A V14= GRAPHITE B
- Thermal plastics: V21=PE low
  V22=PE high
  V23=EC low
  V24=EC high
- Type of forming fiber: V31=Natural V32= Syn 50/50
  V33=Syn C V34=SYN D V111-3
- Amount of forming fiber: V41=A V42=B
  V43=C V44=D

- Amount of resin V51=A V52=B
  V53=C V54=D

The DOE design matrix is given in the Table 1. Hyper-Greco-Latin Squares is used to construct the design matrix.

Table 1

	V11	**V12**	**V13**	**V14**
V21	V31V41V51 **Exp.9**	V32V43V54 **Exp. 1**	V33V44V52 **Exp. 13**	V34V42V53 **Exp. 5**
V22	V32V42V52 **Exp. 10**	V31V44V53 **Exp. 2**	V34V43V51 **Exp. 14**	V33V41V54 **Exp. 6**
V23	V33V43V53 **Exp11**	V34V41V52 **Exp. 3**	V31V42V54 **Exp. 15**	V32V44V51 **Exp. 7**
V24	V34V44V54 **Exp. 12**	V33V42V51 **Exp. 4**	V32V41V53 **Exp. 16**	V31V43V52 **Exp. 8**

There are total 16 experiments. Table 2 is the detailed composition of these 16 experiments. Composition is selected that the ration of graphite/graphite fiber Fortafil is fixed at 50/15.

Table 2

Exp. #	**Graphite**	**Thermal plastic resin**	**Type of forming fiber**	**Amount of forming fiber**	**Amount of resin**
9	A	PE low	Natural	A	A
10	A	PE high	Syn B/Syn C 50/50	B	B
11	A	EC low	Syn C	C	C
12	A	EC high	SYN D 111-3	D	D
1	B	PE low	Syn B/Syn C	C	D
2	B	PE high	Natural	D	C
3	B	EC low	SYN D 111-3	A	B
4	B	EC high	Syn C	B	A
13	A	PE low	Syn C	D	B
14	A	PE high	SYN D 111-3	C	A
15	A	EC low	Natural	B	D
16	A	EC high	Syn B/Syn C	A	C
5	B	PE low	SYN D	B	C

			111-3		
6	B	PE high	Syn C	A	D
7	B	EC low	Syn B/Syn C	D	A
8	B	EC high	Natural	C	B

Experimental Procedure

The typical processing is as follows:

- 30 min deflaking of forming fiber with 10 ml defoamer solution (in mixing tank.
- Pump fiber slurry to holding tank. Then add to mixing tank.
- Add slurry into mixing tank for batches required..
- Add resin slurry that is prepared using Silverson mixer for 5 minutes.
- Prewet graphite fiber and PE if required. Then add to batch along with 10 ml defoamer solution.
- Prewet graphite powders, add to batch along with 10 ml defoamer solution; deflake entire batch for five minutes
- Transfer fiber water slurry back to mixing tank.
- pH was adjusted to maintain at PH=6 in mixing tank with nitric acid or ammonium hydroxide.

Output

1. Bubble point/PERM

    - Flat plates 4x4" was pressed to the following density for BP/PERM measurement 1.18g/cc; 1.2 g/cc; 1.22 g/cc; 1.24g/cc; 1.26 g/cc
    - Bubble Point/PERM measurement on finished molded plate
    - PERM measurement

2. Strength

Strength was measured using biaxial method at Oak Ridge National Laboratory. The test fixture was made of Delrin, an engineering plastic. The support ring was 0.75 inch diameter. The loading ring was 0.375 inch diameter. No interface material was used between the sample and the support and loading rings. It wsa thought that the contact between the Delrin and the

graphite composite parts was sufficiently low in friction that no Teflon or silicone compliance layer was required.

3. Sheet Uniformity

- Sheet to sheet uniformity was judged on the whole wet sheet weight variation (Normalized Stdev. on Mean).
- Within sheet uniformity was characterized on the weight variation (Normalized Stdev on mean) of punched discs on dried sheet according to the pattern below

4. Pressing:

Molded plated was pressed using standard die.

5. Conductivity

Conductivity testing was run on 4x1 specimens.

Results and Discussion

Table 3 summarizes all the output properties as a function of variable and variable levels. There are several interesting observations.

- Sheet to sheet uniformity deteriorates as the amount of fiber increases
- Within sheet uniformity improves as the amount of fibers increases
- Plate width shrinkages increases as the amount of fibers increase
- The PERM decreases as the amount of resin increases

The bubble point value is generally good, although experiments with graphite Graphite A are better. PERM data is not impressive. The future composition should be focused on the improvement of PERM.

Nominal density of plates was calculated using its thickness (not true or equivalent thickness)

Table 3 Output properties vs. Variables and Variable Levels

		Conductivity Siemens/ CM, 1x4 coupons	**Bubble Point KPa, on 4x4 Coupons**	**Strength psi**	**Within Sheet Uniformity**	**Sheet to Sheet Uniformity**	**Predicated PERM on molded plates**	**Predicated Nominal Density of Plates g/cc**
Graphite	Graphite A	**692**	**87**	6441	5.12%	9.54%	12.22	0.80

	GRAPHITE B	631	**58**	5375	5.66%	**5.47%**	**17.17**	**0.81**
Pore Former	Low PE	**691**	73	6290	6.99%	5.25%	13.23	0.8
	High PE	672	73	5487	5.44%	10.09 %	10.82	0.8
	Low EC	**682**	74	6194	5.53%	**4.85%**	21.17	0.81
	High EC	602	71	5663	**3.61%**	9.32%	13.57	0.81
Forming Fibers	Natural	640	74	5616	4.76%	5.12%	19.21	0.78
	Syn B/Syn C	**704**	73	5570	4.85%	6.42%	15.53	**0.83**
	Syn C	661	72	6577	4.72%	5.77%	9.97	0.86
	SYN D 111-3	641	71	5869	7.22%	12.44 %	14.08	0.74
Level of Fibers	A Fibber	656	75	5915	8.18%	5.17%	20.36	0.8
	B Fiber	639	72	6206	5.08%	7.17%	14.11	0.82
	C Fiber	661	75	5871	4.25%	8.64%	11.46	**0.83**
	D Fiber	691	68	5641	4.05%	9.05%	12.86	0.76
Level of Resin	A Resin	657	74	5915	5.56%	7.57%	23.6	0.81
	B Resin	666	68	6206	5.88%	6.88%	18.61	0.79
	C Resin	676	73	5871	5.76%	5.82%	**8.95**	**0.86**
	D Resin	647	76	5641	4.36%	9.76%	7.63	77

Table 4 shows the best selection of variables and variable levels based on their contributions to output properties. Take fiber level and conductivity for example, D fiber level (691 Siemens) will give the highest conductivity amount all four levels. The other levels of addition are making about the same contribution to conductivity, though exact conductivity values are decreasing from C level (661 Siemens), A level (656 Siemens) to B level (639 Siemens).

Table 4 Best Selection of Variables and Variable Levels Based on Their Contribution to Output Properties

Properties		Graphite	Resin Level	Fiber Type	Fiber Level	Additive
Conductivity	1	A, B	C, B, A, D	Syn B/Syn C,	*D*	Low PE, low EC, high PE,
	2			Syn C, Natural, SYN D	*C, A, B*	High EC
Bubble Point	1	Graphite A	D, C, B, A	Syn C, Natural, SYN D, Syn B/Syn C	B, A, D, C	Low PE, low EC, high EC, high PE
	2					
PERM on molded Plates		B	A, B	Natural, Fbrel/Syn C, SYN D	A, B	Low EC
			D, C	Syn C	C, D	High EC, low PE, high PE

Sheet Uniformity Within	1	B , A	D, A, C, B	Syn C, Natural, Syn B/Syn C	D, D, B	High EC, high PE, lowEC
	2			SYN D	A	Low PE
Sheet Uniformity Sheet to Sheet	1	B	C, B	Natural, Syn C , Syn B/Syn C	A	Low EC, low PE
	2		A, D	SYN D	B, C, D	High EC, high PE
Width Shrinkage	1	Graphite A	A	Syn C	A, B	Low PE, low PE
	2		C, B, D	SYN D, Natural, Syn B/Syn C	C, D	Low EC, low EC
Strength	1	Graphite A	B	Syn C	B	Low PE, low EC
	2		C, D, A	SYN D , Natural , Syn B/Syn C	A, C, D	High EC, high PE

Porous Composition Experiment (DOE#2)

Introduction

This report details findings from the second porous material investigation. Results from the first investigation identified key variables that influence product permeability and bubble pressure. The investigation found that low to no forming fiber addition and lower levels of resin addition are beneficial to product porosity characteristics (in terms of bubble pressure and permeability). Further, it was shown that the graphite powder selection drives bubble pressure, where coarser grades produce lower bubble pressures than finer grades. The goals of this investigation were to further explore the variables producing desirable bubble pressure and permeability characteristics, and to explore an additional set of graphite materials.

In this investigation, measurement parameters included product moldability, bubble pressure and permeability. Strength and conductivity were not evaluated due to time constraints and because no flat sheet was manufactured in this experiment.

Variables and levels

The compositional DOE #2 consists of four variables evaluated in eight experiments. Two mid-point experiments were examined as well (experiments 9 and 10). The design matrix is given in the Table 1. In this experiment, the resin and pore former levels are set, the carbon fiber addition level is constant, and the graphite level is allowed to float to accommodate the various ingredient levels investigated in the matrix. Corrections for composition weight loss were made to attempt to achieve consistent product final density after carbonization.

Table 20. Experimental matrix.

Exp.#	Graphite	Pore Former	Resin level	Resin Type
1	GA	PF1	RL1	A
2	GB	PF1	RL1	B
3	GA	PF2	RL1	B
4	GB	PF2	RL1	A

5	GA	PF1	RL2	B
6	GB	PF1	RL2	A
7	GA	PF2	RL2	A
8	GB	PF2	RL2	B
9	GC	PF3	RL3	B
10	GC	PF3	RL3	A

GA – Purified graphite powder
GB – Purified graphite powder
GC –Graphite powder

PF1 – Additive low level
PF2 – Additive high level
PF3 – Additive mid level

RL1 – Resin addition low level
RL2 – Resin addition high level
RL3 – Resin addition mid level

RA – Resin type A
RB – Resin type B

Measurements

The goals of this experimental design are to improve product permeability, bubble pressure and mold-ability. Also of importance is the products uniformity in manufacture. Measurements include product bubble pressure and permeability using the standard vacuum fill preparation technique. Additional parameters of measurement included product weight loss on carbonization, coupon uniformity and dimensional shrinkages. The product was molded on PFCT 100 ton compression test using a two-sided molding die with rib dimensions similar to UTCFC product.

Experimental Results and Discussions

Weight loss on carbonization

Accurate weight loss on carbonization value is very important, as it influences the final product density and dimensional control. Table 2 shows the measured weight loss on carbonization along with the predicted values on some experiments. It is assumed that pore formers lose 100% of their weight in the carbonization process (verified through independent tests), and the carbon yield from the resin used is 50%. The values reported in Table 2 are the measurements of several plates in each case. A significant degree of variation occurred in the some experiments, most notably experiment 9. In this experiment, it is thought that a batching error occurred driving the actual product weight loss to much lower values than predicted. In other experiments, batching inaccuracies or process variation led to off-predicted weight loss results.

Table 2

Exp.#	Measured weight loss on firing	Predicted weight loss on firing	Difference %
1	13.00%	12.33%	0.67%

2	12.04%	12.33%	-0.29%
3	19.8%	21.33%	-1.53%
4	Data not collected	21.33%	Data not collected
5	Data not collected	14.15%	Data not collected
6	14.11%	14.15%	-0.04%
7	21.48%	23.15%	-1.67%
8	22.43%	23.15%	-0.72%
9	**14.44%**	**17.74%**	**-3.30%**
10	16.96%	17.74%	-0.78%

Shrinkage and sheet uniformity

The width and total plate thickness of pressed plates and carbonized plates were measured to calculate composition shrinkage numbers. Table 3 shows the shrinkage data.

Table 3

Exp.#	Width Shrinkage	Thickness Shrinkage
1	0.69%	6.35%%
2	0.71%	6.46%
3	0.64%	5.74%
4	Data not collected	Data not collected
5	Data not collected	Data not collected
6	0.92%	4.74%
7	0.9%	5.4%
8	0.96%	6.15%
9	0.64%	5.8%
10	0.87%	3.35%

Bubble Point and Permeability

Bubble pressure and permeability were measured using the standard measurement and sample preparation techniques (vacuum fill). The data was evaluated two ways, through average parameters corrected for consistent product density, and through a linear curve fit between composition bubble pressure and permeability, as was done in the previous porous composition experiment. In table 4, the permeability is listed for each variable of investigation. Table 4 also shows average values for bubble pressure and permeability corrected for average experiment density.

As seen in the table, Graphite B shows advantage over Graphite A in generating both higher bubble pressures and higher permeabilities. Pore former level 1 (no pore former addition) shows benefit over pore former level 2, and resin type B is a better choice than resin type A. Resin level had a lesser effect, but level 1 may be better than level 2. Some differences in trends occur between the modeled results and the density corrected average results in permeability trends with resin level. The differences are not statistically significant.

Table 4

Variables	Average Predicted Perm at BP	Average Predicted Perm at BP	Average BP (density corrected)	Average Perm (density

	= 50	= 80		corrected)
Graphite A	19.1	7.0	75.0	7.8
Graphite B	42.0	11.7	81.3	12.2
T-ratio			0.98	1.52
PF Level 1	44.0	13.7	78.2	13.0
PF Level 2	17.1	4.9	78.0	6.9
T-ratio			0.03	2.60
Resin Level 1	37.8	10.6	79.9	9.0
Resin Level 2	23.3	8.1	76.3	10.9
T-ratio			0.53	0.59
Resin Type A	23.3	6.7	72.9	9.7
Resin Type B	38.8	11.9	83.4	10.2
T-ratio			1.93	0.14

Best Selections

The best combination of variables in this experiment are the following:

- Graphite B
- No additive
- Resin type B
- Either resin level is acceptable

A model was built from the data of this experiment. Using the best selections, the predictions from this experiment for bubble pressure and permeability are as follows:

- Bubble pressure = 87 kPa
- Permeability = 14.2 x 10^{-16} m^2

An experiment matching this formulation was made in the experimental investigation (experiment #2). The average results from this experiment showed:

- Bubble pressure = 80.6 kPa
- Permeability = 19.5 x 10^{-16} m^2

It should be noted that in this experiment, the average permeability varies significantly at relatively constant bubble pressure. Figure 1 shows the trend for this experiment. For bubble pressures near 80 kPa, permeability varied from less than 10 to more than 20. A good trend between bubble pressure and permeability for this experiment was not obtained. The results are averages for the experiment, and, while promising, the experiment contained both parts that passed and did not pass BP/perm requirements.

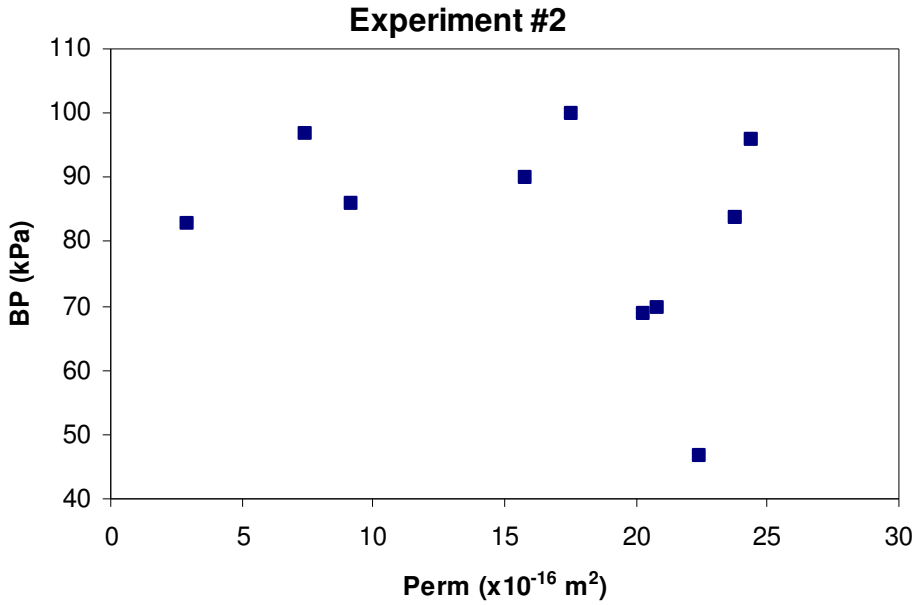

Figure 7. Bubble pressure vs. permeability plot for experiment #2 of this DOE.

Comparison to DOE #1 Results

From the results of the previous DOE, it was found that the trends showed many of the same results found in this experiment:

- Lower quantity of pore former is more beneficial to bubble pressure and permeability
- Lower resin quantity is more beneficial
- Finer particle size graphite powder was more beneficial in optimizing both bubble pressure and permeability

From the previous experimental investigation, an optimal composition was defined as:

- Graphite B (Graphite A in this experiment)
- Low additive
- No Forming fiber
- Moderate Resin (Resin A in this experiment)

Predicted results (comparable to actual results in the experiment) showed:

- Bubble pressure = 87
- Permeability = 24

Significant Differences Between Previous DOE Results and this DOE and Next Steps

In both experiments, it was found that lower amounts of pore former additive improved BP/Perm results. In this experiment, it was not clear if resin amount played a strong role in improving

product permeability. Average analysis of the data indicated that there was minimal if any effect over the range of resin addition studied. Resin type influenced results, pointing to the preferred use of one product over another. Additional study is required to evaluate if the resin type produced any differences in product strength. The graphite type also influenced results strongly. Graphite B in this study is a grade that is made on the supplier's mechanical mill, rather than on their air-jet mill. The end product would be more expensive, have more contaminants and be made with less process control characteristics, so would not be attractive to use despite its better performance results produced in this study. More investigation is warranted here, including an evaluation of the product strength and repeatability using this graphite supply.

Conclusion

This experiment was performed to optimize the porous material composition and uncover the relationship between various ingredients and the plate porosity properties (bubble pressure and permeability). Results showed that some trends continued to hold true, including the trend of improving material properties with decreasing levels of pore former addition. Product permeability was significantly higher with pore former addition of low level as compared to high. The previous experiment showed similar behavior when comparing moderate addition levels. The results of this investigation also pointed to a benefit in porous properties when using different raw material ingredients. Despite the improved properties, it is unknown if the use of this product would otherwise benefit in manufacture, as the manufacture of the product is less controlled and subject to higher manufacturing costs and potential contamination. Additional study is recommended. Also revealed in this experiment is the benefit of using an alternative source of resin. This will also be investigated in further experimentation, but does not provide any foreseeable drawbacks in material supply, cost or purity.

Of concern when evaluating the results of this experimental study is the fact that the overall property numbers are much lower in both bubble pressure and permeability, compared to the results of the previous investigation (referred to here as DOE #1). In that experiment, the best composition showed values that achieved bubble pressure approximately 87 and permeability approximately 24. In this experiment, the use of those same raw material ingredients produced model predicted values much poorer (BP~61, perm ~13). This composition, of course, includes no pore former material. No experiment had these material combinations, but two had similar compositions. Experiment #5, which was the same composition except that the resin type was B instead of A, produced BP ~85, perm ~13. The difference in ideal cases between this DOE and the previous need additional study.

5.2 Investigate Pressing Parameters

PRESSING UNIFORMITY EVALUATION

PRESSED MEASUREMENTS

Introduction

Standard molded parts were pressed in the die at various pressures to evaluate the effect of press pressure on part thickness uniformity achievement. The parts were then measured for thickness in 24 places using a deep-throat dial micrometer. The data collected was evaluate for plate molding uniformity and change with pressing pressure.

Procedure

Parts were pressed on the die at press setpoint pressures (press hydraulic pressure) of 500, 1000, 1500, 2000, and 2500 psi. This equates to approximately 20, 40, 60, 80 and 100 tons, and to part pressing pressure of 360, 720, 1080, 1440, and 1800 psi on the part during the pressing operation. The parts were pressed under the standard press time and operation (standard degas and cure time conditions). After pressing the parts were removed, marked for orientation in the press and measured for thickness in 24 places. Thickness measurement was taken in the flow field pattern area, as shown schematically in Fig 1. Three lines of eight measurements were taken on the plates in the flow field areas. Two of the measurements landed in the uncut water port area (which is the same level as the flow field rib tops). The data is numbered from the top left to the bottom right. Along the top line, the measurements are labeled 1 through 8. The middle measurements are 9 through 16 (left to right), and along the bottom line 17 through 24.

Data and Results

The measurements taken are tabulated at the end of this report. Figure 2 shows the plates overall average thickness vs. pressing pressure. This figure shows a steep reduction in average plate thickness from 500 to 1500 psi (press hydraulic pressure). At 1500 psi and higher, little additional reduction in average plate thickness is seen. Observations of the pressing quality showed that, even at 500 psi, reasonably good mold filling occurred.

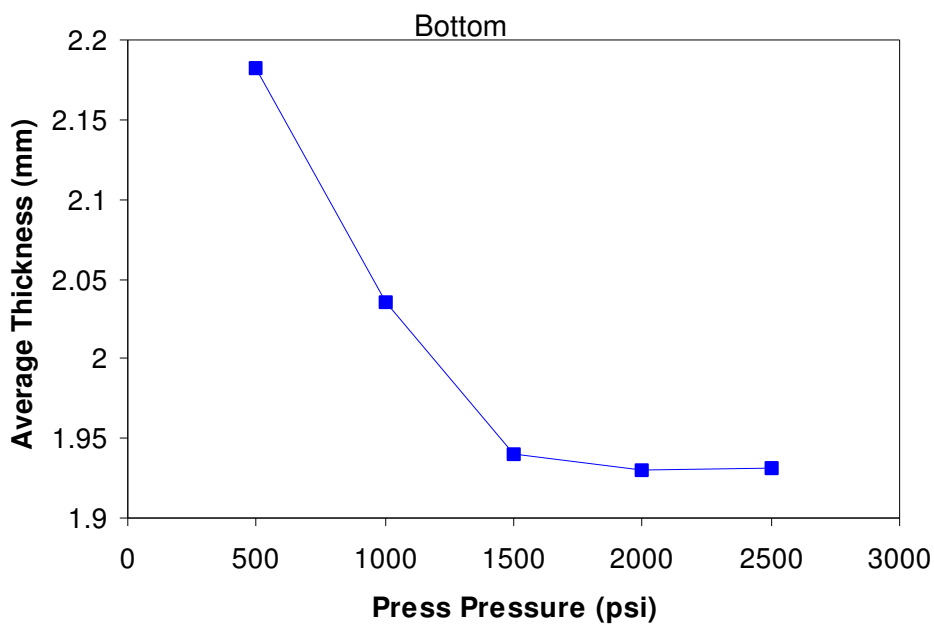

Figure 2. Average part thickness variation with pressing pressure.

From evaluation of the measurements it was apparent that one side of the plates is always thicker than the other side after pressing. This is shown in Figure 3, where the overall plate thickness

average vs. position is plotted. Also apparent in this figure is that the parts are thinner in the middle of the plate (from top to bottom) than at the ends.

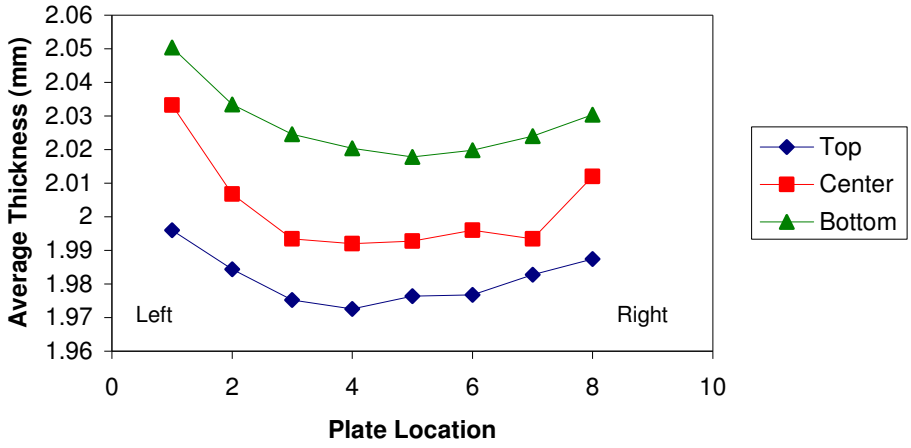

Figure 3. Overall plate average thickness plotted against plate location.

The effect of pressure on the plate is seen to increase the variation in thickness from the left or right to the center of the plate, and reduce the variation from top to bottom. This can be seen by the figures 4 – 8. From these figures, it appears that as tonnage is increased, the plates tend to become thinner in the middle of the plate and thicker on the left and right ends. This is especially apparent in Fig. 7 where the plate was pressed at 2000 psi, but appears less severe with the plate measured at 2500 psi (Fig. 8).

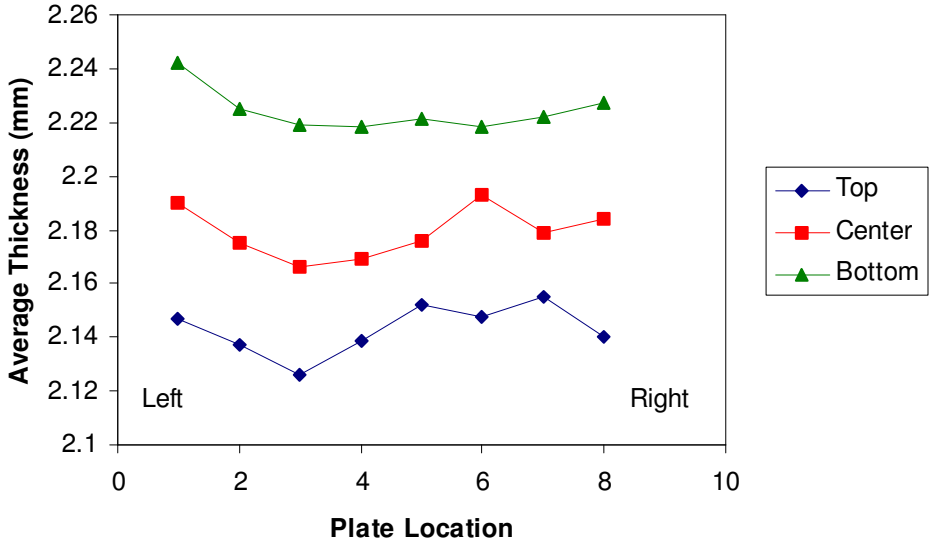

Figure 4. Dimensions measured from plate pressed at 500 psi hydraulic pressure.

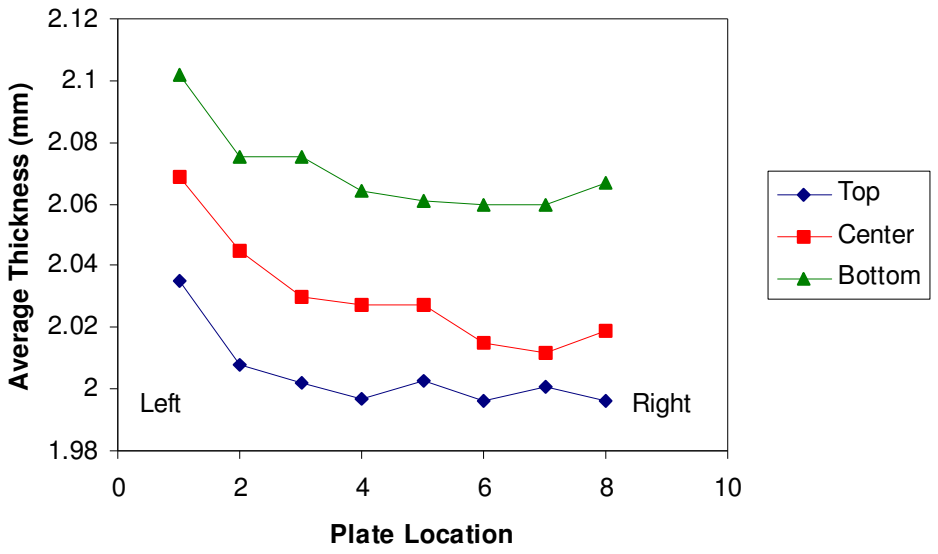

Figure 5. Dimensions measured from plate pressed at 1000 psi hydraulic pressure.

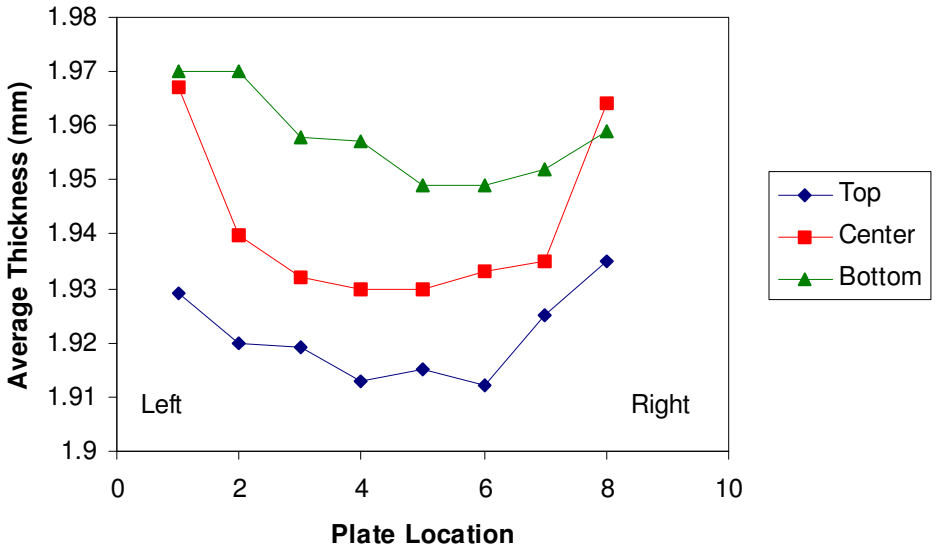

Figure 6. Dimensions measured from plate pressed at 1500 psi hydraulic pressure.

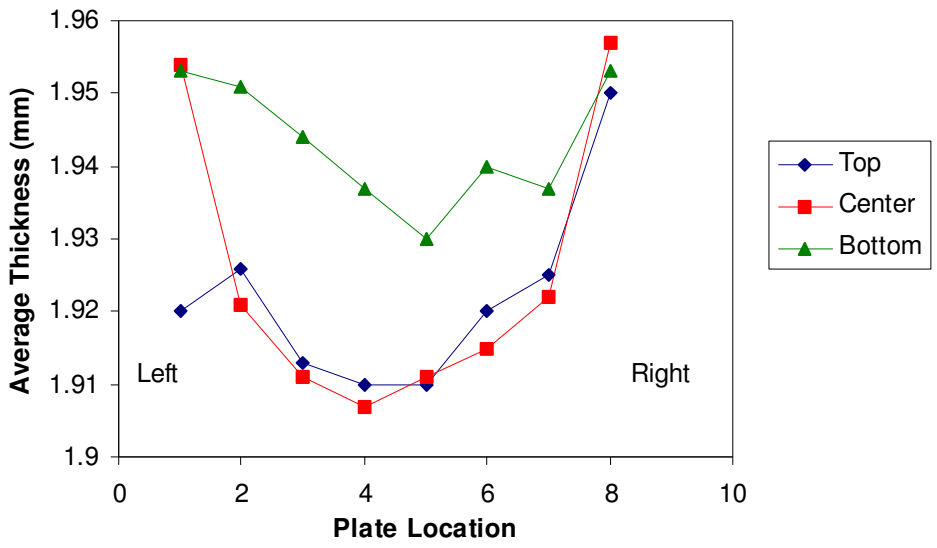

Figure 7. Dimensions measured from plate pressed at 2000 psi hydraulic pressure.

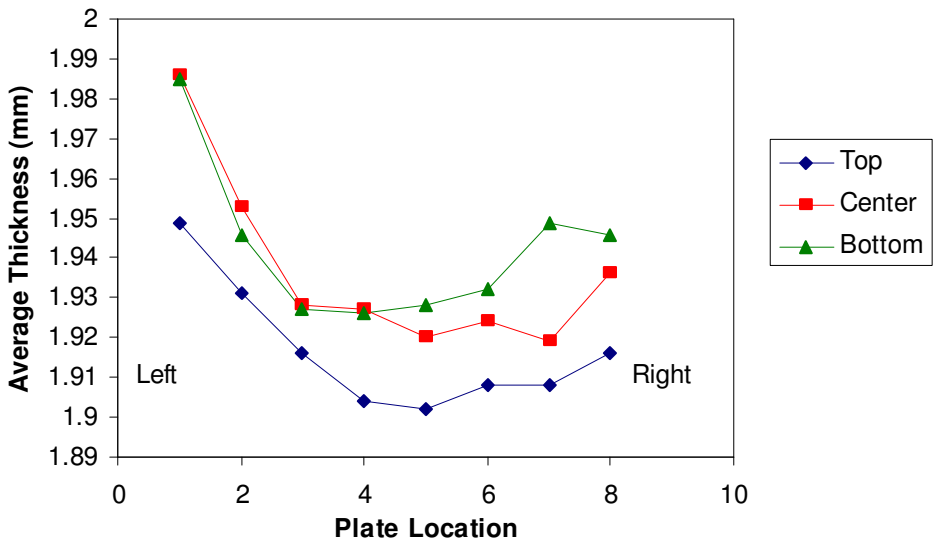

Figure 8. Dimensions measured from plate pressed at 2500 psi hydraulic pressure.

Another item for evaluation is how much the parts are out of dimension, and what impact this may play in the final properties of the plate. Figure 9 shows the maximum deviation for each plate as a function of press pressure. As is seen, the deviation decreases with increasing press pressure, except for the plate pressed at the highest pressure. The trend is probably associated with the practice of plate molding, where pressure is required to push the material fully into the die. The increase in deviation may be caused by die deflection at these higher pressing pressures. The values in inches are also plotted to better provide an understanding of the state

of the pressing uniformity. Most of the deviation appears to come from the centerline of the plate as seen in Figure 10.

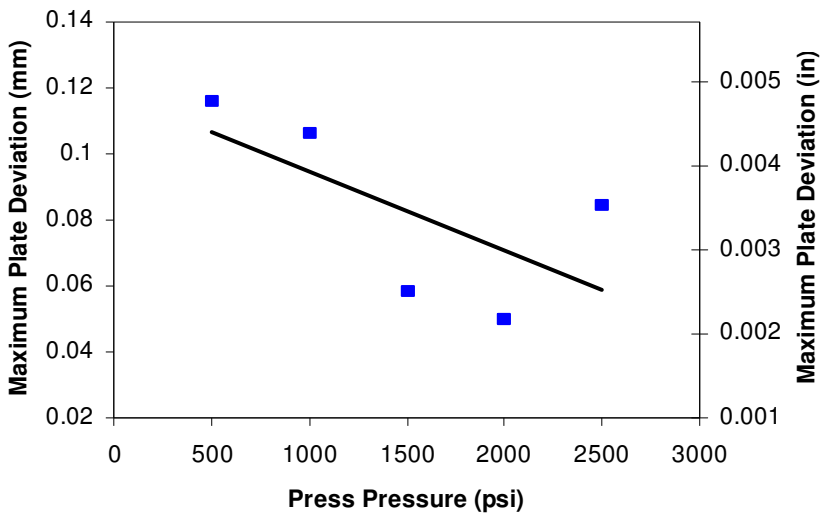

Figure 9. Maximum plate deviation as a function of pressing pressure.

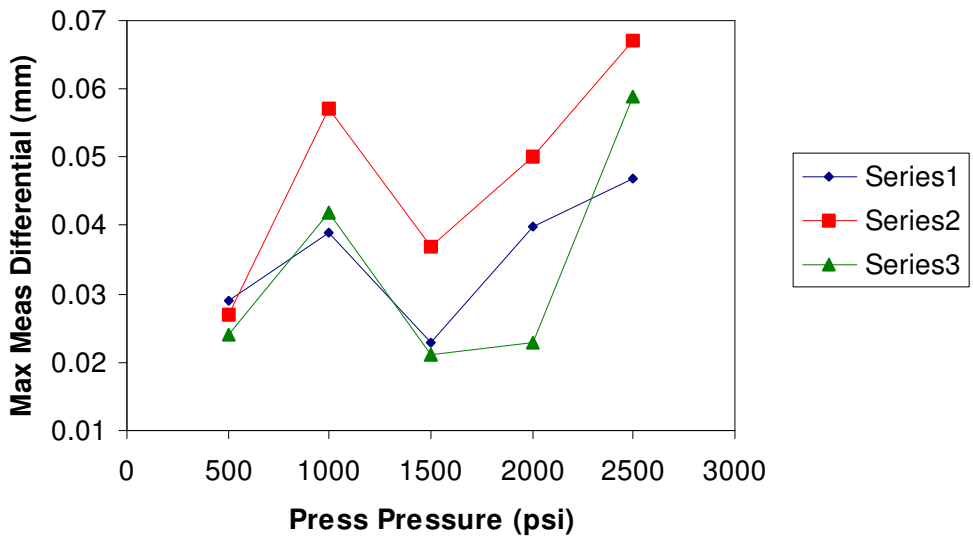

Figure 10. Maximum plate deviation as a function of measurement position and pressing pressure.

Assuming highly uniform initial paper, the effect on density variation as impacted by non-uniform pressing is evaluated. A deviation of 0.02 mm in thickness is approximately 1% of a part that is nominally 2 mm thick. This will lead to local density variations of 1% in the part. For the above samples, it would appear that the parts are somewhat more dense in the middle and toward one side of the plate – the ends being less dense. For the 2000 and 2500 psi parts, this variation is estimated to be approximately as shown in Figures 11 and 12. From the figures, a swing of between 0.04 and 0.06 g/cc would be expected. This density variation can impact product

permeability significantly, depending upon the material composition. A factor of more than two difference between the low and high permeability areas would be an approximation (e.g., 10 in the high density areas and more than 20 in the low density areas), as permeability falls off quickly with density increase.

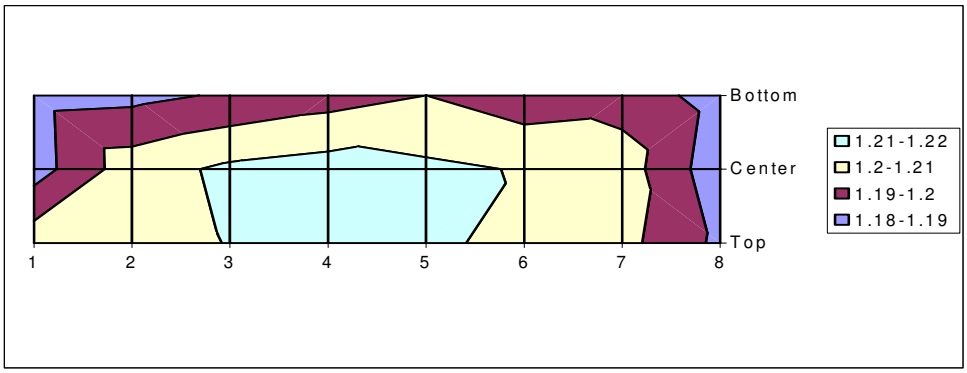

Figure 11. Estimated thickness variation impact on material density assuming average density = 1.20 g/cc for 2000 psi pressed plate.

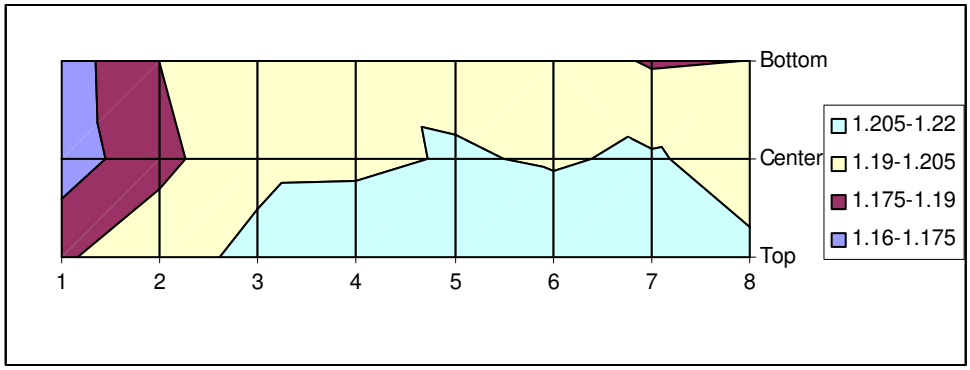

Figure 12. Estimated thickness variation impact on material density assuming average density = 1.20 g/cc for 2500 psi pressed plate.

Conclusion

This report details the impact of press pressure on part uniformity and within part thickness variation resulting from the pressing operation. The study found that the middle of the plate becomes thinner, while the ends remain thicker as press pressure increases. One side of the plate is always thicker than the other (bottom side thicker than the top side), regardless of the press pressure. The report showed that this thickness variation could impact part permeability in areas of higher density. It is possible that die deflection causes some of the thickness non-uniformity. A few specific actions need to be taken to improve pressed part thickness uniformity.

1) Investigate the cause of the significant side-to-side variation – this is most likely a die layout/insertion issue and can be solved quickly.
2) Continue to investigate die deflection with pressure applied
3) Investigate part pressing to pressures sufficient to densify the material, but not excessive such that die deflection results.
4) Investigate mold base modifications that can eliminate die deflection that may occur

5) Investigate pressed plate thickness uniformity capability with a more rigid mold tool and mold base

From this analysis, it appears that the pressing operation imparts more variation than had been anticipated. Elimination of this source of part variation will greatly improve the quality of the plates manufactured.

5.3 Investigate Carbonization Conditions

CARBONIZATION STUDY, BIPOLAR PLATES

Introduction

The carbonization rate significantly effects product cycle time and may influence product properties. This experimental plan is designed to identify key carbonization variables that influence part properties and to identify a faster carbonization cycle.

Experimental Plan

Key variables associated with operating the carbonization process in a vacuum furnace include the following:

Process heating rates
Process hold times and temperatures
Process gas flow rates
Process gas flow injection locations
Process operational pressures
Process gas type
Part configuration
Part density
Loading configuration
Material composition

For this study, we focused upon the following key variables, which can lead to a lower-cost carbonization process:

- Middle Temperature Heating Rate (°C/min)
- Peak Temperature (°C)
- Peak Temperature Hold Time (Hrs)
- Furnace Operating Pressure Setpoint (Torr)

The experimental arrangement is as follows:

Experiment	Heating Rate (°C/min)	Peak Temp (°C)	Hold Time (hrs)	Pressure (Torr)
1	1.5	Low	Short	Low
2	3.0	Low	Short	High
3	1.5	High	Short	High
4	3.0	High	Short	Low
5	1.5	Low	Long	High

6	3.0	Low	Long	Low
7	1.5	High	Long	Low
8	3.0	High	Long	High

Procedure

With each experimental run, load in the following:

- 10 flat sheets loaded in two stacks of 5, one on top of the other, and loaded with graphite block weight
- 5 S500 cathode molded sheet, loaded in one stack of 5, and loaded with graphite block weight
- 5 S500 cathode molded sheet, loaded in 5 stacks of one plate, with graphite felt.
- 3 stacks of 5 graphite plates and graphite block to simulate a furnace load.

After each carbonization cycle, the following was recorded:

- Part length (3 places), width (2 places) and thickness (10 places)
- Molded plate flatness on singly-loaded plates
    - Both overall and ripples
- Plate damage exhibited (blisters, cracks, etc)
- Flat sheet strength (4-point bend)
- Flat sheet conductivity (in-plane)

Results

The experiment was performed as described above, except for experiment #4, which was run at high pressure instead of low. This difference was accounted for in the evaluation of the experiment. The data for flat plates was evaluated principally, as more accurate measurements of dimensions, strengths and conductivities are possible. The molded plates were used for evaluation of product warpage and qualitative observations.

Batches 111 through 116 were used for the flat sheet in this experiment. The carbonized data do not differ significantly from one batch to another, as seen in Table 1.

Table 21. Flat sheet batch shrinkage and weight loss results.

Analysis	Shrinkage Thickness	Lg	Wd	Wt Loss
111	7.34%	0.99%	1.12%	13.27%
112	6.96%	0.94%	1.09%	13.12%
115	7.26%	0.91%	1.07%	13.39%
116	7.48%	0.92%	1.17%	13.35%

The exception was batch #112, which showed somewhat less shrinkage in thickness and overall less material weight loss than the other batches. Material from 112 was used in equal proportions with material 111 in experiments 1 through 4 of this experimental investigation. In general, however, it is not thought that the differences in shrinkage and weight loss shown in the

table are significant when considering the variables investigated in this study. It should be noted that the weight loss is measured between a pressed and a carbonized part.

Heat Rate (C/min)	Thickness Shrinkage	Length Shrinkage	Width Shrinkage	Weight Loss	Conductivity (S/cm)	Strength (psi)	Warp on Plates (mm)
1.5	7.30%	0.94%	1.11%	13.22%	607	5168	4.72
3	7.23%	0.94%	1.12%	13.35%	602	5219	4.97
Peak Temp (C)							
Low	7.12%	0.90%	1.08%	13.03%	512	4608	4.77
High	7.40%	0.98%	1.14%	13.54%	697	5779	4.91
Hold Time (hours)							
Short	7.15%	0.97%	1.10%	13.20%	591	4945	4.56
Long	7.37%	0.92%	1.12%	13.37%	618	5442	5.13
Pressure (Torr)							
Low	7.21%	0.91%	1.13%	13.18%	584	5058	4.56
High	7.24%	0.92%	1.07%	13.24%	564	5085	5.21
Expt Average	7.26%	0.94%	1.11%	13.28%	604	5193	4.84

The data shows that there is very little dependence of the carbonization conditions on part measurements, except for peak temperature and perhaps hold time. Part warp was measured on S500 molded plates using a drop gauge. The measurement is difficult to make accurately, and the results are evaluated and used with caution in this report.

The peak temperature and hold time at temperature were found to have the following influence on the carbonization of the parts:

Higher peak temperature:

- Induces greater material shrinkage
- Induces higher part weight loss
- Results in significantly higher conductivity (~30%)
- Results in significantly higher strength (~20%)

Longer hold time at peak temperature was also found to improve product strength and conductivity. Longer hold times:

- Induces greater material shrinkage
- Induces greater part weight loss
- Results in somewhat higher conductivity (~5%)
- Results in somewhat higher strength (~10%)

In this experiment, it is thought that the parts evaluated were thin enough and of low-enough density that there was no difference in part properties resulting form the heating rate of the furnace. With larger parts and higher density parts, the heating rate could become a factor in limiting part damage, as a slower up-front cycle may be needed to successfully drive off the decomposition gases as the resin in the product breaks down. The average flat plate carbonized density for these experiments was 1.16 g/cc, with a standard deviation of ~5%.

Part warp on the S500 cathode plates was measured for overall bowing. The values measured were similar in all experiments, but the data shows that some variables may induce greater plate bow than others. In general longer hold times and higher furnace pressures resulted in somewhat worse plate bow measurements. Heating rate and peak temperature showed little influence on plate warp.

Implications of Learning

This experiment showed that for parts of this density range, the heating rate can be safely increased to without adversely effecting the properties of the plate. This value should be further evaluated to evaluate the possibility of reducing cycle time.

This experiment showed that there was essentially no effect of furnace pressure on part measurements, except perhaps with the degree of plate warp. The latter should be investigated further, but the other measurements indicate that it should be safe to carbonize at higher pressures without harming product properties. Additional evaluation could include atmospheric pressure carbonization in an inert environment.

This experiment showed that peak temperature and hold time duration impact product shrinkage, strength and electrical conductivity. Improvements were found for product strength and conductivity for higher temperatures and longer hold times. A correlation between product strength and shrinkage, and product conductivity and shrinkage were found (Figures 1 and 2). As part shrinkage increases, part strength and conductivity also increase. Results also found that part weight loss was somewhat higher.

If part strength and conductivity is acceptable at 900°C, it may be possible to carbonize these parts in a belt-type atmospheric furnace, and so reduce cycle times and carbonization costs.

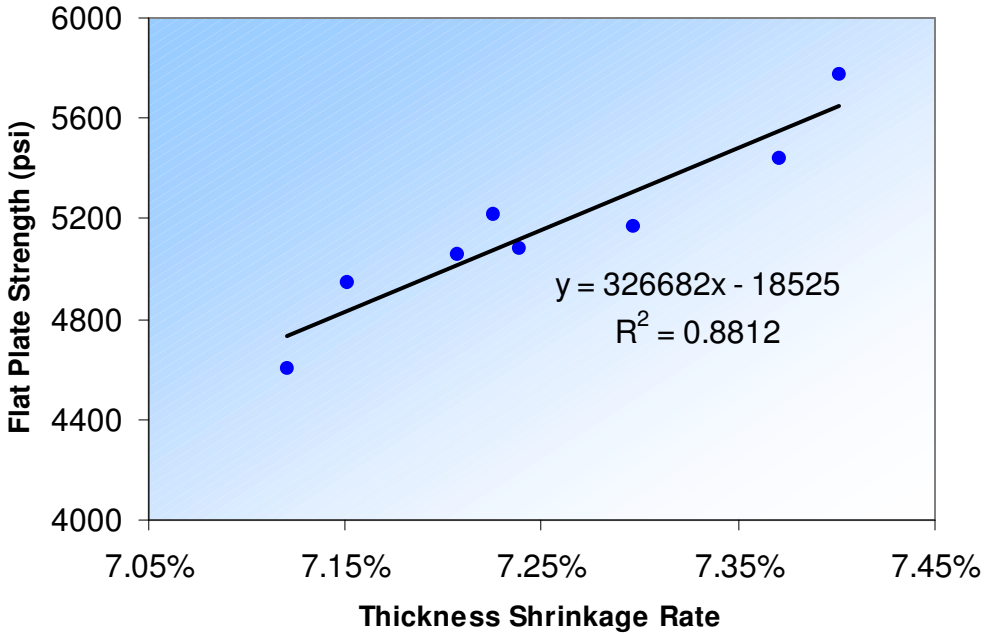

Figure 1. Correlation between flat plate strength and thickness shrinkage rate.

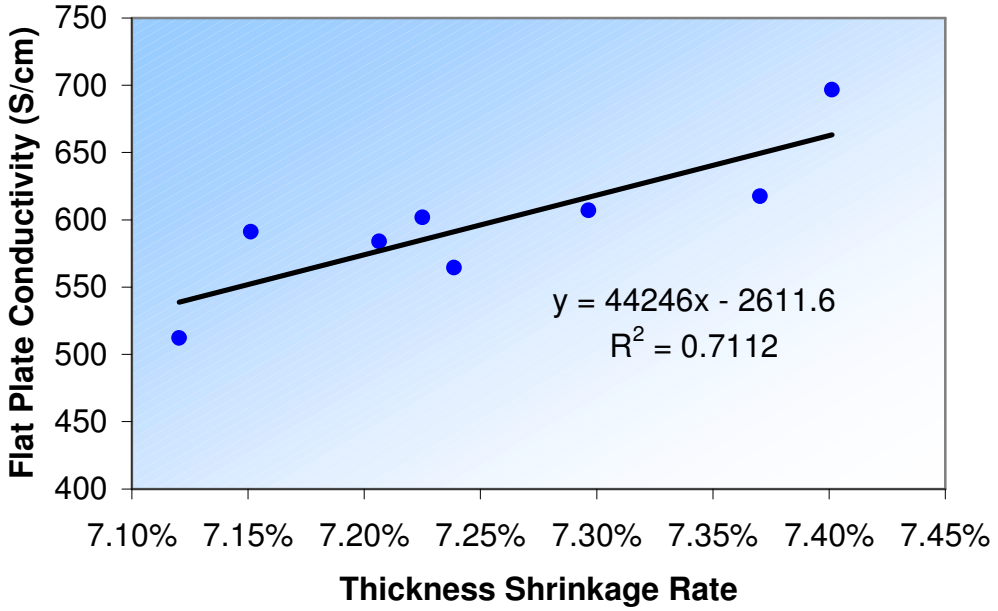

Figure 2. Correlation between flat plate conductivity and thickness shrinkage rate.

Results and Recommendations

This experiment shows that the heating rate can be safely increased to at least 3°C/minute with no apparent impact on product properties, except (possibly) for molded plate overall bow.

Further investigation must be performed to determine if this heating rate can be used with minimal impact on molded part flatness and bow.

This experiment also showed that there is little impact on plate properties with furnace pressure. This indicates that equivalent material properties and characteristics may be achievable under atmospheric pressure conditions, which can lead to substantially reduced carbonization process costs. Further investigation at atmospheric is recommended.

This experiment shows that strength and conductivity are highly dependent upon the cycle peak temperature and somewhat dependent upon the hold time at temperature. The highest strengths and conductivities result from high temperature, long soak duration conditions. However, even at the low temperature conditions investigated in this study, the properties are still reasonable for bipolar plate use. An evaluation of the product requirements and the cost of high temperature operation needs to be investigated to determine if carbonization costs can be reduced by reducing peak soak temperatures in combination with atmospheric and rapid heating cycles.

5.4CVD Sealing Process

In Phase I, we learned about how to apply carbon coatings to the surface of our plates to create an effective hydrogen seal. Variables influencing the uniformity of the coating, and the coating rate were defined. In subsequent work, we applied CVD carbon coatings to several candidate plates for our sealed plate customers, tested the plate seal in-house, and submitted samples for customer evaluation. Feedback from the samples indicated that the seal effectiveness after customer plate bonding and assembly was sporadic. Some plates passed pressure testing at our customer site well, while others failed. Failure analysis generally found very small pinholes or cracks in the surface that led to plate leakage over the required specification.

Evaluating the CVD carbon seal on the plate, it is found that the coating consists as a hard, dense carbon layer adhered to the plate surface. Fig 5.4.1 shows a photograph of the coating at the surface of the plate. The coating consists of multiple layers of very thin carbon, that form when cycles (pulses) of reactive gas is introduced into the reaction chamber. These layers are found to improve the durability of the coating, by enabling crack propagation suppression between layers of the coating. However, this mechanism alone was insufficient to overcome other issues associated with the process including uniformity of the coating from all surfaces of the plate and the sensitivity of the coating to damage from impact and abrasion. Figure 5.4.2 shows a plate area that was damaged in assembly and resulted in part leaking.

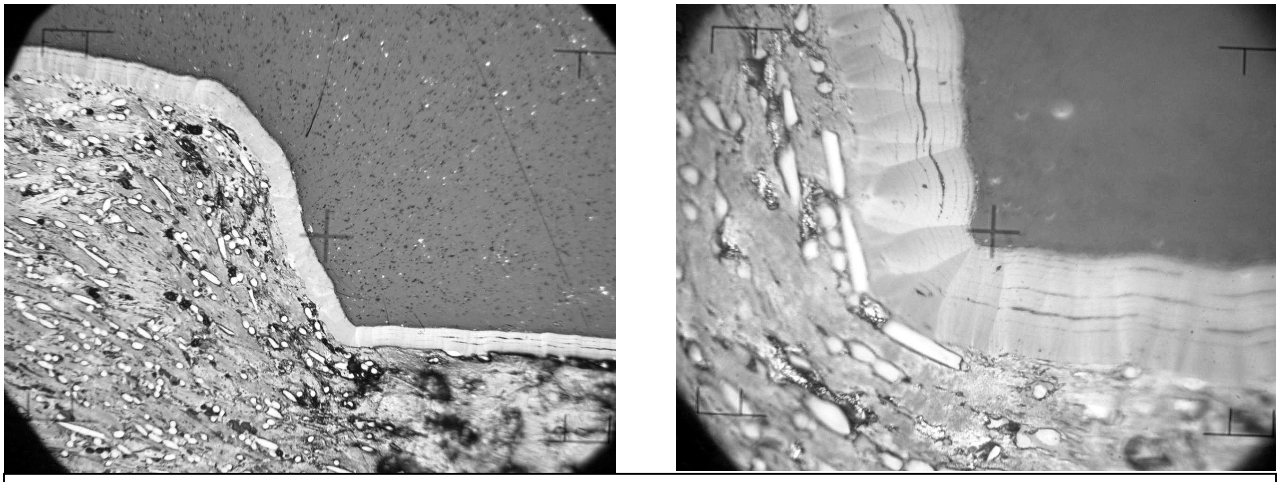

Figure 5.4.1. Cross section of bipolar plate section showing the CVD seal layer, and including a closer view of the layer. Shown are layers applied through reactive gas pulsing.

Further, it was found through customer evaluation of the CVD-coated plates that the coating generates additional contact resistance between the plates. This is represented in Fig. 5.4.3. This chart shows that sealed plates without additional treatment (machining, sanding, etc) designed to improve the contact between anode and cathode yields a high surface-to-surface contact resistance. Plates unsealed (remaining in their original carbonized form without CVD treatment) have extremely low surface-to-surface contact resistance. This is an inherent limitation to the CVD sealing process. Parts that are machined after sealing to improve contact resistance no longer pass hydrogen permeability tests. For this reason, after this learning, our focus to sealing plates changed from CVD sealing to another technology, as discussed in Phase III of this program.

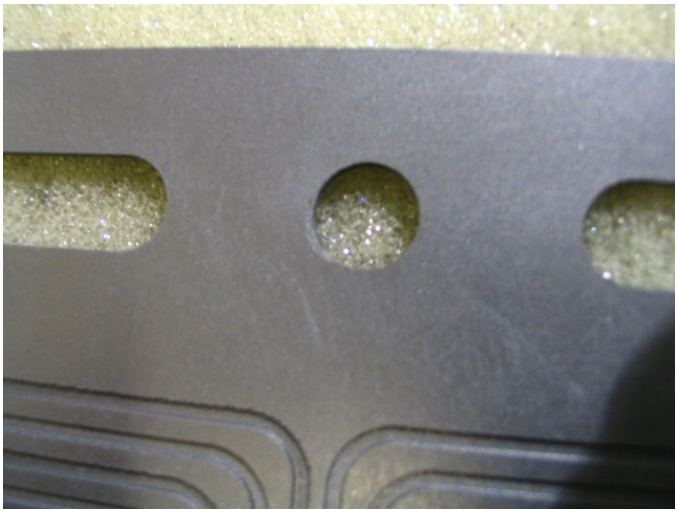

Figure 5.4.2. CVD-coated plate showing scratches resulting in seal failure from assembly operations.

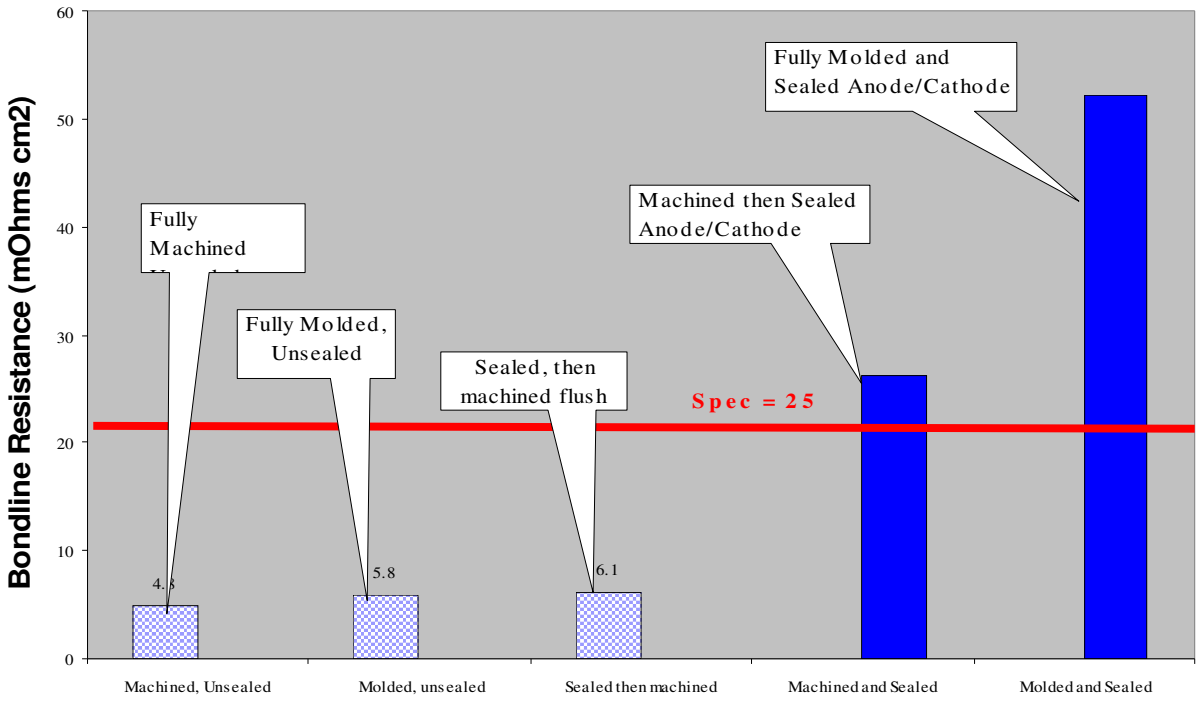

Figure 5.4.3. Chart of plate contact resistance as varies by plate condition (carbonized only, sealed, sealed and machined).

5.5 Optimization and Characterization of Molding Process

POROUS MATERIAL EXPERIMENT

EVALUATION OF RESIN CONTENT, USE OF CHOPPED CARBON FIBER AND USE OF ADDITIVE

Introduction

A short experiment was performed to evaluate the effect of resin content, the use of chopped carbon fibers and the use of polyethylene powder in porous plate manufacture. The UTCFC S600 single-sided anode die set was used. This die set is the most challenging die set to use for mold filling and generating good product permeability. The parts were measured for dimensions, evaluated for mold filling success, and measured for water permeability.

Experiment

Four material batches were made, each producing about 20 useable sheets. The following experimental plan was used:

Ingredient	Expt.1 (Batch 81)	Expt.2 (Batch 82)	Expt.3 (Batch 83)	Expt.4 (Batch 84)
Resin	Low	Low	High	High

Additive	Low	High	Low	High
forming Fiber	High	Low	Low	High
Chopped C-Fiber	Low	High	High	Low

The basis weight target for the materials was 1100 g/m^2. The parts were pressed using the Lawton press at standard process temperature and pressing conditions. The pressed part thickness was changed over a wide range during the pressing of the parts to yield a range of final product density. This was done by shimming the die hard stops sequentially to produce parts that ranged from very poorly filled to very highly filled (and resulting in low to high end product density).

The parts were then carbonized in the batch vacuum furnace (Thermal Tech) with 10 plates stacked together, all constrained under weight. Following carbonization, the parts were measured for length (2 plcs), width (3 plcs), thickness (10 plcs), weight, channel depth (1 place), and permeability (2 plcs).

Results

The data were analyzed to determine the effect of the variables in producing higher permeability and better-filled product. Molding quality was evaluated for product that was judged “good” and “great” with parts that passed permeability requirements (perm of 13). The results of various parameters used to judge product perm and mold fill are shown in the table below:

	Batch 81	Batch 82	Batch 83	Batch 84
Average Rib Height	0.826	0.847	0.812	0.843
Average Plate Thickness	1.394	1.395	1.335	1.352
Estimated Shrinkage	5%	5%	9%	7.5%
Max density w/ good perm (g/cc)	1.20	1.23	1.20	1.18
Min density w/ good mold fill (g/cc)	1.15	1.10	1.15	1.13
Mold Fill Parameter (range 1-5, 1=perfect, 5 = very poor)	3	2	3.5	4.5
Min shim for good perm	0.109	0.109	0.109	0.112
Average Perm for good mold fill	13.9	30.5	18.0	19.0
Good Perm/Mold Fill Density Window (g/cc)	0.05	0.13	0.05	0.05

The charts shown below provide trend information over plate corrected density

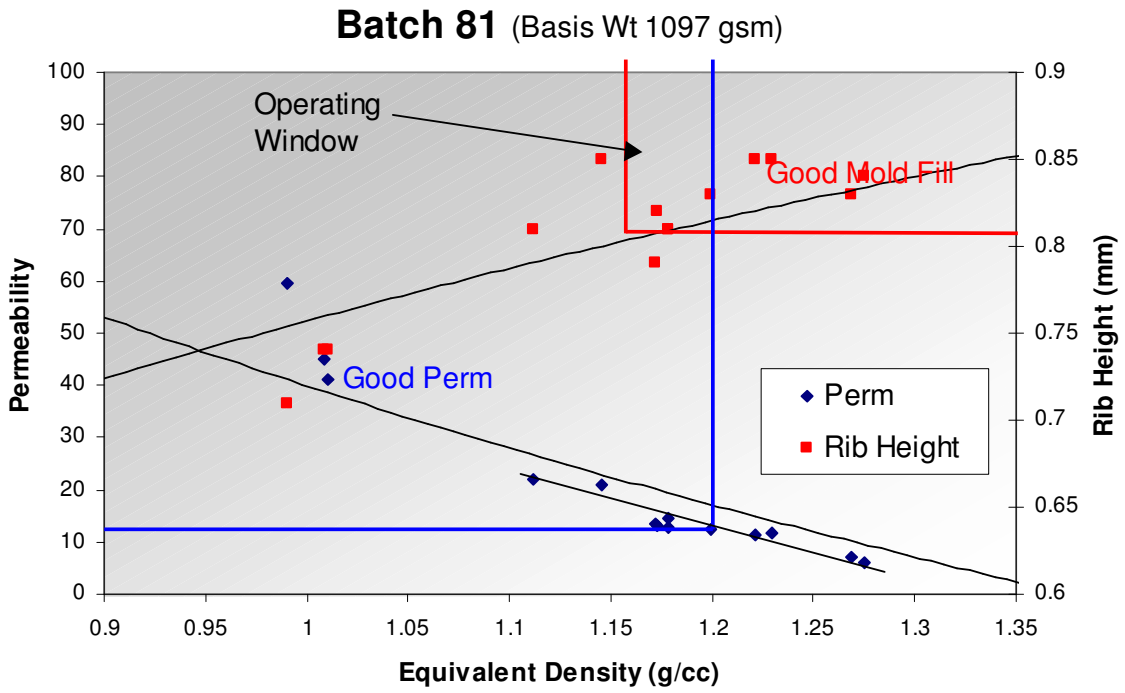
Batch 81 (Basis Wt 1097 gsm)
Operating Window
Good Mold Fill
Good Perm
Perm
Rib Height
Permeability
Rib Height (mm)
Equivalent Density (g/cc)
100
90
80
70
60
50
40
30
20
10
0
0.9
0.85
0.8
0.75
0.7
0.65
0.6
0.9
0.95
1
1.05
1.1
1.15
1.2
1.25
1.3
1.35

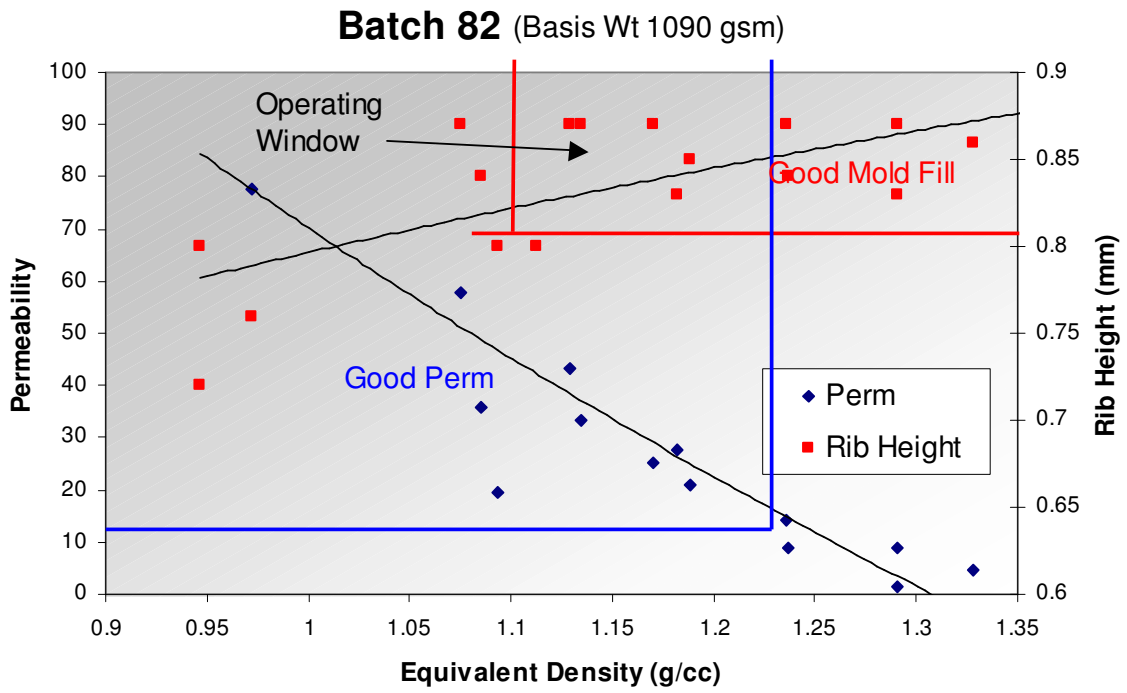
Batch 82 (Basis Wt 1090 gsm)
Operating Window
Good Mold Fill
Good Perm
Perm
Rib Height
Permeability
Rib Height (mm)
Equivalent Density (g/cc)
100
90
80
70
60
50
40
30
20
10
0
0.9
0.85
0.8
0.75
0.7
0.65
0.6
0.9
0.95
1
1.05
1.1
1.15
1.2
1.25
1.3
1.35

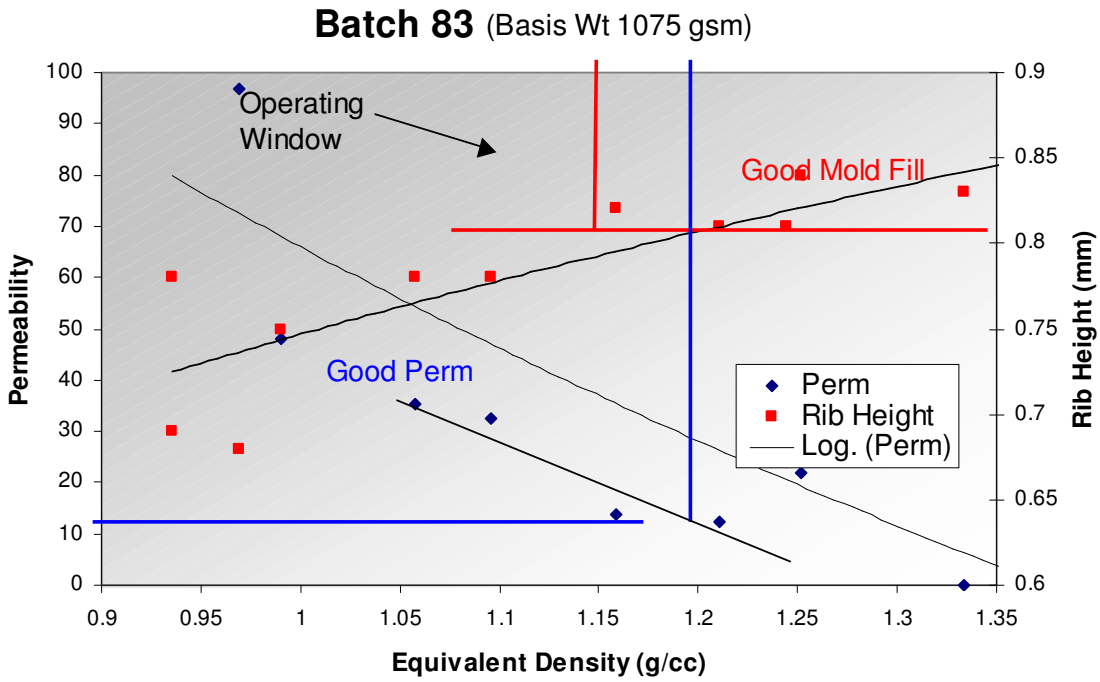
Batch 83 (Basis Wt 1075 gsm)
Operating Window
Good Mold Fill
Good Perm
Perm
Rib Height
Log. (Perm)
Permeability
Rib Height (mm)
Equivalent Density (g/cc)
100
90
80
70
60
50
40
30
20
10
0
0.9
0.85
0.8
0.75
0.7
0.65
0.6
0.9
0.95
1
1.05
1.1
1.15
1.2
1.25
1.3
1.35

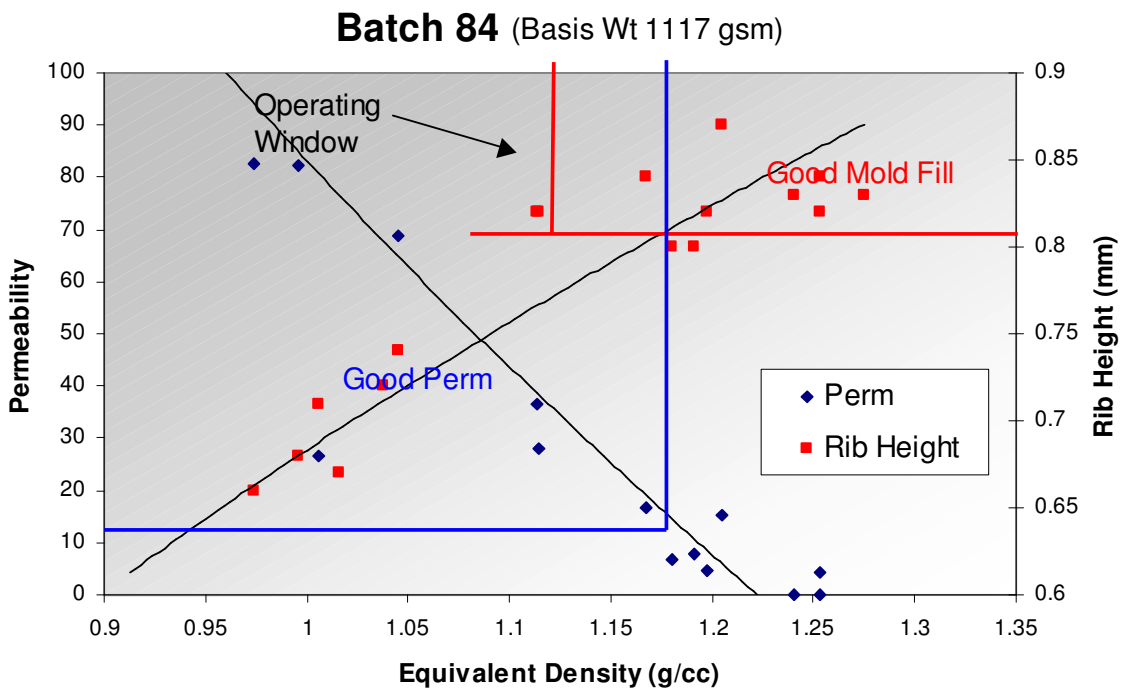
Batch 84 (Basis Wt 1117 gsm)
Operating Window
Good Mold Fill
Good Perm
Perm
Rib Height
Permeability
Rib Height (mm)
Equivalent Density (g/cc)
100
90
80
70
60
50
40
30
20
10
0
0.9
0.85
0.8
0.75
0.7
0.65
0.6
0.9
0.95
1
1.05
1.1
1.15
1.2
1.25
1.3
1.35

Of the runs made, batch 82 exhibited excellent performance. This batch was identical to the standard batch materials, except in the use of the long chopped carbon fiber (replacing the acrylic fiber generally used). The results for this composition showed somewhat better performance than the standard composition.

Batch 84 exhibited the worst performance of the group. While rib heights were generally deep enough to indicate good rib molding, inspection of the molded ribs showed that they were not well filled.

Product using the chopped fiber exhibited fiber presence in the structure of the material after carbonization. The fibers tended to be clumped together on the surface of the sheet, indicating that dispersion should be improved when using the chopped carbon fiber.

Effect of Variables:

	Shrinkage (%)	Mold Fill Parameter	Average Perm (Good Mold Fill)	Operational Density Window (g/cc)
Resin Content – High	8.25	4	18.5	0.05
Resin Content – Low	5	2.5	22.2	0.09
Additive - High	6.25	3.25	24.8	0.09
Additive – Low	7	3.25	16	0.05
Chopped C-Fiber - High	7	2.75	24.2	0.09
Chopped C-Fiber - Low	6.25	3.75	16.5	0.05

Because there were only four experiments, concrete conclusions will not be drawn from the results of this experiment. However, strong trends were noted as follows:

The resin content was found to have the greatest impact of product manufacture and properties. Higher resin contents were found to increase product shrinkage, and to reduce mold fill effectiveness and product permeability. It is possible that lower resin contents add to widening the operational density window as well.

The use of polyethylene powders was found to benefit the molding quality and permeability in this study. Prior experiments have shown that the use of PE powder has no effect on product permeability, however. The best and worst mold fill materials both used PE powder (82 and 84).

Use of chopped carbon fiber showed improved mold filling and better permeability than when not using the chopped fiber. These results are surprising, given that the carbon fibers are generally longer and stiffer than the acrylic fibers normally used. Additional study is needed to confirm the trends seen with the use of the chopped fiber. Qualitatively, no benefit in product strength was noticed with the use of the chopped carbon fiber.

Conclusion

This experiment was designed to take a quick look at some variables of interest in the generation of molded S600 porous bipolar single-sided anode plates. Mold quality and permeability were

judged through qualitative inspection and quantitative measurements. The results showed the following major conclusions:

- Increased resin content does not aid molding quality and hurts product permeability
- Increased resin content increased product shrinkage significantly
- Use of polyethylene powders was found to benefit molding quality and product permeability (although previous experiments found no effect of PE powder use)
- Use of chopped carbon fiber instead of acrylic fiber was found to benefit molding quality – additional study is needed to confirm this benefit.

6.0 Fuel Cell Performance Testing and Construction of Deliverable Fuel Cell Stack.

Test parts were manufactured to demonstrate the process, to evaluate the consistency and capability of the process and to provide test plates to our program partner, UTC Power.

As a first investigation, a production trial was run. Below is a summary of that activity.

Production Trial DOE #1 - Summing It All Up

OBJECTIVE

All of the DOEs conducted by the bipolar plate development group during the first five months of 2004 have focused on a single aspect of the process - chemistry, composition, mixing, or forming. From these experiments, we have learned a great deal about how to make preforms more uniform. Many of the variables we have investigated have clear-cut "preferred" levels. For example, it is clear that bottom filling the Saturn 6 batching cylinder is preferred over top filling because less foam is generated that way.

The present experiment is designed to look at one or two variables in each of the processing areas in a system-wide experiment. We have set the processing conditions at the optimum levels for all the variables we are not examining - e.g., mixing the Saturn 6 the entire time we are filling it.

PROCESSING CONDITIONS FOR THE EXPERIMENT

Mixing

The mixing variable was the length of time the entire batch was mixed through the mixer.

Forming

The forming variable was the type of fill head configuration used - the standard 4-head spider vs a 4-head pinwheel arrangement. The forming conditions included bottom fill in the Saturn 6 fill tube, mix the entire time the tube is being filled and for an additional 30 sec after it is filled, a non-throttled vacuum for standard time. Parts were formed at size and basis weight.

Pressing

Parts were pressed in the S-300 die to a range of shim sizes. We were shooting for a range of densities between 1.1 and 1.35 g/cm^3. Unfortunately, we did not achieve the full range of densities for all compositions. We made note of how the parts pressed, especially whether there were problems with parts sticking in the die.

DOE Inputs

The plan for the DOE is set out in Table 2. It is an 8-experiment Taguchi design with seven variables at two levels each. Only main effects can be extracted from the outputs and all outputs are confounded.

DOE Outputs

We measured and/or observed the following outputs for each experiment within the DOE:

1. Sheet weight for each sheet formed
   (Sheet weight vs sheet number slope was derived from those data)

2. Coupon weights for the eleven standard coupons from the 4th and every 6th sheet after that. From these data, we calculated average coupon weight and variance of the coupons within a sheet.

3. Pressing behavior - mainly whether the parts stuck in the die

4. Permeability and bubble pressure

RESULTS AND DISCUSSION

The results of the experiments are summarized in Table 3 and in Figure 1. The Mean Value analysis is summarized in Table 4. Of the seven variables examined, the use of polyethylene powder had the biggest effects followed by the type of fill head, the type of mixing in the holding tank, and the mix time. The amount and type of latex used to flocculate the suspension had little effect on forming (although it did affect sticking in the die). The type of defoamer had the smallest effect.

Table 2. Design for UTCFC Production DOE #1

Exp #	Additive Type	Additive Level	Mix time (min)	Holding Tank Blade	Fill Head (4-spout)	Other	Defoamer
1	A	Low	Short	A	Standard	No PE	A
2	A	Low	Short	B	Pinwheel	PE	B
3	A	High	Long	A	Standard	PE	B
4	A	High	Long	B	Pinwheel	No PE	A
5	B	Low	Long	A	Pinwheel	No PE	B
6	B	Low	Long	B	Standard	PE	A
7	B	High	Short	A	Pinwheel	PE	A
8	B	High	Short	B	Standard	No PE	B

Table 3. Outputs for UTCFC Production DOE #1

********** **OUTPUT VARIABLES** **********

Exp	Trimmed Slope	Coupon Weight	Coupon Variance	Coef of Variance	Variance/ mean^2	Behavior in Pressing	Foam	Water flow at 1.3 g/cm^3
	(g/sheet)	(g)	(g^2)	(% of mean)	(unitless)	0 - no stick	1 - high foam	(g/min)
						1 - stuck	0 - low foam	
1	2.40	2.06	0.0045	3.23	0.0010	**0**	1	3.2
2	**0.07**	2.03	**0.0018**	**2.12**	**0.0004**	**0**	**0**	**4.7**
3	1.25	2.11	0.0039	2.98	0.0009	**0**	**0**	4.4
4	1.25	2.30	0.0413	8.83	0.0078	1	**0**	0
5	1.45	1.91	0.0302	9.13	0.0083	1	1	0.97
6	0.72	**2.51**	0.0043	2.61	0.0007	1	**0**	3.8
7	1.87	2.26	0.0030	2.43	0.0006	**0**	**0**	1.4
8	0.16	2.21	0.0129	5.14	0.0026	0	1	3.2
Max	2.40	2.51	0.0413	9.13	0.0083	1	1	4.7
Min	0.07	1.91	0.0018	2.12	0.0004	0	0	0.0

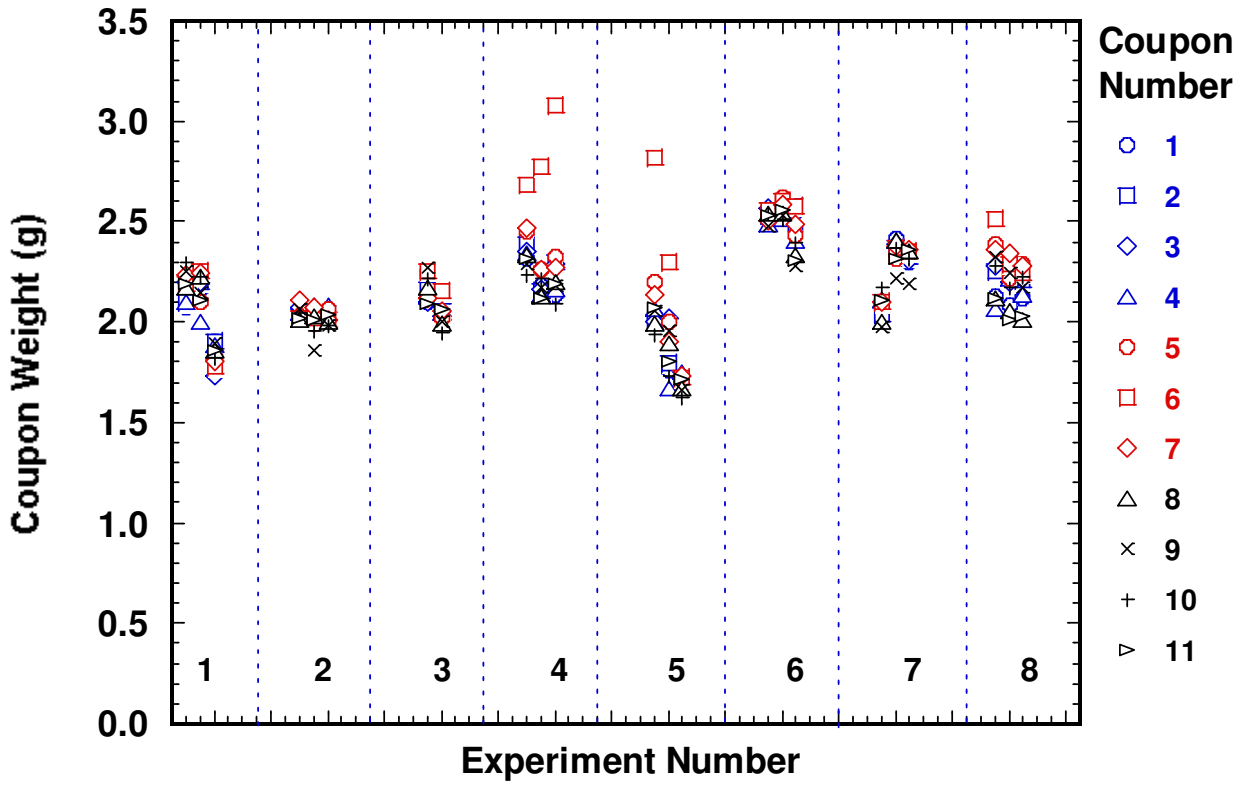

Figure 1. Overview of coupon weights for the eight experiments.

Table 4. Mean Value Analysis for Production DOE #1								
Trimmed slope (lower is better)								
	Level	**Additive**	**Additive**	**Mix time**	**Holding Tank Blade**	**Fill Head**	**Composition**	**Defoamer**
		Type	**Level (g)**	**(min)**	**400 RPM, CCW**	**(4-spout)**		
	1	1.243	1.159	1.126	1.743	1.133	1.316	1.559
	2	1.050	1.134	1.167	**0.550**	1.160	0.977	**0.734**
t-statistic	1.94@0.1	0.317	0.042	0.066	**3.193**	0.045	0.568	**1.610**
	2.45@0.05							
Coupon Weight (higher is better)								
	Level	**Additive**	**Additive**	**Mix time**	**Holding Tank Blade**	**Fill Head**	**Composition**	**Defoamer**
		Type	**Level (g)**	**(min)**	**400 RPM, CCW**	**(4-spout)**		
	1	2.125	2.125	2.138	2.083	2.221	2.120	**2.282**
	2	2.218	2.219	2.205	**2.260**	2.122	2.224	2.062
t-statistic	1.94@0.1	0.679	0.680	0.478	1.440	0.721	0.762	**1.982**
	2.45@0.05							
Coupon Variance (lower is better)								
	Level	**Additive**	**Additive**	**Mix time**	**Holding Tank Blade**	**Fill Head**	**Composition**	**Defoamer**
		Type	**Level (g)**	**(min)**	**400 RPM, CCW**	**(4-spout)**		
	1	0.013	0.010	**0.006**	0.010	0.006	0.022	0.013
	2	0.013	0.015	0.020	0.015	0.019	0.003	0.012
	Ratio	1.022	1.499	**3.594**	1.448	**2.990**	**6.806**	1.085
Variance/Mean^2 (lower is better)								
	Level	**Additive**	**Additive**	**Mix time**	**Holding Tank Blade**	**Fill Head**	**Composition**	**Defoamer**
		Type	**Level (g)**	**(min)**	**400 RPM, CCW**	**(4-spout)**		
	1	0.0025	0.0026	**0.0012**	0.0027	**0.0013**	0.0050	0.003
	2	0.0031	0.0030	0.0044	0.0029	0.0043	**0.0007**	0.003
	Ratio	1.204	1.134	**3.740**	1.065	**3.265**	**7.600**	1.218

Table 4 (cont). Mean Value Analysis for UTCFC Production DOE #1								
Sticking During Pressing (lower is better)								
	Level	**Additive Type**	**Additive Level (g)**	**Mix time (min)**	**Holding Tank Blade 400 RPM, CCW**	**Fill Head (4-spout)**	**Composition**	**Defoamer**
	1	**0.25**		**0.25**	**0.25**	0.50	0.75	0.50
	2	0.75	0.50	0.75	0.75	0.50	**0.25**	0.50
Foam Generation (lower is better)								
	Level	**Additive Type**	**Additive Level (g)**	**Mix time (min)**	**Holding Tank Blade 400 RPM, CCW**	**Fill Head (4-spout)**	**Composition**	**Defoamer**
	1	0.25	0.50	0.50	0.50	0.50	0.75	0.25
	2	0.50	0.25	0.25	0.25	0.25	**0.00**	0.50
Water flow @ 1.3 g/cm^3 density (ml/min) (higher is better)								
	Level	**Additive Type**	**Additive Level (g)**	**Mix time (min)**	**Holding Tank Blade 400 RPM, CCW**	**Fill Head (4-spout)**	**Composition**	**Defoamer**
	1	3.08	3.17	3.13	2.49	**3.65**	1.84	2.10
	2	2.34	2.25	2.29	2.93	1.77	**3.58**	3.32
t-statistic	1.94@0.1	0.575	0.731	0.658	0.333	**1.776**	**1.572**	1.005
	2.45@0.05							

Additive powder

Adding additive powder to the mix had the following effects -

1 - it dramatically reduced the within-sheet coupon weight variance (variance was six times lower with PE)

2 - it eliminated foam in the forming box

3 - it greatly reduced sticking in the die

4 - it increased the permeability of the parts by a factor of two

Mixing in the holding tank

Using two B blade instead of A blade greatly reduced the sheet-to-sheet variability (slope of the dry sheet weight vs sheet number went from 1.743g/sheet to 0.550g/sheet with a t-ratio of 3.193). The type of mixing in the holding tank had essentially no effect on the within-sheet uniformity.

Fill head configuration

Using the standard 4-spout spider (opposed flow) was much better than the 4-spout pinwheel (flow clockwise). The within-sheet variance was reduced by a factor of three. The permeability also increased by a factor of two.

Mix time

A shorter mix time lead to lower coupon weight variance (three times lower variance) and higher permeability (about 50% higher)

Permeability and uniformity

Three of the variables greatly reduced within-sheet variance - use of polyethylene powder, using the spider fill head configuration, and short mix time. All of these variables also showed improved permeability. Figure 2 shows a plot of water flow at a density of 1.3 g/cm^3 (the only density where we had data for all experiments) vs uniformity (as variance/mean^2). Clearly, as the uniformity increases (variance decreases) the permeability increases. This is a somewhat surprising result; however, it points out yet another advantage to achieving high part uniformity.

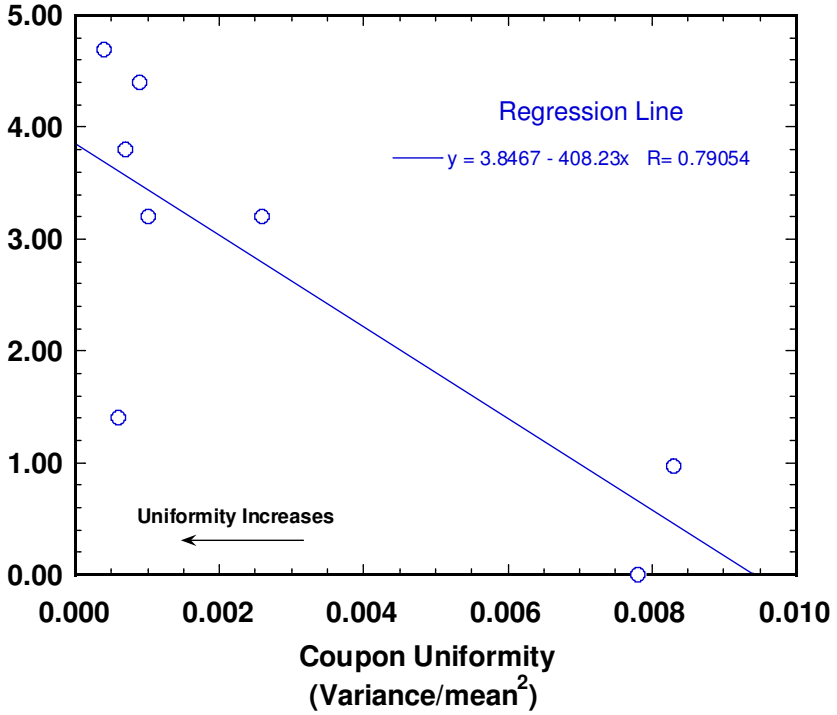

Figure 2. Permeability increased with increasing within-sheet uniformity.

Table 5. Summary of Performance and Prediction of "Best" Settings

Overall Best

Level	Additive Type	Additive Level (g)	Mix time (min)	Holding Tank Blade Type	Fill Head (4-spout)	Composition
1	**4***		**3, 4**	4(?)	**3, 6**	
2				**1, 2, 5**	4 (?)	**3, 4, 5, 6**
*Key	1 - slope		4 - pressing			
	2 - coupon weight		5 - foam			
	3 - coupon variance		6 - water flow			

"Best" Settings

Level	Additive Type	Additive Level (g)	Mix time (min)	Holding Tank Blade Type	Fill Head (4-spout)	Composition
1						
2	**NW-1845K**	**Either**	**5 min**	**2-10s**	**standard**	**w/ PE**

6 Fuel Cell performance Testing and Construction of Fuel Cell Test Stack

In this section, we manufactured parts for fuel cell testing, and evaluated the properties and measures defined as important in characterizing the materials in-house. This information was presented to UTC Power prior to their construction of a fuel cell test stack from these parts. A summary process capability report follows:

DATA REVIEW, PLATES SUPPLIED FUEL CELL EVALUATION

Introduction

Following improvements to the forming system to improve within sheet uniformity, several batches were made to manufacture parts for cell testing at UTCFC. The data shown in this report are taken from the batch sent to UTCFC for evaluation – batch 195. These plates were fully measured and characterized prior to shipment to UTCFC. The measurements included in-process measures (dry weights, press weights, carbonized weights, thickness and dimension. In-process uniformity measurements included the standard basis weight coupon measures. Pressed plate uniformity measurements were not made with this batch.

Dry, Pressed and Carbonized Weights

Figure 1 shows the dry sheet weights. The sheets were not trimmed for these runs, as a net dimension forming pan was used. The data shows one outlier point in the sheet weight consistency (sheet #2). Pressed weights are shown in Fig. 2, carbonized weights in Fig. 3.

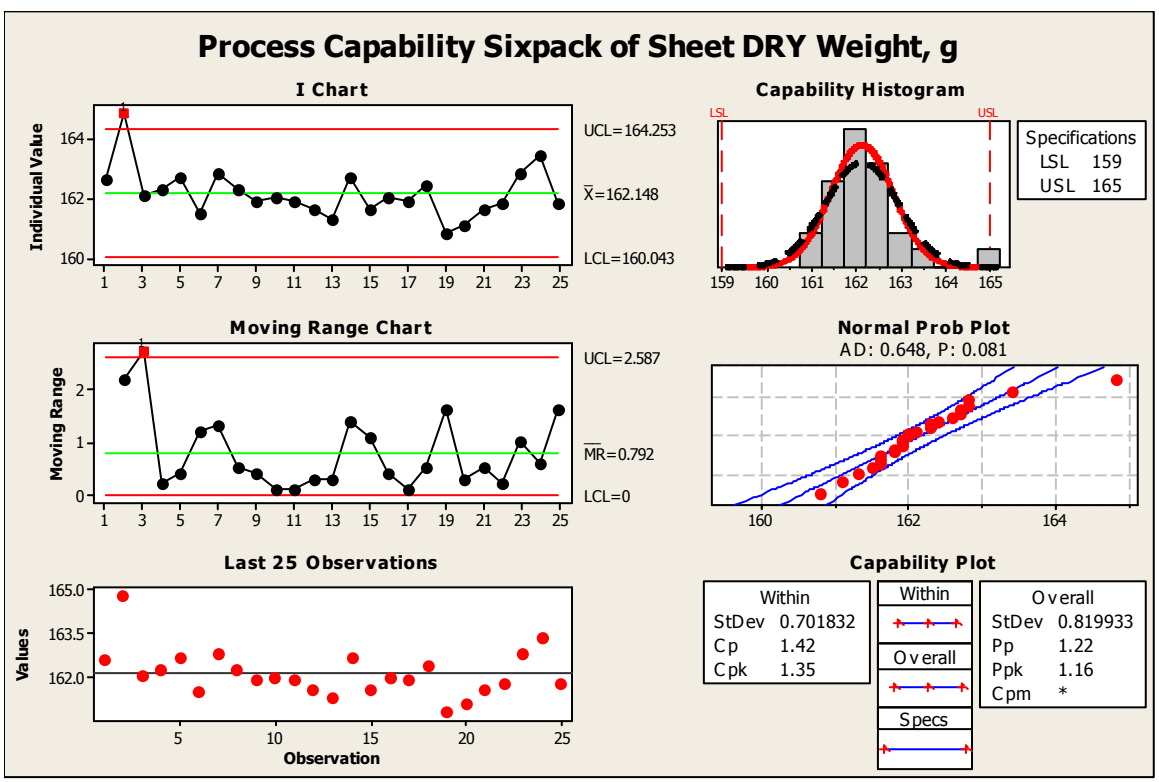

Figure 7. Dry sheet weight capability for batch 195.

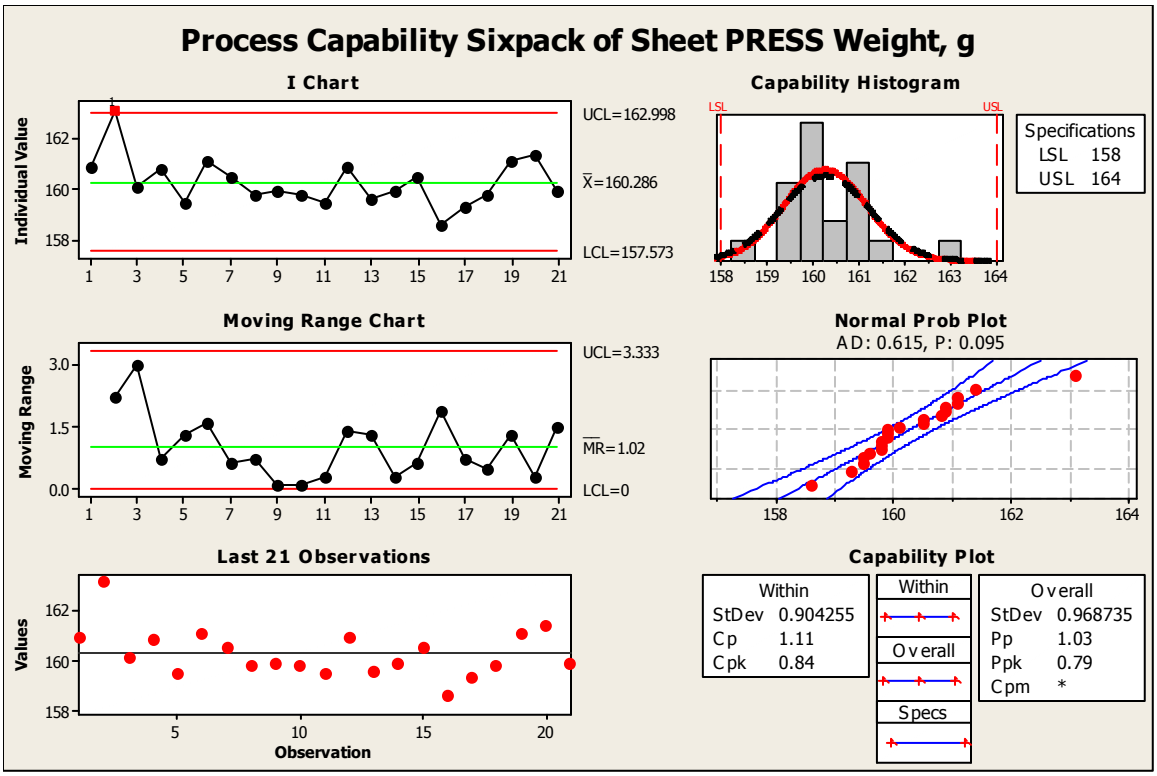

Figure 2. Pressed sheet weight capability for Batch 195.

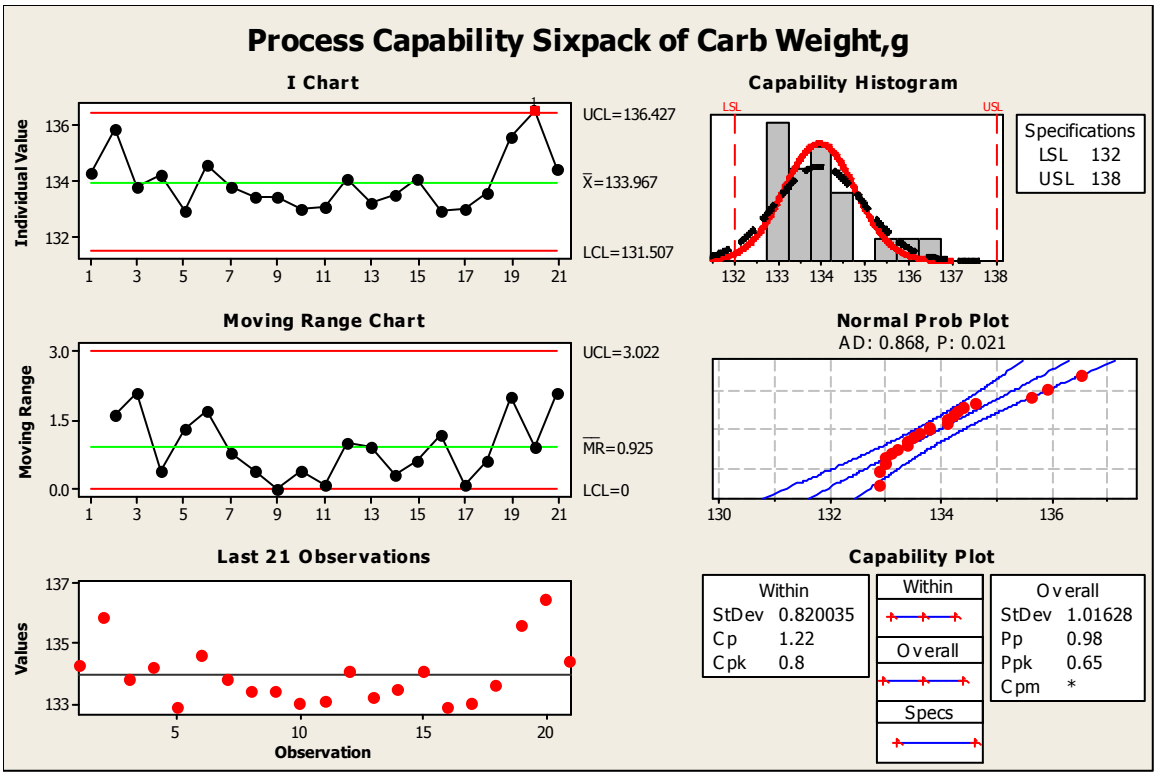

Figure 3. Carbonized weight capability for Batch 195.

Carbonized Dimensions

Figure 4 shows the final average thickness of the plates. Figures 5 and 6 show the average length and width before final trim. Length and width are as formed with no part trimming. The edges of the parts prior to trimming were not straight or parallel.

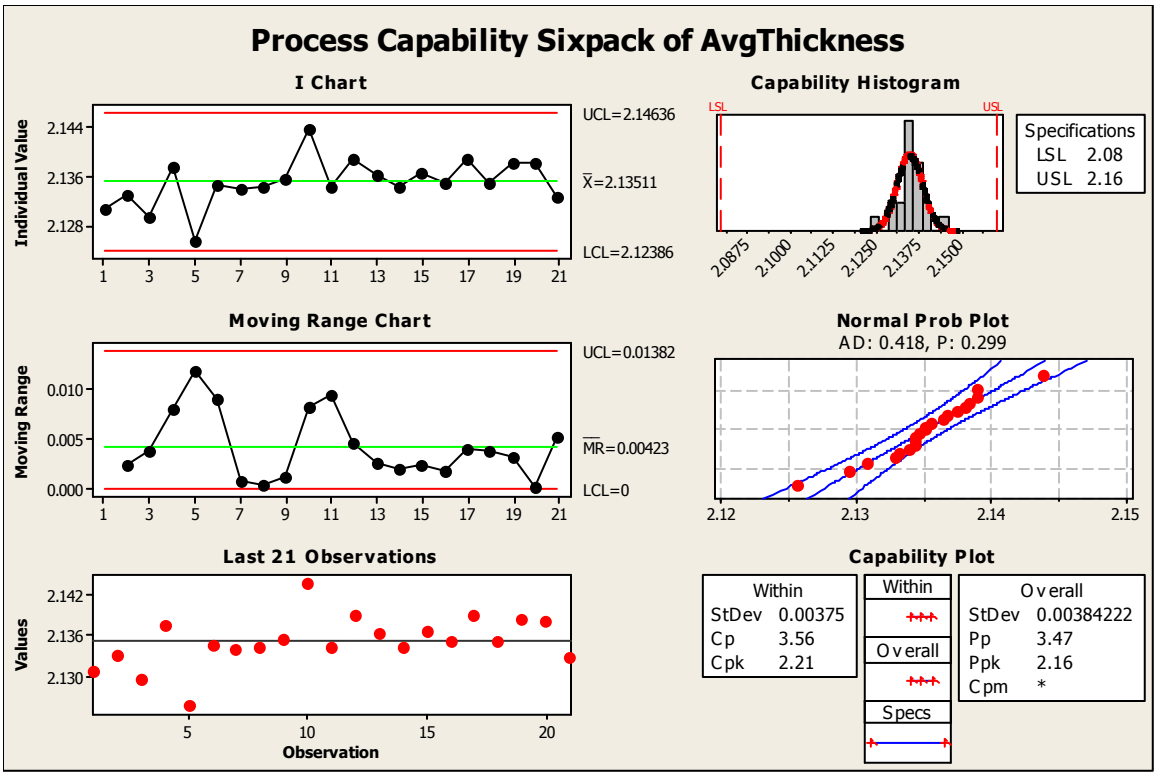

Figure 4. Final plate average thickness capability for batch 195.

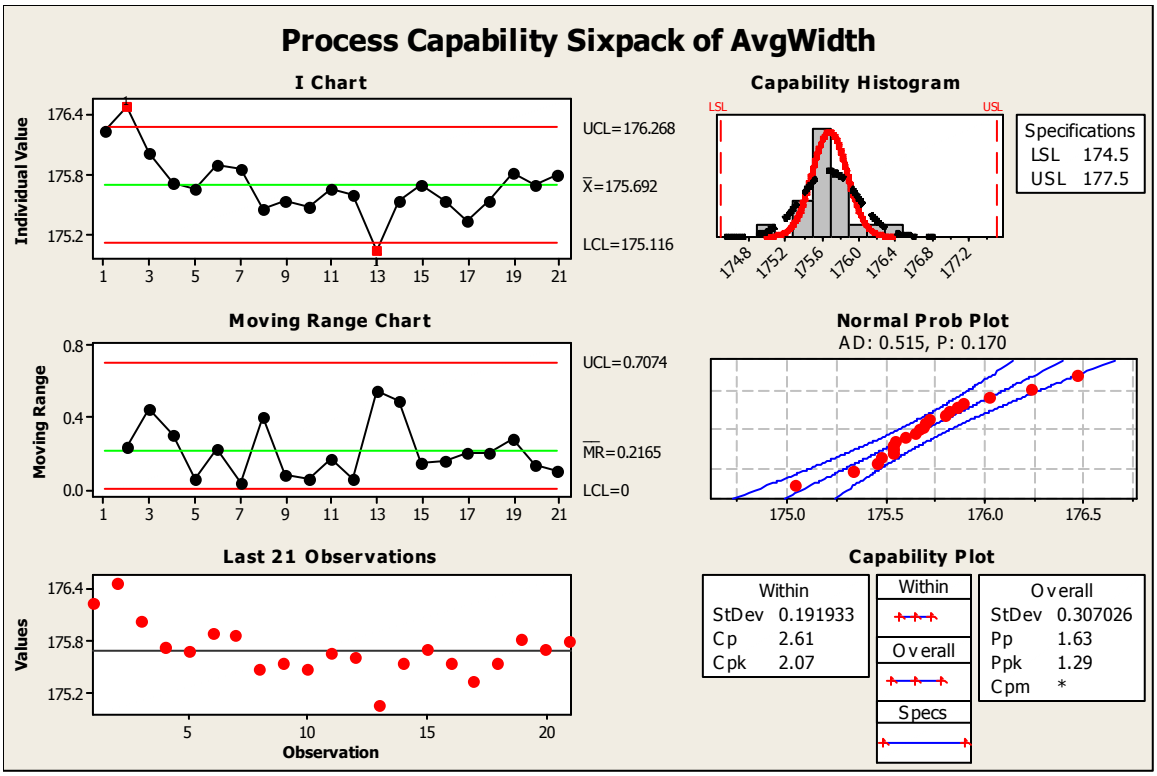

Figure 5. Final plate average width capability for batch 195.

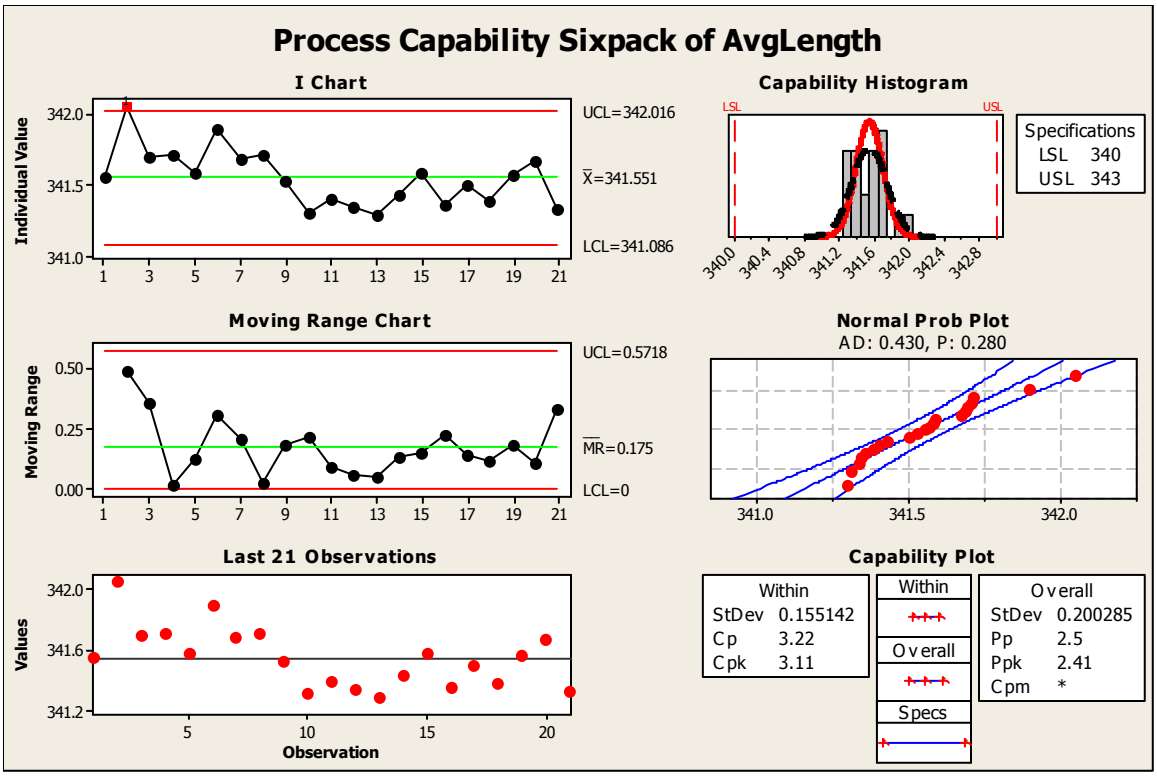

Figure 6. Final plate average length capability for batch 195.

Measured Density Capability

The plate density was calculated from weight and dimension measurements. The data is shown in Fig. 7. The density data should be considered an estimate at this point as the length and width measurements are approximate based upon the rough and non-uniform character of the un-trimmed edges of the plates. The data shows one outlier point (point #20, sheet #24).

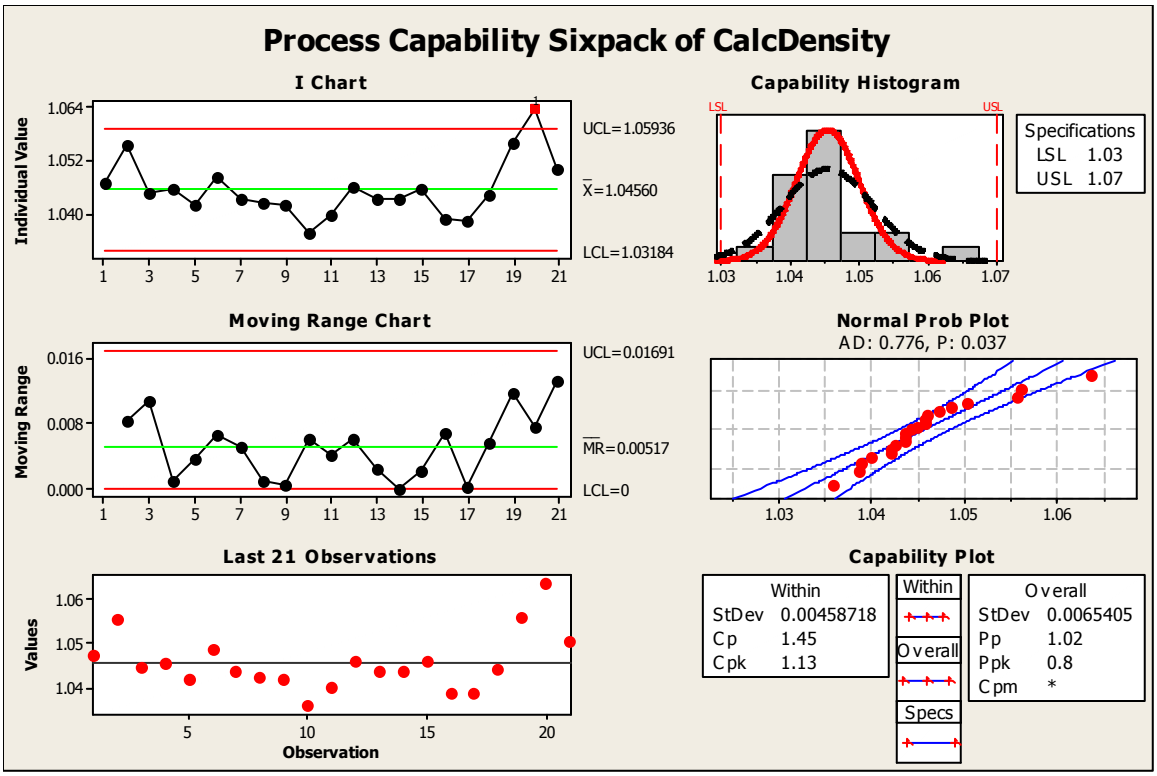

Figure 7. Final plate calculated density capability for batch 195.

Coupon Uniformity

Figure 8 shows coupon uniformity data from the batch (4 sheets measured in 11 locations each).

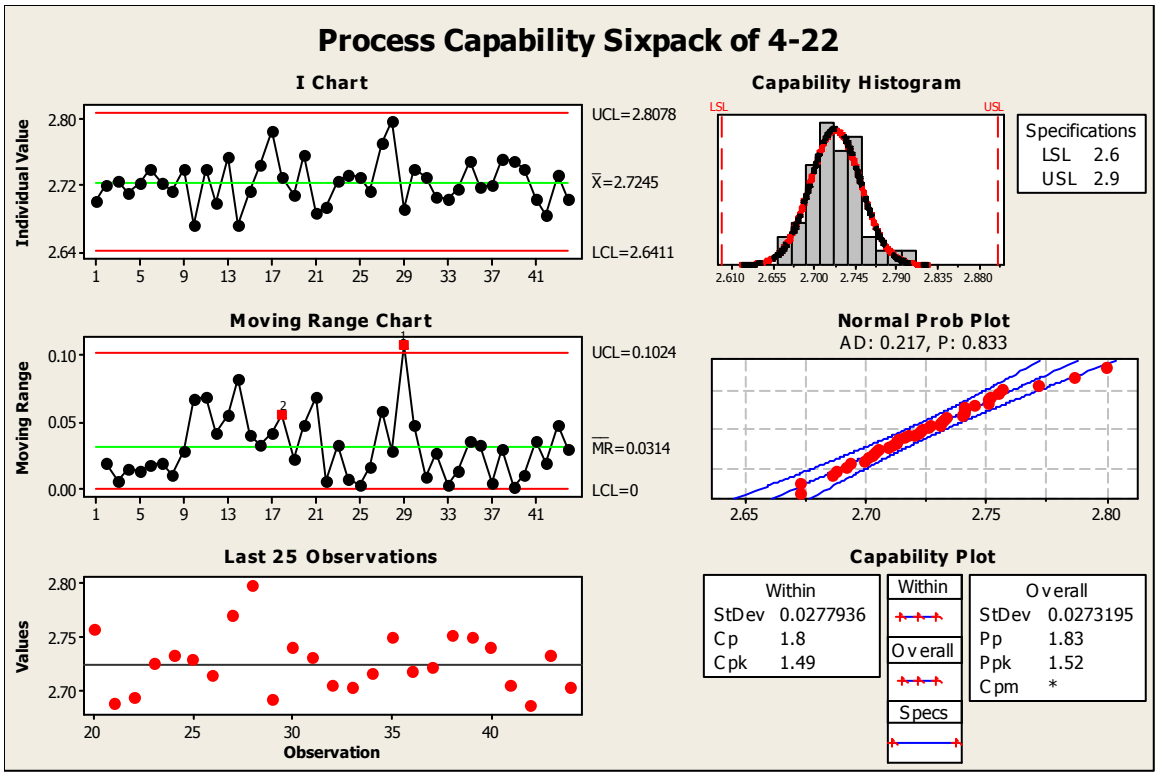

Figure 8. Coupon weight capability from batch 195.

Fuel Cell Testing

UTC Power performed a battery of tests on the net-shape molded parts delivered to them. On arrival at UTC Power, UTC proceeded to characterize the materials for contact resistance, strength, and conformance to print. Following this, the parts were assembled into single and 20-cell test configurations and tested through their standard procedures. Much of the UTC testing data is proprietary, but some polarization curves have been made available for reporting to the DOE. These are shown in Fig. 1 through 3 below.

Generally the data show excellent fuel cell performance, passing UTC's qualification criteria. Stability after start-up was good, as was performance at a variety of current densities.

An observation from UTC regarding our products is that they take longer to break in than their standard bill of material machined plate. The break-in period is where the cell steadily increases in performance over time as the plates are exposed to operation. No theory was

developed to explain the difference, except the fact that the Porvair plates are more porous than the bill of material plates.

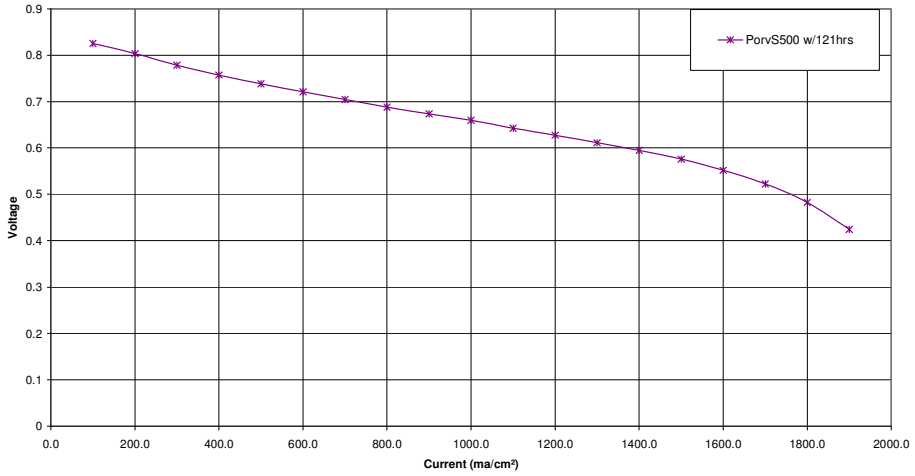

Figure 1. Polarization curve for test stack, as tested at UTC Fuel Cells

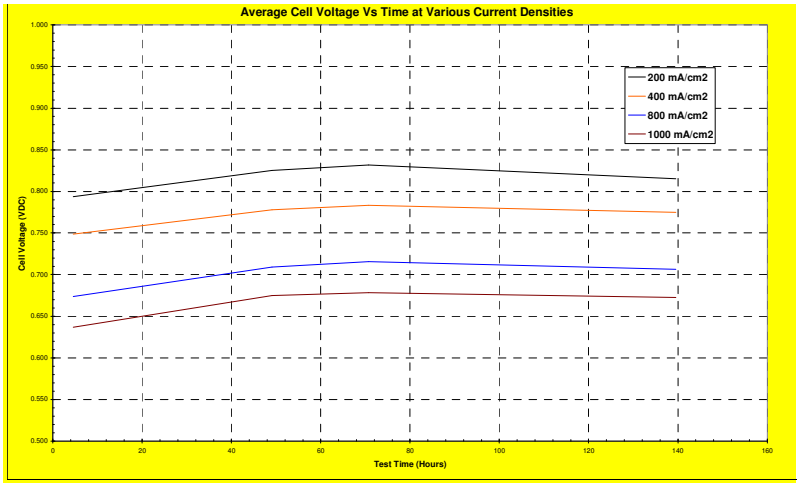

Figure 2. Stability of operation for test fuel cell stack.

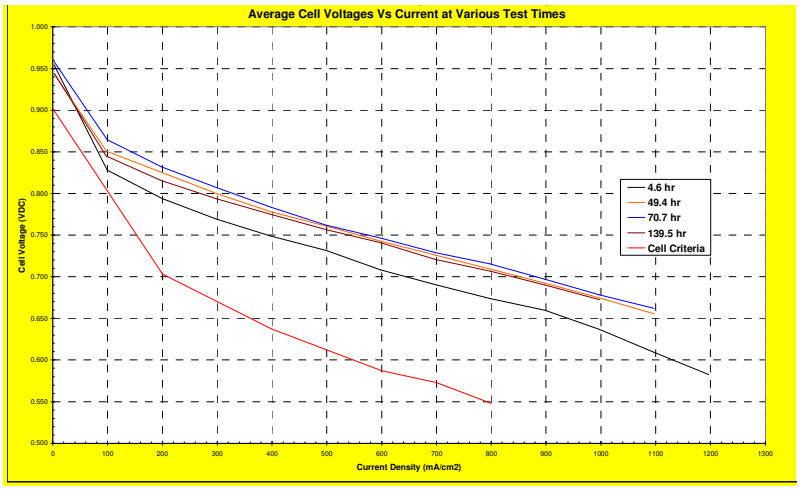

Figure 3. Load calibration polarization curves for test stack.

7.0 Write Formalized Quality Assurance Plan

In the performance of this program, we followed our internal product development program. This program follows the guidelines of ISO9001 for product development, and includes the performance of several items associated with developing a robust manufacturing operation. Included in this activity were the development of formalized control plans, operating instructions, failure mode and effects analyses, continuous improvement activities, data review and statistical evaluation, approval and review of product specifications, qualification of raw material suppliers, and associated audits of suppliers, and evaluation of the fit and function of the product for the intended use.

For the purposes of this program, the activity was principally associated with generating the process control plan and generating specific operating procedures for aspects of the project covered by the grant. These procedures, however, are proprietary to Porvair and will not be included in this final report.

8.0 Review Meeting

A meeting was held May 22, 2005 at the 2005 DOE Hydrogen Fuel Cells & Infrastructure Technologies Program Review in the DC area. A review of the project progress and potential was provided at this meeting.

Phase III

III-1. Develop and Demonstrate Net-Shape Molding Technology

1.1 Investigate Molding of Varied Geometries –This task investigates molding of different flow field geometries, and characterizes product shrinkage and uniformity as a function of flow field geometry and configuration. Molding studies were carried out on 3 different geometric flow field patterns specific to customer designs.

The characterization of flow channel shrinkage is critical to the success of molding accurate bipolar plate flow field geometries. Earlier in the program, it was discovered that the Porvair material shrinks through processing in a very unique manner. The following report was written that summarizes the shrinkage characteristics of the Porvair materials.

MOLDED PRODUCT SHRINKAGE EXPERIMENT

Introduction

The product has shown different shrinkages that were estimated before the die set was ordered. This experiment is designed to evaluate product shrinkage through changes to the composition. The idea is to decrease the fiber level and induce greater shrinkage in the rib width without significantly impacting overall length and width shrinkage.

Experiment

The experimental design is as follows (Table 1):

Experiment	Graphite	Powder	Fiber	Resin
1	Low	Low	Low	Balance
2	High	Low	High	Balance
3	Low	High	High	Balance
4	High	High	Low	Balance

The target trim size is 11”x6.8”. The target trim size is 57 gm.

Results

The experiments as above were performed. The parts after pressing were carbonized and cut into strips for dimensional measurements. Length and width were measured using calipers resting on the outer-most molded features of the plate in two locations each. Overall thickness was measured using micrometers. Channel depth and width, and rib width were measured from the strips on an optical comparator.

The table below shows the data for this experiment (Table 3):

Expt	**Length**	**Width**	**Thickness**	**Ch Depth**	**Rib Width**	**Ch Width**
1	242.6	155.2	1.480	0.6397	0.9343	1.764
2	244.1	156.8	1.515	0.6406	0.9186	1.780

3	243.8	156.3	1.496	0.6448	0.9240	1.768
4	243.8	156.2	1.497	0.6422	0.9303	1.760

In the measurement of channel dimensions, a good deal of variation was found. It is not known if this variation is in the parts themselves, or in the measurement method. The measurement method needs to be evaluated for accuracy and repeatability. Because of the variation in measurements found, no data showed statistically significant trends with the independent variables of the investigation. However, trends did reveal themselves through averages, and this report will focus upon this learning as much as possible.

The data trends are shown in Table 4:

	Length	**Width**	**Thickness**	**Ch Depth**	**Rib Width**	**Ch Width**
Low Graphite	243.21	155.93	1.488	0.6422	0.9292	1.766
High Graphite	243.96	156.48	1.506	0.6414	0.9245	1.770
Low PE Powder	243.38	156.01	1.498	0.6401	0.9265	1.772
High PE Powder	243.79	156.40	1.497	0.6435	0.9272	1.764
Low Fiber	243.22	155.69	1.488	0.6409	0.9323	1.762
High Fiber	243.95	156.72	1.506	0.6427	0.9213	1.774

While no significant differences were found among the data, some trends were noticed:

- PE powder did not impact measurements to any noticeable degree, except perhaps in channel depth (use of PE powder led to slightly deeper channels)
- Higher graphite and fiber levels led to thinner ribs (fiber impacting the data more than the graphite)
- Experiment 1, with much higher resin content than the other experiments showed significantly more overall length, width and thickness shrinkage, but not rib dimensions were not considerably different
- Rib width and channel width trended inversely to each other in general (total rib spacing was consistent, except with experiment 1, which showed higher shrinkage than the other experiments)

Higher levels of fiber lead to thinner ribs (the most significant trend found in the trial). A weak trend can be said to exist with graphite level, and no trend with PE content. Data shows that reducing resin content leads to thinner rib width.

Figure 1 shows the relationship between channel width and rib width measured. As would be expected, as rib width decreases, channel width increases, except in the case of experiment #1, which did not follow the same trends – probably due to the significantly higher resin content for this experiment.

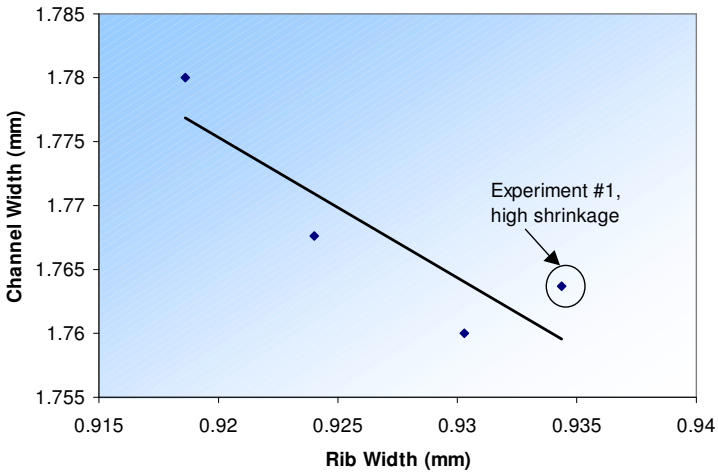

Figure 1. Relationship between channel depth and rib width found in experiment.

Predictive Model

A simple linear model was fit to the data to predict channel depth and rib width. The models are as follows;

Rib Width = 1.1042 – 0.00163*Gr – 0.00596*Fib – 0.00046*Res

Chan Depth = 0.8656 – 0.00245*Gr – 0.00136*Fib – 0.00224*Res

Where Gr = Graphite content
Fib = Carbon fiber content
Res = Resin content

Figures 6 and 7 show the prediction trends, which correlate very well, indicating that this model may be used successfully within the range of the experiment.

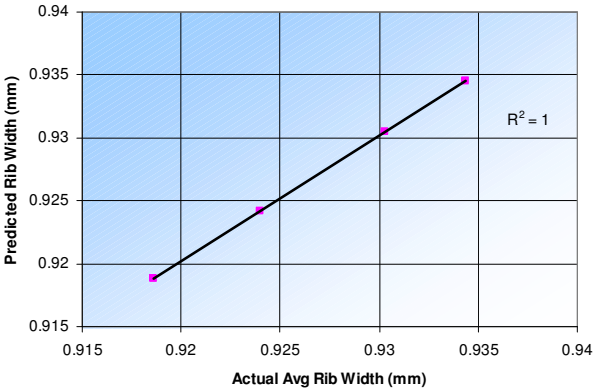

Figure 6. Model prediction for rib width.

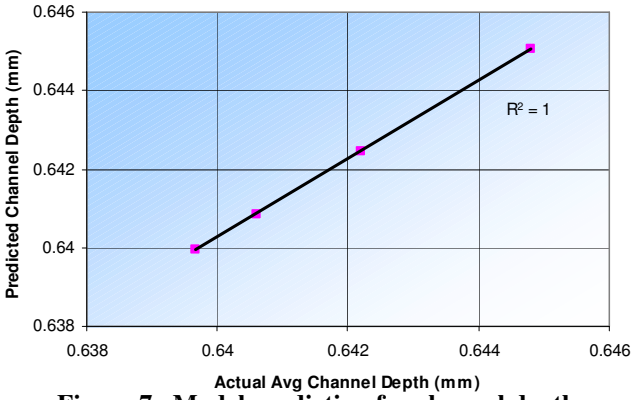

Figure 7. Model prediction for channel depth.

The models were used to predict compositions that would lead to thinner ribs in finished part. It is apparent that increasing the fiber level in the composition most significantly impacts the rib width. While the results are shown to be dependent upon resin content, this parameter impacts rib width less significantly than either graphite content or fiber content. It does, however, significantly impact overall product shrinkage. It is desired that resin content be maintained at value near its present value.

While the trends are slow with relatively significant changes in composition, the data does show a trend in the direction that leads toward reducing rib width to the point that it is moved into product specification. It is likely that the moving the material composition to higher fiber levels will reduce product bubble point. A re-targeting of basis weight may be needed to maintain product bubble pressure and permeability requirements.

MOLDED PRODUCT SHRINKAGE EXPERIMENT #2

Introduction

In the previous experiment, data showed that the molded ribs could be controlled to drive the rib width thinner without significantly impacting overall plate length and width. Results showed that by increasing carbon fiber and graphite powder content, rib widths would decrease while channel depths and widths would increase – a direction required in molding as the standard product shows off-tolerance rib and channel widths.

Experiment

The experimental design for this experiment is as follows (Table 1):

Expt	**Resin**	**Graphite**	**Fiber**
1	Low	Low	Balance
2	High	Low	Balance
3	Low	High	Balance
4	High	High	Balance
5	Mid	Mid	Balance

The target trim size is 11”x6.8”. The target trim size is 57 gm.

Results

The parts after pressing were carbonized and cut into strips for dimensional measurements. Length and width were measured using calipers resting on the outer-most molded features of the plate in two locations each. Overall thickness was measured using micrometers. Channel depth and width, and rib width were measured from the strips on an optical comparator. Rib width was re-measured using micrometers, as the optical comparator data varied greatly. Only rib width results as measured with the calipers is reported below.

The table below shows the data for this experiment (Table 3, in mm):

Expt	Length	Width	Thickness	Rib Width
1	244.8	157.7	1.509	0.954
2	244.6	157.9	1.501	0.955
3	244.5	157.5	1.510	0.957
4	244.3	157.8	1.500	0.957
5	244.7	158.0	1.516	0.950

In the measurement of channel dimensions, a good deal of variation was found using the optical comparator. The measurement method needs to be evaluated for accuracy and repeatability. Because of the variation in measurements found, no data showed statistically significant trends with the independent variables of the investigation. However, trends did reveal themselves through averages, and this report will focus upon this learning as much as possible.

The data trends are shown in Table 4:

	Length	Width	Thickness	Ch Depth
Low Graphite	244.7	157.8	1.505	0.954
High Graphite	244.4	157.6	1.505	0.957
Low Resin	244.7	157.6	1.509	0.955
High Resin	244.4	157.8	1.500	0.956
Mid Ponit	244.7	158.0	1.516	0.950

Focusing upon control of rib width, no significant trends were found with this data. It appeared that none of the variables investigated drove rib width significantly.

This experiment was set up to evaluate the impact of fiber content on rib width. There exists a very mild trend for narrower ribs with increasing fiber content. However, the difference is slight and projecting the trends to reasonable additional increases in fiber content will not substantially impact the results.

Conclusions and Next Steps

No additional analysis was performed with this experiment because of the very mild differences noted in the rib width results. On one hand these results are disappointing as it reflects little ability to control the results through small composition changes. However, because the results

are stable, good process control and capability to maintain consistent channel dimensions will result when manufacturing molded product.

SUMMARY OF CHANNEL SHRINKAGE FOR VARIED CHANNEL GEOMETRIES

Introduction

It is vital that the shrinkage rate vs. geometry of any die set is fully understood so that the Porvair bipolar plate product is manufactured on-target. This report is a review of all of the data available in the molding of three different plate designs. Correlations between the channel dimensions and shrinkage rates have been generated and will be reported, along with an uncertainty analysis relative to the channel dimension tolerances.

Shrinkage Rates and Variations in Channel Dimensions

Porvair has the most experience and data related to the design. The tooling has been measured and inspected by the mold manufacturer, and also checked at Porvair.

Die Measurements

The tooling maker provided a measurement report to Porvair after the die set was built. The measurements were performed using a CMM machine. The die sets were also checked at Porvair for channel characterization. The channel depths were checked with a drop gauge and pin on a granite slab. The channel widths were measured from a no-shrinkage casting of the channels using the same method that is used to measure plates. The actual channel measurements for the tools are proprietary to UTC Power, and so is not shown in this report. Although generally good agreement was noted between measurements at the tooling manufacture, and Porvair's measurements, some differences were noted. The water-side tool is one example, where measurements were somewhat larger than those taken at Porvair. In the analysis of the data, Porvair measurements were used for the data analysis, even though more variation with the channel width measurement was found in measurements taken at Porvair. The high variation probably is a result of the difficulity in the measurement method at Porvair, where measurement samples must be made, cut, mounted and evaluated. Variations in the angle of cut and the quality of the sample will induce variation. A better, faster measurement method needs to be developed. Data were taken from Porvair measurements of these die sets.

Part Measurements

Parts were taken from stock for measurements. Next generation parts were made as well as possible using the standard material recipe and using our best estimate for the ideal basis weight for each plate. These plates were not checked for final density, permeability or bubble pressure. With the new flow field design, it was noted that some of the measured fuel and water channels were not well filled (as seen from the optical photos taken during the channel measurement process). It is thought that the basis weight for this plate was made too low. This poor rib filling introduced error in the measurements, indicating falsely high rib height shrinkage. For this reason, these measurements for water and fuel height were eliminated from the data set. No re-measurements were made as the plates used for these measurements were already cut up and disposed of, and time does not permit re-working these parts.

For all parts measured, the plates were cut and the cut-face lightly sanded. The samples were labeled and measured on the stereomicroscope. Images were captured and software, calibrated to the camera and focus, was used to measure the rib height and width. An earlier gage R&R study on this method showed this to be a decent measurement method.

Expected Trends

In evaluating the shrinkage characteristics, it is beneficial to evaluate the structure of the preform that is made and the flow of material into the channels during the molding process. The preform is composed of a large quantity of milled carbon fiber. During forming, these fibers lay down so that they are randomly distributed in the plane of the sheet. The fiber axis is very unlikely to lie in the z-direction to any significant degree. However, when molding the preform, channels are filled as the material is pushed into the rib spaces of the die set. Micrographs show the directional flow of the materials in the rib areas. As such, the ribs exhibit fiber alignment with the height of the rib (see Fig. 1).

Product shrinkage rates are very strongly correlated with fiber direction. For a flat sheet, our material is found to shrink approximately 9% in thickness and 1.2% in length and width. The fibers, having their axes lying in the plane of the material prevent excessive shrinkage in the plane direction, while normal to the fiber axes, high shrinkage rates result.

Given the nature of the shrinkage and its dependence upon fiber alignment, the shrinkage rates would be expected to be dependent upon the aspect ratio of the plate rib. Very short, wide ribs would be expected to shrink in height similarly to the thickness of a flat sheet, and in width similarly to the length/width of a flat sheet. A very tall, narrow rib, where the fibers have essentially aligned themselves with the rib, would be expected to shrink in rib height similarly to the length/width of a flat sheet, and in width similarly to the thickness of a flat sheet. With this understanding, it is thought to be appropriate to evaluate the shrinkage rates with respect to the aspect ratio of the rib of the design (height of rib divided by width of rib). From a fundamental standpoint, the shrinkage rates for the height of a rib and the width of a rib should follow a trend shown schematically in Figure 2.

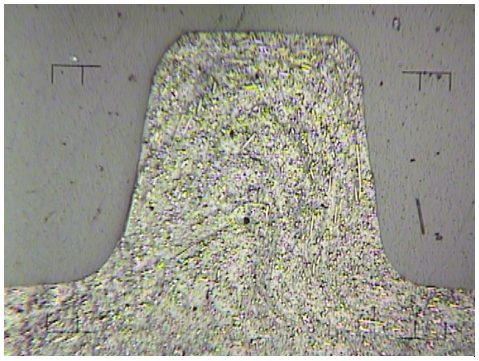

Figure 1. Internal Rib structure – shows tendency of fibers to align with rib height.

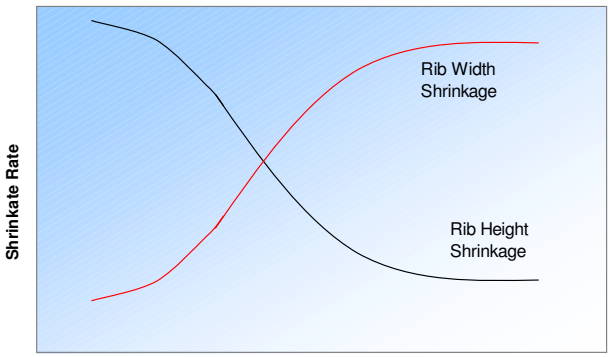

Figure 2. Expected trends in shrinkage. At high rib height/width ratios, the rib width shrinkage is expected to approach the shrinkage rate of a flat plate in the thickness direction. Rib height is expected to approach the shrinkage rate of a flat plate in the length/width direction.

Summary of Shrinkage Data

The variation seen in the measurements was relatively high. Higher measurement variation was seen primarily in molded parts, but some die measurements also showed high measurement variation.

While the same measurement methods were used in gathering the data, multiple operators performed the measurements over a wide time horizon. Some, measurements that show significant variation (as in tool measurements and the anode height measurement) may reflect more measurement variation than others, whereas others (tool width, for example) may reflect reasonably well the variation in the tool. Local machinists made the die quickly, and the quality of the tool was not up to expectations. This is likely reflected in the variation seen in the die measurements. However, most all other measurements appear to have reasonable variation.

In the analysis that follows, it will be assumed that the average values measured represent well the actual average value for the parts and the tools. Most of the measurement histograms show that this is a reasonable assumption.

Shrinkage Trends

Figures 3 and 4 show the trends in rib height shrinkage and rib width shrinkage for the parts measured. As seen in the figures, the data follows the expected trends. Rib height shrinkage decreases as the ratio of rib height to rib width increases. Rib width shrinkage increases as the ratio of rib height to rib width increases. The data also appears to be well represented by the curves shown in the figures. The R^2 values are 0.80 and 0.70 for height and width shrinkage respectively. The data trends are shown to be relatively flat in this region of interest.

Another item of note is that the height on the shortest-rib side (water-side) of double-sided plates varies considerably in rib height. This is caused by the influence to the shrinkage rate of the ribs on the opposite side of the plate. When ribs are running parallel on both sides of the plate, with one rib directly on top of another rib, the rib height is shorter. For ribs running perpendicular to each other, the rib height is greater.

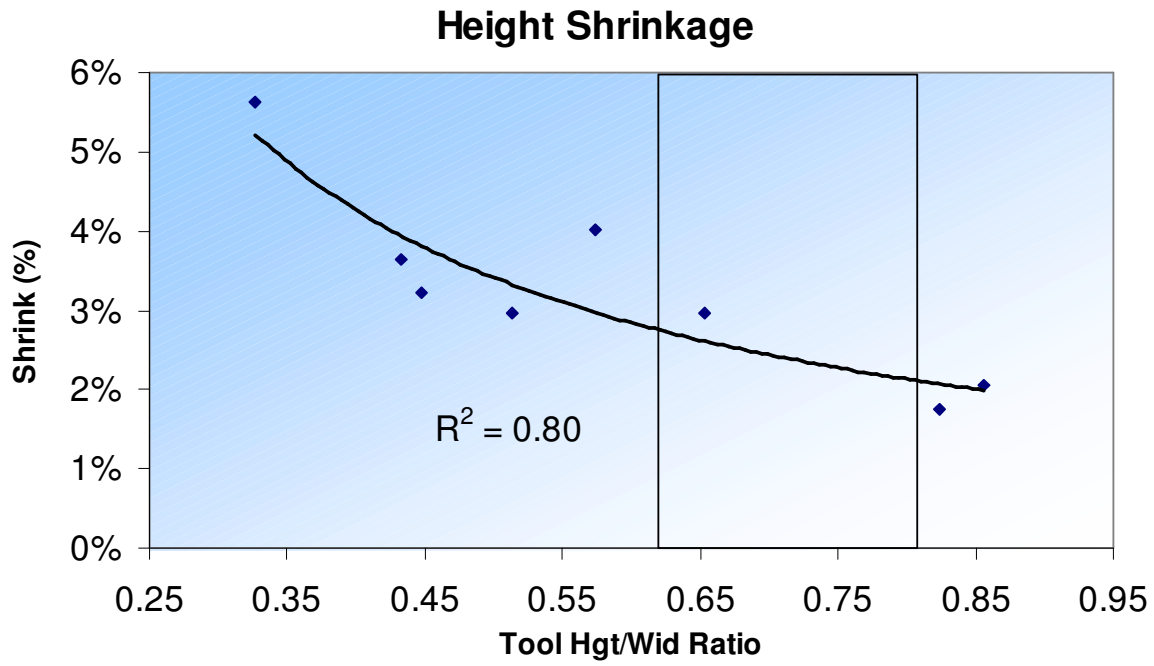

Figure 3. Rib height shrinkage as a function of the tool rib height to width ratio.

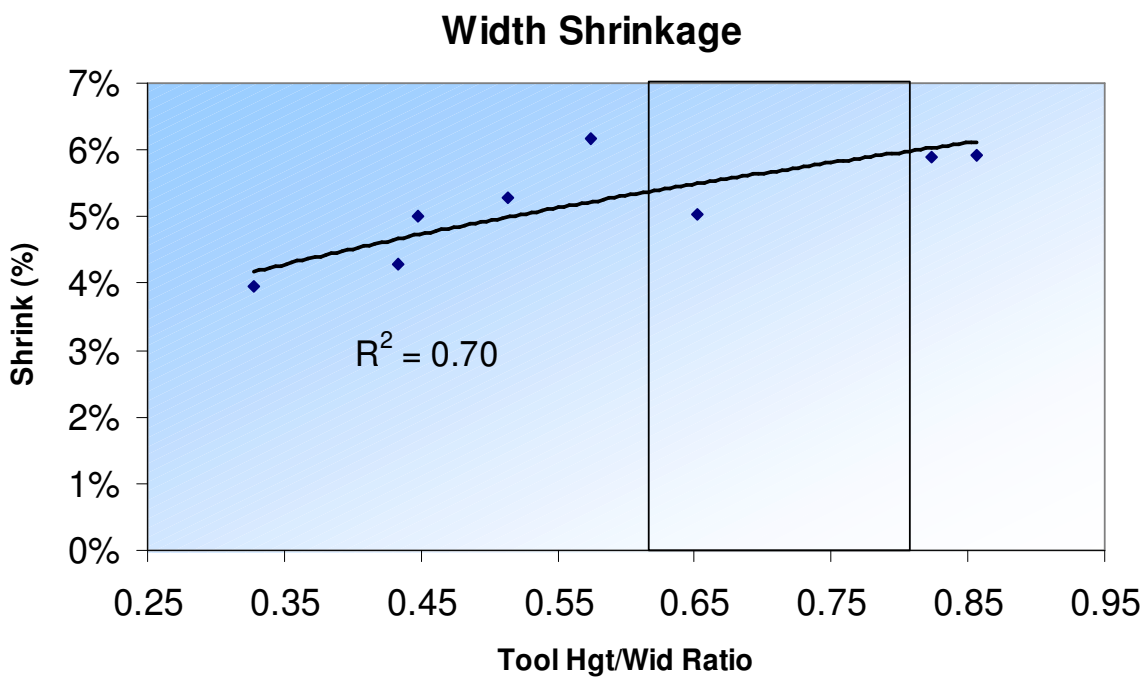

Figure 4. Rib width shrinkage as a function of the tool rib height to width ratio.

Conservatism in Design

Through lessons learned in previous efforts, it may be prudent to design new tooling so that there is a high degree of confidence that the final parts will land on the high side of nominal for rib height and on the low side of nominal for rib width. The combined effect of this would be to make the flow field channels slightly larger than nominal, and so minimize the impact of missed final dimensions on system flow and pressure drop. From the above evaluation, it may be wise to assume a larger shrinkage rate for rib height and a smaller shrinkage rate for rib width.

In this example, the design expected dimension would be larger in height and narrower in rib width than the print design by a small amount (about 1.5%). Moving further away from the design shrinkage with the goal of generating even larger flow channels can further reduce the likelihood that under-sized channels will result in the final product. As an estimate of this effect, a 1% change in height shrinkage rate will lead to approximately 0.007 mm difference in channel height, and a 0.009 mm difference in rib width. Figure 5 shows the impact of having a shrinkage different from the target for channel height and width for a hypothetical channel cross-section. In the figure, the box represents the limits of part channel cross-sectional area. The maximum area was based upon assuming the tallest and narrowest rib allowed by the typical channel tolerances. The minimum area was based upon the shortest and widest rib allowed by the print tolerances. Assuming that the design point reflects the nominal shrinkages calculated in this report (shown as the design point in the figure), the figure shows the error in shrinkage rates that can be tolerated and still yield an acceptable average channel cross-sectional area. The figure also shows where shrinkage rates would be for specific features to become out of spec (labeled on the print for height shrinkage, and above 9% or below 3% for rib width.

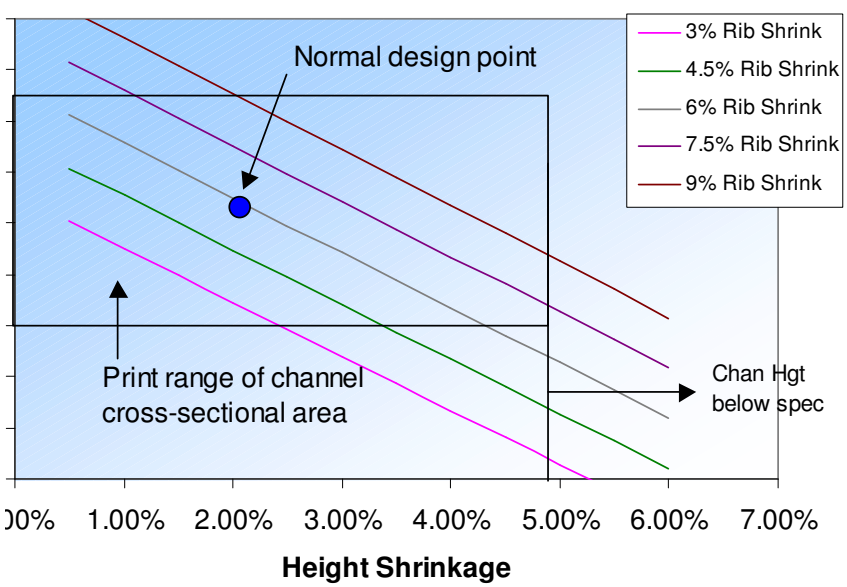

Figure 5. Diagram of the impact of shrinkage variation on the final flow cross-section and the regions beyond which shrinkage of the part induces out of spec features.

Final Design Recommendations

The recommendation is to error on the high side of rib height, but use the nominal rib width shrinkage rate. In this way we will be more confident that the product will be in-spec for rib height without yielding an average rib height that is too tall. Because of the low rib height shrinkage rate, it will be impossible for the rib height to be out of spec high (the tool depth will actually be less than the upper limit of the print tolerance). Biasing the channel depth high ensures that the rib height will not be too short and will be more likely to ensure that larger channels are obtained. Further, from the measurements and analysis, it is likely that the final rib width shrinkage will be within about 1% of the predicted shrinkage rate. Targeting the nominal rib width shrinkage rate should yield a rib width within the specification of the print. In the event that the shrinkage rate is more than predicted, the additional rib height will help to offset the reduction in channel area, and helps to further ensure that the height is also in spec.

Further, it is recommended that sample parts be verified in dimension between Porvair and the final tooling manufacturer to be sure that the measurement methods yield the same results. This activity will likely be relatively time consuming and expensive, as it will be necessary to measure sample materials to an accuracy better than 0.25 mil. Additionally, an understanding of the variation in chrome coating depth must be understood prior to tooling order placement. And, the tooling manufacturer must be sure to account for this coating in the manufacture of the die set (see next section for further discussion of this point).

It should be noted that there will still be variation in the dimensions across the plate and from plate-to-plate. As noted in our measurements of channel data from production plates, the variation seen in channel dimensions is generally greater than +/- 0.03 mm. The variation comes primarily from product and process variation, but will also include variation in the tool set. If for example, the average channel dimensions are within spec, but off target somewhat, the variation in the dimensions will surely mean that there will be regions of plates that have channel dimensions beyond the specification. As with the plates, it is expected that there will need to be an evaluation of the dimensions that are produced in the process, and this information will need to be transferred to the print to enable an acceptable manufacturing process. While the data suggests that the target dimension should be achieved with reasonably good confidence, it will be unlikely that the dimensions will match exactly to the print.

1.2 Manufacturing Improvement Activities

This task is associated with manufacturing improvements required to improve the net-shape molding quality and consistency of the bipolar plate. The most important characteristic in obtaining excellent molding quality and consistency is the uniformity of the perform sheets prior to hot press molding. A study is shown below that identified key process parameters that influence sheet uniformity.

Sheet Uniformity Improvement Study

PURPOSE

The objective of this study was to improve the sheet uniformity to a goal of within 1% standard deviation. Improvements were made to both the current operating and forming system as well as to the batch material composition.

BATCH TRIALS

A number of batches were run the week of 8/15/2005 as trials for improving sheet uniformity. Results from previous sample cup trials dictated the direction for full batch testing. The following table describes the changes per each experimental batch.

Batch	Batch Description
179	Standard Batch Recipe—baseline
180	Standard Batch Recipe—baseline
181	Standard Batch PLUS dispersant added to batch
183	Half Solids Content—Standard Batch Recipe cut solids loading in half
184	More defoamer some mixed with Forming and some mixed with matrix pre-mix
185	defoamer plus dispersant
186	Less disperser, used defoamer, rotated spider 180° half-way through the run, aligned screens in forming pan
187	More dispersnat, NO Defoamer
188	Less defoamer
189	Repeat of Batch 188, spider enhancements, evenly mis-align forming pan screens
190	Even Less defoamer
191	No defoamer

Table 1 Experimental Batch Trial

Beginning with Batch 179, all batches were run with the forming pan addition to lengthen the distance across which the vacuum is pulled and to achieve more uniform suction across the forming part. All sheets were formed in the Net-shape hat with the spider 2 configuration. See Figure 1. The material for one sheet flows down into the spider in the center hole drawn and then flows out in the pattern marked by the arrows and into the pan where the vacuum pulls the water out and a sheet is formed. The actual diameter of the spider is 1 inch.

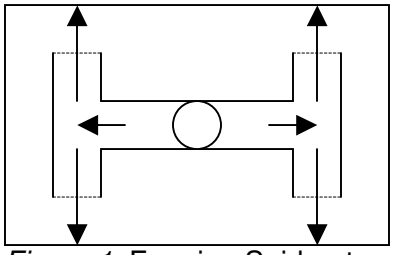

Figure 1 Forming Spider, top view.

RESULTS

Within-Sheet Uniformity

Eight sheets per batch were pulled and eleven coupons were punched out of each sheet and weighed. Figure 2 displays the layout of the sheet with the coupons. The goal for sheet uniformity is to reach below 1% standard deviation of coupon weight for each sheet. Our standard batches, 179 and 180, produced sheet uniformities averaging 1.02% and 1.1%, respectively. This is very good. See table 2 for the trial batch data.

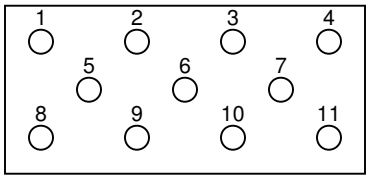

Figure 2 Location of 11 coupons per sheet.

Table 2 Coupon Weight and Variation by Batch

Batch	Avg Coupon Weight, g	Percent Standard Deviation
179	2.8712	1.023962
180	2.9028	1.105829
181	2.8234	1.218389
183	1.4471	1.195494
184	2.8662	1.406043
185	2.8979	1.830291
186	2.90274	1.514707
187	2.913444	1.647157
188	2.915253	1.0266
189	**2.910565**	**0.976032**
190	2.917898	1.554235
191	**2.88165**	**0.894418**

Batch 189 produced 8 sheets with average coupon variation of 0.976%. The process parameters for batch 189 were the same as 188, which produced a variation of 1.027 %. Batch 191 produced a variation in sheet uniformity of 0.89%, the best overall. Batch 191 was similar to the recipe for 188 and 189 except for defoamer. This batch originally called for no defoamer. Once the batch of materials was mixing all together, it was evident defoamer was needed. The defoamer was then added to the entire batch of materials just before it was pumped over to the holding tank. This is different from the usual order of addition for our batch process. In a typical standard batch, 10 ml of defoamer is added to the fiber while deflaking for 30 minutes. The rest of the defoamer is added to the fiber while the rest of the batch of materials is pumped over from another tank.

Figure 3 is a chart of the variation of coupon weight by batch. The maximum and minimum sheet uniformity variation by sheet in each batch is also depicted. The target is to be within 1% for optimum sheet uniformity. Table 3 lists the sheet uniformity for each of the 8 sheets per batch.

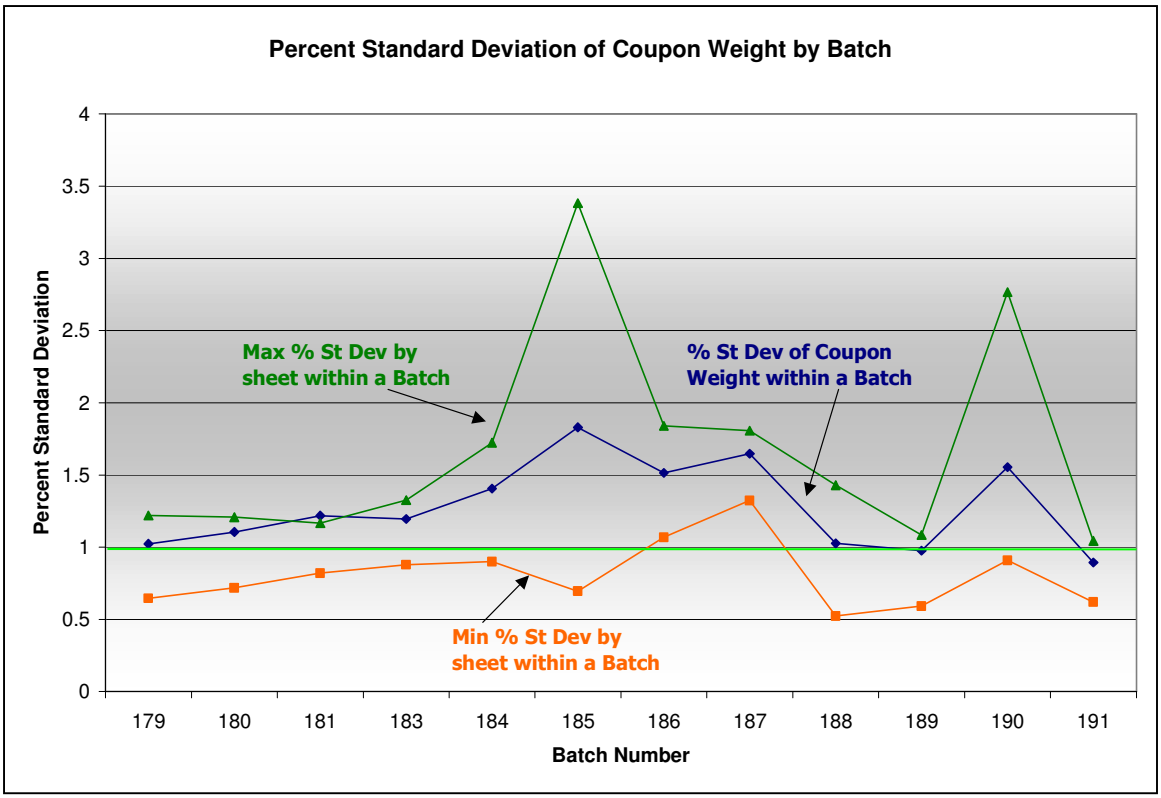

Figure 3 Variation of Sheet Uniformity per Batch

BATCH	Sheets 3	4	7	10	13	16	19	22
179	1.0282	0.8046	1.0535	1.1911	0.9242	1.2195	0.6456	0.7036
180	1.1257	1.1067	1.0934	0.9838	0.7183	1.1549	1.2079	0.8116
	Sheets 4	**10**	**16**	**22**				
181	0.8521	1.1372	0.8197	1.1664				
	Sheets 4	**5**	**10**	**11**	**16**	**17**	**21**	**22**
183	1.0882	1.3259	1.0078	0.9055	1.1399	1.2008	0.8995	0.8790
184	1.6534	1.2338	1.5127	1.1528	1.3528	1.7237	0.8999	0.9551
185	1.2166	0.6951	1.4203	1.2396	1.3657	3.3834	0.9930	1.2218
186	1.5178	1.0686	1.1821	1.5057	1.5825	1.7639	1.8398	1.6773
187	1.8073	1.7924	1.7398	1.6684	1.6834	1.5882	1.5112	1.3231
188	0.6000	1.4297	0.7972	1.0320	0.6184	1.2944	0.5229	1.0650
189	1.0233	0.5922	0.6920	1.0848	1.0431	0.9651	0.9240	1.0744
190	0.9409	1.3095	1.3218	1.3358	0.9087	0.9148	2.7660	1.7677
191	0.6200	0.7412	0.7363	0.8561	0.8517	0.8602	0.9951	1.0432

Table 3 Percent St. Dev. of Uniformity for each of the sheets examined per Batch

Vacuum Levels

The valve for the vacuum pull was throttled to different levels for the latter half of batch 191. Standard batches are formed with the valve open at roughly 50%. Batch 191 was run at 50% open up through sheet 13. The changes in the openness of the valve are rough estimates. Sheet 14 was run at 10% open. The vacuum was not strong enough to pull the water out during the 60-second pull-down. Sheet 15 was run at 15% open. This sheet was very wet, making it difficult to remove the sheet from the screen. Sheets 16 through 18 were run at 20% open. These sheets were still heavier after the vacuum pull but enough water was removed to enable the screen to peel off the sheet. Sheets 19 through 22 were run with the valve at 100% open. The wet weights of these sheets were within the range of those run at 50% open. Sheets 23 through 25 were formed with the valve open further than its 90-degree open/close allowance. Thus it appears the valve is over-extended. It is hard to determine whether this had an effect on the sheets formed because they are at the end of the batch. The dry weights for all of these sheets does not appear to be outside the normal range of dry weights, regardless of vacuum pull. Table 4 lists the corresponding data for batch 191.

Notice that the variation for sheet uniformity for sheet 15 is very high, 1.37%. This is also the sheet that was formed under vacuum open only 15% and was pretty wet. Once dry, sheet 15 weighs just slightly lighter than the rest of the batch. This points to a possibility that the vacuum may have an impact on the uniformity. Plus, the sheet did loose some material with the removal of the forming screen.

CONCLUSIONS

Batches 189 and 191 are well within the target of 1% variation for sheet uniformity. Therefore, it is advisable to freeze our forming process following the recipe of these batches. The only difference between the 2 batches is the order of defoamer addition.

Vac open →	50%	50%	50%	50%	15%	20%	20%	Open	Open	open > 90deg
Vac pull, in HG→	21-22	21-22	21-22	21-22	16	19	19	23	23	21
Wet Wt. g →	282	280.6	278.9	280.8	435.2	315.2	310.4	283.3	281.7	289.4
Dry Wt. g →	172.3	171.9	171.2	171.2	170.3	173.9	171.4	171.3	171.8	172
Coupon	**Sheet 4**	**5**	**10**	**11**	**15**	**16**	**17**	**21**	**22**	**23**
1	2.8398	2.8372	2.8571	2.8662	2.9309	2.8533	2.8845	2.8276	2.8106	2.8673
2	2.8615	2.8515	2.8691	2.8683	2.9358	2.8803	2.8589	2.8565	2.8708	2.872
3	2.9035	2.8689	2.9059	2.8647	2.9252	2.8915	2.8918	2.9032	2.8814	2.8894
4	2.8786	2.9019	2.8795	2.8985	2.9632	2.9145	2.8373	2.9028	2.8644	2.8954
5	2.8725	2.8733	2.9009	2.8783	2.9679	2.9129	2.8759	2.8799	2.8817	2.9291
6	2.9029	2.9091	2.9106	2.9231	2.9392	2.9098	2.9134	2.9345	2.931	2.9759
7	2.8787	2.8823	2.8486	2.8899	2.8919	2.9442	2.8533	2.907	2.8972	2.868
8	2.8791	2.8776	2.8719	2.9056	2.9125	2.897	2.8985	2.9125	2.88	2.9226
9	2.8836	2.8631	2.8698	2.8408	2.8444	2.9263	2.8392	2.8972	2.8445	2.8794
10	2.8885	2.8573	2.8559	2.9052	2.8859	2.9029	2.889	2.8932	2.878	2.9145
11	2.8745	2.8867	2.8639	2.8592	2.981	2.9256	2.8644	2.8942	2.8674	2.9025
average	2.878473	2.873536	2.875745	2.8818	2.925264	2.9053	2.873291	2.891691	2.873364	2.901464
stdev	0.017848	0.021298	0.021175	0.02467	0.040081	0.024745	0.024717	0.028775	0.029974	0.032782
%stdev	0.620046	0.741164	0.736344	0.856071	1.370175	0.851712	0.860238	0.995084	1.043179	1.129838

Table 4 Uniformity and Forming data for Batch 191

Product micrographs were analyzed to evaluate the microstructure of the Porvair net-shape molded material and to evaluate a small crack seen on the surface of the plate near a rib. Because the defect region had the appearance of a crack, the plate was sectioned and the region evaluated under optical microscopy.

As seen in the figures below, the defect was found to be higher than normal porosity in the area, rather than a crack in the plate. It was likely caused by a region of product non-uniformity (such as an accumulation of forming fibers or other non-carbon-forming binders used in the process). The issue is not thought to be common in the material and process, but improved mixing could help to eliminate such occurrences.

The micrographs are also useful in examining the microstructure of the material in response to net-shape molding. As seen in the figures, the porosity of the general material is found to be greater in rib regions than in channel regions. This follows from the behavior of our material in net-shape molding. The material compresses and flows to fill mold features by extrusion of the material from one area to the next. Compaction of the material in highly compressed regions results.

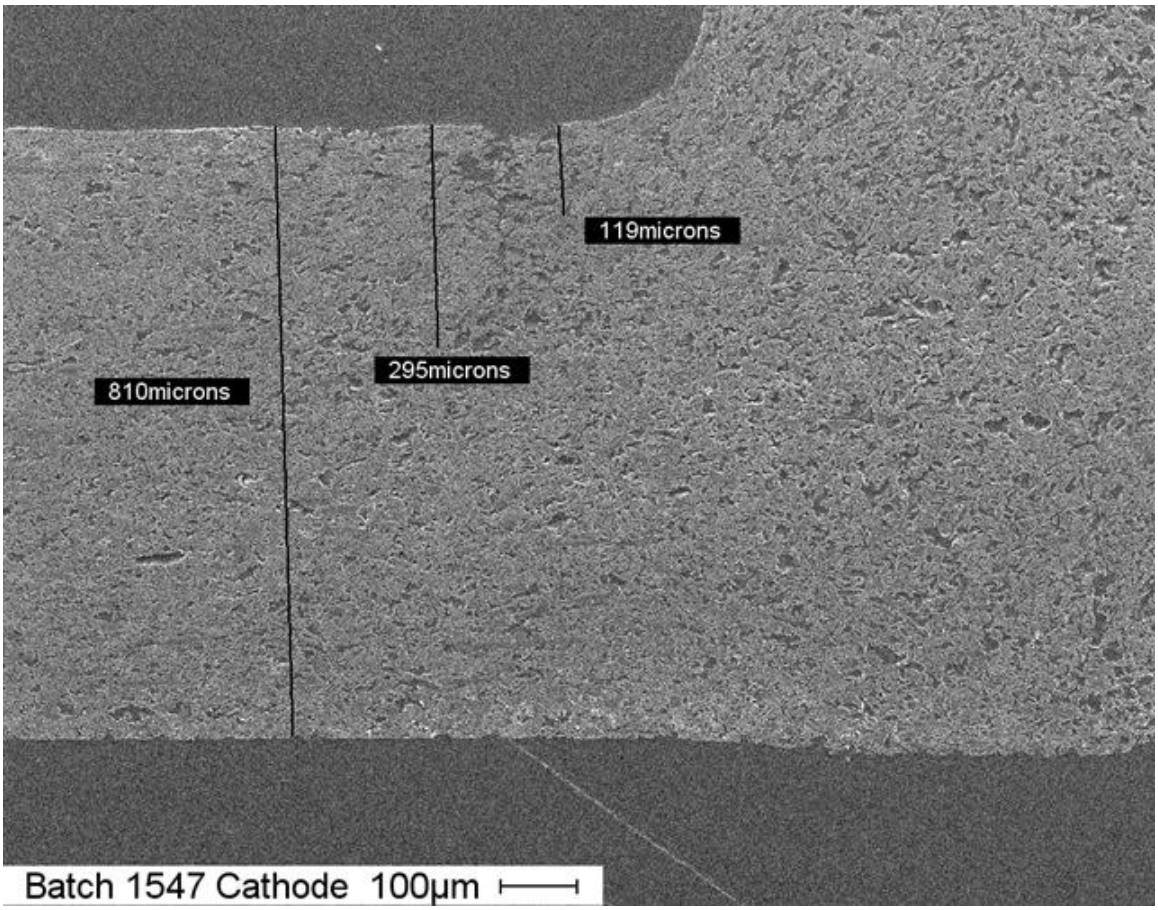

Plate from Batch 1547, Feature A, magnified 75x

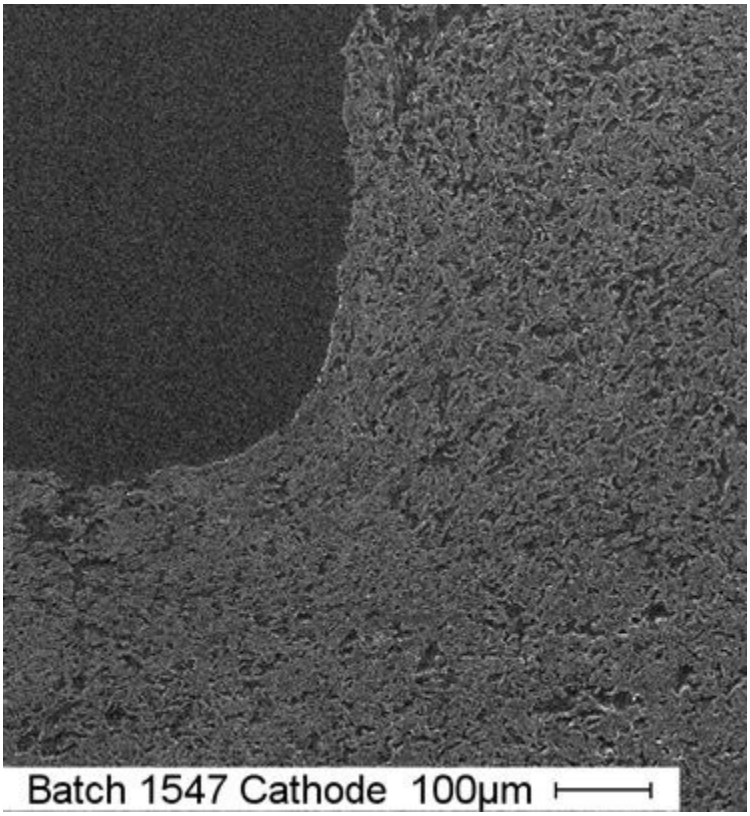

Plate from Batch 1547, same Feature A, magnified 85x, lower left section of picture is the feature

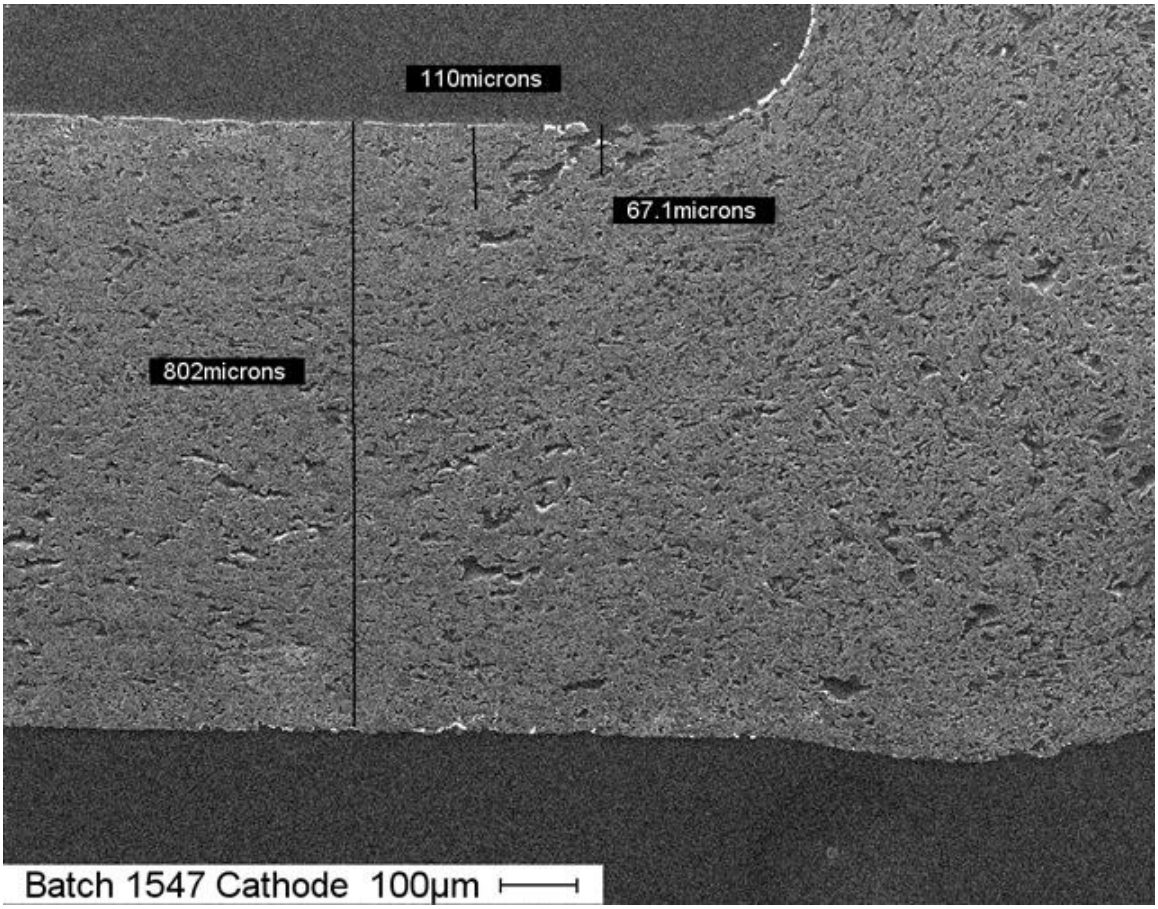

Plate from Batch 1547, Feature B, magnified 75x

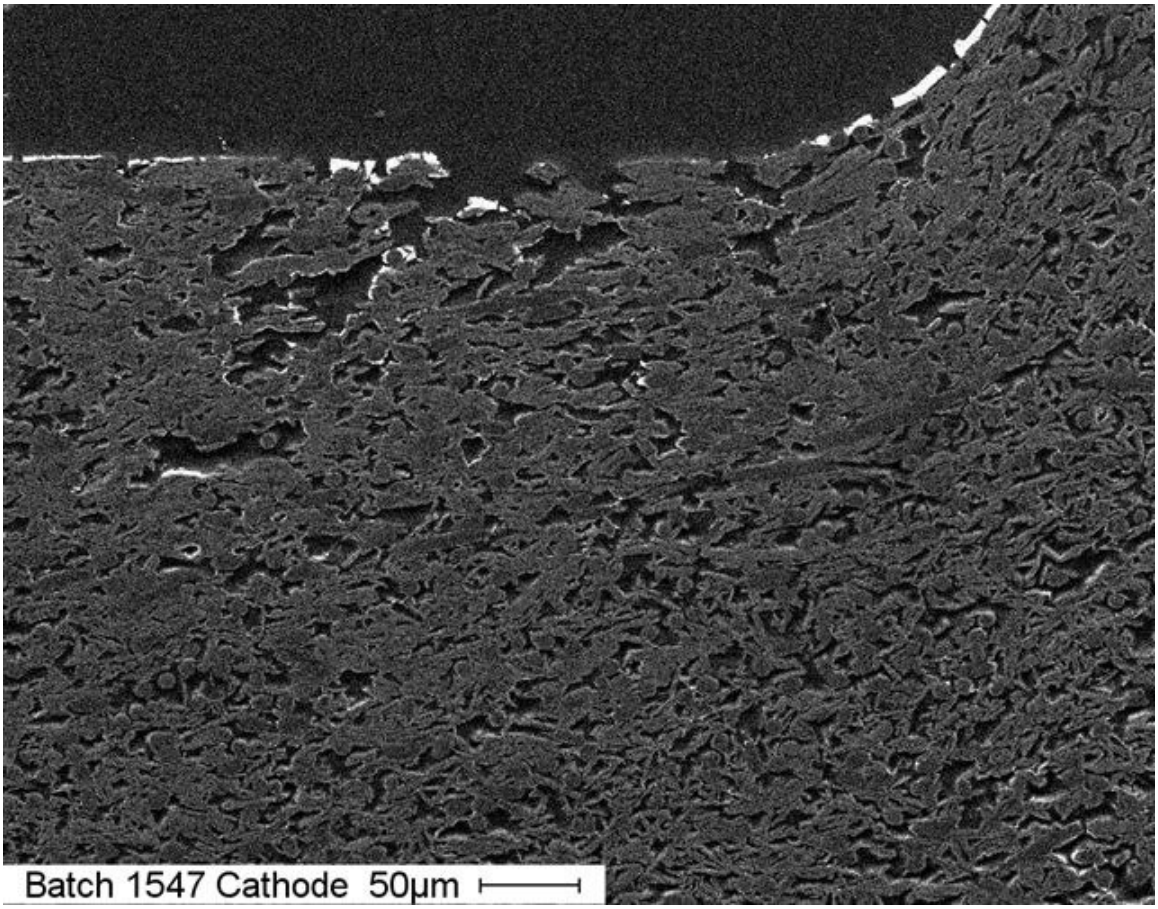

Plate from Batch 1547, same Feature B, magnified 200x

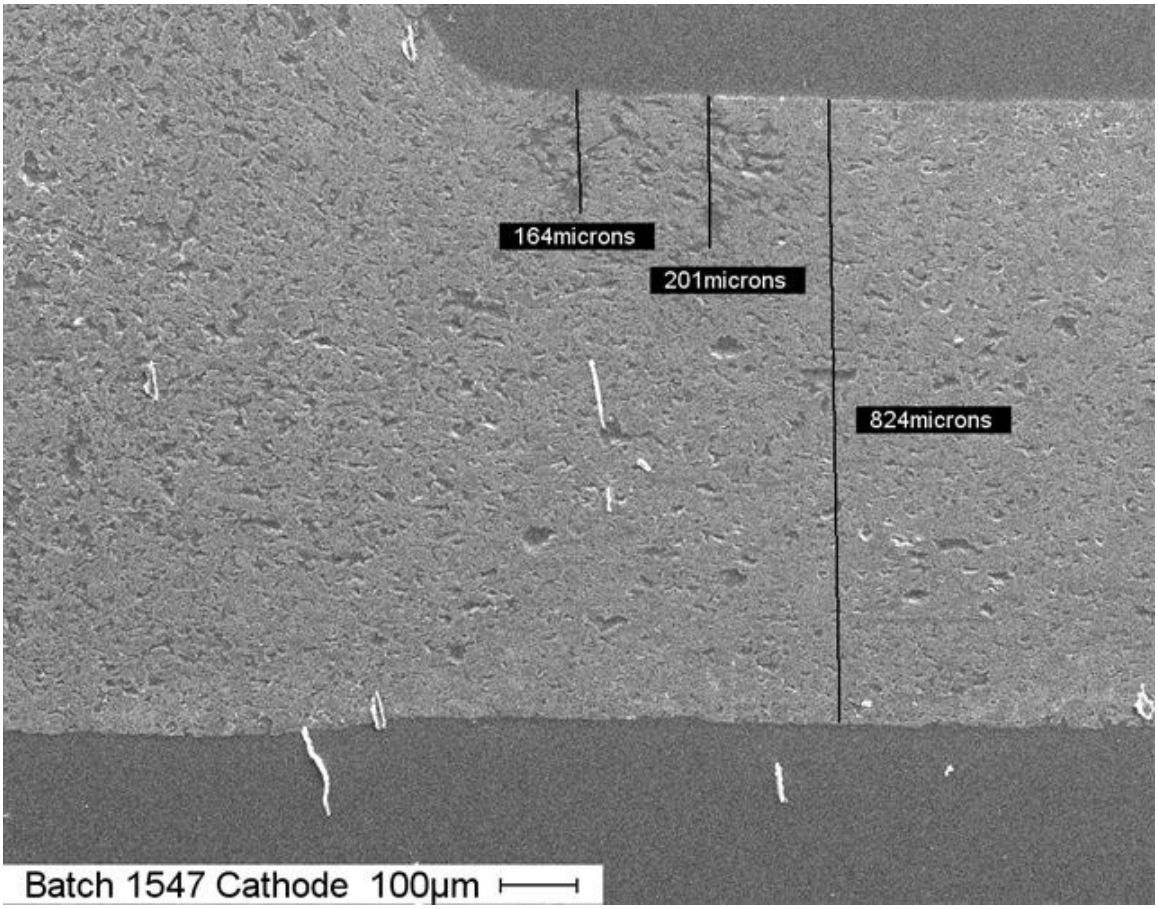

Plate from Batch 1547, Feature C, magnified 75x.

1.3 Flatness Improvement

As experienced early on in the manufacture of molded product, plate warping is a function of the flow field pattern in the plate. Significant steps were taken to reduce and even eliminate the plate warping all together.

It was found in our process that overall plate warping occurred as we began net-shape molding product with thin web sections. This results because of differential shrinkage in the web regions as compared to the rib regions, where the densities of the material as molded are considerably different. The warp was found to be easily corrected through bending the product in the opposite direction of the experienced warp in the original carbonization process. The following is a report of a study of the warp found in plates with straight and parallel flow channels.

In the picture below, the plate on the left is warped. This phenomenon occurs in the carbonization process during which the plate shrinks.

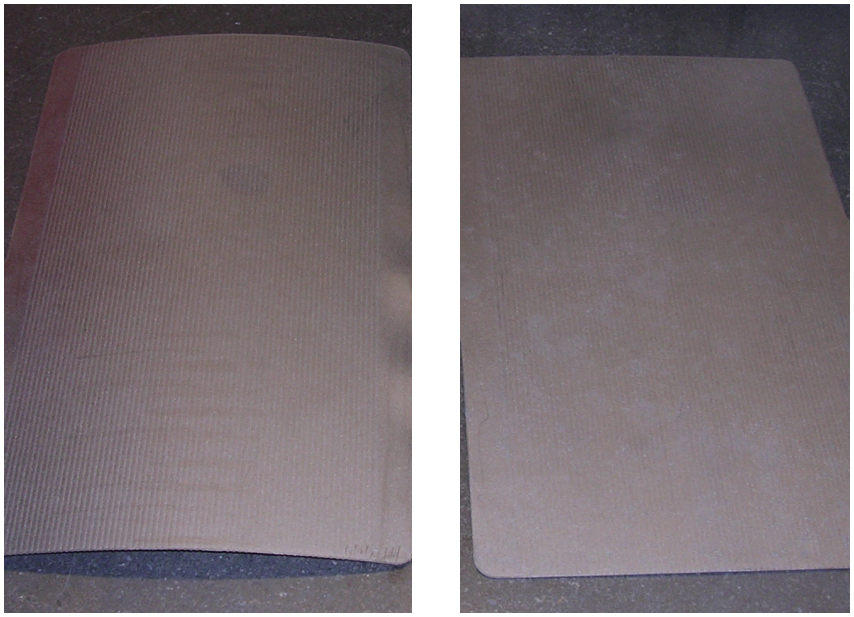

Figure 2 Warped (left) and Flat (right) Anode Plates

To eliminate warp, plates are fired in a curved fixture to correct the warp movement during carbonization. The plate on the right in the above picture, Fig. 2, was fired in a curved fixture. That plate has significantly less warp than the plate on the left. Figure 3, below left, depicts the curved fixture for the cathode plates (channels on both sides). Figure 4, below right, depicts the curved fixture for the anode plates (channels on one side). The plates are placed inside the fixture and the fixtures are stacked on top of one another and loaded into the furnace.

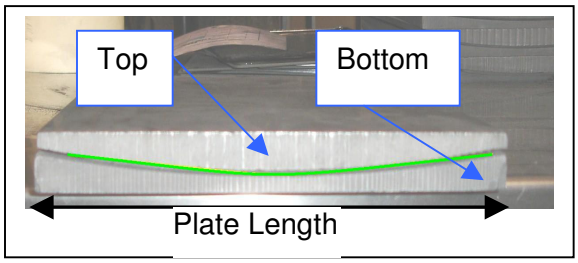

Figure 3 Cathode Plate Carb Fixture

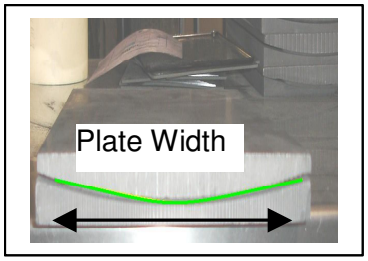

Figure 4 Anode Plate Carb Fixture

Results from a designed experiment for the anode plates revealed that fewer plates stacked together in each curved fixture produced less plate warp. Further study revealed that the orientation of the stacks in the furnace plays an important role in flatness. See figures 5 and 6 for orientation diagrams. Figure 6 depicts our current stacking orientation in the furnace during carbonization.

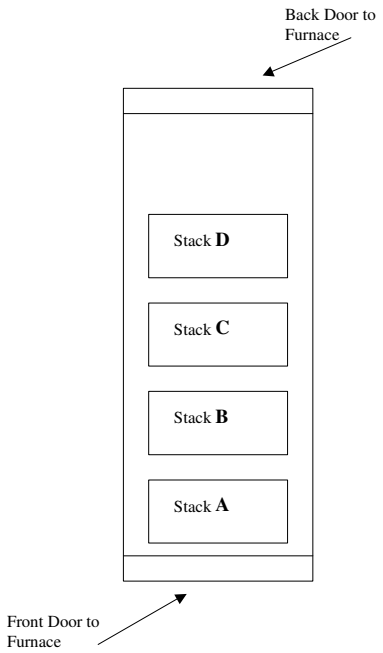

Figure 5 Original orientation of the stacks in the furnace, top view

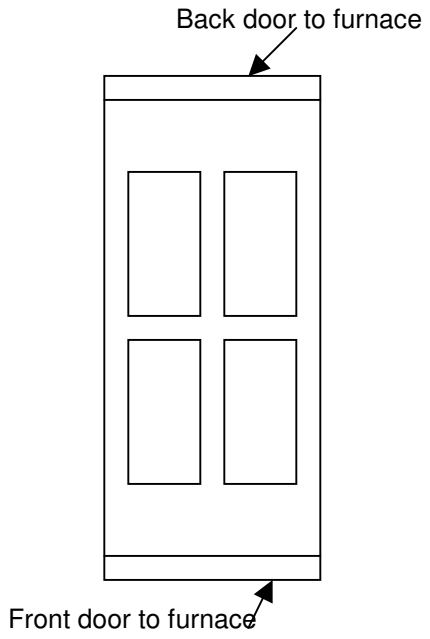

Figure 6 Optimal orientation of the stacks (90 degree rotation), top view

Key Variables to Study

- Ramp Rate (Standard vs. Slow)
- Loading Precision (in line vs. out of line)
- Number of Plates in a Fixture (10 vs. 3)
- Number of Fixtures in a Stack (5 vs. 2)

Ramp Rate	Loading Precision	Number of Plates in Fixture	Number of Fixtures in Stack
+	+	+	+
-	+	+	-
+	-	+	-
-	-	+	+
+	+	-	-
-	+	-	+
+	-	-	+
-	-	-	-

*First Run

Stack	Standard Ramp Rate
D	1 Stack of 5 fixtures with 10 plates in each fixture all in line during loading
C	1 Stack of 2 fixtures with 10 plates in each fixture all out of line during loading
B	1 Stack of 2 fixtures with 3 plates in each fixture all in line during loading
A	1 Stack of 5 fixtures with 3 plates in each fixture all out of line during loading

*Second Run

Stack	Slow Ramp Rate
D	1 Stack of 2 fixtures with 10 plates in each fixture all in line during loading
C	1 Stack of 5 fixtures with 10 plates in each fixture all out of line during loading
B	1 Stack of 5 fixtures with 3 plates in each fixture all in line during loading
A	1 Stack of 2 fixtures with 3 plates in each fixture all out of line during loading

Measureables

- Overall plate warp.

<u>Furnace Layout</u>

The following diagrams best depict the actual plate location in the furnace.

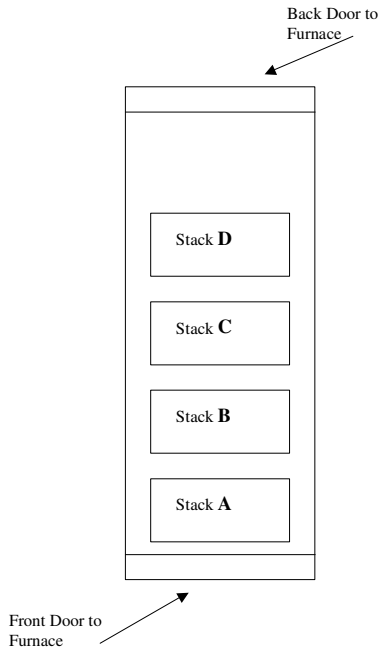

Figure 1, to the left, is a top view of the inside of the Thermal Tech vacuum furnace with the stack A closest to the front door and the rest of the stacks followed back behind.

Figure 2, the lower diagram, is a side view of the Thermal Tech vacuum furnace. The front door is to the left-hand side of the picture. In each stack are 5 fixtures labeled 1, being the bottom fixture in the stack, to 5, being the top fixture in the stack. Some stacks only had 3 fixtures, other stacks had 5, depending on the experimental design plan.

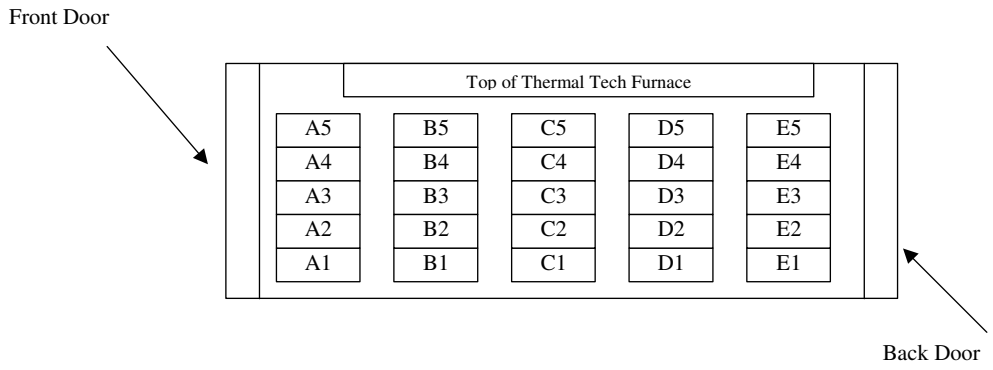

	Fast Profile			Slow Profile		
Segment	Start (°C)	End (°C)	Rate (°C/min)	Start (°C)	End (°C)	Rate (°C/min)
1	20	350	3	20	150	1.5
2	350	750	1.5	150	300	0.2
3	750	1350	5	300	750	0.75
4	1350	1350	Hold 2 hr	750	1350	1.5
5				1350	1350	Hold 2 hr

Results

Figures 1 & 2 chart the warp measurements for each plate in the carbonization run by location in the stack and stack location in the furnace. In both cases, those plates stacked with only 3 plates per fixture (A and B) warped less than those stacked 10 high in a fixture (C and D).

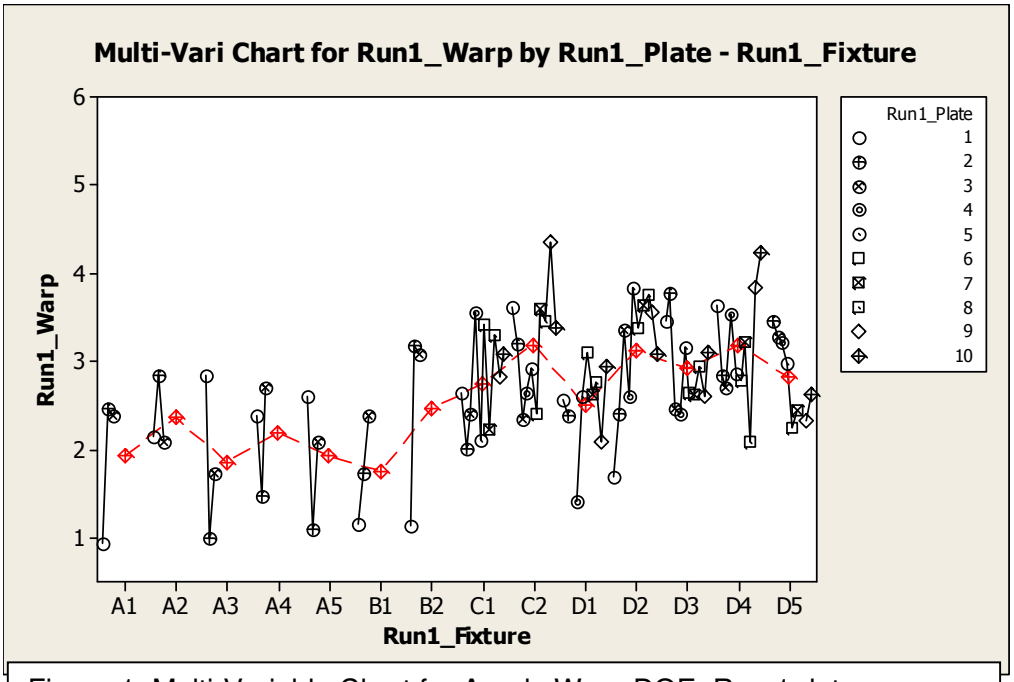

Figure 1 Multi-Variable Chart for Anode Warp DOE, Run 1 data

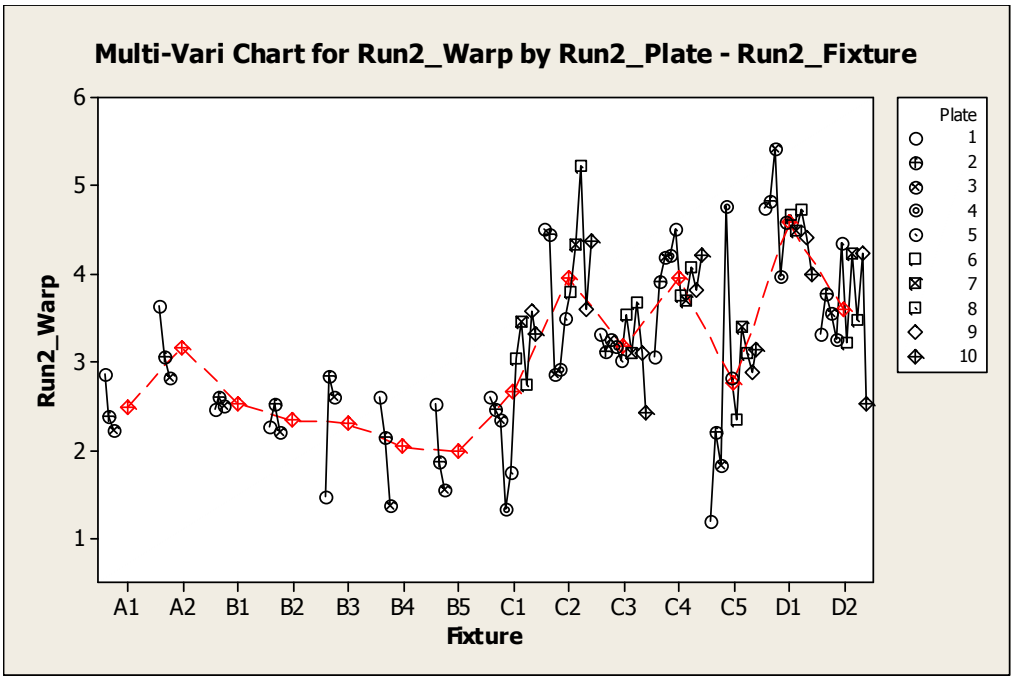

Figure 2 Multi-Variable Chart for Anode Warp DOE, Run 2 data

The influence of the variables of the investigation is as follows:

Table 22. Summary of test results.

Variable	Level	Average Warp (mm)	Significant Effect
Ramp Rate	Fast	2.51	Yes
	Slow	3.12	
Sub-stack Alignment			
	Precise	2.84	No
	Poor	2.79	
# Plates in Fixture			
	3	2.31	Yes
	10	3.32	
# Fixtures in Stack			
	2	2.66	No
	5	2.97	

The data shows that a fast ramp rate is preferred over a slow ramp rate and that fewer plates in a fixture lead to less plate warp. Surprisingly, sub-stack alignment did not show an influence in

overall plate warp. The number of fixtures in a stack also showed no significant influence (although fewer fixtures in a stack did show less warp on average).

While the experimentation did produce some individual plates with warp less than 2 mm, none of the conditions tested produced plates with average warp less than 2 mm. There was a high degree of variation in the data, with warp min recorded 0.93 mm (fast cycle, 3 plates/fixture, 5 fixtures per stack, poor alignment), and warp max 5.42 mm (slow cycle, 10 plates/fixture, 2 fixtures per stack, good alignment). Figure 3 shows a histogram of typical data (stack of 10 plates/fixture, 5 fixtures/stack, slow cycle, poor alignment).

While the experiment showed important trends, a clear pathway to consistently producing low warp plates was not found. For this reason additional experimentation was performed.

In these additional experiments, it was theorized that the direction of the stack and the use of felt could influence the overall part warp. In these experiments, the stack direction was turned such that the long axis of the plate is in-line with the furnace long axis – 90deg from the alignment of the 1st experiment of this report. Further, some of the additional trials used graphite block to separate the test stack from the retort. This was to investigate the potential of non-uniform heating – effectively forcing the heating to be more uniform by adding thermal mass to the perimeter of the test stack. The testing and results are summarized in Table 2.

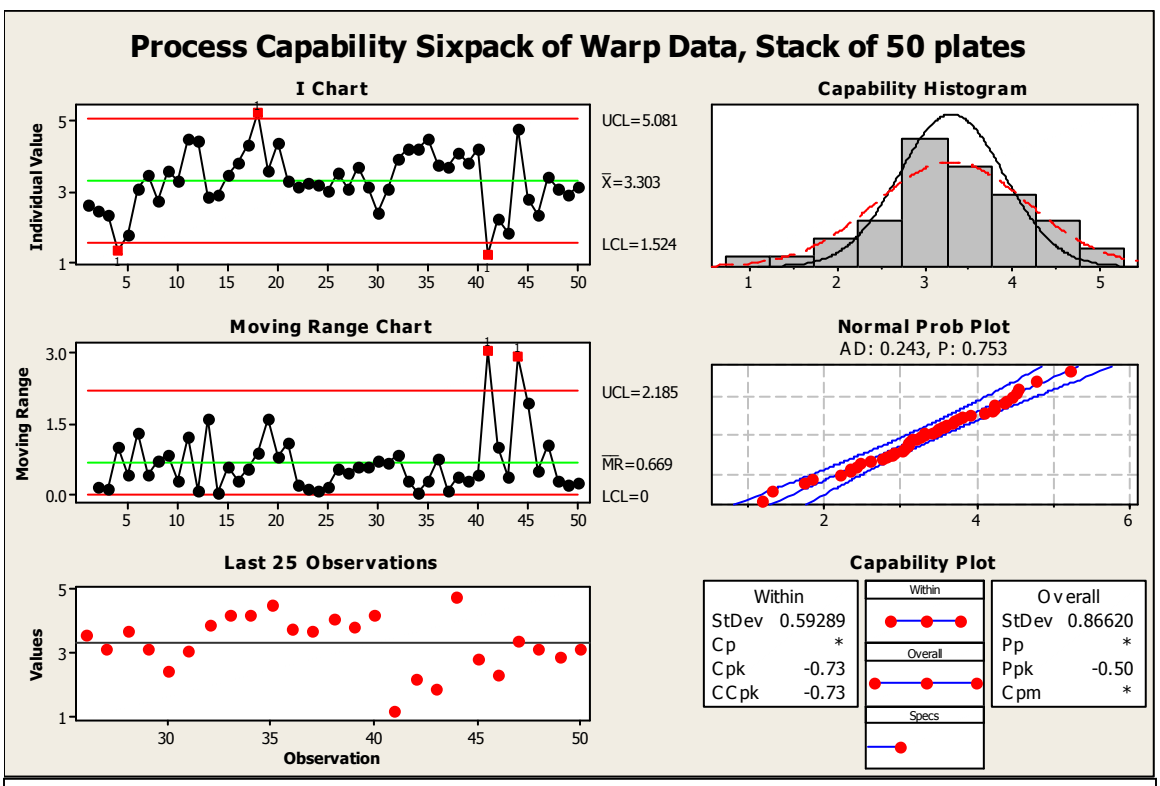

Figure 3. Example process capability for anode warp from this experiment.

Table 23. Summary of additional anode experiments.

Experiment	#/fixture / # fix/stack	Felt Use	Alignment	Perimeter Blocks	Re-fire Plates used	Average Warp	Warp Stdev.
1	5 / 3	yes	W/furnace	Yes	No	1.34	0.54
2	5 / 3	No	W/furnace	Yes	Yes – Base Stack	1.31	0.53
3	5 / 3	No	W/furnace	No	Yes – Base Stack	1.14	0.48
4	5 / 3	No	W/furnace – 2 side by side	No	Yes – 2 Base Stacks side-by-side	1.01	0.46
5	5 / 5	No	W/furnace	No	No	1.21	0.35
6	5 / 8	No	W/furnace	No	Yes – 7 base fixtures, both stacks side-by-side	1.01	0.46

Conclusion

Results from the additional experimentation found that the plate warp was significantly improved over previous trials. It appears from the testing that removing felt and eliminating perimeter blocks improved warp. However, there is such a dramatic improvement over the DOE results that the important variable might be aligning the plates with the furnace axis. It is also possible that the overall size of the load has an influence. This will be investigated in further testing when additional plates have been made.

The variables found to be important in reducing the degree of anode warp include:

- Using fewer plates per fixture
- Using the faster furnace ramp rate
- Eliminating felt
- Eliminating use of perimeter blocks
- Possibly aligning the parts with the furnace axis

It is not thought that the root cause to the anode warp change from low warp to high warp has been found. Additional testing will take place to investigate if the stack alignment influences results or if other loading parameters influence warp (full load vs small test loads for example). However, from the additional tests of this study, a pathway to low warp with the potential of good loading capacity has been defined.

1.4 Manufacturing Trials

The goal of this task was to demonstrate net-shape manufacturing capability using plate designs from two different customers. Plate physical dimensions and properties were collected, along with manufacturing efficiencies and yields.

A manufacturing trial was run with a set of net shape molded parts (anodes and cathodes) ran after finalizing the manufacturing process through a series of qualification runs that were designed to discover any key sources of product variability. The trial evaluated the consistency of product produced from a list of measures including:

- Part trim weight
- Part press weight
- Part carbonized weight
- Part final length, width and thickness
- Part channel dimensions at select locations
- Part porosity properties specific to our customer

Because much of the information is proprietary (and not necessarily germane to the study here, which is focused more on dimensional achievement than on property achievement), porosity parameters will not be reviewed in this report. Further, final part channel dimensions sensitive to our customer will be normalized to yield information reflecting our capability of achieving consistent dimensions rather than focusing on the actual dimensions themselves.

The focus of the study was on obtaining capability data for achieving channel dimensional tolerances important to the final product. In Figures 1.4.1 through 1.4.6 below statistical "6-pak" charts are shown for measurements of anode, air and water channel width and depth. The average feature dimension has normalized the tolerances in the charts as well. Channel depth was measured with a drop gauge. Channel width was measured optically, as described above in section 1.1. The data reflect tolerances modified slightly from the original to improve product capability as compared to machined plate tolerances (which are generally +/- 0.05 mm). We find that the process, despite considerable shrinkage that occurs through plate processing, achieves repeatable performance.

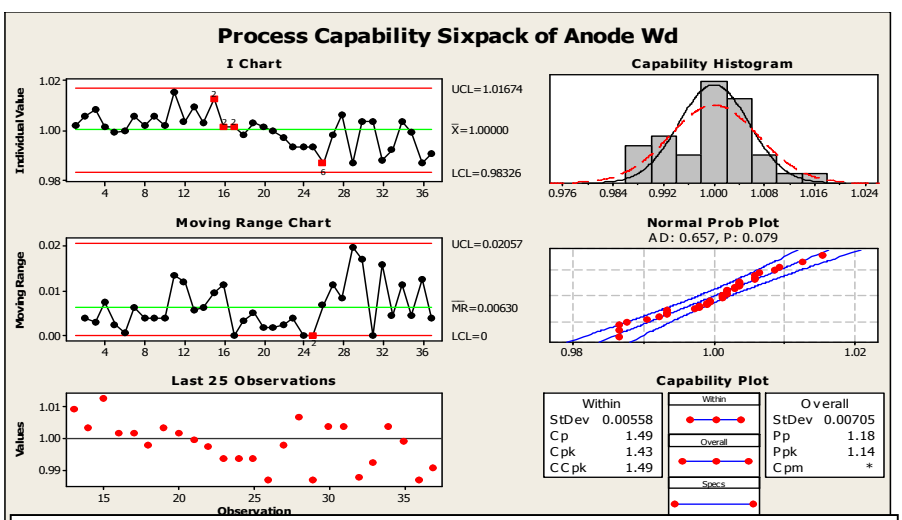

Figure 1.4.1. Anode channel width (normalized) capability.

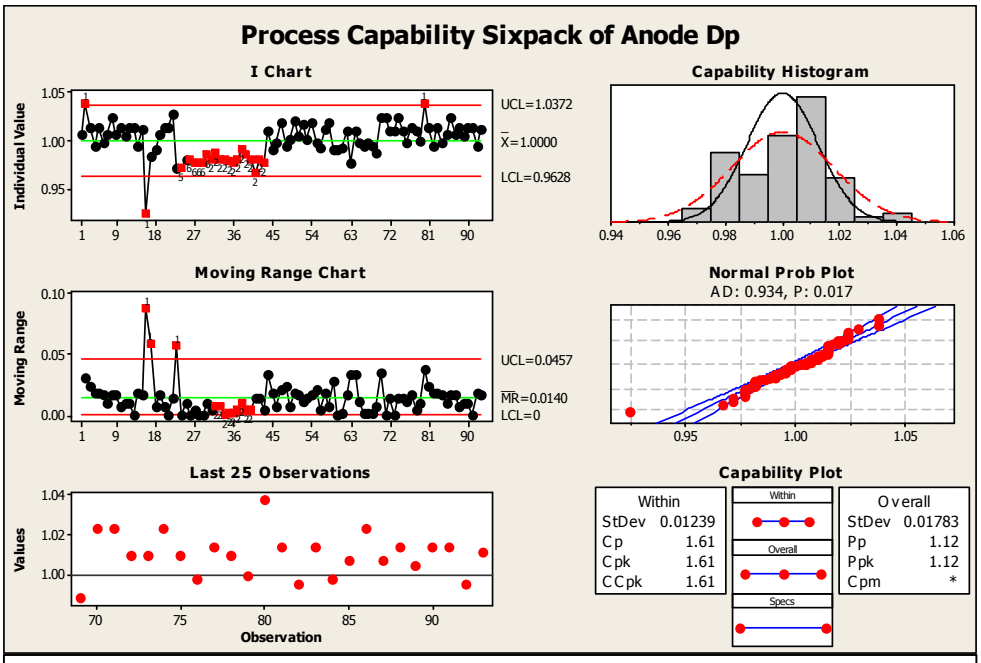

Figure 7.4.2 Anode channel depth (normalized) capability.

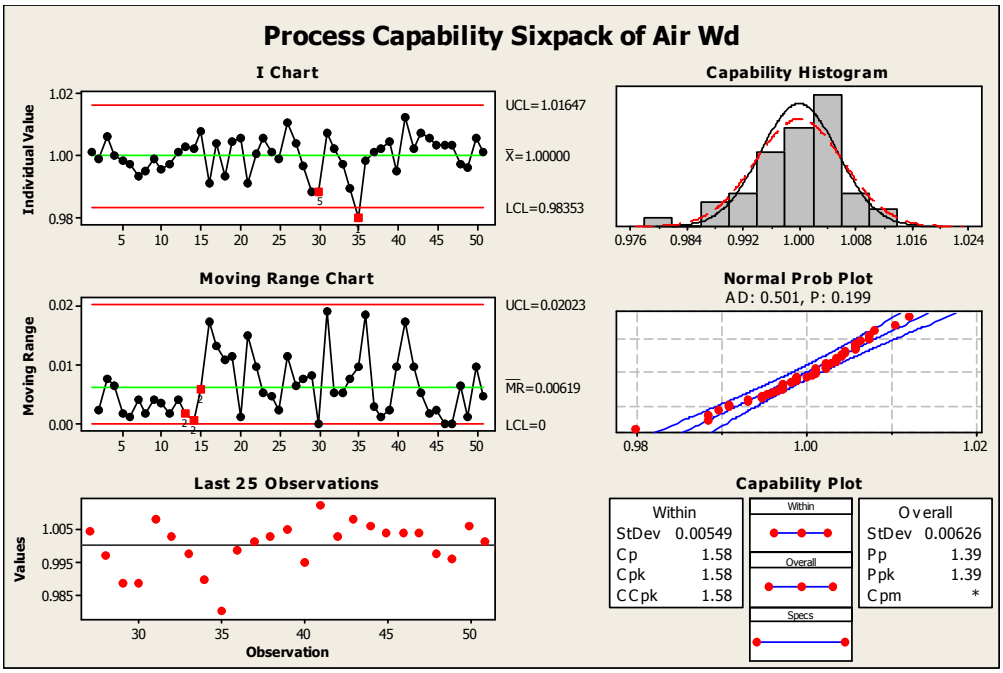

Figure 1.4.3. Air-side channel width (normalized) capability.

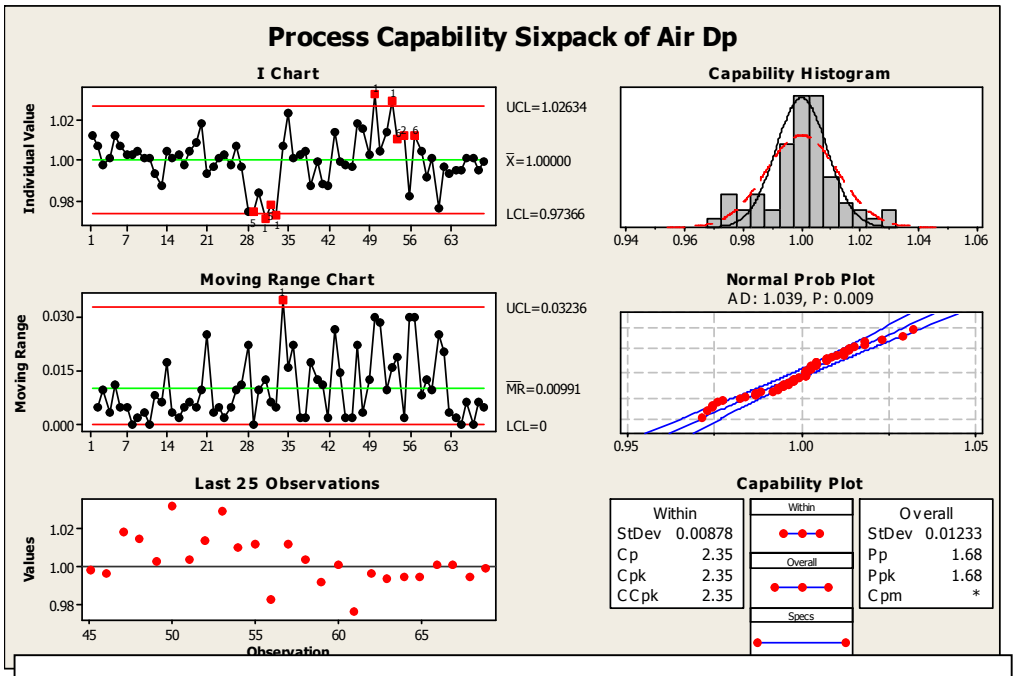

Figure 1.4.4. Air-side channel depth (normalized) capability.

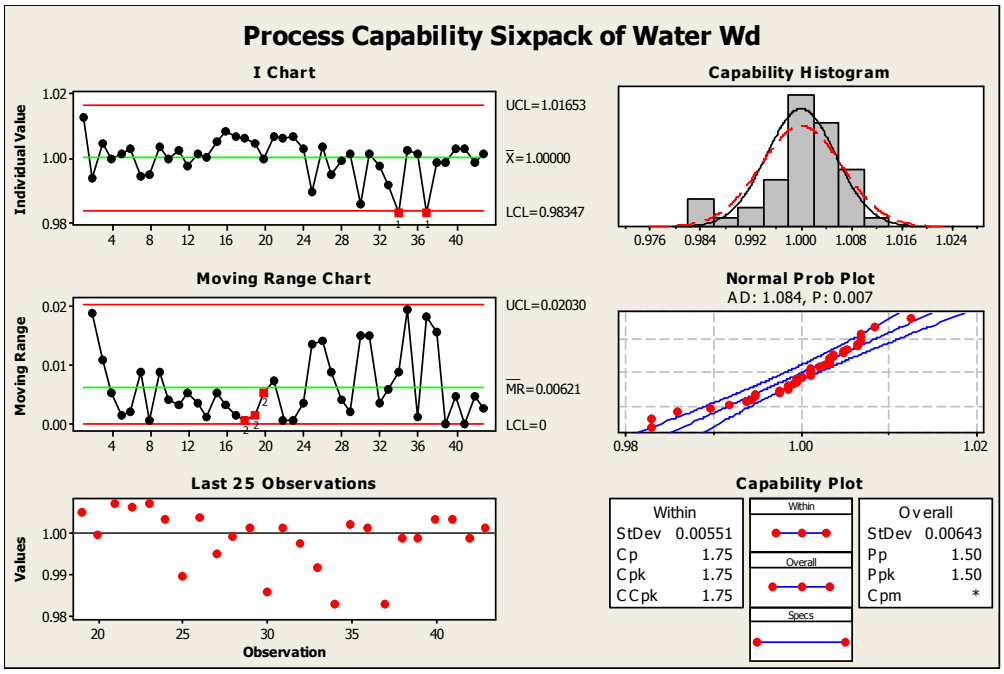

Figure 1.4.5. Water-side channel width (normalized) capability.

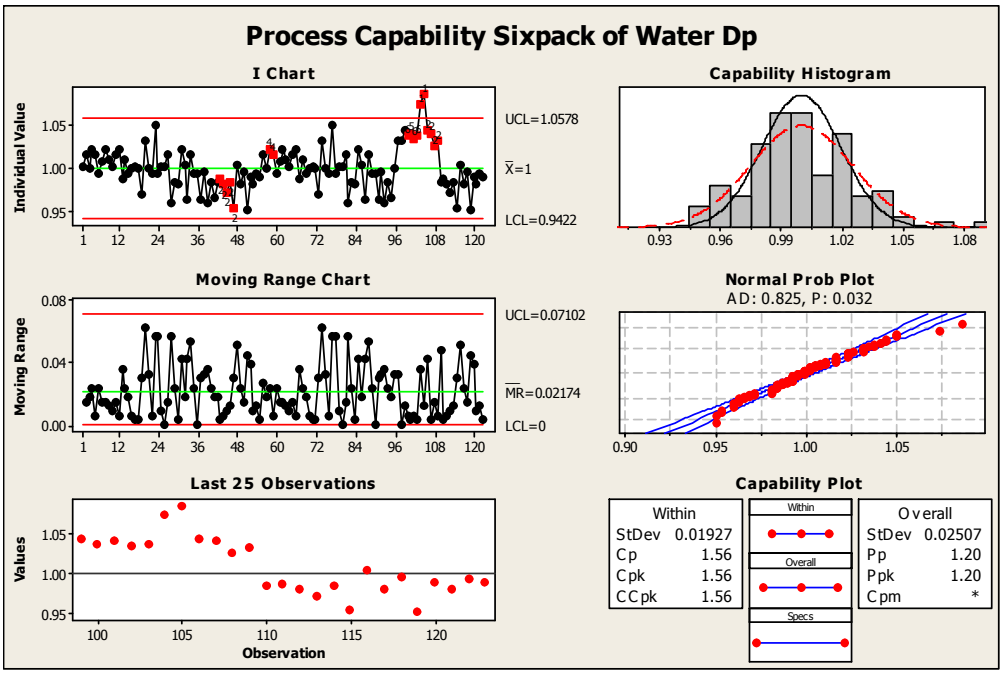

Figure 1.4.6. Water-side channel depth (normalized) capability.

2.0 Develop and Evaluate Robust, Low-Cost Plate Sealing Method

This topic area was included in this program after realizing the issues found with the use of the CVD process (namely the increase in electrical contact resistance, and the sensitivity to damage of the seal surface. See section II. 5.4). Alternative means of sealing plates were investigated in this program, and several trial stacks were built and evaluated by customers.

2.1 Investigate Potential Porosity Seal Materials

In this portion of the program, it was desired to fill the pores of the Porvair product with a set-in-place polymer in a simple, low-cost operation. The polymer material would be applied to the bipolar plate after the carbonization process, and yield a product that is a composite material consisting of the carbonized bipolar plate material and a sealing polymer.

In selecting candidate systems, the following characteristics were considered critical:

1) Chemically compatible with fuel cell systems (i.e., corrosion resistant, non-poisoning)
2) Low viscosity sufficient to penetrate the pores of the material
3) High solids content to limit migration, entrapment and open pores resulting from evaporating solvents and thinners
4) Easily cleaned from the surface of the product
5) Low-cost and readily available in the marketplace

After investigating alternative materials through a round-robin study, we quickly discovered to significant issues that limit the application of this approach. The first is obtaining a suitable

sealing product with a viscosity low enough to penetrate the pores of the bipolar plate product. The porosity of the bipolar plate material is very fine, generally below 1 □m in dimension. The pore size restricts effective penetration of the sealant into the pores of the material, even under vacuum conditions. The second issue is the ability to clean and maintain a clean surface while the material cures within the porosity of the product.

Epoxy products are generally too high in initial viscosity (100 Cp or higher), yielding a product that is limited in sealing effectiveness. Polyethylene and vinylester resins were found similarly unsuitable. However, low-viscosity (~10 Cp) resins were found to be effective in penetrating the porosity of the product, and were able to be cleaned effectively from the surface.

2.2 Develop Robust, Low-Cost Sealing Method

In this program, it was found that the development of the process and the material was hand-in-hand. The material performed best when vacuum impregnated into the pores of the product, then blotted dry. The parts then placed in a convection oven to heat and cure-place sets the resin (schematically illustrated in Fig. 2.2.1). A unique feature of this material is that the surface of the plate, if properly applied, is as clean and free of resin as a fully carbonized plate. Figure 2.2.2 shows the resulting contact resistance for a Porvair net-shape molded plate sealed with resin, as compared with a CVD coated plate. The sealed plate has the same low contact resistance as an unsealed Porvair all carbon plate. The CVD sealing process significantly increases the surface contact resistance (hurting fuel cell performance).

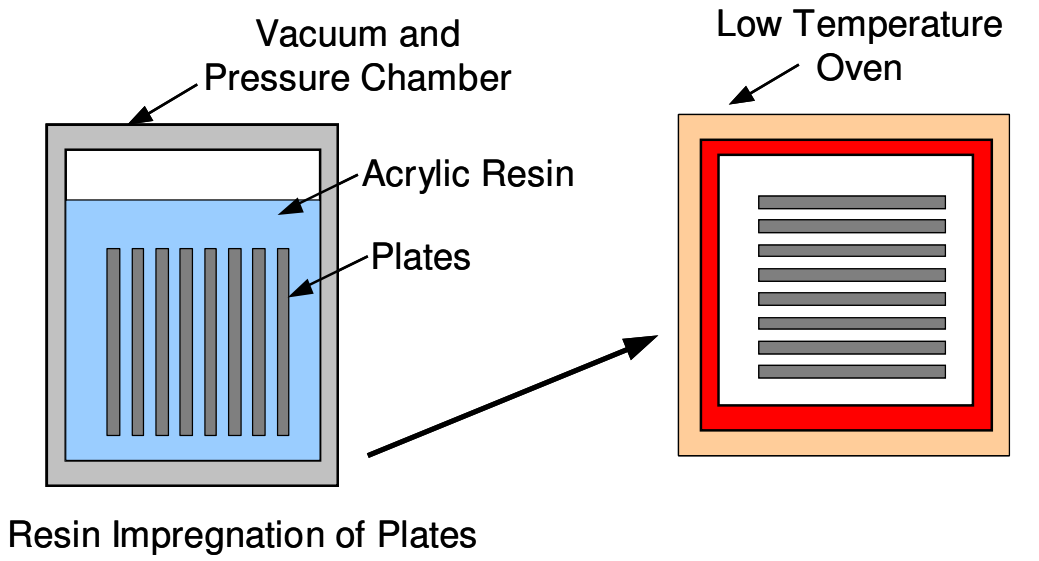

Figure 7.2.1. Schematic illustration of sealing process.

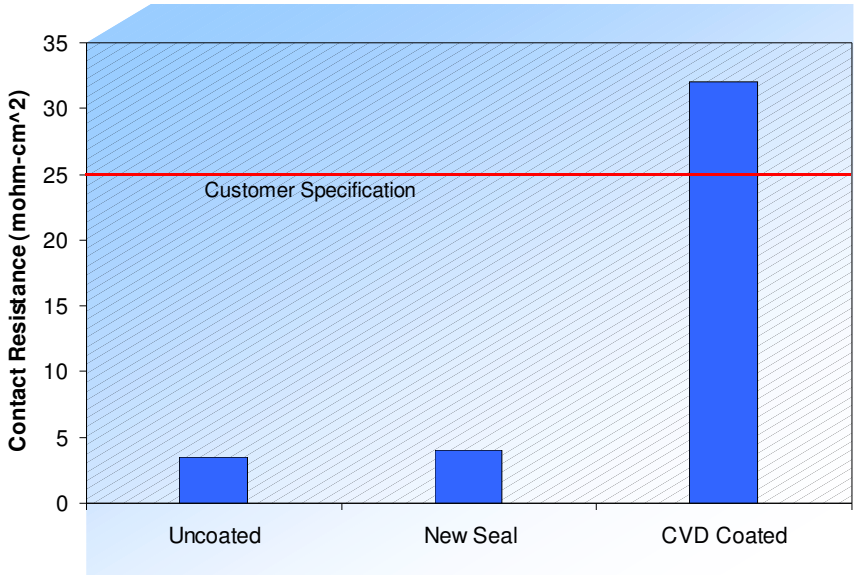

Figure 2.2.2. Contact resistance of sealed, unsealed and CVD coated net-shape molded bipolar plates.

Overall, it was found that the use of the material was beneficial to product sealing, but additional challenges remain. Figure 2.2.3 shows a photograph of a cross-section of an sealed plate. The sealing material is not visible under optical microscopy.

- Sealing Advantages
  - –Good resistance to fuel cell environment
  - –Plate maintains its original electrical conductivity
  - –Contact resistance is low (like a porous plate)
- Sealing Challenges and Disadvantages
  - –Achieving excellent hydrogen seal (we have demonstrated to near DOE target, but have not hit target to date)
  - –Keeping surface of plate free of resin in curing process
  - –Maximum use temperature of ~140 C
  - –Leaves plate with mid-range wettability

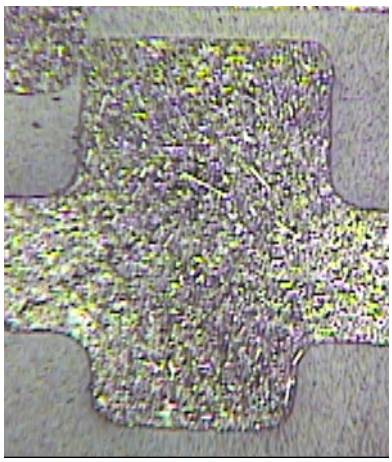

Figure 8.2.3. Cross-section of an sealed bipolar palte. Sealing medium is not visible.

2.3 Develop Hydrogen Permeability Test Method for Patterned Plates

Introduction

In the development of the sealing method, it was found that leakage problems with the plates that we sealed for them for initial product testing. The information gathered was that the plates showed approximately 20 cc/min leakage under pressurization test, when only 0.5 cc/min is allowed from either the anode or cathode to the water side of the bipolar plate. The supposition was that the Porvair coating was allowing the gases to pass from the anode or cathode to the water side of the plates.

Investigation

In the investigation, we cut rectangular sections from the interior of the plates (approximately 12cm x 20 cm) to test for through-plate gas permeability. In this test we applied nitrogen pressure at a maximum of 30 psi (206 kPa) to one side of the plate, and positioned a gas flow meter (20 cc/min maximum indication at standard pressure and temperature) upstream of the plate. The plates were fitted with compressible foam gaskets around the perimeter and compressed in a testing fixture to make a seal. Any flow indicated from the flow meter would indicate gas crossover or leakage across the gasket material. In this test we found that one plate had no leaks, while the other showed leakage of approximately 15 cc/min at 30 psi pressure.

New Test Fixture

We then re-designed our test fixture to fit the trial parts and proceeded to test the remaining 3 plate pairs for leaks. The test fixture looks similar to the drawing in Figure 2.3.1. It allows us to pressurize any of the three plate ports together or independently to evaluate the plate leakage.

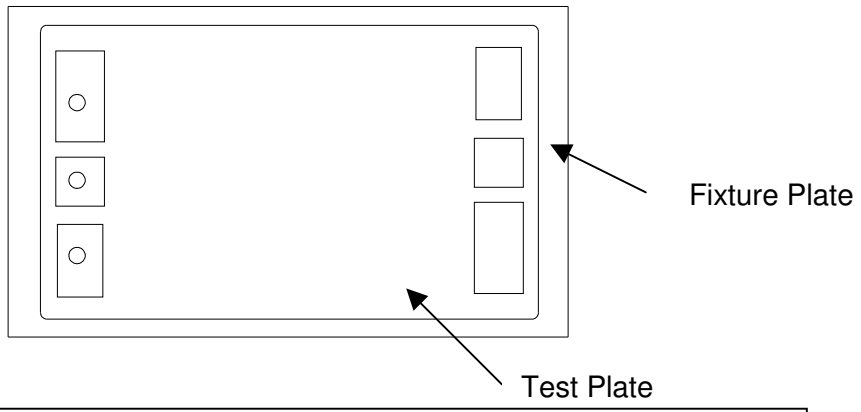

Figure 2.3.1. Schematic diagram of the test fixture developed for seal testing an entire bipolar plate design.

The fixture also allowed us to view the plate during test to attempt to determine where the leak is coming from, as shown schematically in Figure 2.3.2:

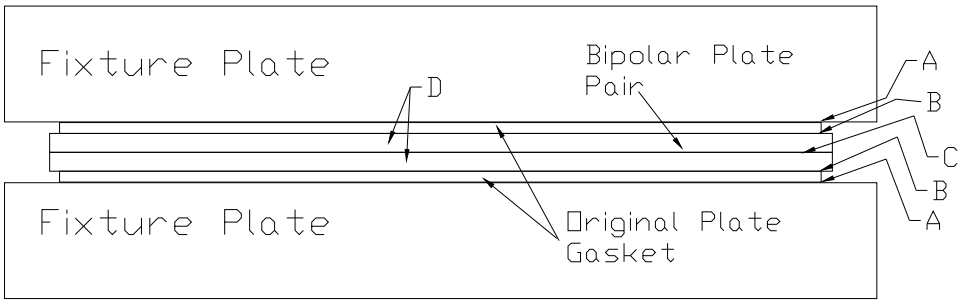

Figure 2.3.2. Schematic diagram of plate testing configuration.

The figure shows four possible leakage locations for visual leakage observation (during the test the plate edges are sprayed with water/soap solution to help in visualizing leaking locations). These are:

A – Leaking between the gasket and the test fixture
B – Leaking between the gasket and the bipolar plate
C – Leaking between the monopolar plates at the bondline
D – Leaking out of the monopolar plates themselves

Additionally, we use a flow meter either upstream or downstream from the plate to determine leak rates.

Test Modes

The test modes are as follows:

1) Pressurize all three ports simultaneously – this test is effective for evaluating leaking from the seal, bondline or plate edges. In this test the flow meter is placed upstream of the plate (on the pressurization side).
2) Pressurize air and fuel ports simultaneously – this test is effective for evaluating leaking from the anode and/or cathode to the water side, or across the gas-to-water bondline between the plates. In this test the flow meter is placed either upstream or downstream of the plate as follows:
    a. Upstream (on the pressurization side) captures all flow leaking to the water side or across the seal, bondline or plate edges.
    b. Downstream of the water port (on the atmospheric pressure side) captures only the flow that leaks through the plate or across the gas-to-water bondline, unless the rubber seal leaks from the gas ports to the water port.
3) Single-side pressurization – should isolate a leaking plate or seal

Results of Testing Plate Pairs

Using the new fixture we found that the plates showed overall leakage rates similar to observation (approximately 20 cc/min), using test mode 1. However, visual observation showed that the leakage was coming primarily from position A (between gasket seal and test fixture plate, as described above).

We made several attempts to reduce the level of this seal leakage, including increasing the pressurization load to the plate up to approximately 1200 lbs (540 kg). We did not want to go further than this and risk damaging more plates. Previous experience shows that this level of load is sufficient to make a seal. However, we tested with the seal dry only (did not attempt to first wet or lubricate the seal material).

We did see some leakage indicated from positions B, C and D. This leakage was very minor compared to the leakage detected from position A.

We next tested the plates using test mode 2a (flow meter on pressurized side of plate). We found approximately the same leakage rates in this mode as we did in test mode 1. Again, our observations were that the bulk of the leakage was across the seal material.

We finally tested the plates using test mode 2b (flow meter on un-pressurized side of plate). We found that the leakage here varied between 5-10 cc/min, depending on the plate tested. We have no way of knowing if this flow indicated leakage across the seal separating the gas ports from the water port.

Summary of Bonded Plate Tests

Using this information, we came to the following conclusions and possibilities:

- A good deal of leakage is occurring across the seal of the plates around the perimeter.
- We did find some evidence of bondline leakage (but leakage was visually minor compared to seal leakage)
- We did find some evidence of plate edge leakage (but leakage was visually minor compared to seal leakage)
- Leakage in test mode 2a is similar to that in test mode 1, indicating the majority of leakage is across the plate perimeter boundary
- Leakage in test mode 2b is between 5-10 cc/min. This leakage could be through the plate, across the plate bondline separating the gas and water ports, or across the gasket seal separating the gas and water ports

Additional Evaluation

Because we found an indication of leakage using test mode 2b, we decided to separate the monopolar plates from each other and evaluate plate leakage through the individual plates. To do this we heat-treated the plates using our standard carbonization cycle. This evaporated the bond material and successfully separated the plates. Some plate surface discoloration resulted

during the process, however. This is likely oxidation to the surface coating resulting from stagnation of the gases evaporated from the bond material.

The separated plates were tested for through-plate leakage by using a compressible gasket material that conforms to the plate channels. We tested only the bulk middle of the plate in a ~12cm x 20 cm rectangular area. We were not able to test the entire plate due to the through-holes in the design.

The plates were pressurized on one side of the plate, with a flow meter positioned on the other side of the plate to indicate through-plate leakage. We used nitrogen gas at a maximum pressure of 30 psi in this test. Because the flow meter was positioned downstream, we were insensitive to small leaks occurring between the gasket and the fixture or plate on the pressurized side.

With the exception of one of the plates then we damaged in our initial evaluation, all plates tested in this way showed zero leakage across the test area.

To evaluate the plates further, we performed the test that we normally use to evaluate for seal effectiveness, but at a higher pressurization pressure. This test involves placing the monopolar plates into a chamber (maximum of 6 plates at a time) for 30 minutes at a pressure of 15 psi using nitrogen gas. For these plates we pressurized to 30 psi instead. After the pressurization, the plates are placed into a water bath and visually watched to identify any leaking regions on the plate surface.

This test has been successful in identifying small regions of plate leakage, and works by allowing gas to leak into any open areas of the seal coating. Over the pressurization time, the internal porosity of the plate is pressurized and leaks slowly from the plate when the plates are removed from the gas pressurization and the leak test is performed.

We found the following in this test:

- None of the plates showed any leaks from the top or bottom faces of the plates
- All of the plates showed small leaks from at least three locations along the plate edge perimeter or edge interior corner of a gas port window

Conclusion

From the evaluation of the leaking of the plates we conclude that the plates themselves showed only minor leaks from edge regions along the perimeter or at a corner of a gas port window. No gas leakage was detected crossing the faces of the plates.

In our testing, we found that the bulk of the leakage was across the rubber gasket seal on the plates and our test fixture surface. We could not reduce this in our testing, but did not try to use any lubricant to improve the gasket seal.

Other leaks observed were minor, and included plate edges and possible the bondline of the bipolar plate.

We believe that the leakage detected from the gasketed bipolar plate tested in mode 2b occurred primarily across the rubber gasket and the plate between the gas and water ports, instead of across the plate face. This is justified by our visual observations of the major leakage locations, as described above.

We believe that the leakage problem is more due to the application of the rubber gasket seal than due to plate leakage or bondline leakage.

2.4 Corrosion and Material Leaching Resistance

Sulfuric acid soaks at 80-95°C temperature were used to judge the corrosion-resistance of the seal (overnight and for 500 hours). Plates were found to discolor somewhat after soaking, but the sealing effectiveness remained at a level near $2x10^{-5}$ ccc/cm^2/sec. Further corrosion and material leaching tests were not performed in this program.

2.5 Evaluate Sealing Method in Fuel Cell Testing

A stack of 30 bipolar plate pairs were prepared for a major customer in this program. The parts were net-shape molded, carbonized, trimmed and sealed, then sent to the customer site. At the customer site, the parts were visually inspected and measured for dimensional accuracy. At the time of this effort (Dec. 2004), the state of dimensional control of the parts was not sufficient to allow the customer to utilize the parts directly in their fuel cell testing equipment. No further work was done in the area of sealed product testing in fuel cells, as the market pricing for net-shape molded composite molded graphite plates made our products look economically unattractive in short-run volumes. Our focus was better placed on net-shape development of our porous plates for our program partner, UTC Fuel Cells.

3.0 Optimization of Plate Materials

In this task, the goal is to optimize materials for permeability improvement for our porous plates, and sealing effectiveness for our sealed plate materials.

3.1 Porosity Optimization with Differing channel configurations

<u>MOLD FILLING EXPERIMENT – COMPOSITION VARIABLES</u>

<u>Introduction</u>

This experiment is designed to investigate the influence of a variety of material ingredients on die mold filling and shrinkage. The key goal is to define materials and processing conditions that reduce or eliminate the bleed-through of the pattern from one side of the plate to the other. The customer B die set is to be used.

Experiment

The experimental design is as follows:

	1	2	3	4	5	6
Resin Amt	High	Low	High	Low	Mid	Mid
PE Amt	High	High	Low	Low	Mid	Mid
Gr Type	New	Standard	Standard	New	Alternative	Alternative
Std Resin	Yes	Yes	Yes	Yes	Yes	No
New Resin	No	No	No	No	No	Yes

Experiments 5 and 6 will be a direct comparison between each to determine the influence of the resin type.

Procedure

Prepare full batches as normal. Form 11 sheets using a probe height of 5.5", then move probe to 10", and form an additional 11 sheets. Discard the balance of the sheets. This will produce sheets with the target trimmed sheet weights:

175 – 185 gm @5.5" probe height.
200-210 gm @ 10" probe height

Record all data as normal, and pull sample sheets as normal (4, 10, 16, 22) for basis weight uniformity.

Press the plates in the cathode die (double-sided) without shims.
Carbonize the plates in a standard carbonization cycle as normal (stacking 4 plates per stack, separated by graphite solid plates).

Following carbonization, check in parts as normal.

Note mold filling quality on a 1-10 scale (10 is perfect, as would be seen with the Plenco pucks, 1 is very poorly filled).

Note appearance and severity of bleed-through pattern on a 1-10 scale (10 is no evidence of bleed through, 1 is severe material depressions, 5 would be like normal parts).

Results of Testing

The parts were made and characterized as above. Because the pattern is easily molded, the rib filling characteristics were not recorded. However, plate warp measurements were taken and provided valuable insight into plate flatness characteristics.

The rib bleed through was difficult to judge. A reference plate (standard material) was used for comparison. From these sets of plates, nearly all of the materials showed better bleed through resistance compared to the standard composition.

The averages from measurements are shown in the two tables below for low density parts and for high density parts

	Average Pressed Wt	Average Carbonized Wt	Avg Wt Loss%	Avg Thikcness	Bleed-Thru Score	Avg Warp Meas
Low Density	177.47	142.05	19.95	1.50	7.37	4.48
High Density	207.73	166.58	19.87	1.52	6.83	6.60

Major conclusions from the data include:

Use of Standard Graphite

The standard graphite is a graphite material that has the unique characteristic of having a high spring-back property. This means that the material does not pack greatly and acts elastic when under compressive loads. This property significantly influences material properties, shrinkage and plate warping. In this study, the plates using the standard graphite had the following characteristics:

- Least thickness shrinkage
- Best bleed-through reduction
- By far the worst plate warpage

The plates using standard graphite were extremely warped, both large scale (plate bow) and small (plate wiggles).

Effect of Resin Content

The study found that higher resin content led to greater part shrinkage and more severe pattern bleed-through characteristics. Part warp was also found to be worse with higher resin content. To summarize, higher resin content leads to:

- Higher thickness shrinkage rates
- Worse pattern bleed-through characteristics
- Worse plate warping

Effect of PE Content

This study also evaluated the effect of PE addition to the mix. The PE powder has been added in the past to improve product-molding qualities without impacting part permeability. It is also

beneficial in reducing foam in the batching and mixing process. In this experiment the use of high levels of PE leads to:

- Higher part shrinkage
- No significant influence on pattern bleed-through
- No significant influence on plate warp

Effect of Plate Density

In this study, two plate densities were targeted for each material made. Half of the batches were made to low target plate weights, and half to high target plate weights. This study found that the plate density had only a small impact on plate shrinkage, pattern bleed-through and warp. Higher plate density leads to:

- Slightly less part shrinkage
- Slightly worse pattern bleed-through characteristics
- Slightly worse plate warping

This study found that within a batch of parts, those made to higher densities were of lower overall quality than those made to lower density. However, strength was not evaluated in this study. Parts made to higher density were noted to be of better strength, qualitatively.

Evaluation of Alternative Graphite, and Alternative Resin

Experiments 5 and 6 were meant to be mid-point comparisons from the main DOE, using a different graphite type and a different resin type, with material quantities placed at the midpoint of the design. A direct comparison between these two batches also provided information comparing the standard resin with the experimental resin.

These two batches produced parts that exhibited less warping than the other batches, except for use of the alternative graphite at low part density. This is probably attributed more to the graphite type than to the other variables in the design.

- Parts made with the alternative graphite exhibit less warp than parts made with standard or new graphite, except at low density, where the alternative and new were nearly the same

The evaluation of the alternative resin is of interest in improving the process, as this material has exhibited improved molding and permeability achievement when manufacturing material. In this study, experiments 5 and 6 were a direct comparison of the use of this resin against the standard resin. This study found that the use of the new resin:

- Imparts slightly more part shrinkage
- Imparts slightly more part warp
- Reduces pattern bleed-through slightly at low part density

The differences were minimal, and may be more attributed to normal process variation than with actual differences. Either resin looks to be a good candidate for use.

Summary

This experiment evaluated in a short DOE the effect of resin content, graphite type, poly ethylene powder content, and use of an alternative resin. Key points of learning from this experiment include the following:

- Standard graphite powder imparts less material shrinkage and bleed through, but produces parts with severe warp characteristics
- Higher resin levels lead to higher shrinkage rates and more severe pattern bleed-through. Plate warp is also worse with higher resin contents
- High levels of PE powder led to higher shrinkage rates, but little effect on plate pattern bleed-through or warpage
- Lower plate densities are beneficial to plate warpage and pattern bleed-through, but worse for plate shrinkage. The effect is relatively minor.
- Either resin standard or alternative resin may be used equally effectively

These results did not consider plate strength. Qualitatively parts made with lower densities and lower resin contents showed lower plate strength.

The recommendations from this experiment are:

- Do not consider the use of standard graphite
- Stick with 3% PE content in the composition
- Avoid the use of resin contents over 30%

The new resin may be used with little impact on part quality

3.2 Optimization of Materials for Sealed Plate Configurations

Based upon the difficulty of displacing an established product with a new product in a risk-averse field (like fuel cells), and upon the state of development of alternative sealed bipolar plate technologies, it was decided to focus our efforts on our porous plate products. No activity was therefore performed in this subtask.

3.3 Develop Low-Cost Material Wetting Angle Method, Material Additives

WETTABILITY TRIALS FOR POROUS PLATES

Introduction

This experiment will evaluate the potential of using the pore sealer in a dilute solution to impart water-wetting characteristics to porous plates without impacting the plate's permeability significantly.

Experiment and Procedure

1) Take 10 dry molded plates already tested for permeability, and having a water flow at test conditions (30 kPa, 30 seconds) of more than 4 grams, and perform a simple water

droplet test. Apply a small droplet of water to the plate in the main flow field area and note the time required for the droplet to wick into the porosity of the material. Record the plate dry weight, original water flow, water wick time and any observations.

2) Prepare three solutions of Loctite 90C resin and alcohol as follows:
    a. 50 ml 90C, 100 ml alcohol
    b. 30 ml 90C, 120 ml alcohol
    c. 15 ml 90C, 135 ml alcohol
3) Impregnate two plates fully with each solution by pouring solution into a shallow pan and soaking the plate into the solution until the part is wet through
4) Allow plates to air-dry overnight in fume hood
5) Heat plates to 100C in oven for 4 hours
6) Record final plate weights
7) Repeat water droplet test and record times and observations
8) Vacuum fill plates and test for permeability – record water flow.

Results and Discussion

The above experimentation went as planned, except that the starting solution consisted of 500 ml sealing resin, and 1000 ml of alcohol. Two parts were soaked in this solution for five minutes and set to air-dry. 500 ml of this same solution was then taken and diluted with 330 ml of alcohol for the second treatment. Following this, 300 ml of the 2nd solution mixture was taken and diluted with 300 ml alcohol to form the most dilute solution. The resulting mixtures were as follows by volume:

a) 33% in alcohol (vol %)
b) 20% in alcohol (vol %)
c) 10% in alcohol (vol %)
d) 0% in alcohol (Vol%)
e) No alcohol or treatment

After soaking for 5 minutes the parts were air-dried overnight and then cured in a convection oven at 100°C for 4 hours. The table below describes plate weight gain for each solution and plate.

Solution	Plate #	Wt Before (gm)	Wt After (gm)	Wt Gain (gm)	%Wt Gain
33%	728-14	37.2	40.2	3.0	7.5%
	728-15	37.3	40.6	3.3	8.8%
20%	728-17	37.4	38.3	0.9	2.4%
	728-18	37.1	38.3	1.2	3.2%
10%	728-19	36.9	37.6	0.7	1.9%
	728-21	37.4	38.0	0.6	1.6%
0%	730-20	36.6	36.6	0.0	0%
	730-21	36.8	36.7	-0.1	0%
Drying only	730-18	36.9	37.0	0.1	0%

Plate wetting characteristics were found to change significantly. The droplet test showed that all of the plates prior to treatment with the solution were non-wettable. Water dropped onto the surface of the un-treated plates remained on the surface for more than one hour without showing evidence of being pulled into the material porosity. After treatment, however, all of the

plates showed very good plate wettability. The droplet test showed that less than 20 seconds was required for the droplet to become soaked into the plates porosity. In some cases, far less time was required (a few seconds only).

The plates were tested for water permeability before and after treatment to discover the impact of the treatment on water perm. The standard vacuum fill method was used to fill the plates with water both before and after solution treatment. The table below shows the results.

Solution	Plate #	Water Flow Before (grams)		Water Flow After (grams)		Average % Reduction	Drop Wick Time (sec)
33%	728-14	5.8	6.0	3.4	3.1	45%	6
	728-15	6.3	7.0	3.4	3.7	47%	17
20%	728-17	5.4	5.9	3.7	4.0	32%	6
	728-18	7.0	7.3	3.8	4.8	40%	12
10%	728-19	6.1	6.5	5.3	4.9	19%	11
	728-21	5.2	5.0	3.3	3.5	33%	10
0%	730-20	5.7	4.6	7.8	5.3	-27%	Long
	730-21	5.5	4.8	6.6	5.6	-18%	Long
Drying only	730-18	7.0	6.7	7.5	7.0	-6%	Long

Water flow in grams reported for standard perm test conditions (30 kPa back pressure, water collected for 30 seconds after flow begins).

It can be seen that there is some degree of significant plate permeability reduction. The drop in perm does correlate with the concentration of the solution, and the resulting water flows are reasonable and would yield plate permeability near customer specification.

Three of the plates were processed without the use of the solution to confirm that the solution does indeed impact plate wetting characteristics independent of the processing conditions (soaking with alcohol and heat treating at 100°C for 4 hours). For these plates, the perm was found to increase after treatment. This is not too surprising of a result, as it has been shown that permeability tends to increase with testing frequency. These three plates did not show evidence of enhanced material wettability.

Conclusion

This short experiment showed that the use of a very dilute solution of resin mixed with alcohol can be an effective way to enhance the plates water wetting characteristics. Even the lowest concentrations were found to benefit plate water wetting. Plate weight gain from the treatment was in proportion to the concentration of the treatment solution. Permeability of the plates decreased significantly for higher levels of addition. However, the permeability was not impacted to an extent where the part would be in danger of no longer passing the customer water permeability specification.

The next step is to discuss the treatment with UTC Fuel Cells, including out-of-cell testing to determine if the treatment can impact fuel cell operation or poison the fuel cell membrane. After some of this basic information is in place, further work internally would be focused around further characterizing the benefit of the treatment.

EXPERIMENT – USE OF NANO-TITANIA POWDER WITH

SEALING TO PRODUCE WETTABLE SURFACE ON SEALED PLATES

Introduction

Surfacae wetting control is a critical element in fuel cell operation. Surfaces must be either highly hydrophobic or highly hydrophilic to operate well in fuel cells. PFCT's sealed materials were thought to produce a highly hydrophilic surface, but evaluation shows that the hydrophilic surface is not stable over time or not wettable enough for use in a fuel cell.

A short experiment showed that applying a thin film of titania-suspended solution (Loctite) to a sealed plate significantly enhanced the wetting characteristics of the material. This experiment will evaluate the potential to use titania in an solution to improve surface wettability. The key characteristics of the coating must be:

- No or little impact on part contact resistance
- Highly durable coating
- Stable for long duration in acidic conditions
- Does not release contaminants that can impact a fuel cell membrane or catalyst

Experiment

1) Determine qualitatively loading of titania in the solution that is possible without making solution too viscous
    a. Prepare 20 grams – allow to warm to room temperature
    b. Add titania in 2 gram increments and shake to disperse until solution is too viscous qualitatively
    c. Prepare a solution to use with the above-determined mixture. Prepare about 100 grams of mixture and label. Store capped in freezer after experiment is done.
2) Prepare four standard coupons from stock sheet (new composition) by cutting to 2" square and drying for at least 1 hour to remove any absorbed moisture in the part. Weight and label the parts 1, 2, 3 and 4.
3) Record contact resistance of samples 1&2, 3&4 and 1&3, keeping mating surfaces consistent (away from labeling scribe marks)
4) Vacuum impregnate coupons 1 and 2 with titania solution using standard vacuum fill conditions and no overpressure for this experiment
5) Cure coupons in water at 90°C for 20 minutes
6) Dry coupons in dryer for 1 hour
7) Record weight
8) Measure contact resistance for samples 1&2, 3&4 and 1&3 as in step 3) above
9) Evaluate surface wettability qualitatively for each sample through droplet test.
10) Soak overnight in 0.1M H_2SO_4 solution in glass beakers large enough to hold the coupons. Place samples 1&2 in one beaker and 3&4 in the other. Attach plastic bag over beaker with rubber band to prevent solution evaporation.
11) Soak overnight (at least 16 hours)
12) Remove coupons from solution, rinse with DI water
13) Dry for 1 hours
14) Record weights
15) Perform contact resistance measurements as in step 8
16) Note wettabiity of surfaces as in step 9

Results and Observations

Solution mixture

Trial	Titania Total in 21 gm resin	Notes
1	1.1	Thin
2	2.2	Thin
3	2.9	Too thick
	Added 1.5 gm resin , total of 22.5 gm	
4	2.9	Thin, good mixture viscosity

Mixed 20 grams titania powder into 179 gm resin for this experiment

Standard composition was used in coupons.

Coupon	Initial Weight (gm)	After Impregnation and drying (gm)	Change (%)	Notes
1	6.0868	6.3121	3.7	Treated
2	6.1425	6.3617	3.6	Treated
3	6.1064	6.1048	0.0	Untreated
4	5.3342	5.3300	-0.1	Untreated

Weight gain on impregnation of mixture was low because during the vacuum cycle, the mixture off-gassed severely and boiled over, resulting in un-covered parts during impregnation. Another impregnation trial will take place to determine if high weight gains can be realized.

Do not believe that titania particles were fully dispersed. The solution showed evidence of small agglomerations of particles when pouring.

Agitated coupons in the hot cure water on entry to clear surface.

Contact resistance:

Test Coupons	Contact Resistance (mohm-cm^2)	Notes
1&2	1.4	Treated-against treated
3&4	1.5	Untreated against untreated
1&3	1.5	Treated against untreated

The titanium dioxide treatment did not appear to impact the contact resistance of the plates. The values measured are as expected for carbonized plates.

Surface wettability:

Water was dropped onto the surface of the coupons after sealing, contact resistance measurements. All coupons were somewhat hydrophilic. The plates with the titania coating, however, were more hydrophilic than the untreated plates. The treated plates tended to spread the water drops out along the surface, wicking outward in circular regions from the original droplet. Drops applied to the untreated samples did not spread. It appears that the titania treatment is effective in aiding surface wettability.

Corrosion tests.

First test used ~0.1N nitric acid. After soaking in nitric acid for 16 hours at ~90°C, and after rinsing the surface and drying the coupons, the surface of the titania treated plates was less hydrophilic than when they were originally produced (Fig. 1). The untreated plates maintained about the same level of hydrophicity (qualitatively). It seems that the acid treatment reduced the hydrophobic character of the plate surfaces somewhat. It is not known if the acid attacked the material, or if it modified the surface titania powder somewhat. The surface, however, was still more hydrophilic than the untreated material.

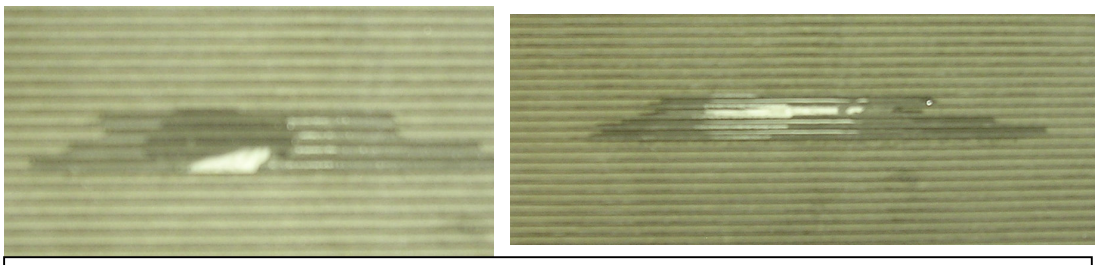

Figure 1. Plate hydrophilic surface without and with titania washcoat with sealing resin to impart improved surface wettablity.

3.4 Material Strength Characterization

Material strength has been historically satisfactory for our product, and early investigations focused upon the measurement of product strength to select and optimize materials. Later in the program, however, the focus on strength was not applied, as the product was suitably strong for the application. However, a study was performed evaluating the compressive strength of the product. The purpose was to evaluate the load bearing capability of the net-shape molded product if a load were applied in a mis-aligned fashion, as shown schematically in Fig. 3.4.1.

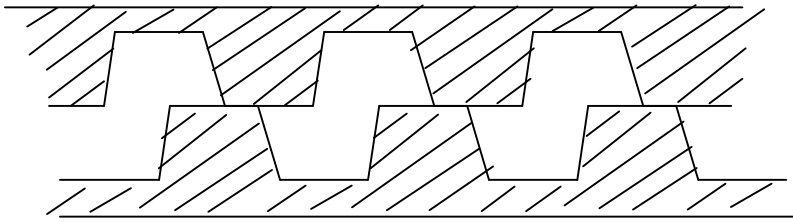

Figure 3.4.1. Schematic diagram of mis-aligned channels.

The testing showed that more than 400 psi of compression pressure was held by the product under the compression test performed with both aligned and mis-aligned flow channels. Typical bipolar plate stack pressures do not generally exceed 100 psi. From this test, we showed that

the material is robust enough to witstand forces generated in stacking, even if a plate is misaligned.

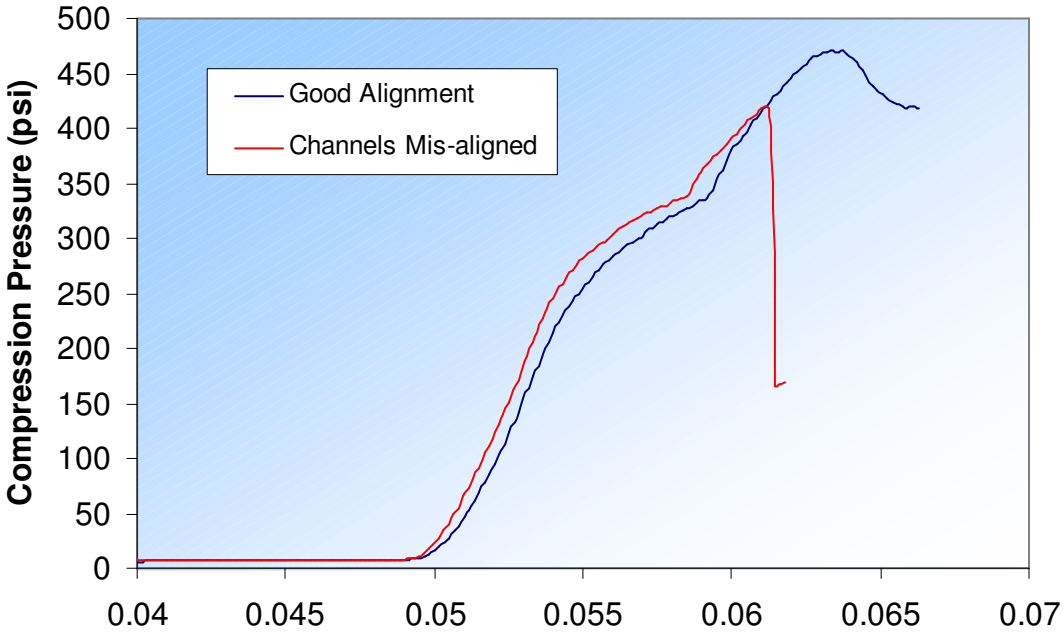

Figure 3.4.2. Chart of compression pressure for bipolar plate samples stacked together as they would be in use. One sample was well aligned while the other was mis-aligned.

3.4.5. Material Contact Resistance Characterization

Contact resistance is a key characteristic that helps to define the performance of a fuel cell. This property was key in our decision to move away from CVD sealing to the sealing described in this report. As shown in Fig. 2.2.2, the contact resistance as measured in-house for our porous and -sealed products is extremely low (about 5 mohm-cm^2, as compared to the value of the CVD seal at around 25. Most competitive products have a contact resistance of 15 mohm-cm^2 or less. Because our going-forward products have a key advantage in this area and are well below customer specification requirements (generally 20 mohm-cm^2), we did not deem it important to optimize this parameter through materials development efforts.

4.0 Develop Low-Cost, Robust Bonding Method

This portion of the work plan was developed sufficiently in prior sections (see Task 4 of section II). Additional work in the area was not performed, as our customers had their own qualified bonding methods and the need was not there. We turned our focus instead on additional process optimization efforts and shrinkage control and characterization efforts.

5.0 Optimize Manufacturing Process

5.1 Develop Comprehensive Quality Assurance Plan

In the execution of this program, we followed our internal New Product Development process, which is part of our plant-wide ISO-9001 certification. In this process, we perform numerous

activities that are designed to transform an emerging technology into an end product. Included in the activities are the following:

- Evaluating the product potential, customer base, competition, potential profitability
- Evaluating statutory and regulatory requirements and safety and environmental issues
- Evaluating intellectual property related to the project
- Defining product performance requirements
- Defining product property measurements to be taken and verifying the accuracy of the measurement system
- Evaluating the material suppliers, their ability to control their processes through statistical analysis, and performing quality audits of the suppliers
- Generating raw material product specifications in concert with the suppliers
- Performing design and process Failure Mode and Effects Analyses (FMEA's)
- Generating a process control plan and all operating procedures for the product and process
- Performing field testing at customer's site(s)
- Establishing product standard costs and bills of materials
- Performing continuous improvement activities

Nearly all of the activities performed in support of our New Product Development process were not associated with this program. The documents created in support of this effort are the proprietary intellectual property of Porvair, and can not be shown in this report.

5.2 Manufacturing Process Improvements

Several studies were performed aimed at generating a more consistent product, or to simplify the manufacturing process. These studies are reported here:

BIPOLAR PLATE DRYER TEMPERATURE PROFILE

Introduction

The temperature of the dryer was measured along its centerline with a type K thermocouple (24 gauge). The procedure was to tie the thermocouple to the dryer belt and allow it to travel the length of the dryer. A data collection system was used to capture the temperature. Two tests were run: one with the dryer empty and another with the dryer loaded during a run (cathode plates). Dryer setpoint was 280°F. After the thermocouple exited the dryer, it was cut free from the belt and drawn back through the dryer (the thermocouple is about 20 feet long).

Results

The measured dryer temperature resided below 200°F and was fairly consistent through the length of the dryer. The small-scale fluctuations most likely represent areas where the thermocouple runs into and out of high velocity air streams (ports in the diffuser panel of the dryer). The dryer under load heated and cooled slightly more slowly than the dryer with no load.

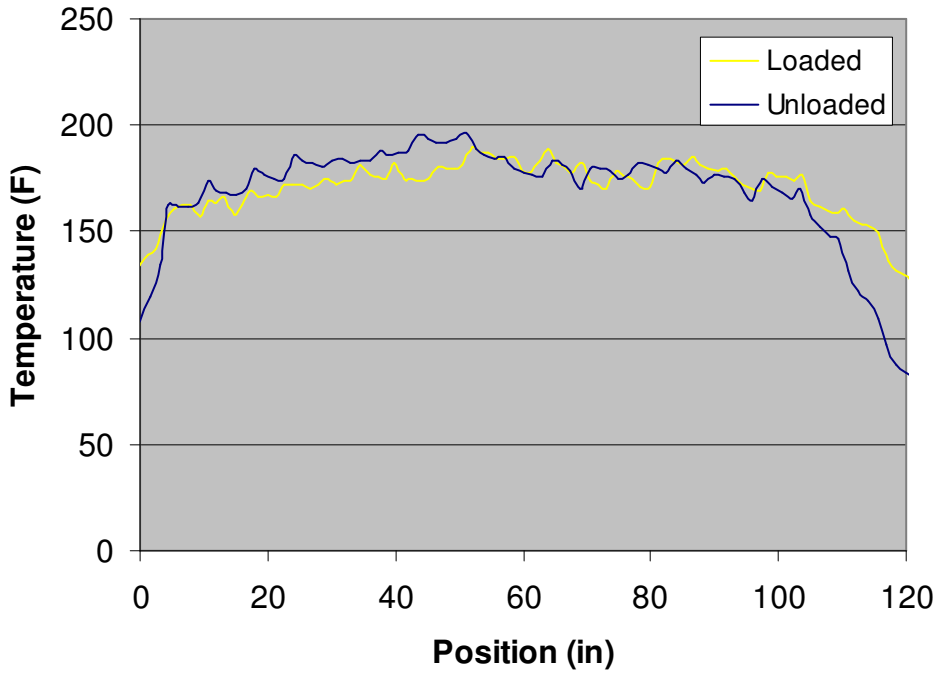

For both the anodes and the cathodes, two randomly selected sheets were chosen from 2 batches formed back to back. The sheets were formed and dried following standard conditions with the rest of the batch. After each of the selected sheets exited the belt dryer, they were weighed and that initial dry weight was recorded. Next, the sheets were placed in a stand-up convection dryer, set to 80C, for an hour. They was removed, weighed and the weight recorded. This was repeated 2 more times, resulting in a total of 4 dry weights taken for each sheet.

The dry weights for both the anodes and the cathodes are displayed below.

	Sheet#	Wet Wt	DryWt #1 belt dryer	DryWt #2 standup dryer	DryWt #3 standup dryer	DryWt #4 standup dryer
			280F @8in/min	80C @1hr	80C @1hr	80C @1hr
Anode	930-12	219	113.8	113.6	113.3	113.2
Anode	930-20	218.6	112.4	111.9	111.9	111.6
Anode	931-14	220	111.6	111.6	111.3	111.3
Anode	931-24	221.5	113.2	113.2	113	112.9
Cathode	934-8	286.1	147.4	147.3	147.1	147
Cathode	934-16	286.9	147.2	146.9	146.3	146.2
Cathode	935-8	287.6	149.3	149	149	148.5
Cathode	935-16	289.6	148.5	148.2	148	147.5

Figure 1 Anode and Cathode Dry Weights

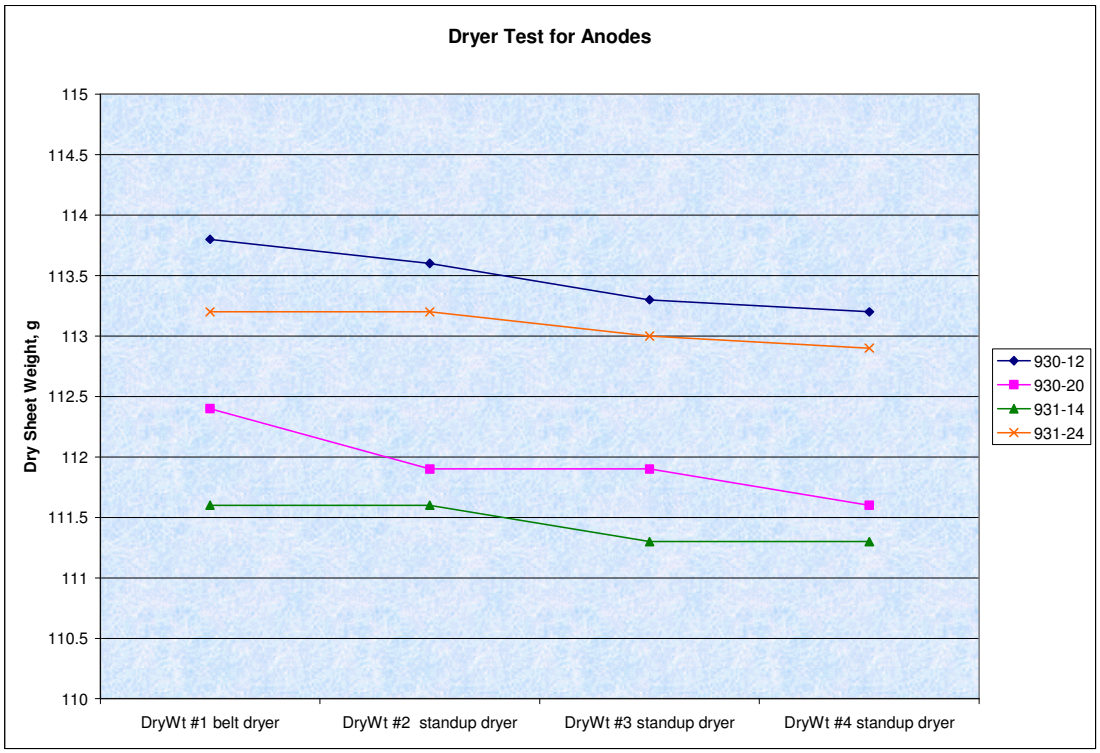
Dryer Test for Anodes
Dry Sheet Weight, g
115
114.5
114
113.5
113
112.5
112
111.5
111
110.5
110
DryWt #1 belt dryer
DryWt #2 standup dryer
DryWt #3 standup dryer
DryWt #4 standup dryer
930-12
930-20
931-14
931-24

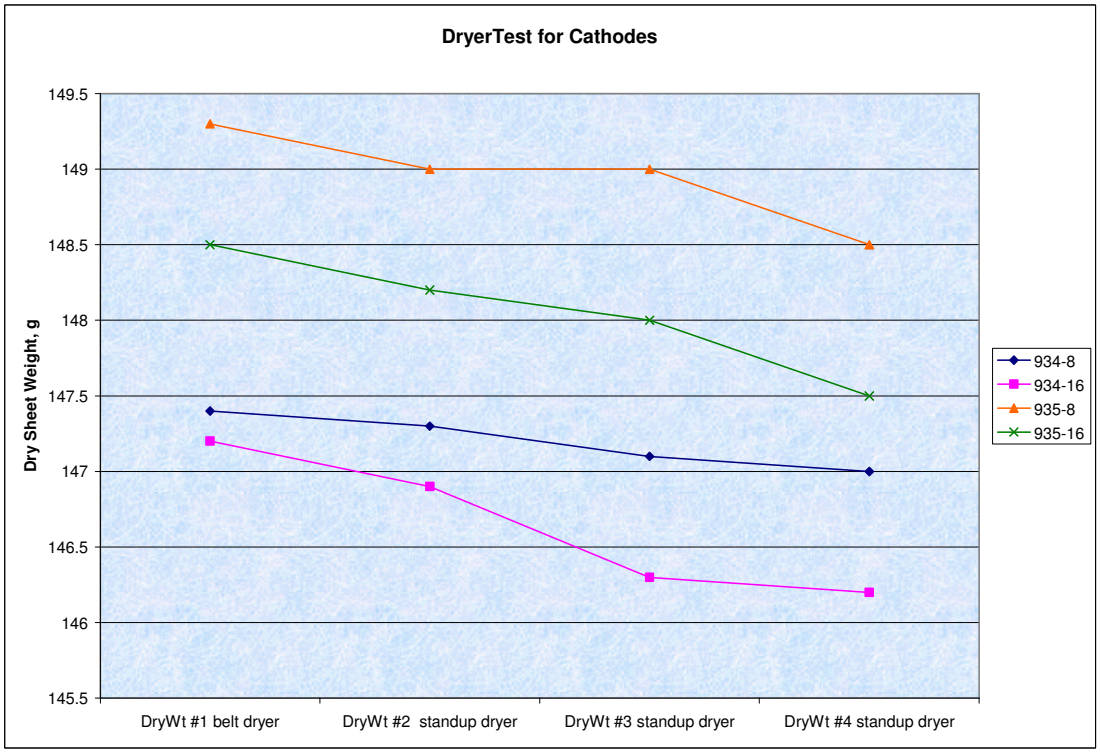
DryerTest for Cathodes
Dry Sheet Weight, g
149.5
149
148.5
148
147.5
147
146.5
146
145.5
DryWt #1 belt dryer
DryWt #2 standup dryer
DryWt #3 standup dryer
DryWt #4 standup dryer
934-8
934-16
935-8
935-16

Dryer Test Results

For the anodes, the difference in weight after the first hour in the stand-up dryer and the weight out of the belt dryer ranges from 0.2 to 0.5 grams. After the second and third hour in the stand-up dryer, the sheets appear to loose a little more weight. The overall range from the initial dry weight to the last varies from 0.3 to 0.6grams, which is less than 1% of the weight.

The difference in sheet dry weight from the initial weight out of the belt dryer and after the 1st hour in the stand up dryer ranges from 0.1 to 0.3 grams. The overall weight range from right out of the belt dryer to the last hour in the stand-up dryer varies from 0.4 to1.0 grams. Again, the weight loss is less than 1% of the sheet weight. The cathodes are about 30% heavier than the anodes.

The results of this study suggest the plates are plenty dry after just one pass in the belt dryer at the standard drying conditions.

Sheet Uniformity Improvement

A study was performed to evaluate the best porous substrate available to filter the sheet materials in the forming system. We have found that a porous plastic (Sheet from Porvair Filtration Group) worked best. The following study was performed evaluating a variety of Sheet sheet materials.

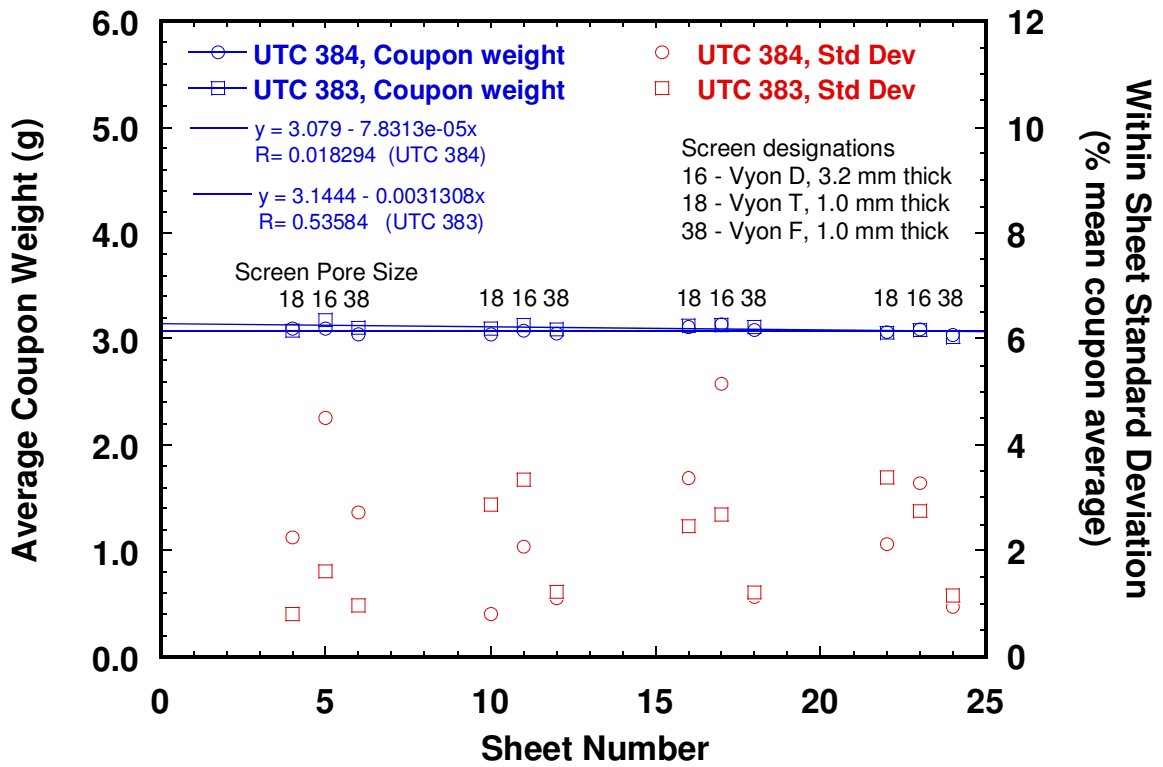

Figure 1. Two bipolar plate preform runs were made using three Porvair Filtration SHEET® porous sheets as the forming screens. Sheets were tested starting with numbers 4, 5, and 6 and then every sixth sheet after that. Coupons were cut from the sheets according to the pattern shown in Figure 2. Coupon weight is the average of all 11 coupons in the sheet. Sheet F at 38 μm pore size gave the best overall performance.

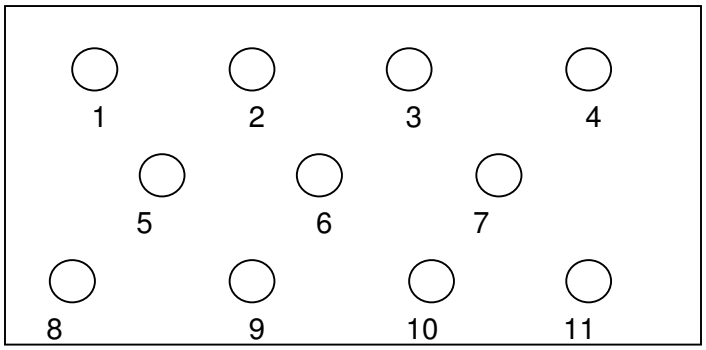

Figure 1. Layout of coupons punched from trimmed dry sheets to determine within-sheet areal density variation.

Table 1. Technical Data For sheet Products Tested at PFCT for Bipolar Plate Preforms

TRADE NAME	MATERIAL TYPE			THICK (mm)	PORE SIZE (μm)			TYPICAL AIR FLOW ($m^2/min/m^{2)}$ AT VARIOUS PRESSURES(mBAR)					REMOVAL EFFICIENCIES (μm)	
	A	B	C		MAX	MEAN FLOW	MIN	1.27	2.45	5.00	10	20	Air Normal	Water Normal
Sheet D	*			3.2 ± 0.18	30	16	8	-	-	2	3	8	6	10
SHEET F	*			**1.00 ± 0.12**	**120**	**38**	**10**	**-**	**22**	**-**	**56**	**92**	**20**	**35**
SHEET HP	*			*2.00 ± 0.20*	*>300*	*91*	*27*	*29*	*46*	-	-	-	*50*	*70*
SHEET T			*	1.00 ± 0.07	40	18	10	-	-	4	8	20	2	10

CARBONIZATION FURNACE TEMPERATURE PROFILE

Introduction

As part of an investigation to find the root cause of recent anode warp issues, a temperature profile of the carbonization furnace was performed. Nine type K thermocouples were inserted into the retort furnace and tied onto a graphite support rack in various locations throughout the furnace. The furnace was run with no other load in the hot zone. Furnace conditions were set for a no gas flow and direct pull vacuum conditions (pumps pulling from retort and main chamber – and furnace blower operating). Vacuum levels less than 1 Torr were typical for this run.

Configuration and Data

The nine thermocouples were positioned as shown in Fig. 1 – thermocouples are labeled A through I.

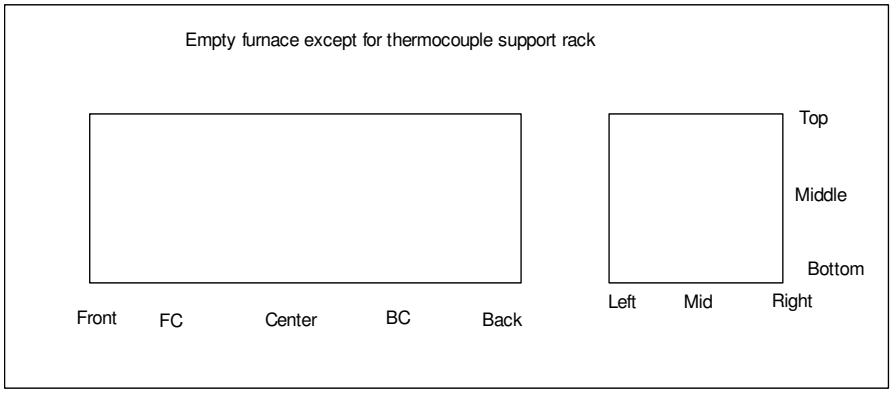

A	Front, Mid, Bottom
B	FC, Left, Bottom
C	Center, Mid, Bottom
D	Front, Mid, Top
E	FC, Right, Top
F	Center, Mid, Top
G	BC, Left, Bottom
H	BC, Right, Top
I	Back, Mid, Top

Figure 8. Furnace profile thermocouple positions.

The temperature profile run was set to the following:

25°C to 600°C at 5°C/min
600°C hold for 30 min
600°C to 1000°C at 5°C/min
1000°C hold for 30 min
1000°C to 1150°C at 5°C/min
1150°C hold for 3 hours
Heat off

The thermocouple temperatures over time are plotted in Figure 2 along with the profile temperature setpoint. As can be seen in this figure, retort box temperatures lag the profile setpoint somewhat and fall generally lower in furnace soak regions. The thermal lag is expected as the retort box must still heat up after the control thermocouple (positioned outside the retort between the retort box and the heaters) achieves setpoint. There was measured a final stable temperature difference between furnace setpoint and the retort of about 40°C at the tests peak setpoint of 1150°C. Retort temperatures also showed some cooling over time in the long soak period. Thermocouple “F” broke during the test run and produced an open signal.

Retort Temperature Uniformity

Figure 3 shows the maximum retort thermocouple temperature difference between all 8 thermocouples in the test array over the test duration. Figure 3 also shows the temperature setpoint for reference.

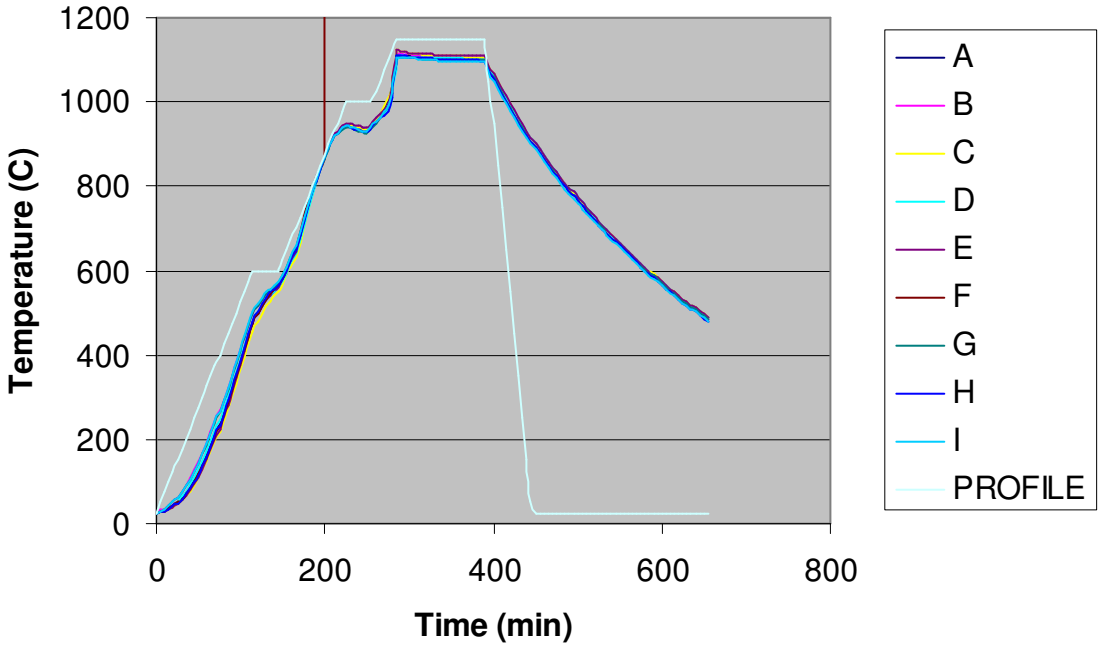

Figure 2. Temperature profile for all thermocouples against furnace setpoint.

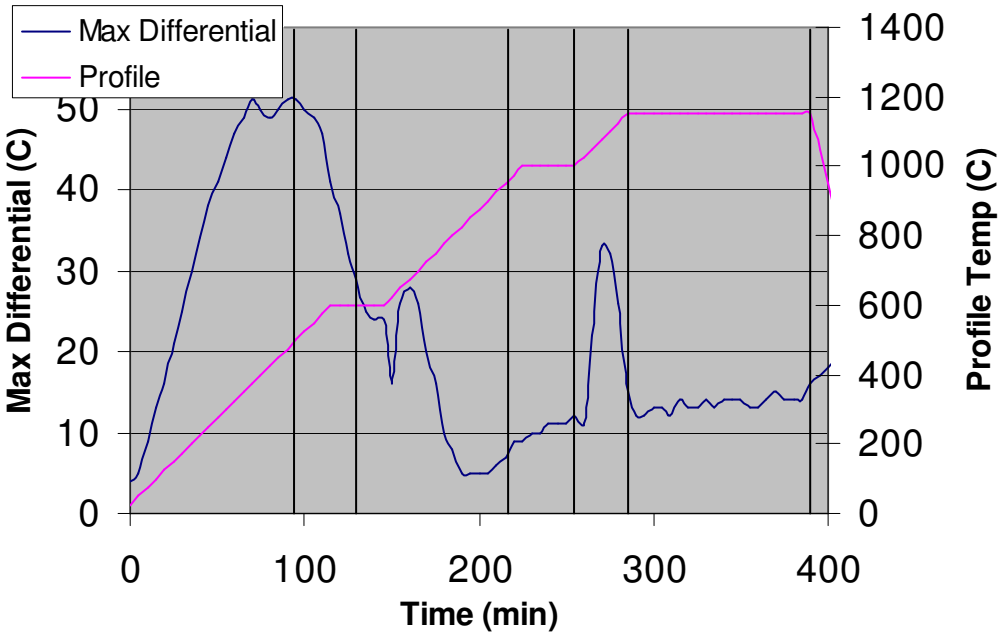

Figure 3. Maximum temperature differential over test duration. Also shown is the furnace temperature profile.

Figures 2 and 3 show that during the initial heating period, the retort box lags the furnace setpoint significantly and the temperature uniformity in the retort becomes erratic. During the initial heating portion of the test cycle, the box temperature can differ by as much as 50°C. Looking at the data in detail, the difference is found to be greatest between the retort box edge and middle, where the edge is at a higher temperature and the middle at a lower temperature. This makes sense relative to the retort design. A chamber below the main retort box exists, which may serve to insulate the bottom center thermocouple from the heating elements, effectively introducing an additional time lag in that region. The thermocouple next to the retort side wall has only the retort wall shielding it from the heating elements, and would be expected to heat more quickly in that area.

On soaking, the thermocouple maximum temperature differential rapidly decreased as the retort box thermally stabilized. On heating to higher temperatures, the differential would increase, but not as significantly as heating to lower temperatures. Once the furnace obtained its 1150°C setpoint, the temperature uniformity was found to slowly increase over time. The uniformity in the box was found to be about within 14°C at its worst.

The temperature profile data was evaluated after the furnace had achieved its target setpoint of 1150°C. Figure 4 shows the average position-by-position temperature on the left during the 1150°C soak time. On the right the data has been evaluated by position within the furnace. The data shows that the ends of the furnace (the front and back) are cooler than the center of the furnace. This reflects the fact that the ends of the furnace are not heated. The data also shows that the back of the furnace is colder than the front by about 6-8°C. This could reflect the need for furnace tuning (re-calibrating setpoint TC's or adjusting their position relative to the retort. Very little difference was noted side-to-side or top-to-bottom.

A	1106.6	Front	1104.9
B	1108.8	FC	1110.6
C	1111.3	Center	1111.3
D	1103.2	BC	1102.3
E	1112.5	Back	1098.8
F	Broken		
G	1101.9	Left	1105.3
H	1102.8	Mid	1105.0
I	1098.8	Right	1107.6
		Bottom	1107.1
		Top	1104.3

Figure 4. 1150°C soak temperatures for the individual profile thermocouples (left) and average values for the furnace positions (right).

A review of the actual furnace profile was performed. The current process temperature profile is as follows:

Segment	Starting Point	Ending Point	Ramp Rate	Hold Time
1	20°C	350°C	3°c/min	N/A
2	350°C	400°C	1.5°C/min	N/A
3	400°C	750°C	1.5°C/min	N/A
4	750°C	1350°C	5°C/min	N/A
5	1350°C	1350°C	N/A	2 hours
6	1350oC	RT	At natural rate	

This profile differs from that indicated to UTC earlier. The profile contains relatively slow ramp cycles from 350°C to 750°C. The cycle was defined about 2 years ago through examining TGA curves for the phenolic resin used. The slow ramp rate was provided in segments associated with high rates of sample off-gassing.

Conclusion

Three potential issues were uncovered in this temperature profile as follows:

1) The back of the retort chamber reads 6-8°C lower than the front at a furnace setpoint of 1150°C. This can be improved through tuning in the front and back zones and re-calibrating or replacing the process control thermocouples there.
2) The stabilized temperature within the retort reads about 40°C lower than the furnace setpoint. It is not known why this temperature difference exists. However, the following actions should be taken to resolve the difference:
    a. Analysis of thermocouple temperature balance to detect potential causes – for example, the TC's used were bare-wire, while the control TC's have carbon-coated alumina sheaths
    b. Calibration of the TC's – survey TC's were not purchased specially calibrated. Control TC's have been in place for at least two years.
    c. Electronics and other causes (cold junction temps, impact of noise reduction, calibration of the electronics for the survey TC's)
3) The 5°C/min heating rate induces a significant temperature difference between the center-line of the retort and the retort walls. With a load in the furnace, this temperature difference may be exaggerated further. The non-uniformity induced on furnace heating was worse at lower furnace temperatures.

5.3 Manufacturing Lean Events

Lean events are a part of the quality culture at Porvair, and are practiced throughout the plant on a regular basis. Most lean events are short in duration (a few hours) and are designed to target one area of improvement – usually in layout of equipment and process flow, or in simplifying the process by eliminating unnecessary process steps. Safety items are also considered in performing a lean event. Throughout the development of the program, we have performed several lean events of this type to improve the bipolar plate manufacturing process. Two major events performed included:

1) A value stream mapping event in the transition of the process from one section of the facility to another.
2) A lifting study and improvement designed to eliminate back strain in workers operating in one specific location of the process.

In transitioning the process into a dedicated location, it was decided to evaluate the process critically and improve upon the process flow, eliminating, reducing or combining process steps. Figures 5.3.1 through 5.3.5 below show the process prior to the lean event. The current state was mapped (Fig. 5.3.6), and the ideal state map created (Fig. 5.3.7).

Figures 5.3.1 – 5.3.5. Photograph of original equipment placement and starting condition for the value stream event.

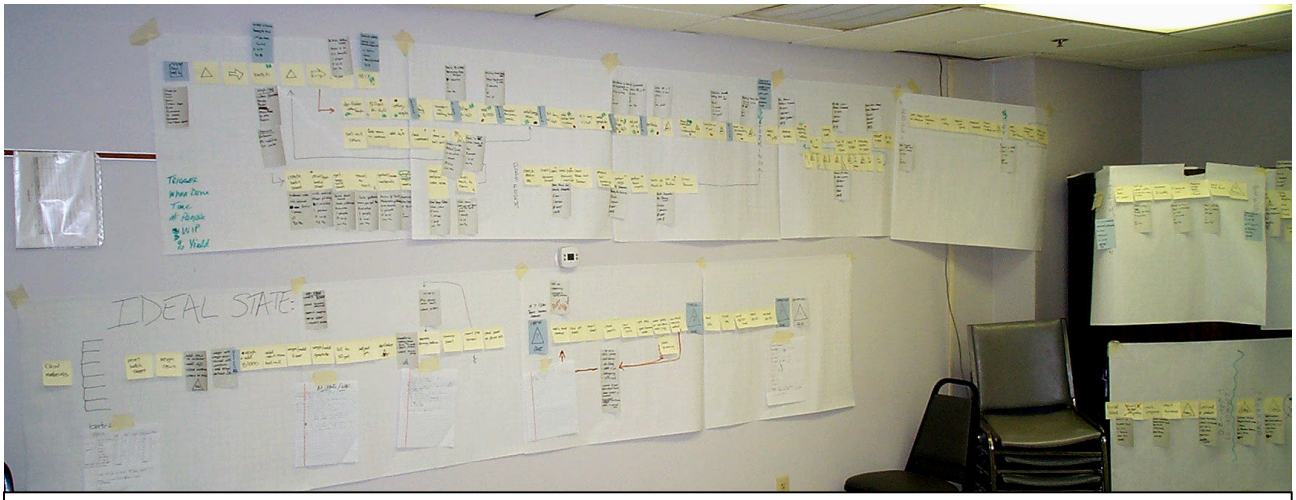

Figure 5.3.6. Current state map, showing numerous process steps and check points.

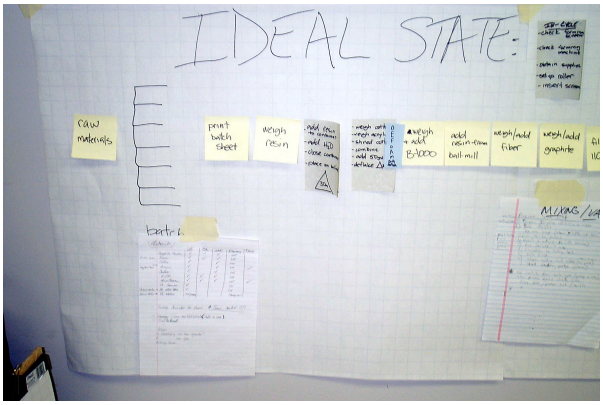

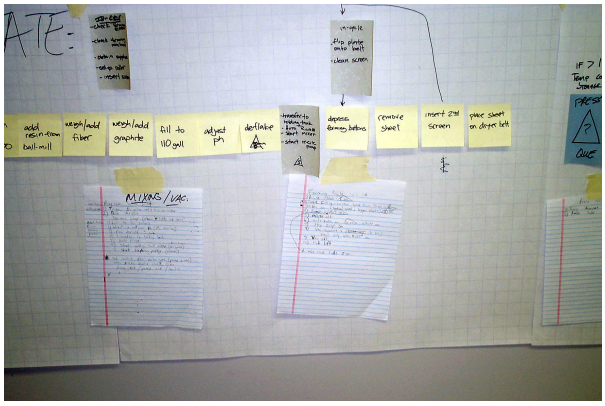

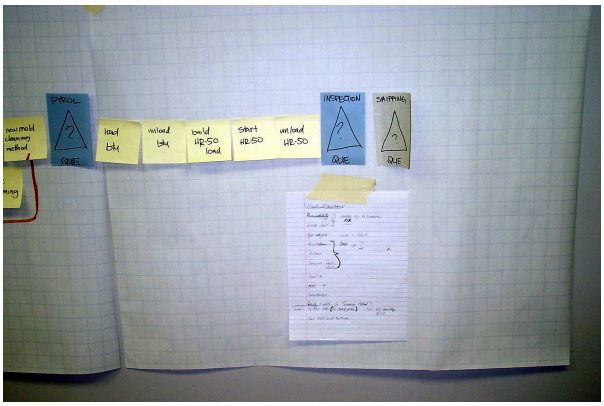

Figure 5.3.7. Ideal state map. Significantly simplified and reduced process layout.

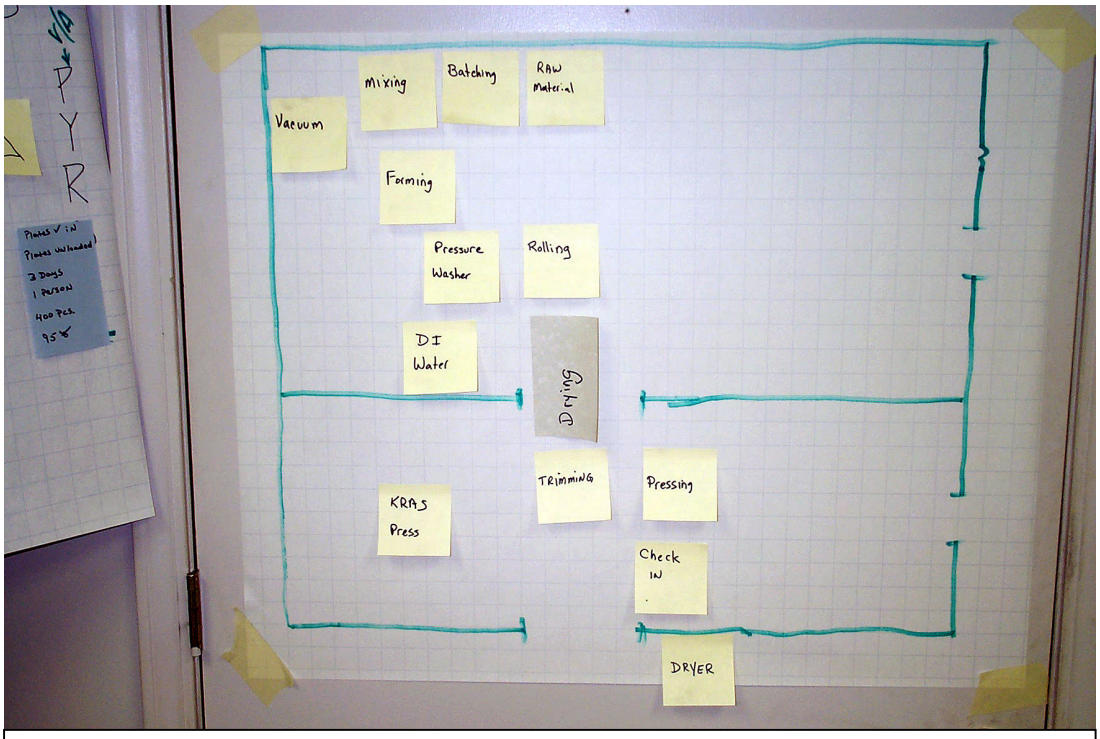

Figure 5.3.8. Ideal state process layout.

The value stream event cumulated with the following accomplishments:

1) Current state mapped
    a. Cycle times
    b. Manufacturing trigger
    c. Current yield
    d. Number of workers
    e. WIP
2) Ideal state mapped
    a. Eliminated non-value added steps
    b. Focused on removing WIP queues
    c. Combined steps that can be done in cycle
3) Generated formal pre-production control plan
4) Performed design FMEA
5) Outlined quality and process measureables
6) Measured and recorded plate travel distances
7) Established plate uniformity baseline from existing process to the ideal state
8) Reduced operator requirements (from 5 to 3)

A second project was performed to investigate process batching. The report below details the activity.

Molded Plate Batching Process Review

The Batching process was audited in order to prepare for writing the SOP and Work Instructions to support this step of our process. Additionally, I was looking for areas that would impact an operator's ability to repeat the batch weights with a high degree of certainty. It was observed that a large amount of airflow passed the scale during weighing and was causing a fluctuation of +/- 4.0 grams. Before batching the next batch of material, a cardboard barrier was placed around the scale and it significantly reduced the instability of the scale. Below is a summary of the issues, which need to be addressed for the batching process:

1. Scale unstable during batching process as discussed above.
    a. Recommend building a "dog house" around the scale to stabilize it or,
2. Scale is being left on a cart that is not stable enough for this step.
    a. Scale should be placed on a solid structure before using or,
3. Scale is not routinely checked / balanced by the operators.
    a. Training and additional auditing.

Changes that we have already made to this process that are significantly improving the batching step are as follows:

1. Switched from Bags to Buckets… This allowed for easier handling and premixing of material.
2. Established tolerances for each material weight to improve consistency.
3. From Roller Ball Milling of Resin to Shear Mixing…

Taking samples representing each batch for Graphite Powder and Resin

A third event was performed to improve worker safety.

In this event, several areas where lifting of materials or components were evaluated from a lifting safety standpoint. An analysis of the lifting operation was undertaken, considering the position of the object to be lifted relative to the operator, how the object is grasped, if the operator must turn in the operation, and how frequently the job must be performed. As part of the evaluation, the chart in Figure 5.3.9 was generated. We decided to focus upon the wettability basket lifting operation because it was the worst for the grasping location, place location and weight. Figure 5.3.10 shows the position that the operator must take prior to improvements. A hoist was installed to improve lifting safety, and resulted in the elimination of the lifting issue in this operation (Fig. 5.3.11).

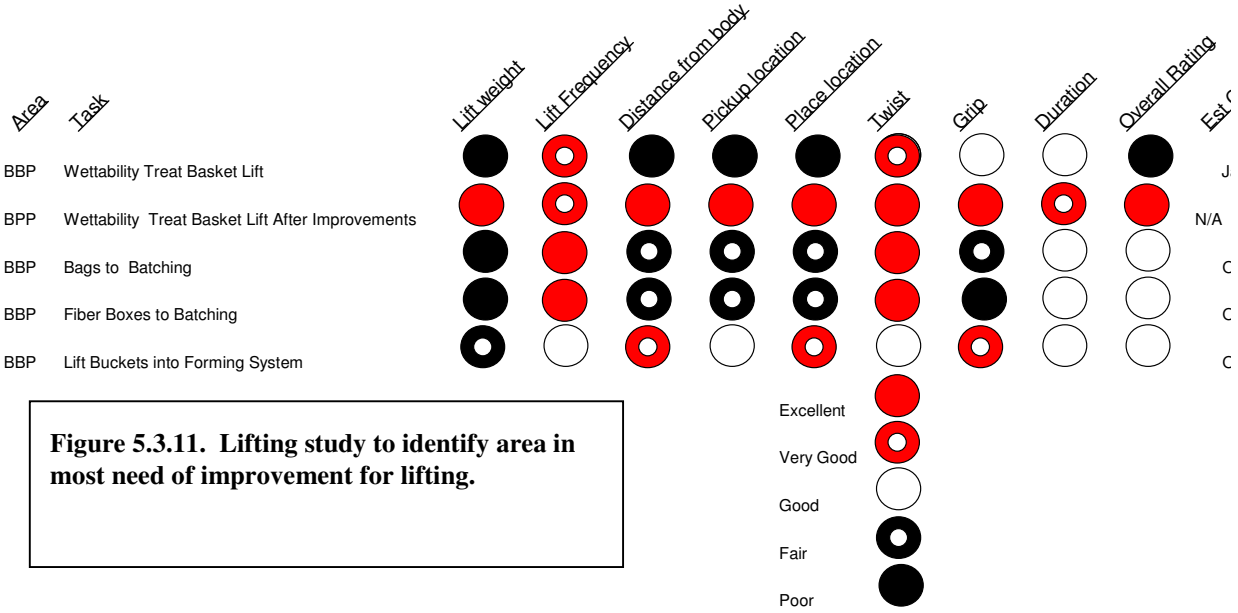

Figure 5.3.11. Lifting study to identify area in most need of improvement for lifting.

Before the improvement, the following was found:

- Part basket is very heavy (49 lbs)
- Part basket must be carried up and down stairs
- Operator must lean into chamber to remove basket
- Terrible lifting configuration
- Study found very small safe lifting load for this operation (< 3 lbs)

To eliminate the hazard, we installed a hoist system, resulting in:

- Hoist system installed
- Eliminated carrying basket entirely
- Eliminated lifting basket entirely

Figure 5.3.12 shows the condition before implementing the improvements. Figure 5.3.13 shows the resulting equipment and the use of the hoist installed.

Figure 5.3.12. Initial lifting requirement for operator. Extremely bad lifting configuration.

Figure 5.3.13. After improvements, no operator lifting required at all.

6..0 Investigation Next-Generation Manufacturing Methods for Ultra-Low Cost Manufacture

The purpose of this section was to investigate potential extensions to the technology having the potential to significantly reduce the cost of part manufacture. Two key areas were envisioned for development – rapid plate molding and early process bonding.

6.1 Rapid Plate Molding

This is the key process identified to be able to introduce a step change in the rate of product manufacture. With current technology, the parts must go through a compression molding step that requires more than 3 minutes per cycle, plus about 1 minute per cycle for die cleaning, waxing, part introduction and part removal. This process bottleneck severely restricts throughput and impacts product cost.

However, because our focus was principally on improving the existing product and process, we did not study rapid plate molding intensively. Rather a couple of small studies for proof of feasibility were performed. In one of these studies, we modified an existing roller unit (used to make foam materials) with a set of channeled rolls (Fig. 6.1.1). The part after initial forming, and while still wet, was rolled through the patterned roll to impart flow channels within the part.

The part was then dried and carbonized to create a demonstration part. We discovered two major issues in the execution of this investigation:

1) The material tended to get stuck in the grooves of the patterned roller.

The material, in a soft, semi-wet state after forming, has very little “green” strength. While it could be effectively pushed into the slots of the roll, the material tended to stay caught in these grooves upon exit from the roller. This caused tear-outs and poor channel filling qualities.

2) The material density after carbonization was too low.

After carbonizing the demonstration parts, the density was found to be in the 0.8-0.9 g/cc range. At this low density, the parts are too weak to be effectively used in fuel cell applications.

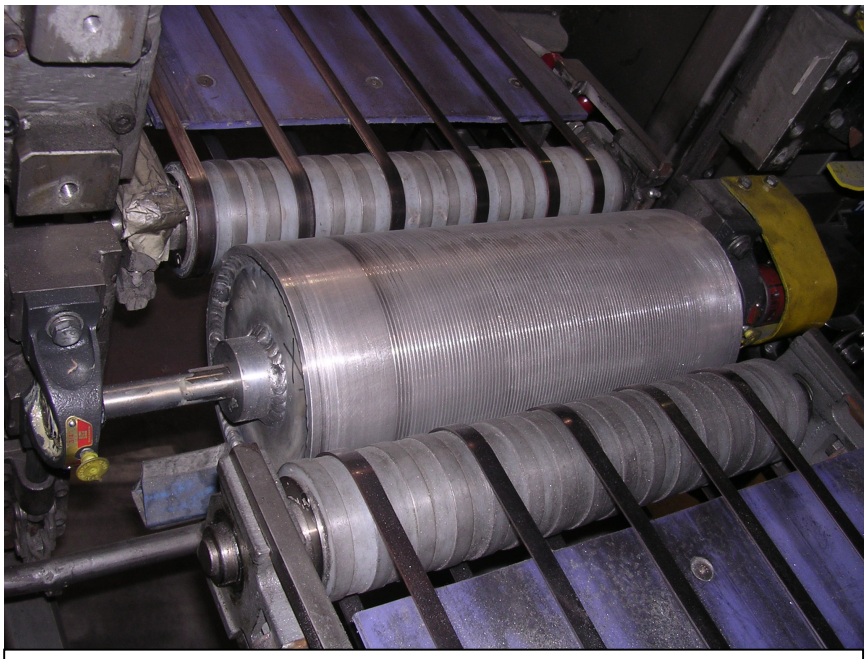

Figure 9.1.1. Prototype rapid molding equipment for proof-of-concept.

While the initial trials were not successful, we still feel that this approach could be taken to dramatically reduce the processing time for the Porvair bipolar plate materials. Further development effort would need to be applied to the concept through both equipment and basic material design.

6.2 Early Process Bonding

Earlier in the program, product bonding was an important topic, as customers were frequently asking if Porvair could perform this function. However, after considerable effort in developing an efficient, robust method, it became apparent that bonding qualification at our customers site is a

long and expensive process. Customers would rather use tried and true methods and materials rather than risk potential project failure by adopting a new (albeit better) bonding method. When we initially wrote this work scope, bonding development was high on our list of desirable development activities. One of the concepts was thought to dramatically improve the product performance and reduce product cost was early process bonding. This is essentially creating a carbon bond between two plates that would significantly reduce the contact resistance between plates. A few informal trials were run to judge the potential of this concept. A summary of one of these trials is included below.

CARBONIZED BONDING TRIALS RESULTS

Introduction

A short experiment was performed to examine the potential of bonding two bipolar plates together with resin and carbonizing the plates to produce a carbon bond.

Summary

Carbonized anode and cathode were used for the test. A mixture of phenolic resin and acetone was prepared in a glass beaker. Acetone was added until the mixture was about the viscosity of syrup. The mixture was then applied to the flat part of the cathode plate with a paint brush in a relatively thin layer (estimate about 5-10 thousands of an inch thickness). The anode plate was then positioned on top of the cathode plate. The plate pairs were then pressed together using the bonding cooling press (pneumatic cylinder) in an arrangement as described below:

- Bottom of press
- Graphite support plate
- Plate pairs with anode plate down
- 1.5” thick foam (40 ppi)
- Graphite support plate
- Spacer plates
- Top of press

The foam was used to provide load to all areas of the plate – especially where the cathode is not fully flat (around the gasket area, which are recessed from the rest of the plate). The assembly was pressed under the load of the pneumatic cylinder overnight until the unit was fully dry. The foam was then carefully removed from the plates (resin mixture was squeezed out of the edges of the plates to flow onto foam). The plate looked very well bonded with a thin bond line and was flat.

The plate was then carbonized using the standard carbonization cycle. The plate was placed anode-side down onto a graphite support plate. Graphite felt was then placed over the cathode side of the plate to provide some gasket land pressure. The felt was 1/8” thick. A support plate was placed over the felt, and graphite blocks were placed on top to provide a compression load (as is done for standard carbonizing cycles).

After the carbonization cycle was complete, the part was removed from the assembly and the following observations were made:

- No bonding occurred between the two plates – anode separated easily from cathode
- Very little carbon residue stuck to anode plate
- Significant carbon residue remained on cathode plate surface

- The carbon material remaining from the resin following carbonization was removed easily from the cathode plate by rubbing or scraping

Carbon was crystalline looking (not uniform film, but many tiny islands of carbon over the plate surface – looks a bit like black dried mud on a small scale).

After this result, we decided to put no further effort into the concept.

7.0 Product Demonstration

7.1 **Next Generation Product Design and Demonstration**

A next-generation plate design from our program partner (UTC Power) was used to generate new fuel cell plates. The shrinkage information gathered in this program was used in generating mold dies that would replicate the original customer design. In this effort a cathode and anode die set was designed and fabricated by Metro Mold (Rogers, MN). The dies were then measured for accuracy using both a CMM technique and with optical characterization of direct molds from the tooling. After establishing that the tooling was fabricated to the tooling prints, the tooling was installed into our process and production trials performed to characterize the new product for all pertinent characteristics:

- Dimensional accuracy of all plate characteristics
- Porosity characteristics
- Product strength
- Product flatness

We found flatness to be a key issue with the new plate design, and expended considerable effort in correcting the issue (see section 1.3). We also found the measurement of the final channel dimensions to be challenging. Sections 1.1 and 3.1 detail investigations that were performed to fully characterize and better predict product shrinkage in response to specific plate features (i.e., channel dimension, land dimension, rib height).

We then characterized the manufacturability of the product through manufacturing trials (section 1.4), and delivered 50 pairs of product to UTC Power.

After fully characterizing the product in-house, UTC Power performed both ex-situ and fuel cell testing on the parts in a single-cell configuration. The specifics of testing at UTC Power is highly proprietary, but some data has been released that indicate excellent performance of this new product design relative to their bill of material product. In fact, it was found that performance of our plate was better than their long-time, and highly expensive product. Figure 7.1.1 shows the polarization curve for this single cell. Other fuel cell performance testing performed in conjunction with this program has been reported in Section I, Task 22, and Section II, Tasks 1.5 and 6.

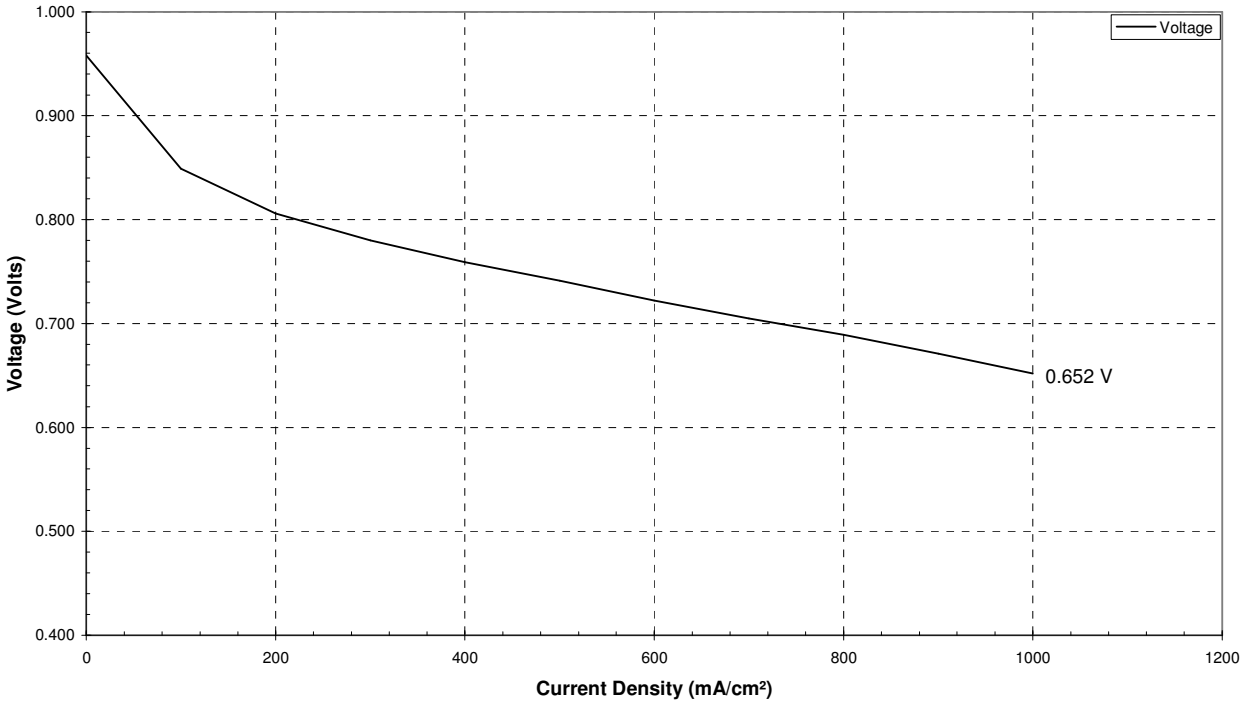

Figure 7.1. Fuel cell performance polarization curve taken of the next generation product design and the Porvair fuel cell plates. Performance was as good or better than the UTC bill of material machined bipolar plate.

Conclusion

The project was highly successful, resulting in the development of a material and process that performed extremely well. Plates were manufactured and used in fuel cell demonstration programs. The plates reportedly exhibited excellent in-the-field performance with no lifetime issues.

The project was left incomplete in the areas of bonding development as it was found that this technology was not needed in the near-term for fuel cell applications (existing methods work well with little cost detriment).